

Durham E-Theses

Luminescent lanthanide complexes as cellular imaging agents or HTRF Assay Components

Montgomery, Craig

How to cite:

Montgomery, Craig (2009) *Luminescent lanthanide complexes as cellular imaging agents or HTRF Assay Components*, Durham theses, Durham University. Available at Durham E-Theses Online: <http://etheses.dur.ac.uk/2108/>

Use policy

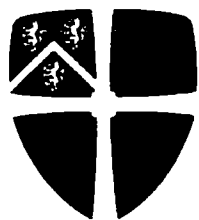
The full-text may be used and/or reproduced, and given to third parties in any format or medium, without prior permission or charge, for personal research or study, educational, or not-for-profit purposes provided that:

- a full bibliographic reference is made to the original source
- a [link](#) is made to the metadata record in Durham E-Theses
- the full-text is not changed in any way

The full-text must not be sold in any format or medium without the formal permission of the copyright holders.

Please consult the [full Durham E-Theses policy](#) for further details.

The copyright of this thesis rests with the author or the university to which it was submitted. No quotation from it, or information derived from it may be published without the prior written consent of the author or university, and any information derived from it should be acknowledged.



Durham
University

**Luminescent Lanthanide Complexes as
Cellular Imaging Agents or HTRF Assay
Components**

Craig Montgomery

A thesis submitted for the degree of Doctor of Philosophy

**Department of Chemistry
Durham University**

2009



25

Abstract

A series of new azaxanthone chromophores has been established as sensitizers of europium and terbium emission in aerated aqueous media. Chromophores incorporating either a pyridyl or pyrazoyl moiety have been devised with large molar extinction coefficients and long excitation wavelengths.

The pyridyl and pyrazoyl-1-azaxanthenes have been incorporated into an array of functionalised macrocycles, to yield a series of emissive europium and terbium complexes, including examples suitable for conjugation. The complexes possess high emissive quantum yields ($\Phi_{Eu} = 25\%$, $\Phi_{Tb} = 64\%$) and long emissive lifetimes (up to 2.3 ms for Tb) in aqueous media. These properties arise from exclusion of coordinated water molecules, as a result of bidentate chelation of the heterocyclic chromophores.

Quenching studies of the lanthanide excited states indicate that non-covalent protein association shields the complexes from quenching by endogenous electron rich species, such as urate and ascorbate. Under simulated cellular conditions, (0.4 mM serum albumin, 0.13 mM urate) the emissive lifetimes remain within 10 % of that observed in water, indicating protein binding does not quench the lanthanide excited states.

Cellular uptake experiments have been performed with CHO and NIH-3T3 cell lines. Examination using fluorescence microscopy reveals cellular uptake, with complexes exhibiting a time-dependent localisation profile partitioning between mitochondrial and lysosomal regions.

Following establishment of an efficient and reproducible method of conjugation, complexes have been covalently attached to benzyl guanine vectors to examine their performance as components in homogeneous time resolved fluorescence (HTRF) assays.

Declaration

The research described herein was undertaken at the Department of Chemistry of Durham University between October 2005 and December 2008. All of the work is my own; no part of it has previously been submitted for a degree at this or any other university.

Statement of Copyright

The copyright of this thesis rests with the author. No quotations should be published without prior consent and information derived from it should be acknowledged.

Acknowledgements

My sincere thanks go to:

My supervisor Prof. David Parker for his support, guidance and expertise during my years at Durham University.

Cisbio International for financial funding. Particular thanks to Dr Laurent Lamarque, Dr Robert Poole and Dr Gérard Mathis for their collaboration throughout this research project.

My co-supervisor Dr Andrew Beeby, and Dr Lars-Olof Pålsson, for acquisition of phosphorescence emission spectra and luminescence quantum yields.

Dr Alan Kenwright, Catherine Hefferman and Ian McKeag for their assistance with NMR spectroscopy. Dr Mike Jones, Dr Jackie Mosely and Lara Turner for their assistance with mass spectrometry.

Dr Bob Peacock (Glasgow University) for his help and expertise in circularly polarised luminescence.

Dr Aileen Congreve for performing flow cytometry experiments, and assistance with HPLC analysis.

Dr Philip Stenson for help with cyclic voltammetry measurements.

Elizabeth New for performing fluorescence microscopy, flow cytometry and cytotoxicity experiments.

The past and present members of the Parker research group for providing an 'entertaining' working environment. Particular thanks to Rachael, Ben, Elena, Elisa, Kirsten, Liz, Phil and Robek for their friendship throughout my PhD.

My parents, Kath and Peter, because without their love and support, none of this would have been possible.

Abbreviations

A	absorbance
Ac	acetate
Ar	aromatic
BG	benzyl guanine
BOC ₂ O	di- <i>tert</i> -butyl dicarbonate
BODIPY	dipyrrromethane boron difluoride; 4,4-difluoro-4-bora-3a,4a-diaza- <i>s</i> -indacene
br	broad
BSA	bovin serum albumin
°C	degrees celsius
CCl ₄	carbon tetrachloride
CHO	Chinese hamster ovarian cells
cm ⁻¹	wavenumber
CD	circular dichroism
COSY	homonuclear correlation spectroscopy
CPL	circularly polarised luminescence
CV	cyclic voltammetry
Cyclen	1,4,7,10-tetraazacyclododecane
d	doublet
DCC	<i>N,N</i> -dicyclohexylcarbodiimide
DCM	dichloromethane
DEFRET	diffusion enhanced fluorescence resonance energy transfer
DIPEA	<i>N,N</i> -diisopropylethylamine
DMF	<i>N,N</i> -dimethylformamide
DMSO	dimethyl sulfoxide
DO3A	1,4,7-tris(carboxymethyl)-1,4,7,10-tetraazacyclododecane
DOTA	1,4,7,10-tetraazacyclododecane-1,4,7,10-tetraacetic acid
dpqC	10,11,12,13-tetrahydrodipyrido-[3,2a:2',3'-c]-phenazine; tetraazatriphenylene

Dy	dysprosium
EDC.HCl	1-ethyl-3-[3-dimethylaminopropyl]carbodiimide hydrochloride
EPA	diethyl ether – isopentane – ethanol (2 : 5 : 5 by volume)
E_T	sensitiser triplet energy
ET (k_{ET})	energy transfer (rate of energy transfer)
Et ₂ O	diethyl ether
EtOH	ethanol
eq.	equivalent
Eu, Eu ³⁺	europium
Fc ⁺ / Fc	ferrocenium / ferrocene
FRET	fluorescence resonance energy transfer
g, mg, μg	gram, milligram, microgram
g_{em}	emission dissymmetry factor
GFP	green fluorescent protein
h, min, sec, ms, μs,	hour, minute, second, millisecond, microsecond
HEPES	4-(2-hydroxyethyl)-1-piperazineethanesulfonic acid
HPLC	high pressure liquid chromatography
HRMS	high resolution mass spectroscopy
HSA	human serum albumin
HTRF	homogeneous time resolved fluorescence
Hz	hertz
IC	internal conversion
I_L	intensity of left circularly polarised luminescence
I_R	intensity of right circularly polarised luminescence
ISC,	inter-system crossing
K	kelvin
L, ml	litre, millilitre
LED	light emitting diode
Ln; Ln ³⁺	lanthanide ion
M, mM, μM	molar (mol dm ⁻³), millimolar, micromolar
MeCN	acetonitrile

MeOH	methanol
mol, mmol,	mole, millimole, micromole
m.p.	melting point
MRI	magnetic resonance imaging
MS	mass spectroscopy
ES ⁺	electrospray using positive mode
ES ⁻	electrospray using negative mode
M	molecular Ion
MTT	3-(4,5-dimethylthiazol-2-yl)-2,5-diphenyltetrazolium bromide
NBS	<i>N</i> -bromosuccinimide
NHE	natural hydrogen electrode
NHS	<i>N</i> -hydroxysuccinimide
NIH 3T3,	mouse skin fibroblast cells
NMR	nuclear magnetic resonance
br	broad
d	doublet
m	multiplet
q	quartet
s	singlet
t	triplet
Ph	phenyl
PPA	polyphosphoric acid
ppm	parts per million
Q	quencher
τ_{1p}	proton relaxivity
rt	room temperature
S ₀	singlet ground state
S ₁	first singlet excited state
SAP	square antiprismatic
sens	sensitiser
Sm	samarium

Tb, Tb ³⁺	terbium
Tf	triflate
TFA	trifluoroacetic acid
THF	tetrahydrofuran
TLC	thin layer chromatography
Trp	tryptophan
TSAP	twisted square
TSTU	<i>N,N,N,N</i> ,-tetramethyl- <i>O</i> -(<i>N</i> -succinimidyl)uronium tetrafluoroborate
UV-Vis	ultra-violet, visible
ϵ	extinction coefficient
η_{ET}	efficiency of the energy transfer process
Φ_{em}	overall emission quantum yield
k_{BET}	rate of back energy transfer
τ_{obs}	observed luminescence lifetime

Contents

Chapter One: Introduction	1
1.1 Overview of Fluorescent Probes	2
1.2 Luminescent Properties of the Lanthanide Ions	5
1.3 Sensitised Emission	6
1.4 Energy Transfer Mechanisms	7
1.5 Eu(III) and Tb(III) Luminescence Characteristics	8
1.6 Lanthanide Luminescence Deactivation Processes	10
1.7 Summary – Essential Requirements for a Sensitising Moiety	14
1.8 Luminescent Lanthanide Complexes	15
1.9 Aim and Objectives	19
1.10 Engineering Lanthanide Complexes for Biological Applications	19
1.11 Using Lanthanide Complexes for Imaging <i>in cellulo</i>	20
1.12 Using Lanthanide Complexes as Bioconjugate ‘tags’	24
References	29
Chapter Two: Synthesis and Photophysical Characterisation	34
2.1 Chromophore Synthesis	35
2.1.1 2-Pyridyl-azaxanthone	37
2.1.2 2-Pyrazoyl-azaxanthone	39
2.1.3 Tetraazatriphenylene	41
2.2 Chromophore Characterisation	42
2.2.1 Absorption Spectra	42
2.2.2 Fluorescence Emission Spectra	43
2.2.3 Phosphorescence Emission Spectra	44
2.2.4 Summary	46
2.3 Ligand and Complex Synthesis	47
2.3.1 DO3A Complexes	47
2.3.2 Tri-Amide Complexes	48
2.4 Complex Characterisation	52

2.4.1 Absorption Spectra	52
2.4.2 Emission Spectra	53
2.4.3 pH and Anion Sensitivity	56
2.4.4 Lanthanide Coordination Environment Studies (¹ H NMR & HPLC)	59
2.4.5 Luminescent Lifetimes	62
2.4.6 Luminescence Quantum Yields	64
2.5 Conclusions	66
References	67
Chapter Three: Dynamic Quenching Studies	69
3.1 Cyclic Voltammetry	71
3.2 Stern – Volmer Constants	72
3.2.1 Quenching Studies with Iodide	74
3.2.2 Quenching Studies with Ascorbate and Urate	76
3.3 Non Covalent Protein Association and Inhibition of Quenching	79
References	82
Chapter Four: Circularly Polarised Luminescence (CPL)	83
4.1 Complex Conformational Studies	84
4.2 CPL Spectra	86
4.3 Emission Dissymmetry Factors	88
4.4 Protein Association	90
4.5 HSA Binding Studies	95
References	97
Chapter Five: Cellular Studies	98
5.1 Cellular Cytotoxicity Profiles	99
5.2 Luminescence Microscopy Studies	102
5.3 Cellular Uptake Mechanism	106
5.4 Conclusions	107

References	108
Chapter Six: Conjugate Complexes	109
6.1 Amide Conjugate Ligand and Complex Synthesis	111
6.1.1 Trans Pendant Arm Synthesis	111
6.1.2 Functionalisation of Cyclen	112
6.2 Complex Characterisation	122
6.3 Anion Sensitivity of [EuL⁸]	123
6.4 HTRF	127
6.4.1 Complex Activation and Conjugation	129
6.4.2 HTRF Application and Screening	132
6.5 Alternative Conjugation Complexes	133
6.5.1 Carboxylate Conjugate Complex Synthesis	133
6.5.2 Carboxylate Conjugate Complex Characterisation	137
6.6 Conclusions	138
Future Work	139
6.7 Chromophore Optimisation	139
6.8 Phosphinate Conjugate Complexes	140
References	142
Chapter Seven: Experimental	144
Ligand and Complex Synthesis	152
7.1 Sensitising Chromophores	152
7.1.1 Pyridyl-azaxanthone	156
7.1.2 Pyrazoyl-azaxanthone	161
7.2 DO3A Complexes	164
7.2.1 Pyridyl-azaxanthone DO3A Complexes	165
7.2.2 Pyrazoyl-azaxanthone DO3A Complexes	167
7.2.3 Tetraazatriphenylene DO3A Complexes	170
7.3 Triamide Complexes	172
7.3.1 Pyridyl-azaxanthone Triamide Complexes	173

7.3.2 Pyrazoyl-azaxanthone Triamide Complexes	178
7.3.3 Tetraazatriphenylene Triamide Complexes	187
7.4 Amide Conjugate Complexes	193
7.4.1 Conjugate Amide Pendant Arm	193
7.4.2 Cyclen Intermediates	200
7.4.3 Pyridyl-azaxanthone Amide Conjugate Complex	205
7.4.4 Pyrazoyl-azaxanthone Amide Conjugate Complex	211
7.4.5 Tetraazatriphenylene Amide Conjugate Complex	214
7.5 Activation and Conjugation of Conjugate Complexes	220
7.5.1 Pyridyl-azaxanthone, [EuL ⁹]	220
7.5.2 Pyrazoyl-azaxanthone, [TbL ¹⁰]	222
7.5.3 Tetraazatriphenylene, [EuL ¹¹]	224
7.6 Carboxylate Conjugate Complexes	226
7.6.1 Carboxylate Conjugate Arm	226
7.6.2 Cyclen Intermediates	227
7.6.3 Pyridyl-azaxanthone Carboxylate Conjugate Complex	230
7.6.4 Tetraazatriphenylene Carboxylate Conjugate Complex	232
References	234
Appendices	235
Appendix 1 – Substituted Pyrazoyl-azaxanthone Characterisation	235
Appendix 2 – Analytical Reverse Phase HPLC Analysis	236
Appendix 3 – Crystal Data and Structure Refinement Parameters	239

CHAPTER ONE:

Introduction



Chapter One: Introduction

1.1 Overview of Fluorescent Probes

Living organisms function by a complex array of cellular processes, utilising their intracellular network of interacting biopolymers, ions and metabolites. Our understanding of *in cellulo* phenomena, including intracellular signalling and recognition processes is of utmost importance for disciplines in biochemistry, drug design and medical diagnostics.^{1,2} At present, the biological characteristics of many biomolecules cannot be examined in their purified, isolated forms, increasing the impetus to monitor biological processes inside living cells.¹ Our ability to visualise, probe and sense intracellular analytes, including characterising their movement, interactions and chemical microenvironment is crucial in developing a detailed understanding of their function.^{3,4}

Recent decades have seen advances in the field of fluorescence microscopy,⁵ ultimately seeking a better understanding of cellular activity. Fluorescence microscopy provides a non-invasive procedure⁶ that is of particular use in examining and imaging living cells.⁷ The technique monitors emitted photons from fluorescent moieties, and has been shown to be capable of analysing subcellular events.⁸ The challenging objective for scientists is to devise responsive optical probes which can either quantitatively signal information of the nature of their local environment, or be targeted to selective organelles.⁹ To date, probes for live cell imaging have been most frequently based on either **recombinant proteins** or **heterocyclic organic fluorophores**.

Recombinant proteins

Since the initial molecular cloning¹⁰ and genetic engineering¹¹ of green fluorescent protein (GFP), continued mutagenesis has led to a new generation of fluorescent proteins.^{4,12,13} These proteins have variable excitation (> 350 nm) and emission wavelengths within the visible region of the spectra,^{14,15} making them well suited for microscopic applications. The primary advantage of fluorescent protein probes over conventional organic dyes is their ability to be chemically manipulated (e.g. conjugation to signalling peptides), without compromising their photophysical characteristics.¹⁶ Other benefits include reduced photodynamic toxicity and compatibility in protein recognition

studies, notably when used as components of fluorescence resonance energy transfer (FRET) studies.¹⁷ In addition to FRET applications, advanced microscopic techniques like time-lapsing imaging and fluorescence recovery after photobleaching have made it possible to extract spatial and dynamic information about fluorescent fusion proteins in live cells under physiological conditions.⁹ These techniques have been instrumental in improving our understanding of how proteins assemble in large protein complexes and function in cellular processes, regulating the maintenance, growth, division, differentiation, and death of cells. However, despite being employed efficiently in biological applications, fluorescent proteins still have limitations. These are primarily related to their sub-optimal photophysical properties, high molecular weight and relatively time-consuming labelling processes.⁹

Heterocyclic fluorophores

Low molecular weight organic fluorophores based on fluorescein (**A**) and rhodamine (**B**) (**Figure 1.1**) have provided luminescent probes that offer an effective alternative to the use of recombinant proteins.^{18,19} These condensed heterocyclic aromatics are highly emissive, possessing large molar absorption coefficients. Unfortunately, their short lived excited states (a few nanoseconds), do not easily allow distinction between their fluorescence and autofluorescence. Furthermore, these moieties exhibit broad absorption and emission bands, with small Stokes' shifts. For these reasons, a large proportion of research has focussed on modifying these dyes. The series of optical probes based on Alexa Fluor[®] and BOPIPY[®] structures provide attractive alternatives.^{20,21} These dyes prove more resistant to photobleaching, exhibit a pH-independent fluorescence and possess high extinction coefficients with emission quantum yields that are typically > 0.5.²²

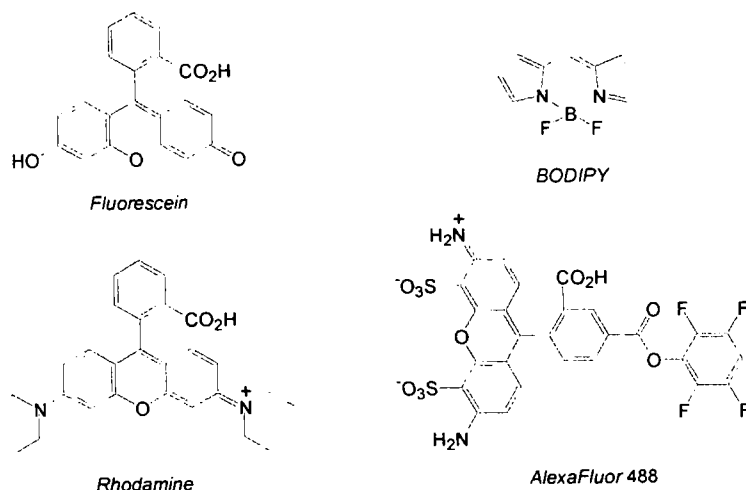


Figure 1.1: The structure of common commercial organic fluorescent dyes and emissive tags

While the number of commercially available fluorescent probes continues to increase, the limitations of such compounds, namely their susceptibility towards interference from light scattering in biological media or natural fluorescence from certain biomolecules, has led to research into possible alternatives.

Over the past decade, attention has grown into the development of biocompatible semi-conductor **quantum dots**. At present their primary application is as replacements for fluorescent proteins in labelling cellular proteins,²³ as their lack of responsiveness to the local environment renders them applicable only as fluorescent tags. The primary drawbacks surrounding the use of quantum dots in biological applications, is their large molecular volume and poor cell permeability.^{24,25,26} Strategies such as attaching appropriate surface vectors (e.g. amphiphilic polymer coatings) are used to enhance solubility and improve their biocompatibility.²⁷

Significant progress has been made in recent years towards the development of highly emissive **lanthanide ion complexes** in aqueous solution, seeking to exploit their unique excited state properties.²² This trend has led to the publication of various reviews, during recent years.^{22,28,29,30} Compared to other optical probes, lanthanide complexes possess sharp emission bands, large Stokes' shifts (separation between absorption and emission wavelengths) and are relatively insensitive towards dissolved O₂ and photobleaching.³¹ A more beneficial property is their long emissive luminescence lifetimes, which allow time-

resolved spectroscopy and microscopy to be employed.³² For europium (Eu) and terbium (Tb), the radiative lifetimes are typically milliseconds in duration. Thus, time-gated acquisitions can afford excellent discrimination between probe emission and background fluorescence or light scattering.

In this thesis, the emerging use of lanthanide coordination complexes as cellular probes is explored. In particular, their application either as components of time-resolved luminescence assays or as probes to target organelles selectively *in cellulo* is addressed. A discussion of the properties of lanthanide complexes which make them suitable as luminescent probes follows.

1.2 Luminescence Properties of the Lanthanide Ions

With the exceptions of Ce^{4+} and Eu^{2+} , the most stable and predominant oxidation state of the lanthanide ions in solution is +3. Consequently, it is the result of the partial filling of the $4f$ orbitals (except for lanthanum and lutetium) that determines their absorption and emission spectra properties. The energy levels of the $4f$ orbitals are not degenerate. Electronic repulsion between electrons ‘lifts’ degeneracy to yield spectroscopic terms with separations between neighbouring terms of the order of $5,000 - 10,000 \text{ cm}^{-1}$. The J levels within each manifold are further separated by about 1000 cm^{-1} .³³

The $4f$ orbitals in the Ln^{3+} ions are highly contracted, so that there is only a very weak interaction between the f orbitals and the ligands in a Ln complex. The shielded nature of the $4f$ electrons has profound effects on the optical spectra of lanthanides. Small ligand-field splittings (typically 100 cm^{-1}) are associated with the Laporte forbidden $f-f$ transitions.³⁴ These effects are, to a first approximation, independent of environment.³⁵ However, changes in the fine structure and the relative intensity of emission bands can be very informative. This is particularly true for Eu^{3+} , for which subsequent alterations in the spectral form allow ratiometric analysis (*See section 1.5*). The forbidden nature of the $f-f$ transitions means that the lowest energy excited states of lanthanides possess long natural lifetimes. The most studied emissive lanthanide ions are europium and terbium. They, and analogous gadolinium systems, are the only lanthanide complexes studied in this thesis.

1.3 Sensitised Emission

The low extinction coefficients ($0.5 - 3 \text{ dm}^3 \text{ mol}^{-1} \text{ cm}^{-1}$)³³ of lanthanide ions mean that efficient population of excited energy states cannot be achieved by traditional sources of irradiation, e.g. flash-lamps. It is therefore necessary to adopt alternative approaches to ensure efficient population of the excited states. One option is the use of laser radiation. Eu and Tb are just two lanthanides that can be excited in this manner; using a rhodamine 110 dye laser at 580 nm (matching the ${}^7F_0 \rightarrow {}^5D_0$ transition of Eu) or an argon ion laser at 488 nm (${}^7F_6 \rightarrow {}^5D_4$ for Tb).³⁵ Laser excitation is currently not a practical method for microscopy applications. Instead, efficient excitation can be achieved by incorporating an organic chromophore into a lanthanide-binding ligand, allowing indirect population of the lanthanide excited state by intramolecular energy transfer.^{36,37}

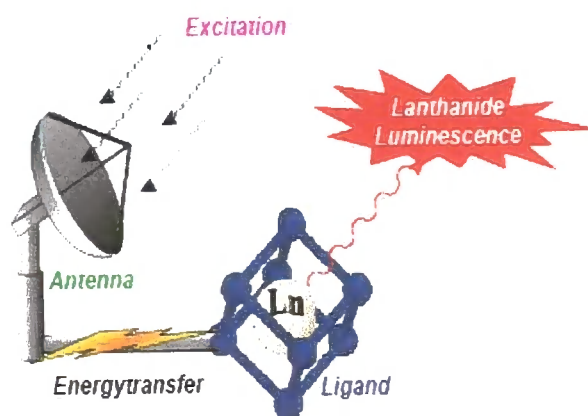


Figure 1.2: Schematic illustrating energy transfer from chromophore to lanthanide metal

The process of sensitised emission and indirect population of the lanthanide excited state (via the chromophore triplet state) is best summarised in a Jablonski diagram (**Figure 1.3**).

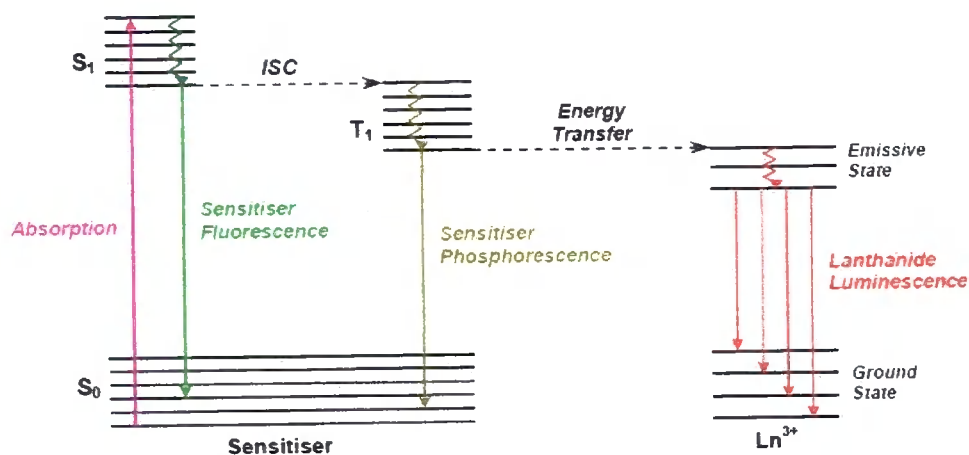


Figure 1.3: Jablonski diagram showing the energy transfer processes during sensitised emission

Prior to excitation, the antenna chromophore is in the ground state S_0 . Upon absorption of a photon, it is raised to a vibrationally excited singlet state (S_n where $n = 2, 3, \dots$). The higher vibrationally and electronically excited state undergoes non-radiative relaxation (**internal conversion IC**) to a high vibrational energy level of the first excited state (S_1) manifold in a process that occurs rapidly in comparison to the competing radiative decay process (i.e. $S_2 \rightarrow S_0$). The excess energy of the S_1 excited state is then lost by **vibrational relaxation** to the lowest level of the manifold. The sensitiser can now either undergo radiative decay by fluorescence, or undergo a change in spin multiplicity ($\Delta S \neq 0$) in the formally forbidden non-radiative process of **intersystem crossing (ISC)**. This populates the triplet state, T_1 . Finally, reverse intersystem crossing to S_1 and sensitiser phosphorescence compete with energy transfer to the lanthanide excited state. The excited Ln^{3+} ion then relaxes to its ground state electronic configuration, resulting in luminescence.³⁸

1.4 Energy Transfer Mechanisms

The energy transfer step between the sensitiser triplet state and the lanthanide (III) ion can proceed via either a **Förster** or **Dexter** mechanism.^{39,40} The Förster mechanism is a

through-space, dipole-dipole interaction which is strongly dependent on the donor / acceptor spectral overlap between the emission spectrum of the donor and the absorption spectrum of the acceptor. The rate of energy transfer k_{ET} is a sensitive function of the mean separation (r) between the donor and acceptor, varying as r^{-6} .

In the Dexter mechanism, a shorter range electron-exchange energy transfer process is involved. This mechanism requires orbital overlap between the donor and the acceptor.

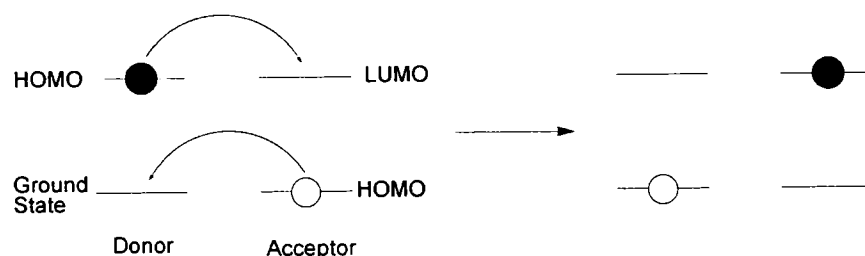


Figure 1.4: Schematic diagram showing electron exchange between donor and acceptor

The process can be regarded as a simultaneous exchange of electrons from the excited sensitizer to the lanthanide ion and vice versa.⁴¹ The rate of energy transfer for the Dexter mechanism varies as $e^{-\beta r}$ (where β is a constant). A sufficiently long-lived donor excited state is required for the energy transfer process to compete effectively with potential deactivation pathways.

1.5 Eu (III) and Tb (III) Luminescence Characteristics

Absorption of light can promote lanthanide (III) ions to any energetically accessible state, but rapid internal conversion to the lowest-lying J state of the first excited spectroscopic term ensures that emission occurs almost exclusively from this state. For Eu and Tb, these excited states are 5D_0 ($17,200\text{ cm}^{-1}$) and 5D_4 ($20,400\text{ cm}^{-1}$) respectively. By examining the partial energy diagram for these ions, it is understandable why emission from these states may occur to several of the various J states of the ground 7F manifold, resulting in a series of well defined, sharp, narrow bands. For Eu in particular, examination of the fine structure and intensity ratio of these bands (**Figure 1.5**) can provide valuable information regarding the coordination environment of the metal ion.

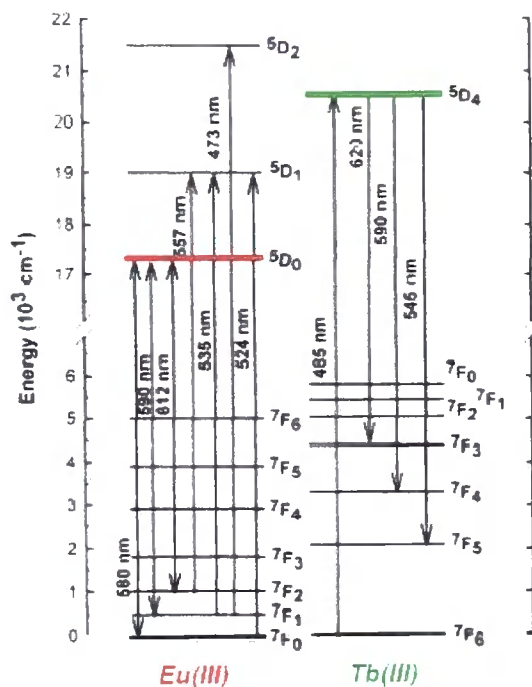


Figure 1.5: Partial energy diagrams of Eu(III) and Tb(III)

With Eu, the dominant emission bands arise at 590 nm ($^5D_0 \rightarrow ^7F_1$, $\Delta J = 1$) and 612 nm ($^5D_0 \rightarrow ^7F_2$, $\Delta J = 2$). The $\Delta J = 1$ transition is magnetic dipole allowed and its form is largely independent of the coordination sphere. The $\Delta J = 2$ manifold is made up of electronic dipole allowed transitions. Each is extremely sensitive to the symmetry of the coordination sphere.³⁷ In a centrosymmetric environment, the $\Delta J = 1$ dominates, whereas the intensity of the $\Delta J = 2$ transition is enhanced as the distortion of symmetry around the ion increases. Since the 7F_0 and 5D_0 states are non-degenerate, the number of $\Delta J = 0$ bands in the emission spectrum is related to the number of chemically distinct environments of the Eu^{3+} ion.

In the case of Tb^{3+} , the hypersensitive $^5D_4 \rightarrow ^7F_5$ ($\Delta J = 1$) emission band at 545 nm is the most intense transition, but it is not as sensitive to the environment as the $\Delta J = 2$ bands of Eu. The unique sensitivity of the europium emission spectral form has driven the development of ‘responsive’ lanthanide complexes, in which changes in the emission profile have been used to signal variations in the local environment, e.g. modulation of pH, $p\text{O}_2$, $p\text{X}$ and $p\text{M}$.³¹ Examples include the pH responsive Eu(III) complex **EuL**¹ which incorporates an azathioxanthone sensitizer and pendant pH sensitive alkylsulfonamide arm.⁴² This complex has been shown to be applicable for pH

determination *in cellulose*, over the pH range 6 to 8. Further examples of responsive lanthanide complexes are described in *section 1.6*.

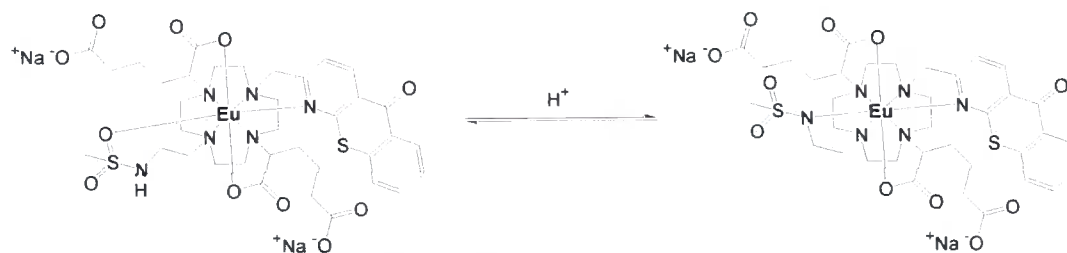


Figure 1.6: Reversible protonation of pH dependent EuL^{I}

1.6 Lanthanide Luminescence Deactivation Processes

The photochemical pathway that defines the kinetic profile of sensitised luminescence reveals that there are three excited states which can be perturbed: (i) the sensitiser singlet excited state; (ii) the sensitiser triplet excited state; (iii) the lanthanide emissive state.⁴³

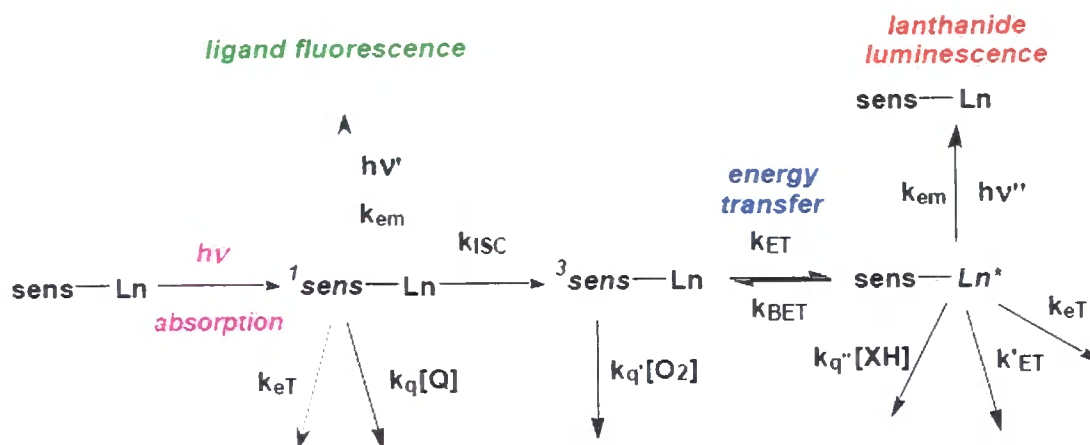


Figure 1.7: Deactivation pathways for sensitised lanthanide emission⁴³

Deactivation of the sensitiser singlet excited state

In addition to ligand fluorescence, electron or charge-transfer processes, which can be inter- or intramolecular in nature, can quench the singlet excited state of the sensitising chromophore. The most comprehensively studied examples are ‘collisional’ intermolecular interactions with halide ions,^{44,45} whilst examples of photoinduced electron intramolecular transfer from the excited S_1 of the chromophore to Ln(III) ion have also been published.⁴⁶ The latter is more common with Eu^{3+} complexes, owing to the ease of reduction of Eu(III) to Eu(II) .

Deactivation of the sensitiser triplet excited state

The energy of the aryl triplet state is arguably the most critical criterion in sensitised emission, as intramolecular energy transfer to the Ln(III) ion occurs from this state. For sensitisation of Tb(III) and Eu(III) luminescence, a singlet-triplet energy gap of less than 7000 cm^{-1} is desirable, with the S_1 state preferably lying less than about $29,000\text{ cm}^{-1}$ above the ground state.

If the aryl triplet state and the accepting excited lanthanide state energy gap becomes less than $1,500\text{ cm}^{-1}$ then the rate of thermally activated back energy transfer is greatly enhanced, leading to a re-population of the 'fragile' aryl state (i.e. deactivation of the lanthanide luminescent state).⁴⁷ However, if the energy gap is too great, then the efficiency of the energy transfer step is diminished. Consequently, a compromise must be established whereby the aryl triplet state should lie between $1,700$ and $3,000\text{ cm}^{-1}$ above the lanthanide emissive state.

A competing process to intramolecular energy transfer ($^3\text{sens}$ to Ln) is collisional quenching of the triplet state by molecular oxygen. For complexes where $k_q[\text{O}_2]$ is competitive with k_{ET} , lanthanide emission intensity and lifetime become sensitive to oxygen concentration. Although appearing problematic, research groups have utilised this process to their advantage, designing oxygen sensitive luminescent lanthanide complexes. One example is the singlet oxygen dosimeter **EuL²** (**Figure 1.8**),⁴⁸ in which reaction of the anthroyl moiety leads to suppression of intramolecular triplet energy transfer between the terpyridyl moiety and the anthracene, switching 'on' Eu emission. The system has limited applicability however, due to a distinct absence of chemical reversibility at ambient temperature.

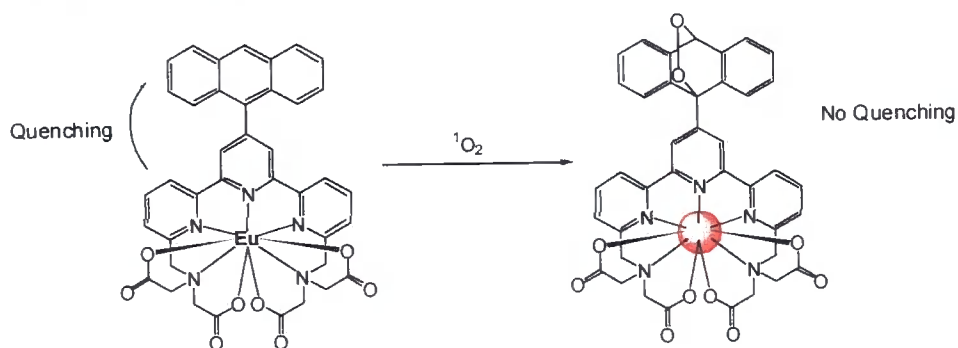


Figure 1.8: **EuL²**, singlet oxygen sensitive phosphorescence 'probe'⁴⁸

Deactivation of the lanthanide excited state

Lanthanide excited states may persist for several milliseconds, during which time they are prone to non-radiative quenching by one of three processes:

1.) Vibrational energy transfer involving high frequency oscillators

The 5D_0 and 5D_4 excited states of Eu^{3+} / Tb^{3+} are prone to deactivation by vibrational energy transfer involving energy-matched X – H oscillators (X = O, C or N). In an aqueous medium, quenching by O – H oscillators is of particular significance. As expected due to the intrinsic r^{-6} dependence of this energy transfer step, directly coordinated water molecules have a more substantial quenching effect than closely diffusing waters.⁴⁹ Quenching by energy matched oscillators arises due to weak vibronic coupling between the f-electronic states of the lanthanide ion and the vibrational states of an O – H group, where the energy gap between the emissive excited state and the highest level of the ground manifold must be bridged by these vibrational states. The energy gaps for Eu^{3+} and Tb^{3+} are approximately $12,000\text{ cm}^{-1}$ and $15,000\text{ cm}^{-1}$, equating to the third and fourth vibrational overtones respectively. It is this lower overtone that makes europium more sensitive towards vibrational quenching than terbium, as the Franck-Condon overlap term is less favourable.

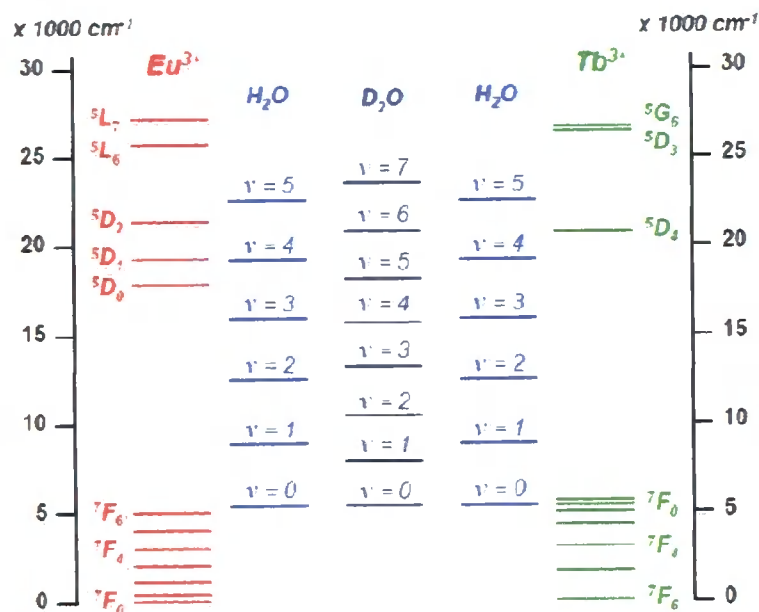


Figure 1.9: Energy level diagram for Eu, Tb, O – H and O – D oscillators

Vibrational quenching in D₂O is much less efficient than H₂O, as the O – D oscillator possesses a lower stretching frequency. Thus, energy matching is only feasible by occupation of higher vibrational states (4th and 5th overtones).⁵⁰ By measuring the difference in rate constants *k* for the depopulation of the lanthanide excited state in H₂O and D₂O respectively, it is possible to estimate a hydration state of a given complex.

Displacement of bound water molecules by inter- or intramolecular anion binding directly to the Ln³⁺ centre may lead to both emission intensity and lifetime increases, with the variation in the emission spectrum allowing ratiometric analyses. Numerous research groups have utilised this property, creating chemoselective sensors for citrate (**EuL³**), bicarbonate (**EuL⁴**) and phosphate anions.^{51,52,53}

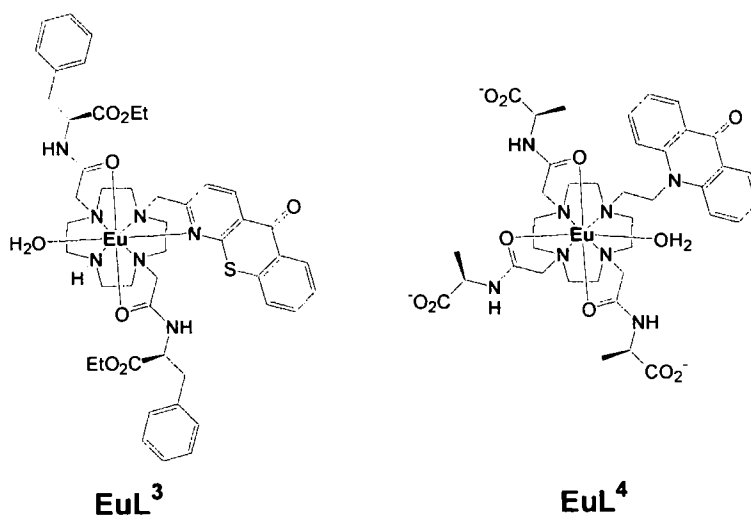


Figure 1.10: Chemoselective citrate (**EuL³**) and bicarbonate (**EuL⁴**) sensors

2.) Energy transfer to an acceptor of appropriate energy

Quenching of the lanthanide excited state by energy transfer may occur to an energy-matched acceptor, usually within a Förster radius of about 9 nm of the complex. This process is the principle behind fluorescence resonance energy transfer (FRET) and will be discussed in more detail in *section 1.12*.

3.) Electron transfer involving the metal-centred excited state

The Tb and Eu excited states lie at 244 and 206 kJ mol⁻¹ above their ground states. This free energy can be used to ‘drive’ various electron transfer processes, including collisional encounters with electron rich anionic species. Species such as halide anions

and the low molecular weight anti-oxidants urate and ascorbate are well known quenching species. Urate and ascorbate typically occur in between 0.1 and 2.0 mM levels in most cell types.^{43,54} Parker and co-workers have used this quenching pathway to their advantage. The dynamic quenching of a tetraazatriphenylene complex (**EuL⁵**, **Figure 1.11**) has been shown to provide a non-enzymatic luminescence assay for uric acid detection, in diluted urine samples. A systematic study of dynamic quenching of lanthanide complexes by selected reductants is discussed in Chapter 2.

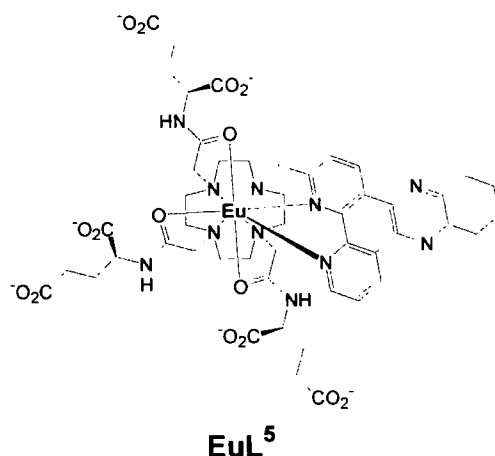


Figure 1.11: Uric acid sensor **EuL⁵**

1.7 Summary – Essential Requirements for a Sensitising Moiety

The choice of sensitizer in lanthanide complexes is determined primarily by the energy of the emissive excited state of the chosen lanthanide. The chromophore must possess an excited state from which there is efficient energy transfer to the lanthanide excited state. Ideally, this equates to a triplet energy of slightly greater than 22,000 cm⁻¹ for Tb (⁵D₄ = 20,400 cm⁻¹) and 19,000 cm⁻¹ for Eu (⁵D₀ = 17,200 cm⁻¹). Other essential criteria for the sensitising moiety can be summarised as follows:

- High extinction coefficient at an excitation wavelength for single photon excitation in the range of 340 – 420 nm. This is to avoid the need for quartz optics and prevent excitation of common biomolecules. Of particular interest are excitation wavelengths that correspond to readily available laser or LED lines (337, 355 or 405 nm).
- Fast rate of intersystem crossing to ensure the aromatic triplet state is populated efficiently, minimising ligand fluorescence.

- Fast energy transfer step, leading to efficient population of lanthanide excited state.
- A high reduction potential, minimising electron-transfer quenching involving electron rich species.

1.8 Luminescent Lanthanide Complexes

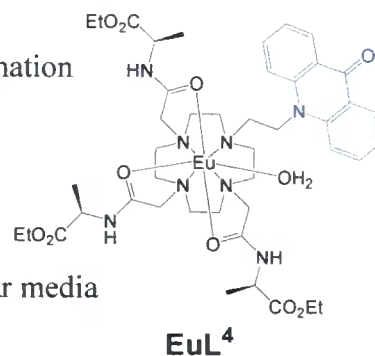
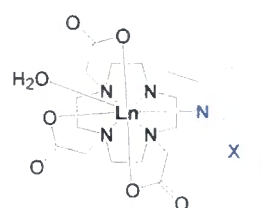
Like the sensitising antenna, the ligand surrounding the lanthanide ion plays a pivotal role in establishing emissive systems. The chromophore must be engineered into a ligand structure, thereby providing a kinetically and thermodynamically stable seven to nine coordinate complex.⁵⁵ The high charge density and low polarisability of Ln^{3+} ions means they exhibit ‘hard acid’ like behaviour. Consequently, lanthanide ions are best accommodated by ligands offering nitrogen or oxygen donors, typically coordinating via ionic interactions.

Complexes derived from a 1,4,7,10-tetraazacyclododecane (cyclen) macrocycle often provide well-defined and highly stable complexes. An advantageous property of cyclen is the ease with which a diverse range of pendant arms can be introduced. Carboxylate, phosphinate and amide groups have all been used to synthesise stable, water soluble lanthanide complexes. Manipulation of these pendant arms allows control over the charge of the complex, while can minimise quenching of the lanthanide excited state by water molecules. The latter is most notably achieved by providing sterically bulky complexes with adequate donor atoms in order to complement the lanthanide’s coordination number, preventing any directly bound water molecules.

In addition to cyclen derivatives, other systems such as cryptates,^{56,57} calixarenes, podands, helicate and bipyridyl-functionalised macrocycles have been employed as chelating agents for lanthanide complexes.⁵⁸ The following examples highlight the diverse range of aromatic chromophores / chelating ligands which have been implemented successfully for sensitised lanthanide emission.

Acridones^{59,60}

- Allow efficient Eu^{3+} sensitisation, without direct coordination
- Excitation at wavelengths > 400 nm
- Two inner sphere bound water molecules
- $\Phi(\text{H}_2\text{O}) = 0.05$,
- Low Φ associated with large ligand fluorescence in polar media

**Azaxanthonones / Azathioxanthonones**⁶¹

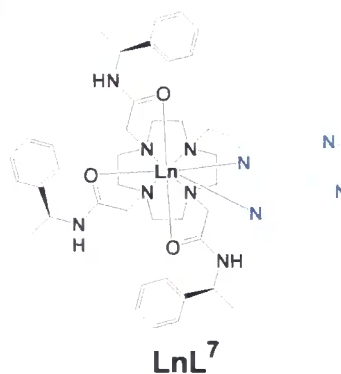
X = O Azaxanthonone
S Thioazaxanthonone

LnL⁶

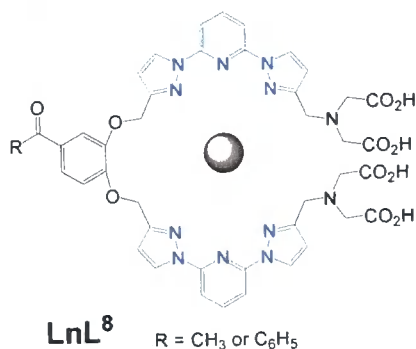
- Allow sensitisation of Eu^{3+} and Tb^{3+} in aqueous media
- Excitation at 336 nm (azaxanthonone) and 380 nm (azathioxanthonone) respectively
- One inner sphere bound water molecule
- $\Phi_{\text{Eu}}(\text{H}_2\text{O}) = 0.07$, $\tau = 0.57$ ms;
 $\Phi_{\text{Tb}}(\text{H}_2\text{O}) = 0.14$, $\tau = 1.82$ ms
- A range of substituents can be incorporated in the benzenoid ring
- Thioxanthonones exhibit modest ligand fluorescence

Tetraazatriphenylene⁴³

- $T_1 = 24,000 \text{ cm}^{-1}$ enabling Eu^{3+} and Tb^{3+} sensitisation
- Excitation at 348 nm
- Serves as a bidentate ligand (no bound H_2O)
- Possesses a fast rate of inter-system crossing.
- High quantum yields in water;
 $\Phi_{\text{Eu}}(\text{H}_2\text{O}) = 0.16$, $\tau = 0.99$ ms;
 $\Phi_{\text{Tb}}(\text{H}_2\text{O}) = 0.40$, $\tau = 1.46$ ms

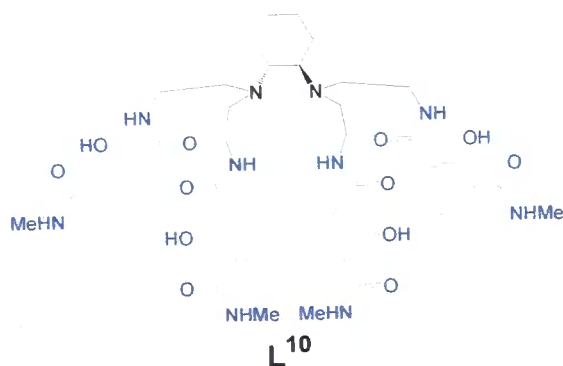


Pyrazolopyridines ^{62,63,64,65,66}



- Both ligands allow Eu³⁺ / Tb³⁺ sensitisation (**LnL⁸** T₁ = 24,500 cm⁻¹, **LnL⁹** T₁ = 26,000 cm⁻¹)
- Ligand **L⁸** has a high extinction coefficient 26,600 cm⁻¹, but a low excitation wavelength 306 – 310 nm.
- These complexes are water soluble and coordinate to the Ln ion via the iminodiacetate groups. This results in a long Ln – chromophore distance and subsequent poor energy transfer.
- Ligand **L⁹** has a low excitation wavelength (294 nm).
- Despite one bound water molecule, an efficient ligand to lanthanide energy-transfer process is observed. This results in a high quantum yield for Tb sensitisation.
Φ_{Tb} (H₂O) = 0.49, τ = 1.85 ms

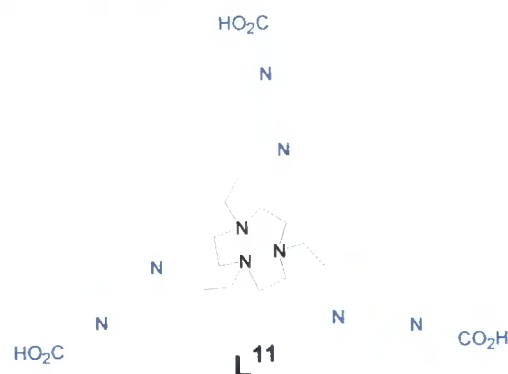
2-Hydroxyisophthalamide (IAM) ^{67,68}



- Enantiopure, octadentate ligand **L¹⁰** incorporates repeating 2-hydroxyisophthalamide units to chelate a Tb ion.
- Excitation at 340 nm (ε = 28,200 M⁻¹ cm⁻¹)

- The absence of water ($q = -0.04$) in the immediate proximity of the Tb(III) ion results in long luminescence lifetime ($\tau_{1120} = 2.28$ ms).
- Forms very emissive Tb system in aqueous media, $\Phi_{\text{Tb}}(\text{H}_2\text{O}) = 0.57$.

Substituted Bipyridyls / Terpyridyls ⁶⁹



Numerous bipyridyl systems have been used in lanthanide sensitisation, including complexes **EuL**¹⁷ and **LnL**¹⁸ which will be discussed in *section 1.12*.

Research in the design of new sensitising moieties is a continually evolving field, with recent publications citing emissive systems incorporating thiophene-derivatised Pybox⁷⁰, quinoxaline⁷¹ and 2-hydroxyisophthalate⁷² chromophores. Although reporting large quantum yield measurements, these systems are rather limited in application, as emission is only observed in organic solvents (e.g. acetonitrile).

In contrast to the intramolecular sensitiser complexes shown above, short peptides have been studied to promote intermolecular lanthanide sensitisation. One example is the synthesis and design of a cyclin fluorescent sensor using Tb³⁺ DOTA.⁷³ The macrocycle is covalently bound to a short cyclin binding protein. This protein has an appropriately positioned Trp amino acid residue that can sensitise the lanthanide ion (at 280 nm) when in close proximity. Imperiali *et al.* have also used this principle to devise new Eu³⁺ and Tb³⁺ sensitising binding tags.⁷⁴ By replacing tryptophan with unnatural amino acids, it has been shown that Eu sensitisation can be achieved with excitation at 337 nm or 390 nm. This method of sensitisation is extremely fragile, with a detailed understanding of protein modelling and structure required. For efficient systems, the Ln ion and amino acid residue must be in close proximity to ensure efficient energy transfer.

1.9 Aim and Objectives

As shown previously, numerous organic chromophores have been utilised as sensitiser for lanthanide emission. Very few of those reported possess a $S_1 - T_1$ energy gap in protic media that is sufficiently small to allow excitation in the range 338 to 410 nm, without depopulation of the sensitiser triplet excited state. This could involve either back energy transfer or competitive quenching by triplet oxygen. Furthermore, the high excited state energies of Eu and Tb reduces the number of compatible candidates.

The objective of this thesis is to devise practicable routes to new highly emissive complexes of Eu and Tb that possess the following characteristics:

- a) can be excited in the range 337 (nitrogen laser) to 420 nm;
- b) possess an overall emission quantum yield in biological media in excess of 10 %;
- c) resist quenching of the intermediate sensitiser and lanthanide excited states;
- d) can be conjugated to appropriate vectors and bio-molecules, as required for their application in a variety of time-resolved luminescence assays, or for their direct application as probes *in cellulo*.

1.10 Engineering Lanthanide Complexes for Biological Applications

Emissive lanthanide complexes that are to be used either as 'responsive' systems or as luminescent 'tags' in bio-conjugates must function in aqueous media. This function must be maintained in the presence of significant concentrations of competing endogenous ligands or buffers (e.g. proteins, phosphorylated anions, citrate, ascorbate, urate and glutathione).²² Complexes are therefore required to be water soluble, non-toxic and have both high kinetic and thermodynamic stabilities with respect to lanthanide ion dissociation, preferably over the pH range 4.5 – 8. The complex should also be stable with respect to photofading and oxidative degradation in air or aqueous solution. Complexes must possess an excitation wavelength in excess of 337 nm, with a high overall emission quantum yield (> 10 % in aqueous medium) and large extinction coefficient at the excitation wavelength.

1.11 Using Lanthanide Complexes for Imaging 'in cellulo'

For a complex to be employed as a cellular probe it must exhibit cell permeability by either passive diffusion or an active transport mechanism. In addition to this, a distinct compartmentalisation profile (i.e. preference to localise in a given organelle) is desirable. The complex must convey information about its local environment (e.g. as a function of a given intracellular analyte) by either changes in its spectral emission profile or lifetime, while resisting competitive quenching from endogenous ions or biomolecules.

Recently, lanthanide complexes have been reported that are taken up by live cells and can be observed by fluorescence microscopy. Examples include complexes **EuL**¹² and **TbL**¹³, which have specific targeting vectors located on a pendant arm of the cyclen macrocycle. In the case of **EuL**¹², the *o*-chlorophenylquinoline moiety reportedly targets benzodiazepine receptors that are over expressed in glioblastoma cells.⁷⁵ Cellular uptake experiments suggest this complex localises in the outer mitochondrial membrane, following an endocytosis uptake mechanism. Excitation of the lanthanide is achieved at 320 nm via an attached quinoxaline group. For **TbL**¹³, the tetrapeptide tuftsin is known to be responsible for activation of macrophage cell lines and is internalised by macrophages.⁷⁶ Luminescence spectra of macrophages incubated with **TbL**¹³ suggest the complex is internalised / bound within macrophage cells, but have not been confirmed by any cell localisation studies. The absence of a sensitising moiety in the complex could present poor sensitivity in vivo, with the complex liable to quenching. At present luminescence is only observed by direct excitation at 366 nm (corresponding to the $^7F_6 \rightarrow ^5G_6$ transition).

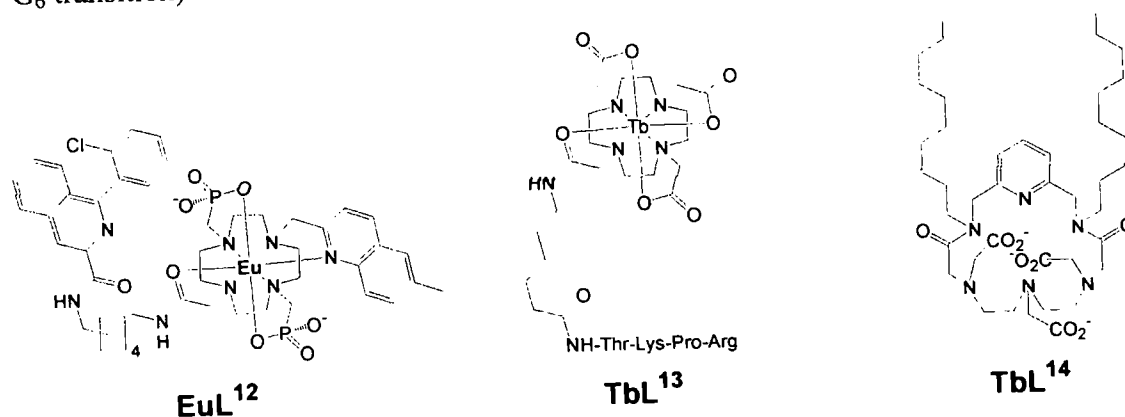


Figure 1.12: Examples of lanthanide complexes used in cellular imaging

Diffusion enhanced fluorescence resonance energy transfer (DEFRET) studies of complex **TbL**¹⁴ were used to determine its cellular localisation.⁷⁷ It has been suggested that this complex labels cells by inserting the two hydrophobic alkyl chains into the cell membrane, with the remainder of the complex in the extracellular medium. Complexes **EuL**¹², **TbL**¹³ and **TbL**¹⁴ demonstrate the use of structural manipulation to provide certain criteria essential for their respective cellular applications.

Azaxanthone and thiazaxanthone containing complexes have also shown interesting cellular behaviour. The two heptadentate macrocyclic complexes, **EuL**¹⁵ and **EuL**³ are just two complexes that include these chromophores, which warrant further investigation.

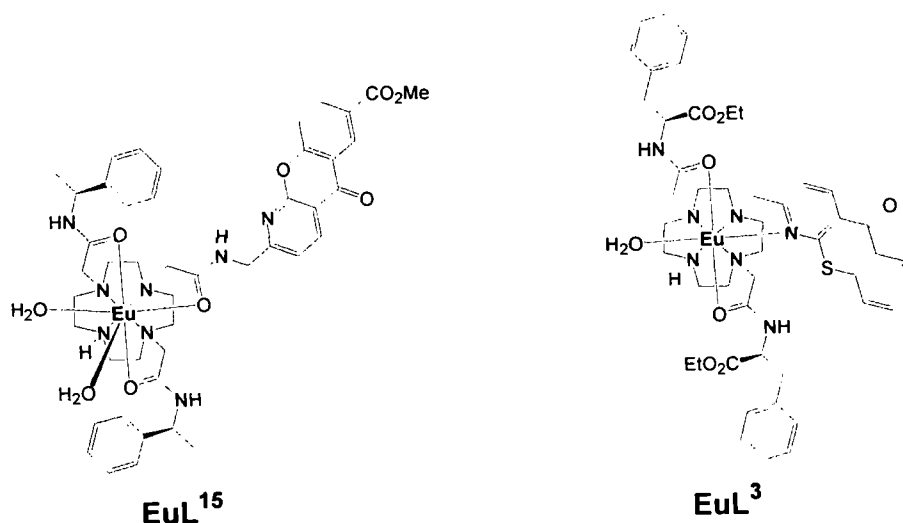


Figure 1.13: Azaxanthone complex **EuL**¹⁵ and thiazaxanthone complex **EuL**³

The localisation of these complexes has been examined by fluorescence microscopy in a range of cell lines.^{78,79} Within 5 minutes of incubation at 50 μ M, complex **EuL**¹⁵ was found to localise in cell mitochondria. This hypothesis was confirmed by co-staining with commercially available Mitotracker GreenTM. After longer incubation periods (> 4 h), **EuL**¹⁵ appears to migrate from the mitochondria to late endosomes/lysosomes (**Figure 1.14**).⁷⁸ This process has been attributed to the complex's ability to bind reversibly with a given carrier protein. This behaviour highlights the need for complexes to resist fast intracellular trafficking, and persist long enough in their desired locations to convey information about their surrounding environment.

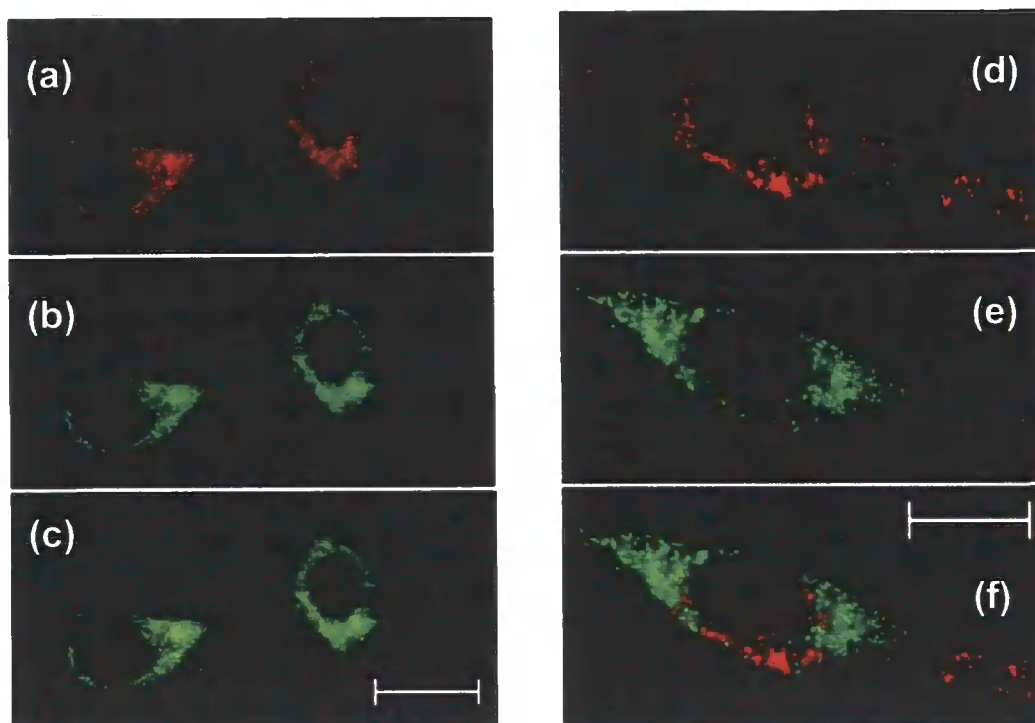


Figure 1.14: Microscopy images for **EuL¹⁵**, showing a mitochondrial localisation profile and subsequent migration of the complex to the perinuclear endosomes/lysosomes.⁷⁸

(a) *Eu complex (50 μ M complex, 4 h incubation)*

(b) *Mitotracker GreenTM*

(c) *Merged image of (a) and (b)*

(d) *Eu complex (50 μ M complex, 24 h incubation time)*

(e) *Mitotracker GreenTM*

(f) *Merged image of (d) and (e) consistent with migration of the complex from the mitochondria to the perinuclear endosomes/lysosomes*

Protein association may also explain the affinity of complex **EuL³** to cross the nuclear membrane and stain the nucleoli of mouse skin fibroblast, Chinese hamster ovarian and HeLa cells. At a 100 μ M concentration, **EuL³**, has been shown to co-localise with SYTO RNA-select,⁷⁹ a fluorescent stain that highlights the position of RNA (free or protein bound).

Despite promising results, the design of single-component luminescent species for a specific cellular compartment remains extremely difficult to predict from structure alone.

This is exemplified by the constitutional isomeric complexes **EuL⁴** and **EuL¹⁶**. Originally developed as HCO₃⁻ anion sensors, these two complexes have been shown to exhibit differing behaviour in mouse skin fibroblast (NIH 3T3) cells.^{52,60}

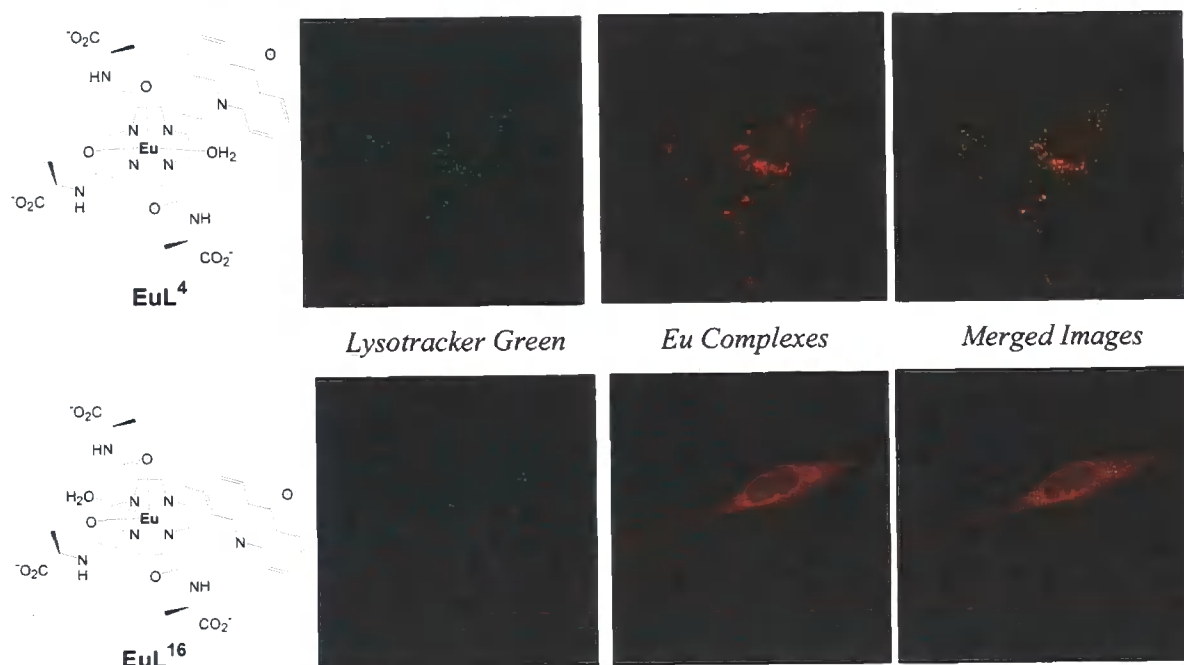


Figure 1.15: Fluorescence microscopic images of complexes **EuL⁴** and **EuL¹⁶**

As shown in **Figure 1.15**, isomer **EuL⁴** distributes well in the cytosol, with fluorescence microscopy and co-staining with Brefeldin A suggesting localisation in the endoplasmic reticulum. In contrast, complex **EuL¹⁶** shows a tendency for compartmentalisation in acidic lysosomal environments.²² This work is part of an extensive study (> 60 complexes) within the Parker research group, seeking to rationalise the cellular behaviour of luminescent Ln complexes (e.g. uptake / compartmentalisation). Preliminary results indicate it is the nature and linkage of the sensitising moiety that defines the extent of the complex's protein interaction. It is believed that this interaction is fundamental in defining the cellular uptake/egress rates and the compartmentalisation profile. The mechanisms of cellular uptake and cellular localisation behaviour will be discussed in Chapter 5.

1.12 Using Lanthanide Complexes as Bioconjugate 'tags'

If luminescent lanthanide complexes are to serve as emissive 'tags', they must possess a suitable reactive functional group to expedite conjugation e.g. pendant acid or primary amine group. The following section highlights some recent literature publications of bioconjugate lanthanide complexes and their respective applications.

HTRF[®] / FRET

Cisbio International, sponsors and collaborators for the duration of this thesis, have developed a technique known as homogeneous time-resolved fluorescence, HTRF[®].⁸⁰ This technique relies on fluorescence resonance energy transfer (FRET) principles, with the time-resolved measurement of fluorescence. FRET is based on the transfer of energy between two fluorophores, a donor and an acceptor, in a process which is distance dependent (r^{-6}).⁸¹ For FRET to occur, the donor and acceptor must have certain compatible criteria. These include:

- non-overlapping emission spectra in order to measure each component's fluorescence individually
- the FRET quantum yield must be as high as possible
- fluorescence emission must occur within a region of the spectrum remote from that naturally produced by proteins

HTRF[®] allows molecular interactions between biomolecules to be assessed by coupling each respective component with a fluorescent label and detecting the level of energy transfer. To date, numerous assays have been devised, among them those which measure protein – protein interactions and kinase / protease enzyme activity. Leading on from the revolutionary work by Prof. J. M. Lehn, Cisbio International have developed long-lived luminescent donors such as Europium cryptate **EuL**¹⁷ and Lumi4-TbTM (a Tb³⁺ cryptate).

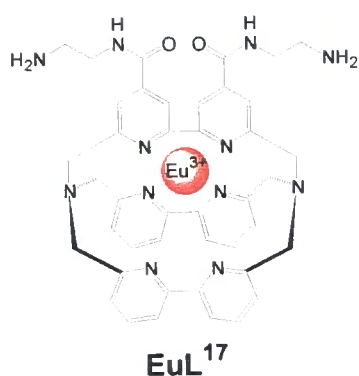


Figure 1.16: *EuL¹⁷ developed by Cisbio international*

These cage structures confer long-lived fluorescence, high emissive quantum yields (λ_{ex} 337 nm) and stability towards photobleaching and ion dissociation. Commercial acceptors used in HTRF[®] include XL665, a 105 kDa cross-linked allophycocyanin protein. It presents a set of photophysical properties matching the TBP Eu^{3+} cryptate **EuL¹⁷**: a high molar absorptivity at the cryptate emission wavelength which allows a high transfer efficiency ($R_0 \sim 9.5$ nm); emission in a spectral range where the cryptate signal is insignificant, high quantum yield ($\sim 70\%$) not quenched in biological fluids.⁸⁰

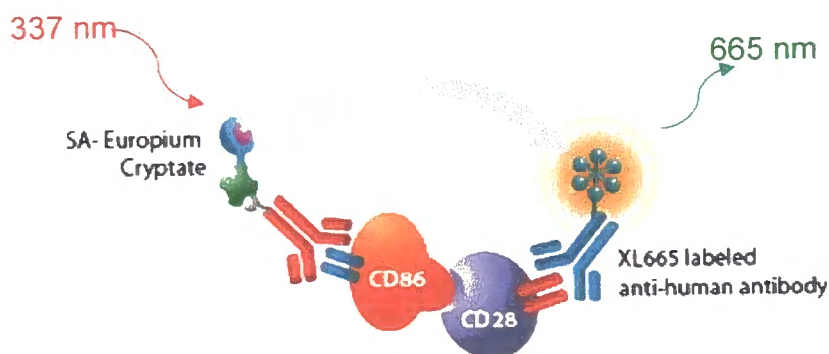


Figure 1.17: *Illustration of fluorescence resonance energy transfer (FRET)*

Following excitation, HTRF[®] emissions are measured at two different wavelengths, 620 nm (donor) and 665 nm (acceptor). This allows ratiometric analysis, with emission at 620 nm used as an internal reference, while emission at 665 nm is used to assess the biological reaction.

Bioconjugate Complexes

Complex LnL^{18} (Figure 1.17) has been cited in the literature to be employed in protein labelling and time-resolved luminescence imaging.⁸² The complex consists of a glutamic acid framework, bis-functionalised with bipyridyl carboxylic acid sensitising moieties. These moieties have a triplet excited state of $22,100 \text{ cm}^{-1}$, enabling both europium and terbium sensitisation. The respective Eu and Tb complexes possess quantum yields of $\Phi_{\text{Eu}} = 0.08$, $\Phi_{\text{Tb}} = 0.31$ in aqueous solution. The extinction coefficient of the bipyridyl system lies in the range of $19,000$ to $21,000 \text{ M}^{-1} \text{ cm}^{-1}$. A terminal carboxylate function in the complex has been shown to be activated into the corresponding *N*-hydroxysuccinimidyl ester using EDC.HCl and *N*-hydroxysuccinimide in DMSO. It is this activated form that has been covalently linked to amino functions (e.g. on BSA) and implemented in time-resolved luminescence imaging.

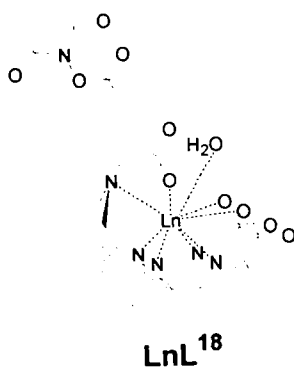


Figure 1.17: *N*-Hydroxysuccinimidyl ester complex LnL^{18}

Despite positive preliminary results, analogous systems have proved unstable when anionic species such as phosphates are present. For this reason, improvements may orientate around changing the chemical structure to provide an additional donor atom. This modification may help exclude the present bound water molecule and therefore increase the emissive quantum yields and lifetimes.

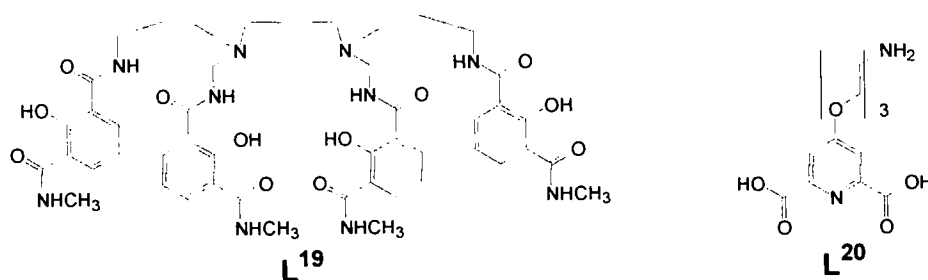


Figure 1.18: Ligands L¹⁹ and L²⁰

Ligands L¹⁹ and L²⁰ (Figure 1.18) constitute two other systems cited as being applicable as bioconjugate complexes.^{67,83,84} The octadentate ligand L¹⁹, incorporates repeating 2-hydroxyisophthalamide chelating units to coordinate to a lanthanide ion (Ln = Eu, Tb, Sm, Dy). The respective Tb complex possesses a λ_{exc} 350 nm with an extinction coefficient of 26,800 M⁻¹ cm⁻¹. These attributes, in addition to an efficient ligand to lanthanide energy transfer process are responsible for a quantum yield of 0.59 in aqueous solution. This value is 30 times larger than the commercially used FRET component EuL¹⁷. Unlike the latter, this system does not require external fluoride ions to prohibit direct water coordination. However, no emission lifetimes or pH / anion sensitivity experiments are evident in the literature, providing no indication as to how these systems might behave in biological media. It can be assumed that the coordinated water molecule will deactivate the lanthanide excited state, providing an area of possible structural improvement.

The dipicolinic acid derivative L²⁰ has been identified as a possible assay component. The incorporation of a terminal amine group situated at the end of a polyoxyethylene linker enables potential vector conjugation. Despite proving efficient sensitizers of Eu³⁺ in aqueous media ($\Phi_{Eu} = 0.29$), these complexes have numerous limitations. A low excitation wavelength of 279 nm is not optimal for biological applications, while the complexes show inconsistent stoichiometries and are often racemic. If complexes are to be used in biological situations, it is essential to have a detailed understanding of their confirmation and chirality. This is due to the fact that racemic complexes may interact with endogenous chiral species with differing affinities, making subsequent changes in behaviour difficult to distinguish.

Although ligands L^{19} and L^{20} have been described as potential candidates for bioanalytical applications, neither has been covalently conjugated or used in biological media. This is extremely important to identify if the respective complexes retain their structural and photophysical attributes that are observed in aqueous media.

References

- 1.) J. A. Prescher and C. R. Bertozzi, *Nat. Chem. Biol.*, 2005, **1**, 13.
- 2.) N. Johnsson and K. Johnsson, *ACS Chem. Biol.*, 2007, **2**, 31.
- 3.) A. Keppler, S. Gendreizig, T. Gronemeyer, H. Pick, H. Vogel and K. Johnsson, *Nat. Biotechnol.*, 2003, **21**, 86.
- 4.) J. Zhang, R. E. Campbell, A. Y. Ting and R. Y. Tsien, *Nat. Rev. Mol. Cell Bio.*, 2002, **3**, 907.
- 5.) N. Weibel, L. J. Charbonniere, M. Guardigli, A. Roda and R. Ziessel, *J. Am. Chem. Soc.*, 2004, **126**, 4888.
- 6.) M. Wartenberg, J. Hescheler, H. Acker, H. Diedershagen and H. Sauer, *Cytometry*, 1998, **31**, 127.
- 7.) C. Bour-Dill, M-P. Gramain, J-L. Merlin, S. Marchal and F. Guillemain, *Cytometry*, 2000, **39**, 16.
- 8.) N. J. Emptage, *Curr. Opin. Pharmacol.*, 2001, **1**, 521.
- 9.) R. W. Dirks and H. J. Tanke, *Chem. Biol.*, 2006, **13**, 559.
- 10.) D. C. Praser, V. K. Eckenrode, W. W. Ward, F. G. Prendergast and M. J. Cormier, *Gene*, 1992, **111**, 229.
- 11.) R. Y. Tsien, *Annu. Rev. Biochem.*, 1998, **67**, 509.
- 12.) B. N. G. Giepmans, S. R. Adams, M. H. Ellisman and R. Y. Tsein, *Science*, 2006, **312**, 217.
- 13.) J. S. Anderson, Y. W. Lam, A. K. L. Leung, S-E. Ong, C. E. Lyon, A. I. Lamond and M. Mann, *Nature.*, 2005, **433**, 77.
- 14.) N. C. Shaner, R. E. Campbell, P. A. Steinbach, B. N. G. Giepmans, A. E. Palmer and R. Y. Tsien, *Nat. Biotechnol.*, 2004, **22**, 1567.
- 15.) V. V. Verkhusha and K. A. Lukyanov, *Nat. Biotechnol.*, 2004, **22**, 289.
- 16.) J. Lippincott-Schwartz and G. H. Patterson, *Science.*, 2003, **300**, 87.
- 17.) N. C. Shaner, P. A. Steinbach and R. Y. Tsien, *Nat. Methods.*, 2005, **2**, 905.
- 18.) www.probes.com and www.invitrogen.com.
- 19.) Y. Urano, K. Kamiya, K. Kanda, T. Ueno, K. Hirose and T. Nagano, *J. Am. Chem. Soc.*, 2005, **127**, 4888.

-
- 20.) T. Yogo, Y. Urano, Y. Ishitsuka, F. Maniwa and T. Nagano, *J. Am. Chem. Soc.*, 2005, **127**, 12162.
- 21.) N. Panchuk-Voloshina, R. P. Haugland, J. Bishop-Stewart, M. K. Bhalgat, P. J. Millard, F. Mao, W-Y. Leung and R. P. Haugland, *J. Histochem. Cytochem.*, 1999, **47**, 1179.
- 22.) S. Pandya, J. Yu and D. Parker, *Dalton Trans.*, 2006, 2757.
- 23.) X. Y. Wu, H. J. Liu, J. Q. Liu, K. N. Haley, J. A. Treadway, J. P. Larson, N. F. Ge, F. Peale and M. P. Bruchez, *Nat. Biotechnol.*, 2003, **21**, 41.
- 24.) A. P. Alivisatos, W. W. Gu and C. Larabell, *Annu. Rev. Biomed. Eng.*, 2005, **7**, 55.
- 25.) N. Kaji, M. Tokeshi and Y. Baba, *Anal. Sci.*, 2007, **23**, 21.
- 26.) J. F. Weng and J. C. Ren, *Curr. Med. Chem.*, 2006, **13**, 897.
- 27.) X. Gao, L. Yang, J. A. Petros, F. F. Marshall, J. W. Simons and S. Nie, *Curr. Opin. Biotech.*, 2005, **16**, 63.
- 28.) S. Faulkner, S. J. A. Pope and B. P. Burton-Pye, *Appl. Spectrosc. Rev.*, 2005, **40**, 1.
- 29.) T. Gunnlaugsson and J. P. Leonard, *Chem. Commun.*, 2005, 3114.
- 30.) D. Parker, *Chem. Soc. Rev.*, 2004, **33**, 156.
- 31.) R. Poole, C. P. Montgomery, E. J. New, A. Congreve, D. Parker and M. Botta, *Org. Biomol. Chem.*, 2007, **5**, 2055.
- 32.) G. Mathis, *Clin. Chem.*, 1995, **41**, 1391.
- 33.) W. T. Carnall in 'Handbook on the Physics and Chemistry of Rare Earths', vol 25, Elsevier, 1998.
- 34.) J. H. Van Vleck, *J. Chem. Phys.*, 1942, **41**, 67.
- 35.) D. Parker and J. A. G. Williams in 'Responsive Luminescent Lanthanide Complexes', ed. A. Sigel and H. Sigel, New York, 2003.
- 36.) J-C. G. Bünzli and C. Piguet, *Chem. Soc. Rev.*, 2005, **34**, 1048.
- 37.) D. Parker and J. A. G. Williams, *J. Chem. Soc. Dalton Trans.*, 1996, 3613.
- 38.) A. Døssing, *Eur. J. Inorg. Chem.*, 2005, 1425.
- 39.) T. Förster, *Discuss. Faraday Soc.*, 1959, **27**, 7.
- 40.) D. L. Dexter, *J. Chem. Phys.*, 1953, **21**, 836.

-
- 41.) A. Beeby, S. Faulkner, D. Parker and J. A. G. Williams, *J. Chem. Soc. Perkin Trans 2.*, 2001, 1268.
- 42.) R. Pal and D. Parker, *Org. Biomol. Chem.*, 2008, **6**, 1020.
- 43.) R. A. Poole, G. Bobba, M. J. Cann, J-C. Frias, D. Parker and R. D. Peacock, *Org. Biomol. Chem.*, 2005, **3**, 1013.
- 44.) D. Parker, P. K. Senanayake and J. A. G. Williams, *J. Chem. Soc., Perkin Trans. 2.*, 1998, 2129.
- 45.) D. Parker and J. A. G. Williams, *Chem. Commun.*, 1998, 245.
- 46.) D. Parker, *Coord. Chem. Rev.*, 2000, **205**, 109.
- 47.) A. Beeby, D. Parker and J. A. G. Williams, *J. Chem. Soc. Perkin Trans 2.*, 1996, **8**, 1565.
- 48.) B. Song, G. Wang and J. Yuan, *Chem. Commun.*, 2005, 3553.
- 49.) A. Beeby, I. M. Clarkson, R. S. Dickins, S. Faulkner, D. Parker, L. Royle, A. S. de Sousa, J. A. G. Williams and M. Woods, *J. Chem. Soc. Perkin Trans 2.*, 1999, 493.
- 50.) Y. Haas and G. Stein, *J. Phys. Chem.*, 1971, **75**, 3668.
- 51.) D. Parker and J. Yu, *Chem. Commun.*, 2005, 3141.
- 52.) Y. Bretonniere, M. J. Cann, D. Parker, and R. Slater, *Org. Biomol. Chem.*, 2004, **2**, 1624.
- 53.) P. Atkinson, Y. Bretonniere, D. Parker and G. Muller, *Helvetica. Chim. Acta*, 2005, **88**, 391.
- 54.) R. A. Poole, F. Kielar, S. L. Richardson, P. A. Stenson and D. Parker, *Chem. Commun.*, 2006, 4084.
- 55.) S. Lis, M. Elbanowski, B. Makowska and Z. Hnatejko, *J. Photoch. Photobio. A.*, 2002, **150**, 233.
- 56.) G. Mathis, *Clin. Chem.*, 1993, **39**, 1953.
- 57.) G. Mathis, *Clin. Chem.*, 1995, **41**, 1391.
- 58.) S. Quici, G. Marzanni, M. Cavazzini, P. L. Anelli, M. Botta, E. Gianolio, G. Accorsi, N. Armaroli and F. Barigelletti, *Inorg. Chem.*, 2002, **41**, 2777.
- 59.) A. Dabadhoy, S. Faulkner and P. G. Sammes, *J. Chem. Soc., Perkin Trans. 2.*, 2000, 2359.

-
- 60.) Y. Bretonniere, M. J. Cann, D. Parker and R. Slater, *Chem. Commun.*, 2002, 1930.
- 61.) P. Atkinson, K. S. Findlay, F. Kielar, R. Pal, D. Parker, R. A. Poole, H. Puschmann, S. L. Richardson, P. A. Stenson, A. L. Thompson and J. Yu, *Org. Biomol. Chem.*, 2006, **4**, 1707.
- 62.) M. J. Remuinan, H. Roman, M. T. Alonso and J. C. Rodriguez-Ubis, *J. Chem. Soc. Perkin. Trans. 2.*, 1993, 1099.
- 63.) E. Brunet, O. Juanes, R. Sedano and J. C. Rodriguez-Ubis, *Org. Lett.*, 2002, **4**, 213.
- 64.) E. Brunet, O. Juanes, R. Sedano and J. C. Rodriguez-Ubis, *Tetrahedron.*, 2005, **61**, 6757.
- 65.) E. Brunet, O. Juanes, R. Sedano and J. C. Rodriguez-Ubis, *Tetrahedron Lett.*, 2007, **48**, 1091.
- 66.) I. Nasso, S. Bedel, C. Galaup and C. Picard, *Eur. J. Inorg. Chem.*, 2008, 2064.
- 67.) M. Seitz, E. G. Moore, A. J. Ingram, G. Muller and K. N. Raymond, *J. Am. Chem. Soc.*, 2007, **129**, 15468.
- 68.) S. Petoud, G. Muller, E. G. Moore, J. Xu, J. Sokolnicki, J. P. Riehl, U. N. Le, S. M. Cohen and K. N. Raymond, *J. Am. Chem. Soc.*, 2007, **129**, 77.
- 69.) R. Ziessel and L. J. Charbonniere, *J. Alloy. Compd.*, 2004, **373**, 283.
- 70.) A. Bettencourt-Dias, S. Viswanathan and A. Rollett, *J. Am. Chem. Soc.*, 2007, **129**, 15436.
- 71.) M. Andrews, R. H. Laye, L. P. Harding and S. J. A. Pope, *Polyhedron.*, 2008, **27**, 2365.
- 72.) L. Benisvy, P. Gamez, W. T. Fu, H. Kooijman, A. L. Spek, A. Meijerink and J. Reedijk, *Dalton. Trans.*, 2008, 3147.
- 73.) E. Pazos, D. Torrecilla, M. V. Lopez, L. Castedo, J. L. Mascarenas, A. Vidal and M. E. Vazquez, *J. Am. Chem. Soc.*, 2008, **130**, 9652.
- 74.) A. M. Reynolds, B. R. Sculimbrene and B. Imperiali, *Bioconjugate Chem.*, 2008, **19**, 588.
- 75.) H. C. Manning, T. Goebel, R. C. Thompson, R. R. Price, H. Lee and D. J. Bornhop, *Bioconjugate Chem.*, 2004, **15**, 1488.

-
- 76.) R. J. Aarons, J. K. Notta, M. M. Meloni, J. Feng, R. Vidyasagar, J. Narvainen, S. Allan, N. Spencer, R. A. Kauppinen, J. S. Snaith and S. Faulkner, *Chem. Commun.*, 2006, 909.
- 77.) Q. Zheng, H. Dai, M. E. Merritt, C. Malloy, C. Y. Pan and W-H. Li, *J. Am. Chem. Soc.*, 2005, **127**, 16178.
- 78.) B. S. Murray, E. J. New, R. Pal and D. Parker, *Org. Biomol. Chem.*, 2008, **6**, 2085.
- 79.) J. Yu, D. Parker, R. Pal, R. A. Poole and M. J. Cann, *J. Am. Chem. Soc.*, 2006, **128**, 2294.
- 80.) H. Bazin, M. Preaudat, E. Trinquet and G. Mathis, *Spectrochim. Acta. A.*, 2001, **57**, 2197.
- 81.) S. Ghose, E. Trinquet, M. Laget, H. Bazin and G. Mathis, *J. Alloy. Compd.*, 2008, **451**, 35.
- 82.) N. Weibel, L. J. Charbonniere, M. Guardigli, A. Roda and R. Ziessel, *J. Am. Chem. Soc.*, 2004, **126**, 4888.
- 83.) S. Petoud, S. M. Cohen, J-C. G. Bunzli and K. N. Raymond, *J. Am. Chem. Soc.*, 2003, **125**, 13324.
- 84.) A-L. Gassner, C. Duhot, J-C. G. Bunzli and A-S. Chauvin, *Inorg. Chem.*, 2008, **47**, 7802.

CHAPTER TWO:

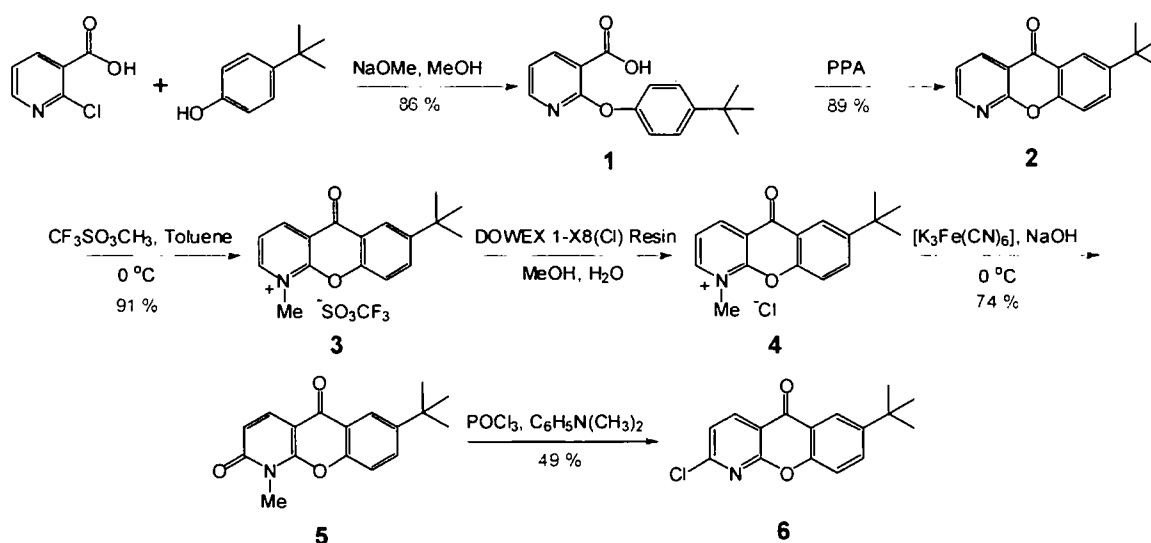
Synthesis & Photophysical Characterisation

Chapter Two: Synthesis and Photophysical Characterisation

As discussed in the previous chapter, ligands containing substituted 1-azaxanthone and azathioxanthenes have been demonstrated to be efficient sensitisers of Eu^{3+} and Tb^{3+} in aqueous media. It was envisaged that by modifying the azaxanthone structure to incorporate an additional heterocyclic moiety, an additional donor atom to bind to the lanthanide (III) ion could be incorporated. This would also extend the conjugation length of the chromophore, shifting the lower energy absorption band of the ligand to a longer wavelength, increasing the molar extinction coefficient. The putative bidentate binding of the chromophore, when incorporated into a macrocyclic structure, creates a nonadentate environment for the Ln ion, excluding any bound water molecules.

2.1 Chromophore Synthesis

The versatile synthetic intermediate 6-*tert*-butyl-2-chloro-9-oxa-1-aza-anthracen-10-one, **6**, was synthesised according to **Scheme 2.1**. The synthesis of 6-*tert*-butyl-9-oxa-1-aza-anthracen-10-one, **2**, was accomplished by a two-step process involving a nucleophilic aromatic substitution reaction between 2-chloronicotinic acid and 4-*tert*-butyl phenol, followed by electrophilic cyclisation under acidic conditions. Methylation of azaxanthone **2** with methyl triflate¹ and subsequent anion exchange chromatography yielded the water soluble azaxanthone **4** as its chloride salt. Oxidative hydrolysis using a literature protocol² with $[\text{K}_3\text{Fe}(\text{CN})_6]$ and NaOH afforded the N-methylpyridone intermediate, **5**, in 74 % yield. The reaction was easily monitored by ^1H NMR, with the loss of pyridine aromaticity accompanied by a proton shift from 7.99 to 6.54 ppm. Finally, chlorination (POCl_3) of intermediate, **5**, yielded the 2-chloro derivative, **6**, in 50 % yield after chromatographic purification on silica.



Scheme 2.1: Synthesis of intermediate 2-chloro-azaxanthone, **6**.

Initial attempts to synthesise the corresponding unsubstituted and CO₂Me derivatives of Cl-azaxanthone, **6**, (i.e. replacing 'Bu by H or CO₂Me) proved unsuccessful. The CO₂Me functional group was seen as a possible route for bioconjugation via an activated ester derivative. However, both compounds exhibited poor solubility in organic solvents, resulting in poor yields. Research studying the photophysical properties of an array of substituted azaxanthone derivatives has been reported in the literature³ (**Table 2.1**). It was shown that substituting a *tert*-butyl group (or methyl carboxylate) into the 7 position of the azaxanthone structure had no significant effect on the λ_{\max} or energy of the triplet excited state. For these reasons, a *tert*-butyl group was introduced into the azaxanthone moiety in the knowledge that it would help enhance solubility, without compromising any photophysical attributes associated with azaxanthone moieties.

Azaxanthone	λ_{\max} / nm (ϵ ; M ⁻¹ cm ⁻¹) ^a	λ_{em} / nm ($I_{\text{em}}^{\text{rel}}$)	E_{T} / cm ⁻¹ ^b
1a	330 (6,900)	405 (1)	24,800
1b	328 (5,270)	392 (1.3)	24,900
1c	336 (9,380)	409 (0.4)	24,600

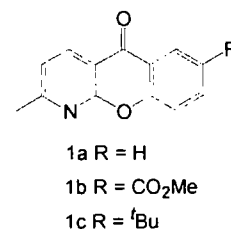


Table 2.1: Photophysical properties of 2-methyl-1-azaxanthone derivatives

^a MeOH, 295 K; ^b 77K in an Et₂O-isopentane-ethanol (EPA) frozen glass with typically a 100 μ s decay)

The chloride functionality of compound **6**, provided a reactive group to utilise for the introduction of heterocyclic moieties. Any potential heterocyclic rings that were to be included into the azaxanthone scaffolding would have to possess the following requirements;

- Extend the conjugation
- Be suitably functionalised as to allow linkage to a cyclen framework
- Be either commercially available or synthetically accessible from an appropriate precursor

A 2-pyridyl and a 2-pyrazoyl group were deemed suitable for this purpose, as the corresponding bipyridyls and 2-pyrazoylpyridines constitute well-studied classes of ligands in coordination chemistry⁴ and have been shown (Chapter 1) to be effective donors in Ln^{III} complexes.

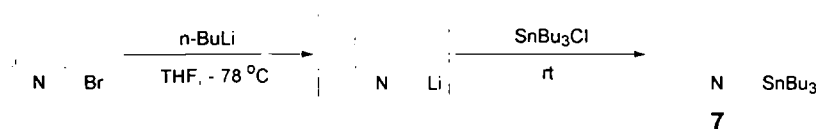
2.1.1 2-Pyridyl-azaxanthone

The Suzuki – Miyaura cross-coupling reaction is the most common way of introducing carbon – carbon bonds in heterocyclic chemistry.⁵ It is often preferred to alternative cross-coupling reactions because of the non-toxic, mild, and air / water stability of boronic acids.^{6,7} The most frequently used substrates are aryl bromides, iodides and triflates, with aryl chlorides often proving unreactive substrates. This poor reactivity is attributed to the reluctance of aryl chlorides towards oxidative addition to Pd (0).⁸ However, recent publications have highlighted the successful coupling of electron- rich aryl chlorides when using tri(dibenzylideneacetone)dipalladium (0) as a catalyst.^{9,10}

This literature precedent prompted us to explore the possibility of coupling **6**, with commercially available 6-methyl-2-pyridineboronic acid *N*-phenyldiethanolamine ester. 6-*tert*-Butyl-2-(6-methyl-pyridin-2-yl)-9-oxa-1-aza-anthracen-10-one, **8**, was isolated in 16 % yield, with reduction of the starting material (Cl → H) constituting a significant by-product. A potential solution was to employ an alternative nucleophilic substrate. Literature shows the Negishi cross-coupling reaction and arylzincs has been used to synthesise bipyridyl systems,^{11,12} using functionalised pyridine chlorides. However, despite

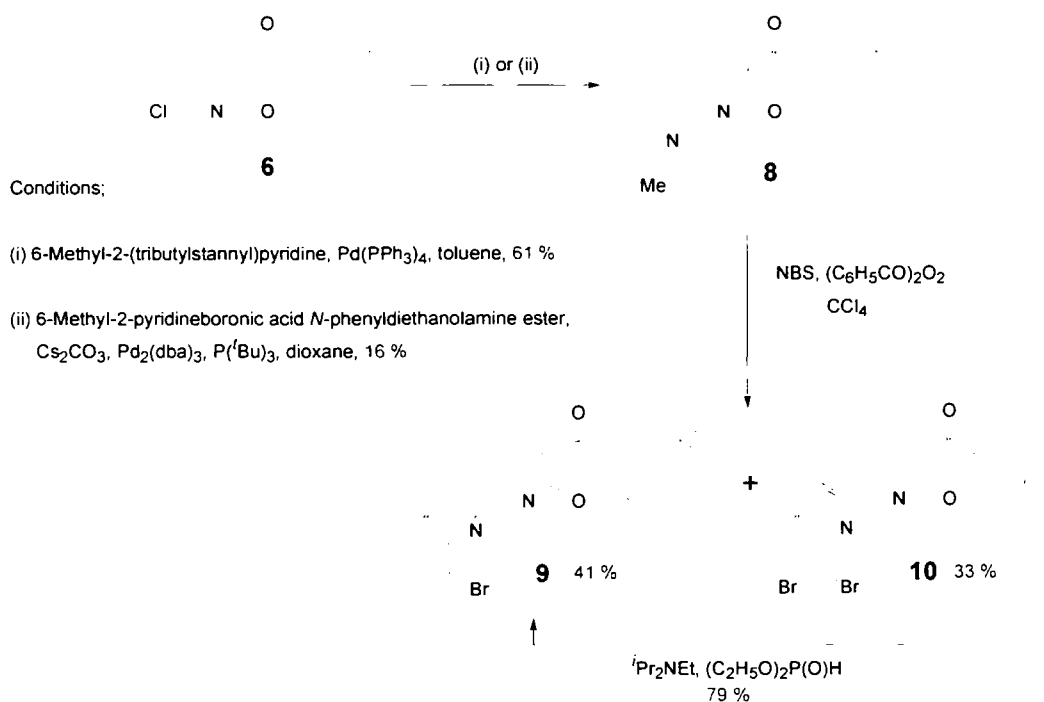
using these literature conditions, attempts to couple 6-*tert*-butyl-2-chloro-9-oxa-1-aza-anthracen-10-one, **6**, with 6-methyl-2-pyridylzinc bromide proved unsuccessful.

An alternative approach investigated was via a Stille-coupling reaction. The reaction of 2-bromo-6-methyl-pyridine with *n*-BuLi, followed by *tri*-*n*-butyl-tin chloride gave 6-methyl-2-(tributylstannyl)pyridine, **7** (**Scheme 2.2**).^{13,14}



Scheme 2.2: Synthesis of 6-methyl-2-(tributylstannyl)pyridine, **7**.

6-Methyl-2-(tributylstannyl)pyridine **7**, was used directly in a Stille-coupling with azaxanthone **6**, without any purification. Using Pd(PPh₃)₄ as a catalyst, 6-*tert*-butyl-2-(6-methyl-pyridin-2-yl)-9-oxa-1-aza-anthracen-10-one, **8** (¹H NMR and X-ray crystal structure are shown in **Figures 2.1** and **2.2**), was isolated in 61 % yield following purification by trituration in diethyl ether (**Scheme 2.3**).



Scheme 2.3: Synthesis of bromopyridyl-azaxanthone, **9**.

Selective bromination of the α -methyl substituent of **8** was performed using radical bromination with *N*-bromosuccinimide and benzoyl peroxide in CCl₄. The reaction was

monitored by ^1H NMR to provide ratiometric analysis of the formation of the desired mono-brominated derivative **9**, and the competing di-brominated analogue **10**. Purification by column chromatography on silica yielded **9** and **10** in 41 % and 33 % yields respectively. Reaction of compound **10** with diethyl phosphite and DIPEA enabled conversion of the di-brominated material to the corresponding mono-brominated analogue, following chromatographic purification.

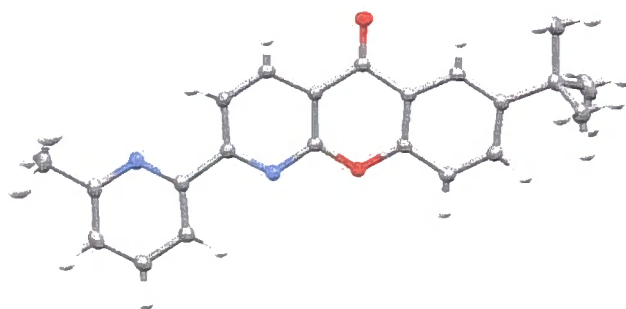


Figure 2.1: X-ray crystal structure of methylpyridyl-azaxanthone, **8**.

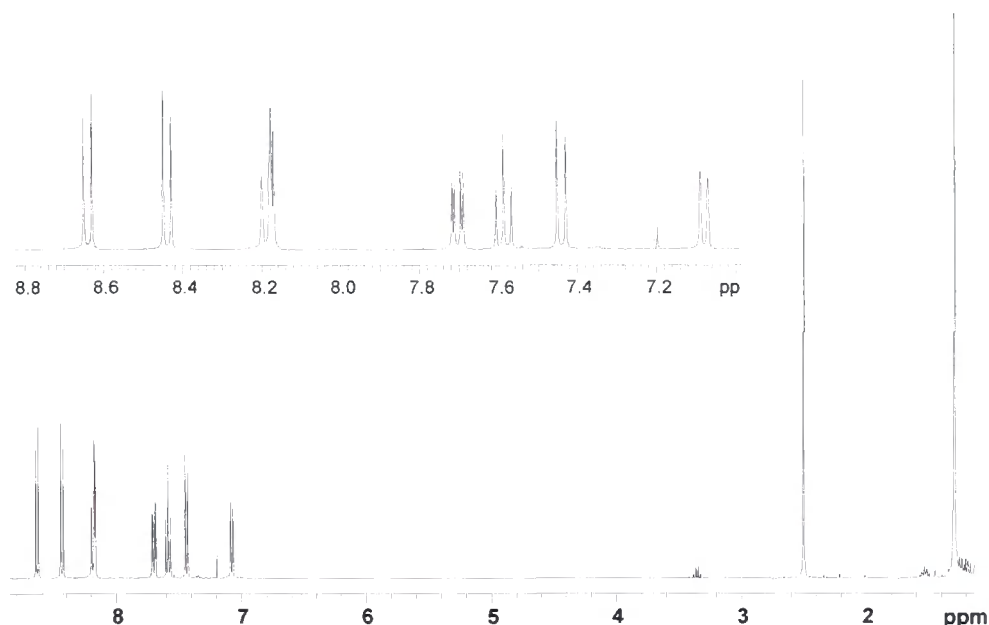
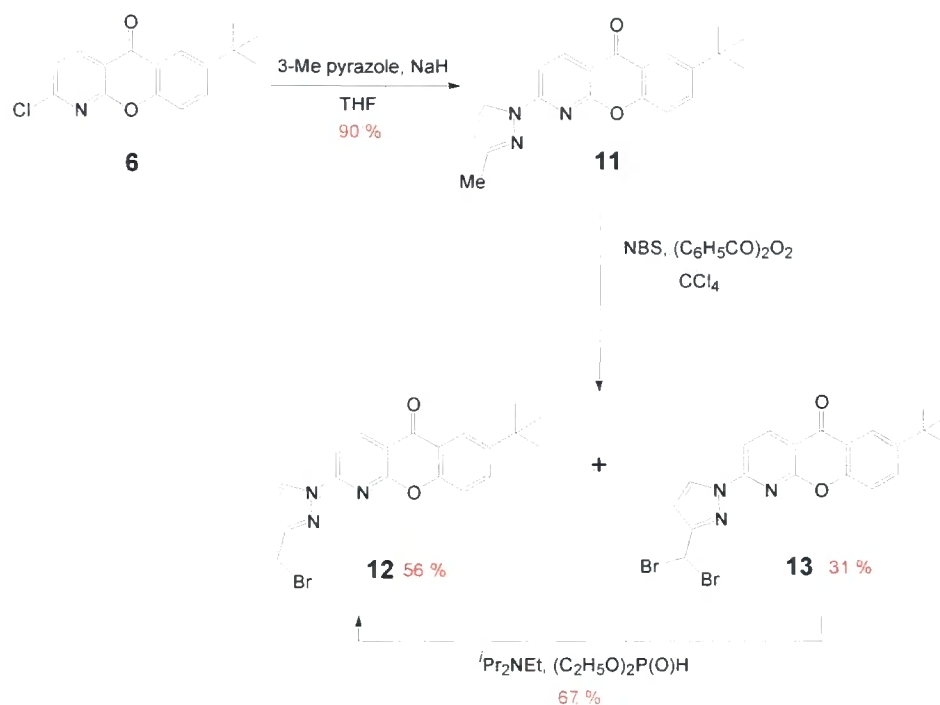


Figure 2.2: ^1H NMR spectrum of methylpyridyl-azaxanthone **8** (CDCl_3 , 700 MHz, 298 K)

2.1.2 2-Pyrazoyl-azaxanthone

The synthesis of pyrazole azaxanthone **11** was achieved in 90 % yield by nucleophilic aromatic substitution between chloro-azaxanthone, **6**, and 3-methylpyrazole, using NaH

as a base (**Scheme 2.3**).¹⁵ Bromination of **11** to the corresponding mono (**12**) and di-brominated (**13**) analogues was performed in an analogous method to that described for pyridyl-azaxanthone, **8**.



Scheme 2.3: Synthesis of bromopyrazoyl-azaxanthone, **11**.

Examination of the X-ray crystal structure of bromopyrazoyl-azaxanthone, **12** (**Figure 2.3**), confirmed as expected, that covalent linkage to the azaxanthone moiety was through the desired nitrogen atom. There was no evidence to suggest that the constitutional pyrazole isomer is formed or reacts during the aromatic substitution reaction.

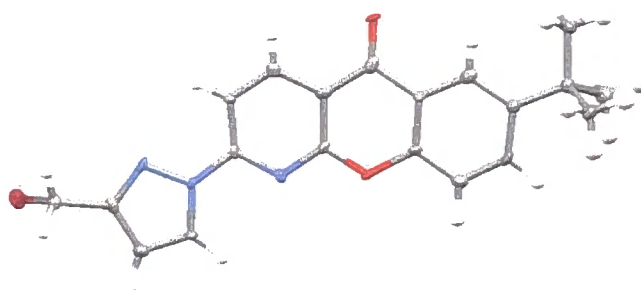


Figure 2.3: X-ray crystal structure of bromopyrazoyl-azaxanthone, **12**.

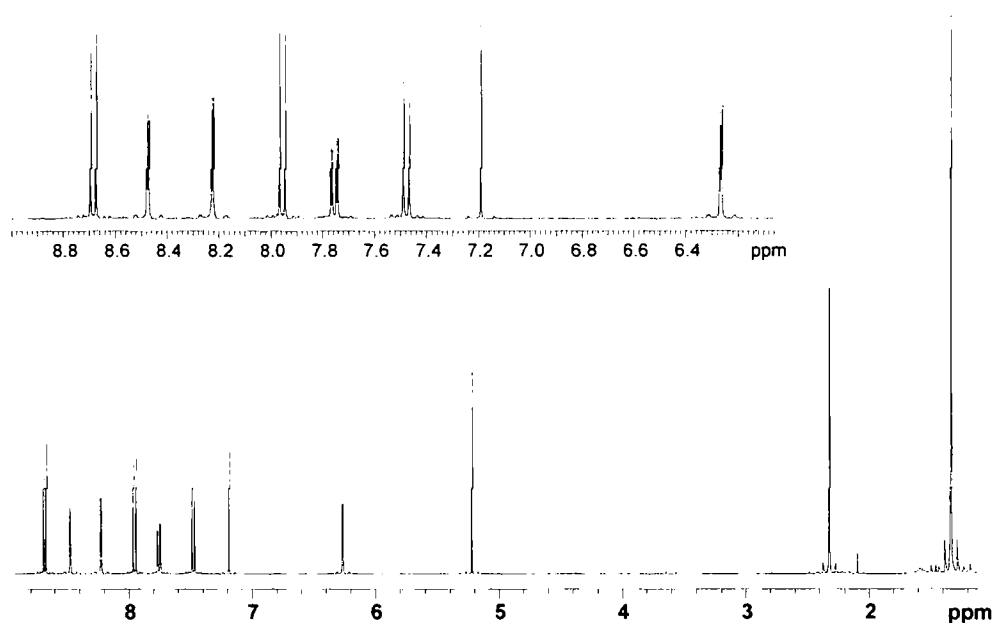
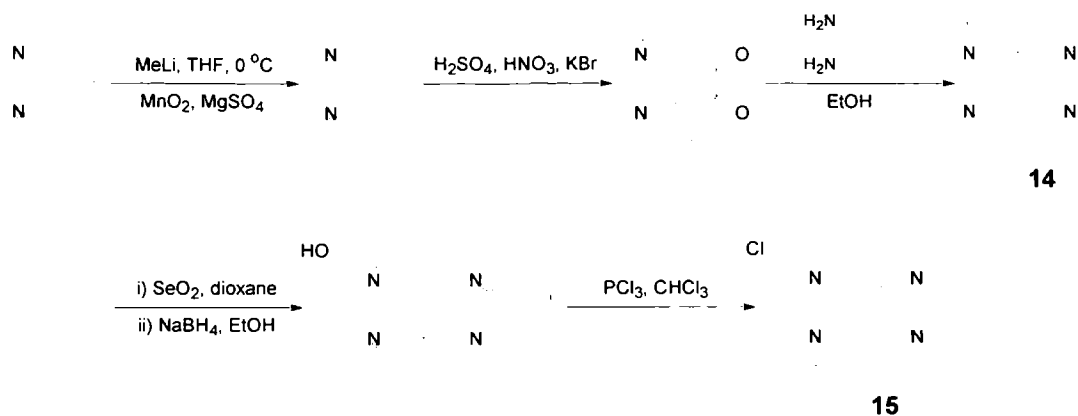


Figure 2.4: ^1H NMR spectrum of methylpyrazoyl-azaxanthone, **11**, (CDCl_3 , 700 MHz).

2.1.3 Tetraazatriphenylene

The tetraazatriphenylene chromophore (dpqC) **14**, is an established sensitiser for lanthanide luminescence. A triplet energy of the order of $24,000\text{ cm}^{-1}$ means that the moiety is suitable for both europium and terbium sensitisation. Furthermore, a fast rate of intersystem crossing ensures the triplet excited state is efficiently populated in aqueous media.¹⁶

The dpqC moiety may serve as a bidentate ligand, binding via two pyridyl nitrogen atoms. This coordination enables nine-coordinate complexes to be prepared based upon a cyclen macrocycle. Such complexes possess no bound water molecules, and for this reason form emissive complexes with an effective sensitiser.



Scheme 2.4: Synthesis of chloromethyl dpqC, **15**.

The 2-chloromethyl dpqC derivative, **15**, is synthesised by reaction of 1,10-phenanthroline with one equivalent of methyl lithium, followed by oxidation with MnO₂ in the presence of MgSO₄. Oxidation of the 9-10-double bond with molecular bromine under strong acidic conditions yields the corresponding dione. Condensation of the dione with 1,2-diaminocyclohexylamine affords 2-methyl-tetraazatriphenylene, **14**. Stepwise derivatisation of the methyl group to the corresponding 2-chloromethyl (**15**) is achieved by oxidation with SeO₂, reduction with sodium borohydride and chlorination with PCl₃.¹⁶ Compound **15** was supplied by Cisbio International for work during this thesis.

2.2 Chromophore Characterisation

Having isolated chromophores 2-pyridyl-azaxanthone, **8**, and 2-pyrazoyl-azaxanthone, **11**, their respective photophysical properties were assessed.

2.2.1 Absorption Spectra

The absorption spectra of chromophores **8** and **11** were recorded in MeOH at 298 K (**Figure 2.5**).

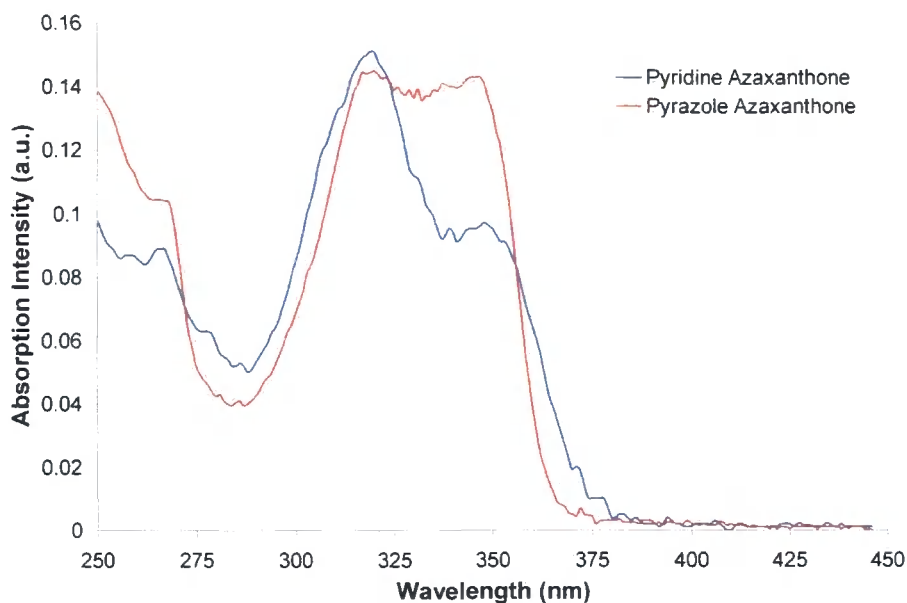


Figure 2.5: Absorption spectra for chromophores **8** (blue) and **11** (red) (MeOH, 298 K)

The absorption spectra of chromophores **8** and **11** show moderately intense long wavelength bands at 348 ($\epsilon = 10,100 \text{ dm}^3 \text{ mol}^{-1} \text{ cm}^{-1}$) and 346 ($\epsilon = 15,400 \text{ dm}^3 \text{ mol}^{-1} \text{ cm}^{-1}$) nm respectively. A strong absorption is also apparent at 355 nm, a common laser excitation wavelength. The extension of the chromophore conjugation is accompanied by a red shift in λ_{max} by ~ 10 nm when compared to the parent *tert*-butyl azaxanthone (**1a** shown in **Table 2.1**). In addition, the molar extinction coefficients show a two fold increase in comparison to the parent azaxanthone and dqpC. This increase indicates an increase in light absorption efficiency and subsequent population of the singlet excited state.

2.2.2 Fluorescence Emission Spectra

Emission spectra of chromophores **8** and **11** were recorded in MeOH at 298 K. Both chromophores were shown to exhibit minimal ligand fluorescence at room temperature, with weak broad bands observed between 390 – 430 nm. This radiative decay of the singlet excited state suggests that the rate of fluorescence is competitive with the rate of inter-system crossing. The fluorescence, which is not observed in the parent azaxanthone systems, is consistent with an enhanced degree of $\pi\pi^*$ character in the singlet excited state of the pyridyl- and pyrazoyl-azaxanthenes.

2.2.3 Phosphorescence Emission Spectra

Phosphorescent emission spectra of chromophores **8** and **11** were measured to distinguish their respective triplet state energies. This would ultimately indicate which lanthanides these chromophores could potentially sensitise. The spectra are shown in **Figure 2.6**, and were measured at 77 K in a diethyl ether – isopentane – ethanol (EPA) frozen glass.

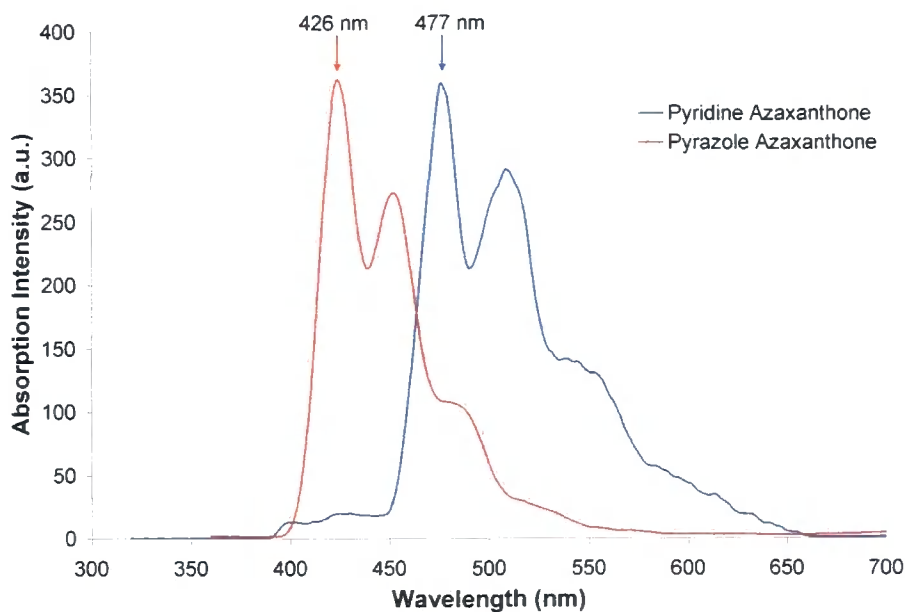


Figure 2.6: Phosphorescence emission spectra for compounds **8** (blue) and **11** (red) (77 K, EPA)

The highest energy vibrational band in each spectra is the 0,0 ($T_1(v=0) \rightarrow S_0(v=0)$) transition band, corresponding to the respective triplet energies of the chromophores. The phosphorescence spectra show that chromophores **8** and **11** have triplet energies (E_T) of 477 nm ($20,960 \text{ cm}^{-1}$) and 426 nm ($23,470 \text{ cm}^{-1}$) respectively.

It can be concluded from this experimental data that pyrazoyl-azaxanthone, **11**, should allow Eu and Tb sensitisation, while pyridyl-azaxanthone **8** is only applicable for Eu sensitisation. The triplet energy of **8** ($20,960 \text{ cm}^{-1}$) is too low to allow efficient Tb sensitisation (${}^5D_4 = 20,400 \text{ cm}^{-1}$) at ambient temperature without the prospect of thermally activated back energy transfer (**Figure 2.7**).

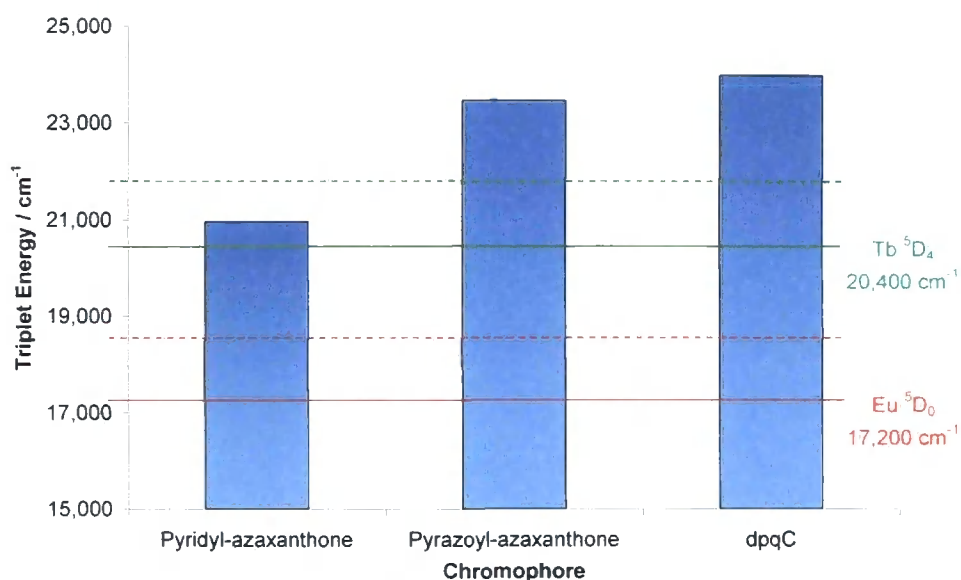


Figure 2.7: Bar chart showing the triplet energies of chromophores **8**, **11** and **dpqC** and the respective lanthanides they can sensitise

Fine structure was observed in both chromophores, with each phosphorescence spectrum exhibiting three bands, separated by $\sim 1650 \text{ cm}^{-1}$. This characteristic is typical of carbonyl vibrational fine structure, behaviour that is distinctive and consistent with dominant $n\pi^*$ character of the triplet states.^{17,18} Confirmation of the $n\pi^*$ triplet character was achieved by recording absorption spectra in media of varying polarity. Here, a small red shift in the longest wavelength band was observed upon increasing the solvent polarity (e.g. for pyridyl-azaxanthane, **8**, a shift from 344 nm (EPA) to 348 nm in MeOH was observed).

2.2.4 Summary

A summary of the photophysical properties of pyridyl-azaxanthone, **8**, and pyrazoyl-azaxanthone, **11**, is shown below, **Table 2**.

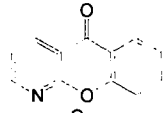
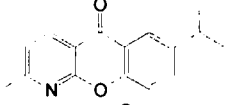
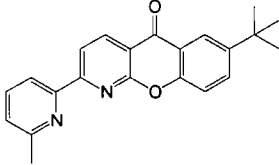
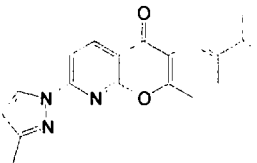
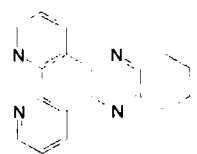
Chromophore	λ_{\max} (nm) ^a	ϵ (dm ³ mol ⁻¹ cm ⁻¹) ^a	E_T (cm ⁻¹) ^b
	330	6,900	24,800
	336	9,380	24,600
	348	10,090	20,960
	346	15,380	23,470
	348	6,400	23,400

Table 2.2: Photophysical properties of selected sensitising chromophores
(^a MeOH, 295 K; ^b 77K in an Et₂O-isopentane-ethanol (EPA) frozen glass)

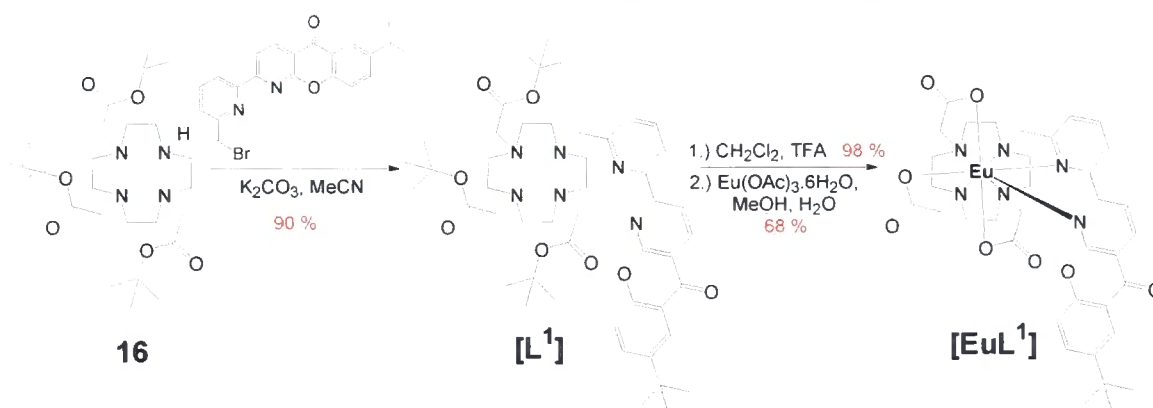
The extended conjugation in the pyridyl- and pyrazoyl-azaxanthone moieties is accompanied by an increase in both λ_{\max} and extinction coefficients (when compared to the parent azaxanthone). Examination of the triplet excited state energies indicate the pyrazoyl-azaxanthone is applicable for both europium and terbium sensitisation. For the pyridyl-azaxanthone, a T_1 of 20,960 cm⁻¹ implies thermally activated back energy transfer would be problematic for terbium sensitisation. Consequently, only europium complexes will be studied using this heterocyclic chromophore.

2.3 Ligand and Complex Synthesis

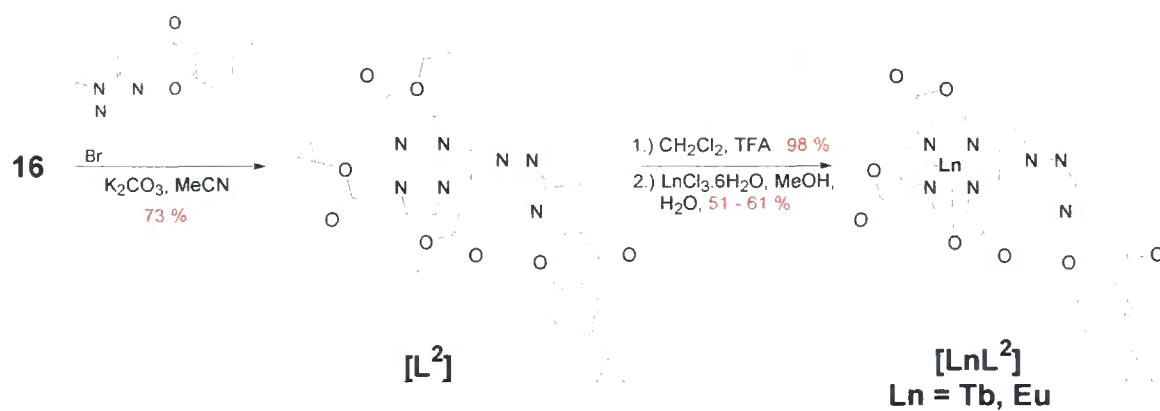
The following section will describe the synthesis of neutral carboxylate and cationic phenyl amide complexes incorporating the pyridyl-azaxanthone, pyrazoyl-azaxanthone and dpqC chromophores.

2.3.1 DO3A Complexes

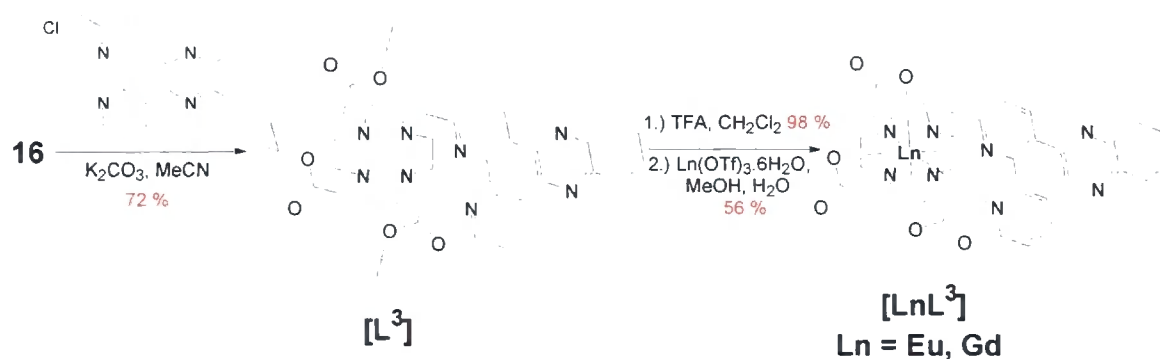
1,4,7,10-Tetraazacyclododecane-1,4,7-triacetic acid (DO3A, **16**) was synthesised from reaction of cyclen with *tert*-butyl bromoacetate, under S_N2 conditions (acetonitrile, K_2CO_3). Purification by column chromatography on silica yielded DO3A, **16**, in 32 % yield. The synthesis of ligands [**L**¹], [**L**²] and [**L**³] involved alkylation of DO3A, with the appropriate halomethyl chromophores. Following chromatographic purification on neutral alumina, treatment with $CF_3CO_2H - CH_2Cl_2$ removed the BOC protecting groups. Complexation of the deprotected ligands was performed using the appropriate $Ln(OAc)_3$ salt in water at pH 5. Removal of excess lanthanide was achieved by precipitation of $Ln(OH)_3$ at pH 10. Finally, chromatography on neutral alumina (20 % $CH_3OH - CH_2Cl_2$) led to the isolation of the neutral complexes [**EuL**¹], [**LnL**²] and [**LnL**³].



Scheme 2.5: Synthesis of ligand [**L**¹] and the neutral complex [**EuL**¹]



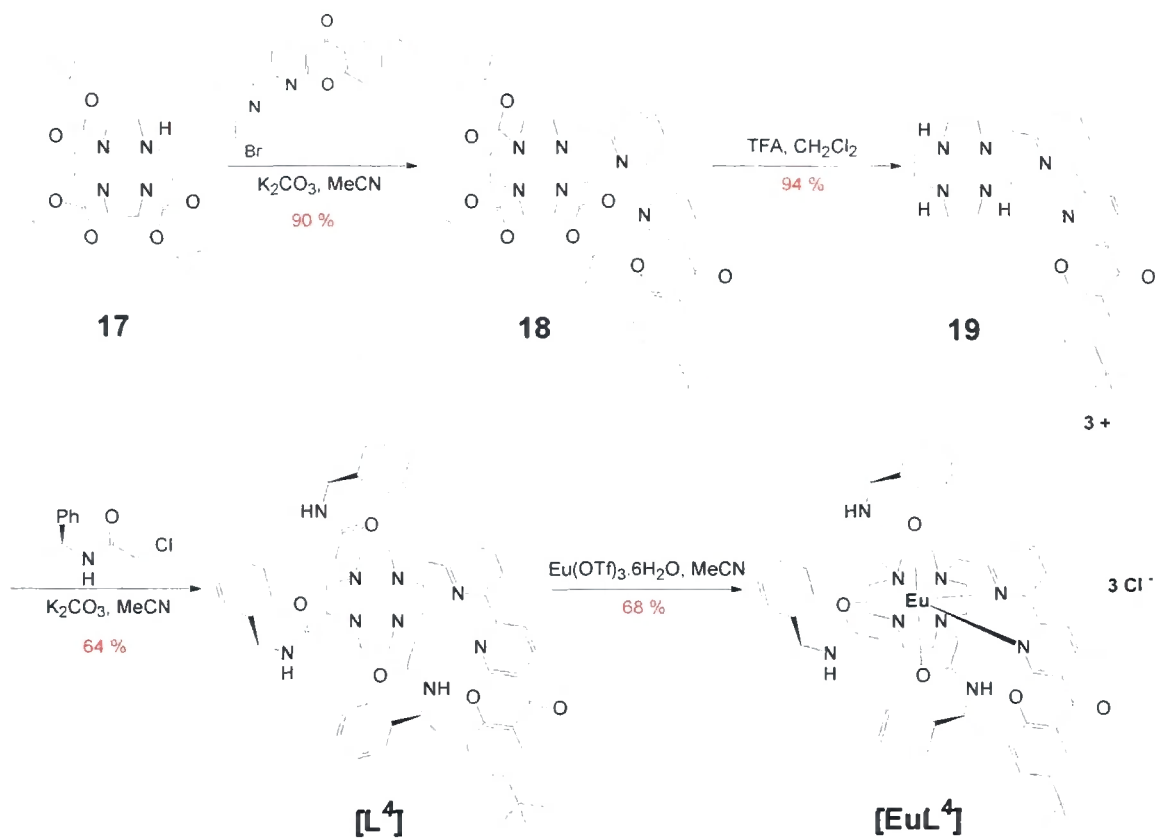
Scheme 2.6: Synthesis of ligand $[L^2]$ and neutral complexes $[LnL^2]$



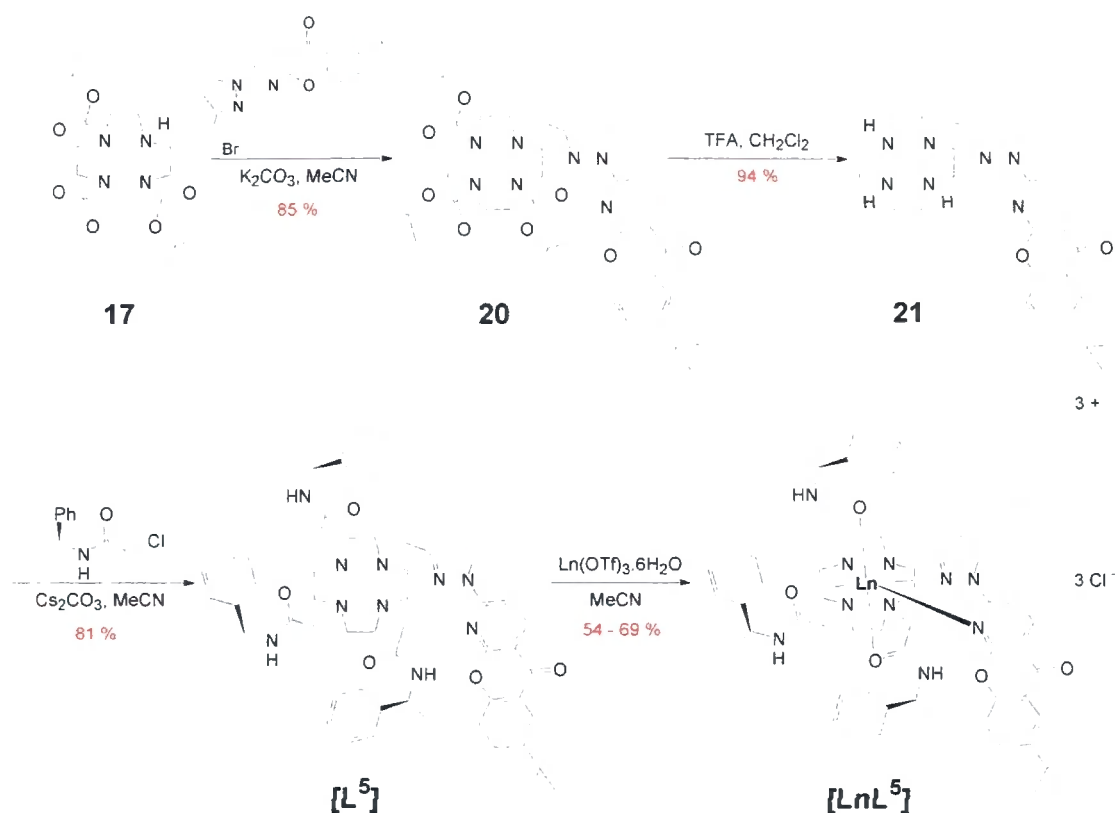
Scheme 2.7: Synthesis of ligand $[L^3]$ and neutral complexes $[LnL^3]$

2.3.2 Tri-Amide Complexes

Selective mono-substitution of cyclen was achieved via alkylation of *tri*-BOC cyclen **17**, under S_N2 conditions (acetonitrile, K_2CO_3), using the respective halomethyl chromophores. Deprotection of the BOC groups (CF_3CO_2H / CH_2Cl_2) yielded the tetraamines **19**, **21** and **23** (Schemes 2.7, 2.8 and 2.10). Alkylation with (*S*)-*N*-2-chloroethanoyl-2-phenylethylamine under basic conditions in acetonitrile afforded the triamide ligands $[L^4]$, $[L^5]$, $[L^7]$ which were purified by chromatography on neutral alumina. Reaction of the triamide ligands with one equivalent of $Ln(CF_3SO_3)_3$ in anhydrous acetonitrile gave the desired cationic complexes as triflate salts. Excess ligand was removed via sonification in CH_2Cl_2 , while trituration in water removed any excess lanthanide salt. Finally, the respective complexes were converted to the more water soluble chloride salts by anion exchange chromatography.

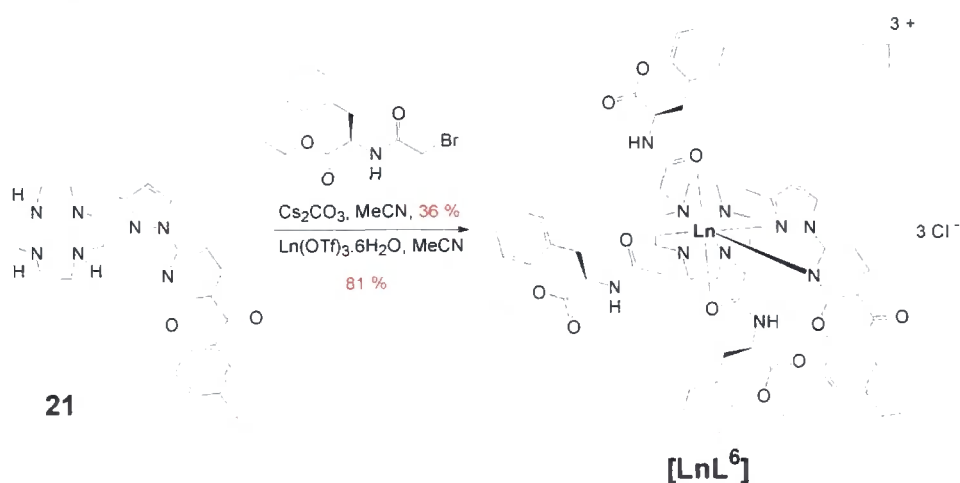


Scheme 2.8: Synthesis of ligand **[L⁴]** and the cationic complex **[EuL⁴]**

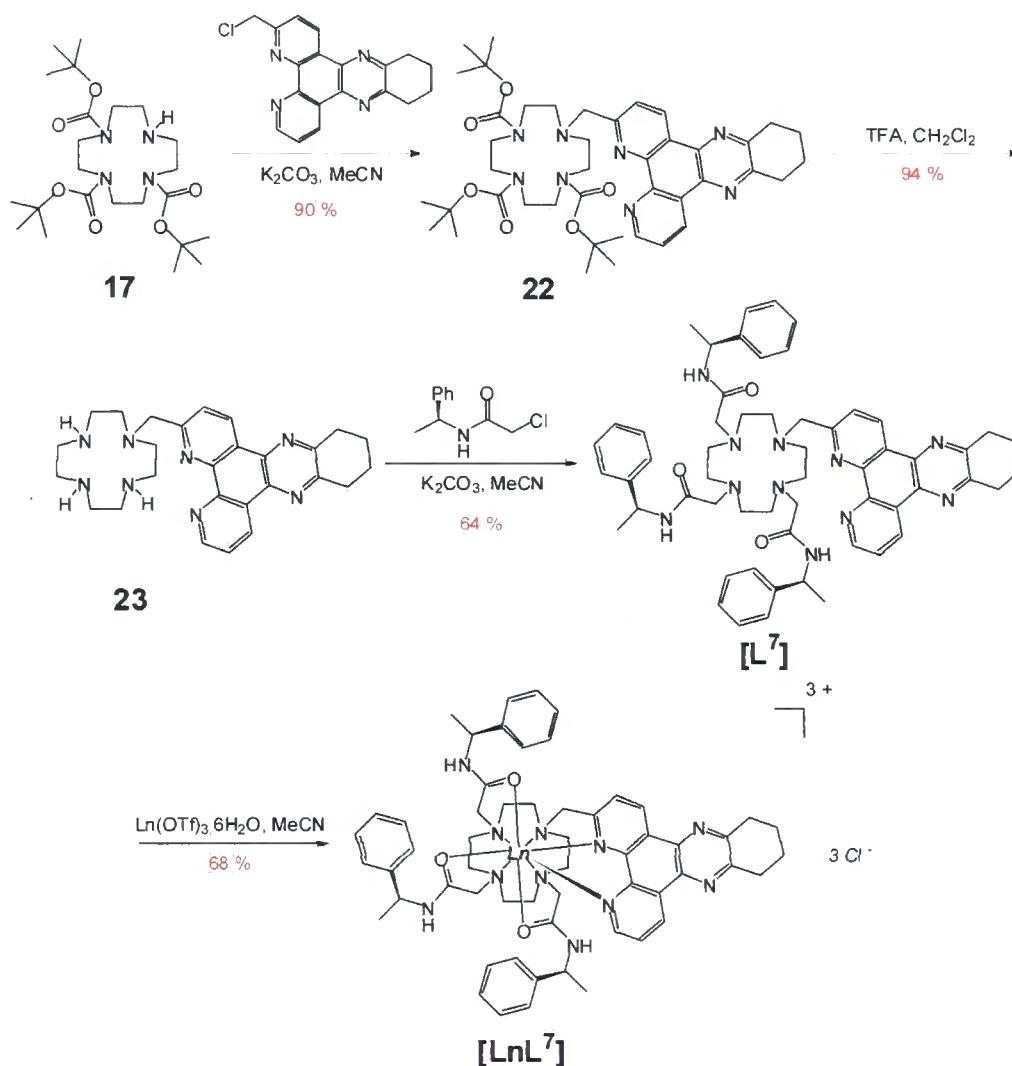


Scheme 2.8: Synthesis of ligand **[L⁵]** and cationic complexes **[LnL⁵]**

Alkylation of tetraamine **21** with (S) -2-(2-bromo-acetylamino)-3-phenyl-propionic acid ethyl ester under $\text{S}_{\text{N}}2$ conditions afforded ligand **[L⁶]**, after purification by trituration in diethyl ether. Complexation of the ligand was achieved in acetonitrile using $\text{Ln}(\text{CF}_3\text{SO}_3)_3$, followed by anion exchange chromatography to yield the water soluble cationic complex **[LnL⁶]**.



Scheme 2.9: Synthesis of ligand **[L⁶]** and the cationic complexes **[LnL⁶]**



Scheme 2.10: Synthesis of ligand **[L⁷]** and the cationic complexes **[LnL⁷]**

Parallel synthetic protocols were followed for complexes **[LnL⁵]** and **[LnL⁷]** using (R) - N -2-chloroethanoyl-2-phenylethylamine. This yielded the opposing chiral complexes **(RRR)-[LnL⁵]** and **(RRR)-[LnL⁷]**. These complexes were examined by circularly polarised luminescence (Chapter 4) and fluorescence microscopy (Chapter 5) to investigate the effect of chirality on complex characteristics, such as cellular behaviour.

2.4 Complex Characterisation

The photophysical properties of complexes $[\text{EuL}^1]$ to $[\text{LnL}^7]$ were assessed and compared to analogous complexes incorporating the parent 2-methyl-1-azaxanthone and 7-tert-butyl-1-azaxanthone chromophores.

2.4.1 Absorption Spectra

The absorption spectra for complexes $[\text{EuL}^1]$ – $[\text{LnL}^7]$ were recorded in water at 298 K. For complexes containing the pyrazoyl-azaxanthone or dpqC chromophores, each spectral profile was consistent with those observed for the ‘free’ chromophores in organic solvent. This behaviour suggests there is a small electronic interaction between these chromophores and the lanthanide metal. Thus, pyrazoyl-azaxanthone complexes exhibited strong absorption at 346 nm, while the dpqC analogues show a major band at 348 nm. With the pyridyl-azaxanthone complexes, $[\text{EuL}^1]$ and $[\text{EuL}^4]$, complexation was accompanied by a change in spectral form. A red shift in λ_{max} was observed to a wavelength > 350 nm, while a gradual decrease in absorption was observed above 350 nm (**Figure 2.8**). This behaviour differs from the free chromophore, which shows a steep decline in absorption beyond 350 nm. In conclusion, the pyridyl-azaxanthone complexes are well suited to excitation at 355 nm, a wavelength of several common lasers.

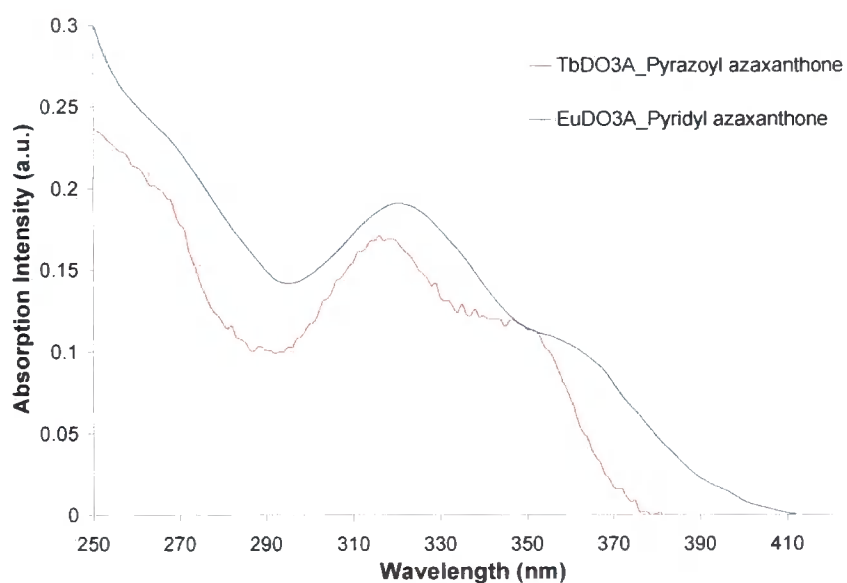


Figure 2.8: Comparative absorption spectra for complexes $[\text{EuL}^1]$ (blue) and $[\text{TbL}^2]$ (red) (295 K, H_2O)

2.4.2 Emission Spectra

The total emission spectra of $[\text{EuL}^1]$ and $[\text{EuL}^2]$ are shown in **Figure 2.9**. Emission from complex $[\text{EuL}^1]$ reveals the expected Eu spectral fingerprint from the $^5\text{D}_0$ emissive state. The spectrum also shows azaxanthone fluorescence centred at 445 nm. This ligand-based emission ($\Phi_{\text{em}}^{\text{f}} = \sim 20\%$), whilst limiting the metal-based quantum yield, provides an observable band for luminescence microscopy and facilitates flow cytometric studies. Interestingly, only very weak Eu emission is observed from the analogous pyrazoyl-azaxanthone complex, $[\text{EuL}^2]$. Instead, the emission spectrum is dominated by ligand fluorescence at 410 nm. Initially, this ligand fluorescence was attributed to uncomplexed ligand. However, further investigation by HPLC analysis indicated the sample was free of any ligand impurity and comprised one species in solution.

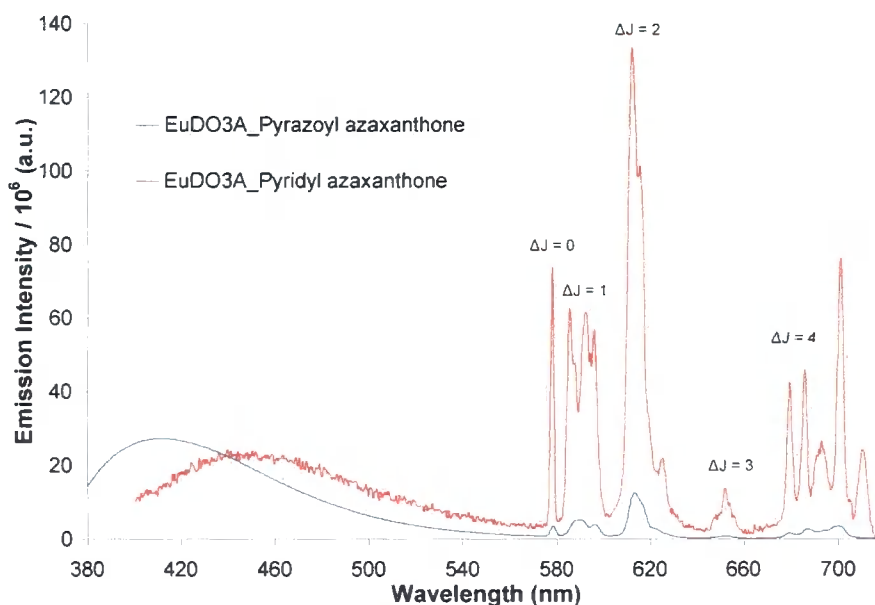


Figure 2.9: Total emission spectra (aerated water, 295 K, λ_{exc} 355 nm) for $[\text{EuL}^1]$ (red) and $[\text{EuL}^2]$ (blue)

Examination of the Tb adduct, $[\text{TbL}^2]$ (**Figure 2.10**), showed the expected Tb $^5\text{D}_4$ decay with weak ligand fluorescence.

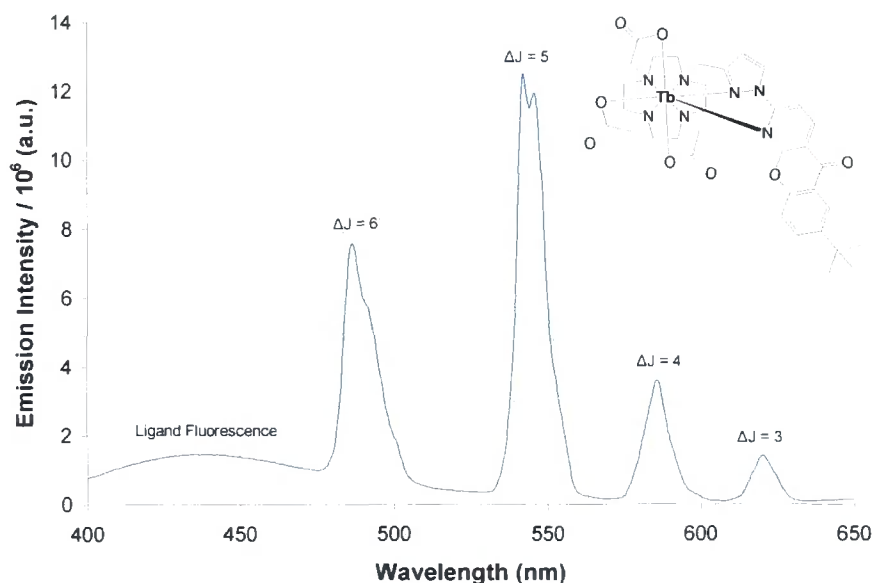


Figure 2.10: Total emission spectra for $[\text{TbL}^2]$ (aerated water, 295 K, λ_{exc} 355 nm)

Measurement of the total emission of complex $[\text{EuL}^2]$ in MeOH (**Figure 2.11**) revealed an increase in europium emission, with a significant decrease in ligand fluorescence. This observation suggests that in aqueous media, the pyrazoyl-azaxanthone is displaced from binding with the lanthanide metal by a water molecule. In methanol however, the chromophore binding is not adversely affected. It can be postulated that the increase in ionic radius from terbium to europium ($\text{Tb}^{3+} = 1.09$ vs $\text{Eu}^{3+} = 1.12$)¹⁹ is significant enough to exceed the pyrazoyl-pyridine nitrogen's 'bite angle'. Consequently, an apparently weak binding interaction between the lanthanide ion and pyridyl nitrogen is observed, which is susceptible to competitive displacement by solvent water molecules.

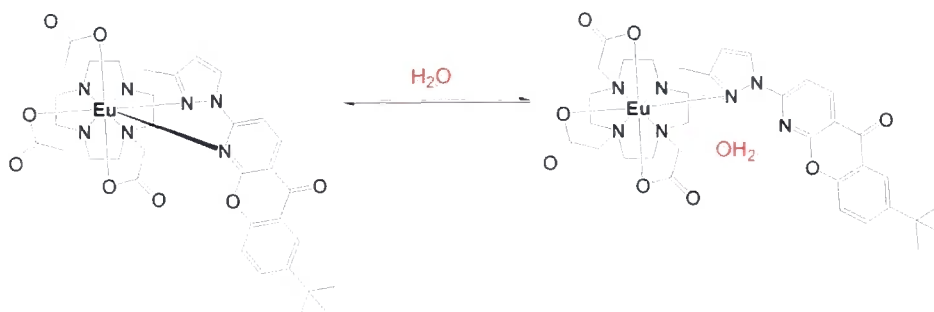


Figure 2.11: Dissociation of pyrazoyl-azaxanthone in $[\text{EuL}^2]$

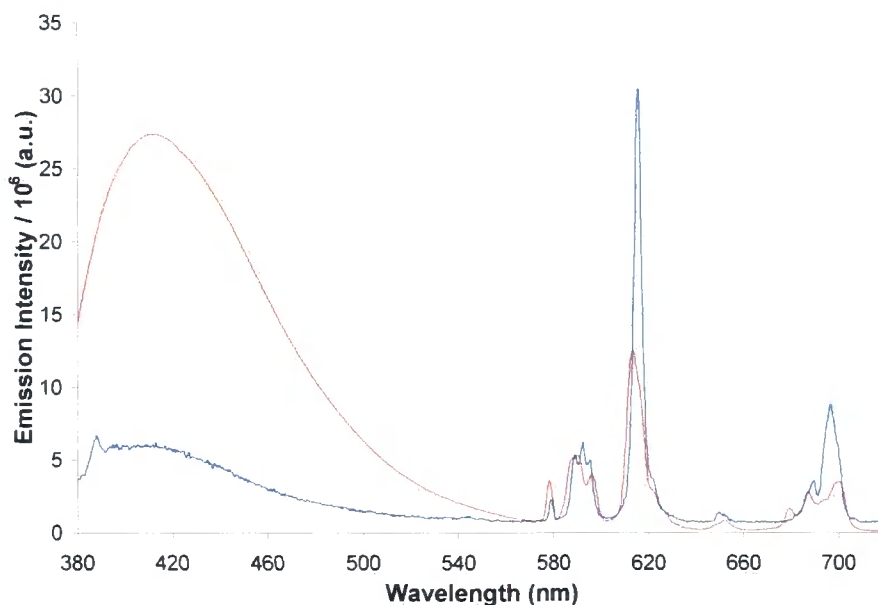


Figure 2.12: Total emission spectra for $[\text{EuL}^2]$ in water (red) and MeOH (blue) at 295 K

The emission spectra of the cationic triphenylamide complexes $[\text{EuL}^4]$ (Figure 2.13) and $[\text{TbL}^5]$ (Figure 2.14) exhibited more intense lanthanide emission compared to their DO3A analogues. Each complex showed less ligand fluorescence, suggesting a more efficient rate of inter-system crossing. The total emission spectral form of complex $[\text{TbL}^6]$ resembled that observed for $[\text{TbL}^5]$.

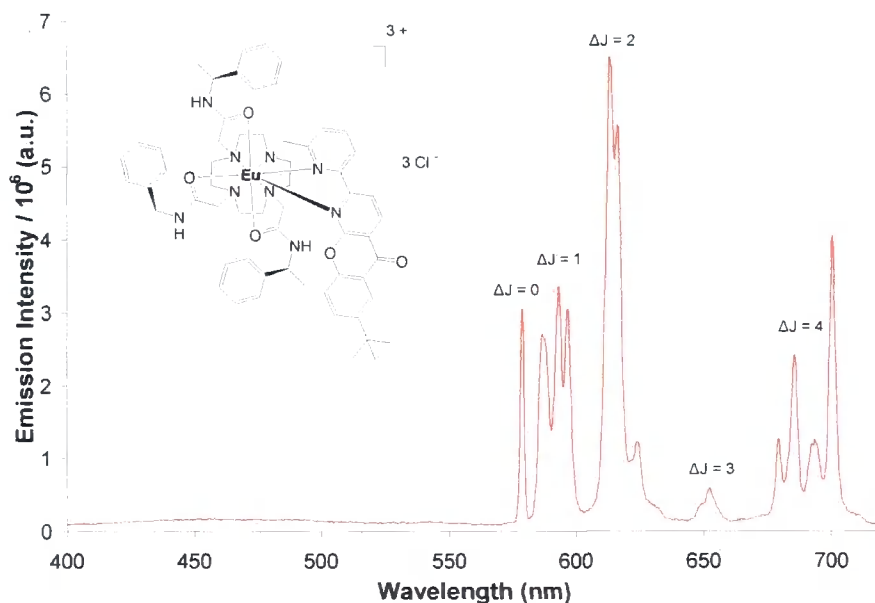


Figure 2.13: Total emission spectra (aerated water, 295 K, λ_{exc} 355 nm) for $[\text{EuL}^4]$

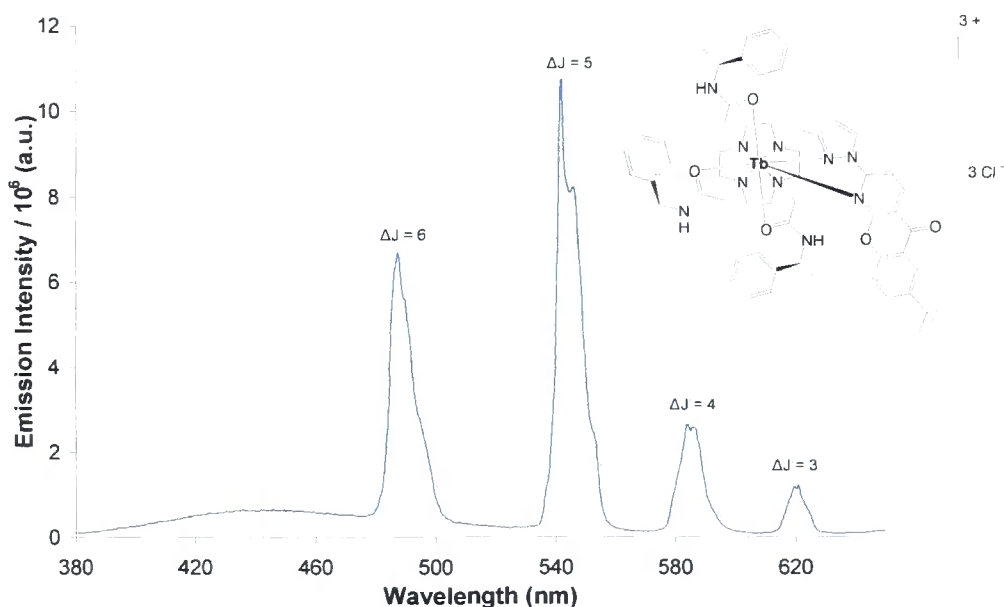


Figure 2.14: Total emission spectra (aerated water, 295 K, λ_{exc} 355 nm) for $[\text{TbL}^5]$

The emission spectral forms of the tetraazatriphenylene complexes $[\text{EuL}^7]$ and $[\text{TbL}^7]$ were found to be identical to those previously published within the literature.¹⁶ The complexes exhibited the expected europium and terbium emission bands, with no observed ligand fluorescence.

2.4.3 pH and Anion Sensitivity

The apparent susceptibility of the pyrazoyl-azaxanthone moiety to undergo dissociation in $[\text{EuL}^2]$, prompted an investigation of the pH and anion stability of complexes $[\text{EuL}^4]$ and $[\text{TbL}^5]$.

Pyrazoyl-azaxanthone, $[\text{TbL}^5]$

Luminescence titrations were carried out to determine any apparent pH sensitivity in aqueous media. As shown in **Figure 2.15**, the emission intensity and ligand fluorescence of $[\text{TbL}^5]$ were found to be pH dependent. This observation coincides with the findings for $[\text{EuL}^2]$, wherein binding of the pyrazoyl-azaxanthone was also susceptible to dissociation. Studies showed that this dissociation is reversible. Addition of anions such as citrate, lactate and carbonate to $[\text{TbL}^5]$, also resulted in a decrease in emission profile,

consistent with pronounced sensitivity towards intermolecular anion ligation and pyridyl nitrogen dissociation.

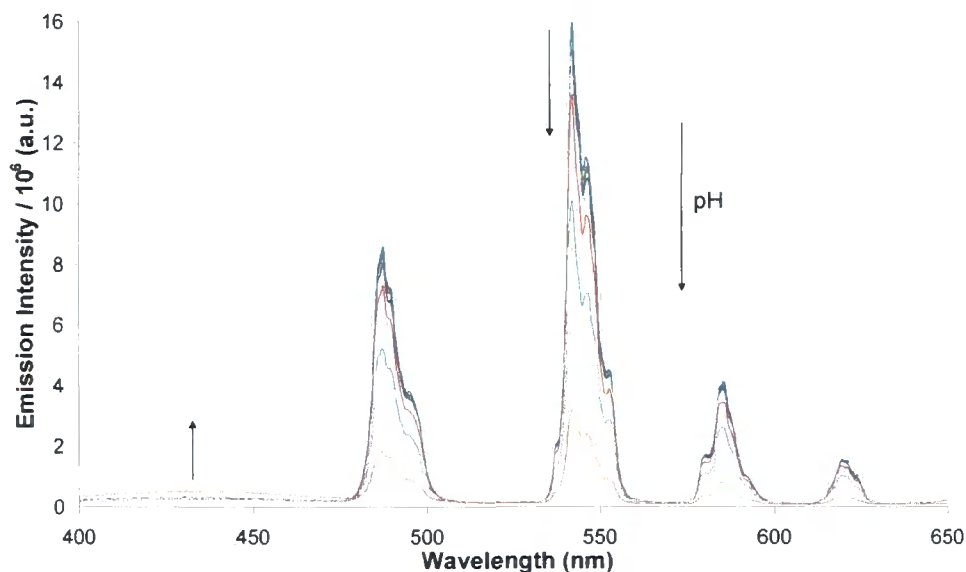


Figure 2.15: Variation of the terbium emission spectrum of $[\text{TbL}^5]$ as a function of pH over the range 3 to 10 ($[\text{Complex}] = 20 \mu\text{M}$, $\lambda_{\text{exc}} = 355 \text{ nm}$, 0.1 M NaCl , 298 K)

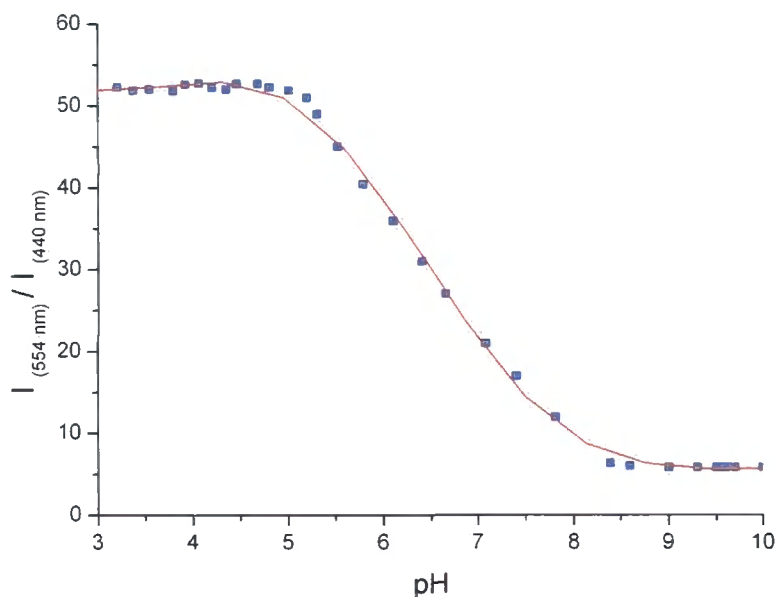


Figure 2.16: Intensity ratio (554 nm / 440 nm) vs. pH plot for complex $[\text{TbL}^5]$

An intensity ratio plot vs. pH for complex $[\text{TbL}^5]$ (Figure 2.16) revealed that the complex has a pK_a of 6.5 in aqueous medium. This value corresponds to the pyridyl nitrogen of the azaxanthone rather than the pyrazoyl binding nitrogen.

Pyridyl-azaxanthone, [EuL⁴]

Luminescent titrations of [EuL⁴] revealed no apparent pH sensitivity of the pyridyl azaxanthone, with luminescent behaviour remaining constant over the pH range 3 to 9. However, incremental addition of biological anions, such as citrate and lactate, caused a change in both the emission intensity and spectral form from the europium (III) ion (**Figure 2.17**). Addition of 0.4 mM HSA also led to modest quenching of the total emission spectra, with similar changes in the spectral form.

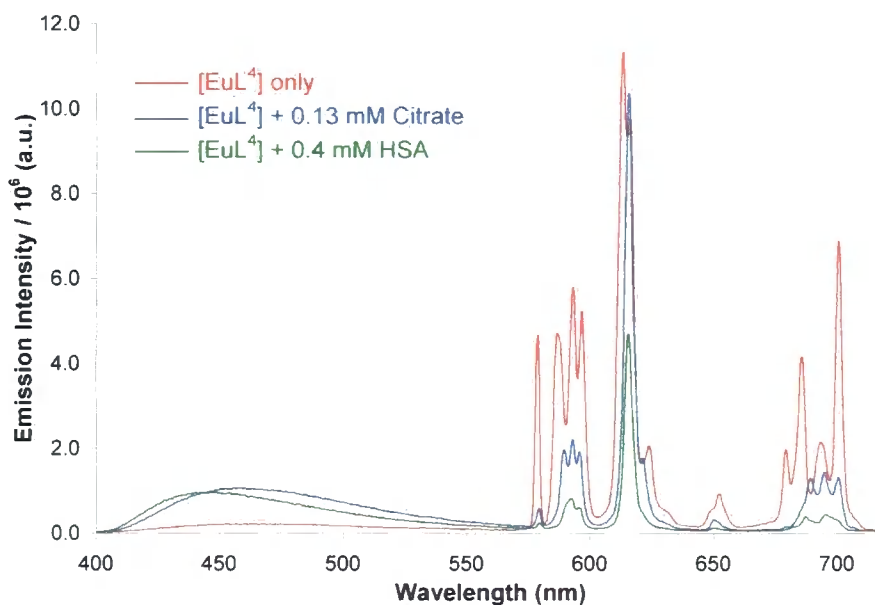


Figure 2.17: Total emission spectra (aerated water, 295 K, λ_{exc} 355 nm) for [EuL⁴] with 0.13 mM citrate (blue) and 0.4 mM HSA (green)

The most notable changes were an increase in ligand fluorescence and changes in the form and intensity of the $\Delta J = 2$ and $\Delta J = 4$ bands (**Figure 2.18**). The loss of the 680 nm emission band is consistent with dissociation of the axial pyridyl-azaxanthone nitrogen atom. This was confirmed by comparison of the absorption spectra of [EuL⁴] in the absence and presence of citrate. Addition of citrate was accompanied by a blue shift in λ_{max} , to reveal a spectrum similar to that of the free chromophore, described earlier (**Figure 2.5**).

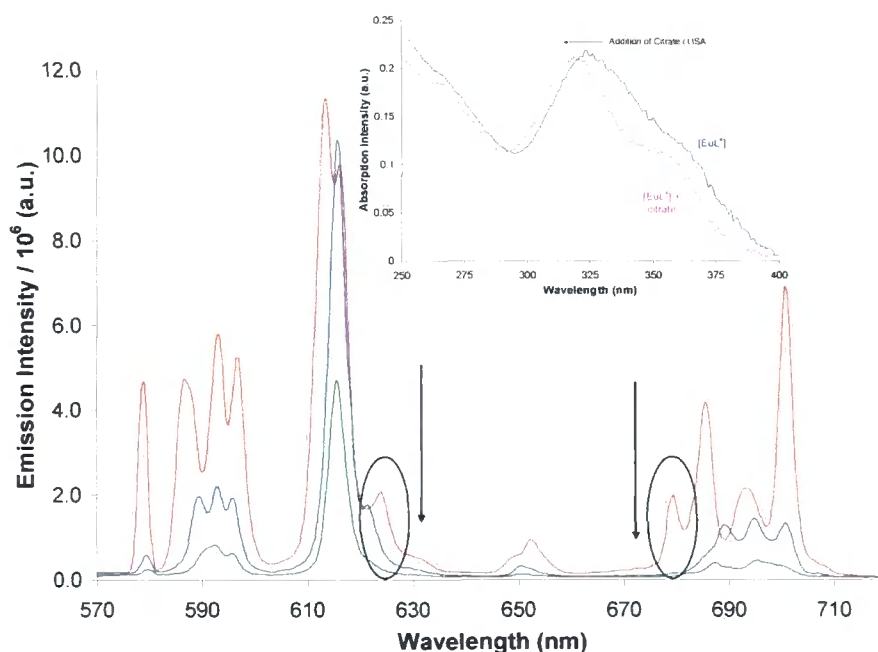


Figure 2.18: Emission spectra (aerated water, 295 K, λ_{exc} 355 nm) for $[\text{EuL}^4]$ with 0.13 mM citrate (blue) and 0.4 mM HSA (green) showing changes in spectral form; (Insert): Absorption spectra of $[\text{EuL}^4]$ without (blue) and in the presence of citrate (red)

Examination of the emissive lifetime of $[\text{EuL}^4]$ following addition of 0.13 mM citrate and 0.4 mM HSA resulted in less than a 10 % decrease compared to that observed in water. Thus, neither the presence of citrate nor HSA significantly quenches the lanthanide excited state.

These observations suggest that in a cellular environment, the pyridyl-azaxanthone is likely to dissociate from the lanthanide ion. However, under such conditions the complex remains emissive, with a strong $\Delta J = 2$ band providing an emissive parameter to measure.

2.4.4 Lanthanide Coordination Environment Studies (^1H NMR and HPLC)

The paramagnetic nature of lanthanide (III) ions has led to their exploitation in the development of shift reagents and MRI contrast agents. The NMR resonances of atoms that are either directly coordinated or that are in close proximity to the metal ion exhibit a signal shift and broadening, the extent of which is dependent on the lanthanide ion.

By examining the total optical emission and NMR spectral properties of a complex, it is possible to form an understanding on the nature and symmetry of the metal ion coordination environment.²⁰ Of particular importance is the group or atom occupying a

position on or close to the principal axis of the complex. The nature and polarisability of this group determines the second order crystal field coefficient B_0^2 that controls the dipolar NMR shift and the degree of splitting of the $\Delta J = 1$ manifold in europium spectra.^{21,22} For cyclen based complexes, this is typically the ‘axial’ ligand. The more polarisable this donor atom is, the greater the relative intensity of the $\Delta J = 2$ emission band. The ^1H NMR spectrum of $[\text{EuL}^4]$ is similar to that observed with $[\text{EuL}^7]$ (298 K, D_2O) (Figure 2.19).

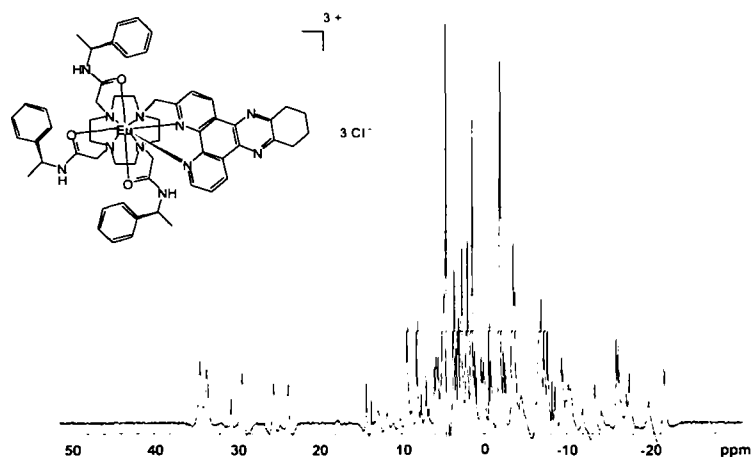
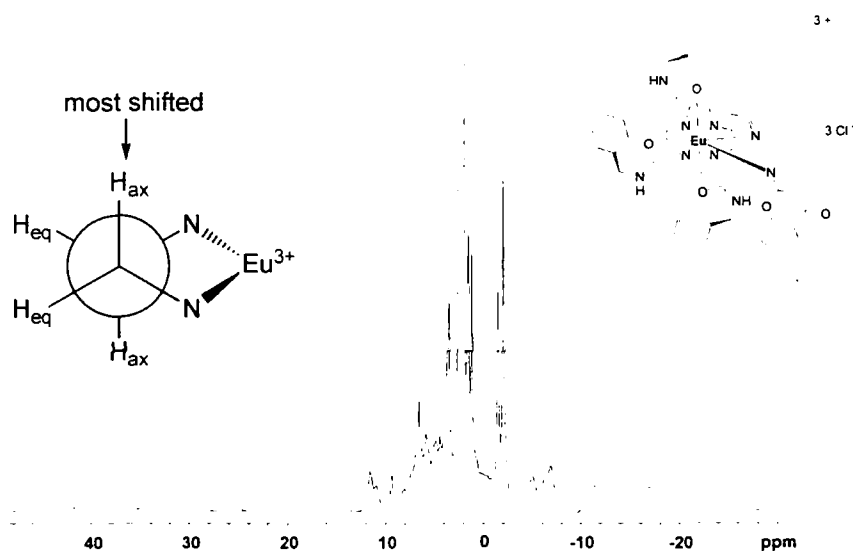


Figure 2.19: ^1H NMR spectra of $[\text{EuL}^7]$ (upper) and $[\text{EuL}^4]$ (lower) (D_2O , 298 K)



Each complex presents 4 distinct axial protons on the cyclen ring. These axial protons, assigned by COSY as between 25 to 42 ppm, experience the largest paramagnetic shielding effect. The spectral behaviour of each complex is consistent with the presence of only one isomeric species in aqueous solution at room temperature. Confirmation of the presence of one isomeric species was obtained by reverse phase HPLC analysis (Figure 2.20).

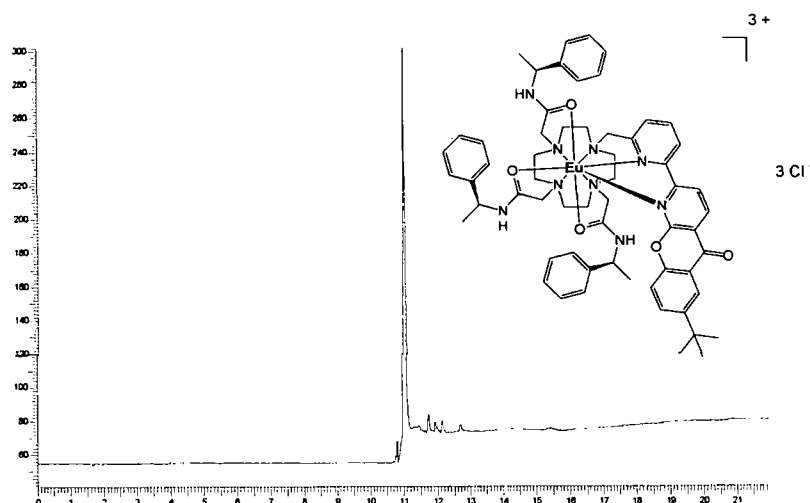


Figure 2.20: Reverse phase analytical HPLC analysis of $[\text{EuL}^4]$

(Chromolith performance RP18e column; Method A;ⁱ $\lambda_{exc} = 355 \text{ nm}$, $\lambda_{em} = 355 / 613 \text{ nm}$)

Detailed analysis of the total emission spectra of $[\text{EuL}^4]$ and $[\text{EuL}^7]$ also provides information regarding the coordination environment of the europium ion. The fine splitting of the respective europium $\Delta J = 1$ bands provides information about the number of structural isomers present in solution. The presence of three transitions for each complex suggests one isomeric species of low symmetry, complementing the observations from ^1H NMR and HPLC analysis.

For $[\text{EuL}^4]$, the relative heights of the $\Delta J = 1$ and $\Delta J = 2$ bands indicate that the polarisability of the axial donor is low. The presence of an emission band corresponding to 680 nm in the respective $\Delta J = 4$ manifolds is consistent with a nitrogen atom as the ‘axial’ donor for complexes of both the tetraazatriphenylene and pyridyl-azaxanthone chromophores.

ⁱ For HPLC solvents and gradients see Chapter 7: Experimental

2.4.5 Luminescent Lifetimes

Long luminescent lifetimes are highly desirable for complexes which are to be considered as practical luminescent probes. As previously discussed in Chapter 1, the excited states of europium and terbium are sensitive to quenching by OH and NH oscillators. The extent to which these emissive states are quenched by H₂O and D₂O is different. Consequently, measurements of the radiative lifetimes in H₂O and D₂O permit an estimate of the number of coordinated water molecules, q . This is achieved using **Equations 2.1** and **2.2**,²³ which account for the quenching effect of second sphere waters and exchangeable NH oscillators of coordinated CO groups.

$$q_{Eu} = 1.2 (k^{H_2O} - k^{D_2O} - 0.25 - 0.07x) \quad (2.1)$$

x = number of carbonyl-bound amide NH oscillators

$$q_{Tb} = 5 (k^{H_2O} - k^{D_2O} - 0.06) \quad (2.2)$$

The lifetimes and respective q values of complexes [EuL¹] to [LnL⁷] are collated in **Table 2.3**, along with analogous complexes containing the parent azaxanthenes. Three D₂O exchanges were performed before each lifetime measurement in D₂O, to ensure complete H / D exchange for each sample analysed.

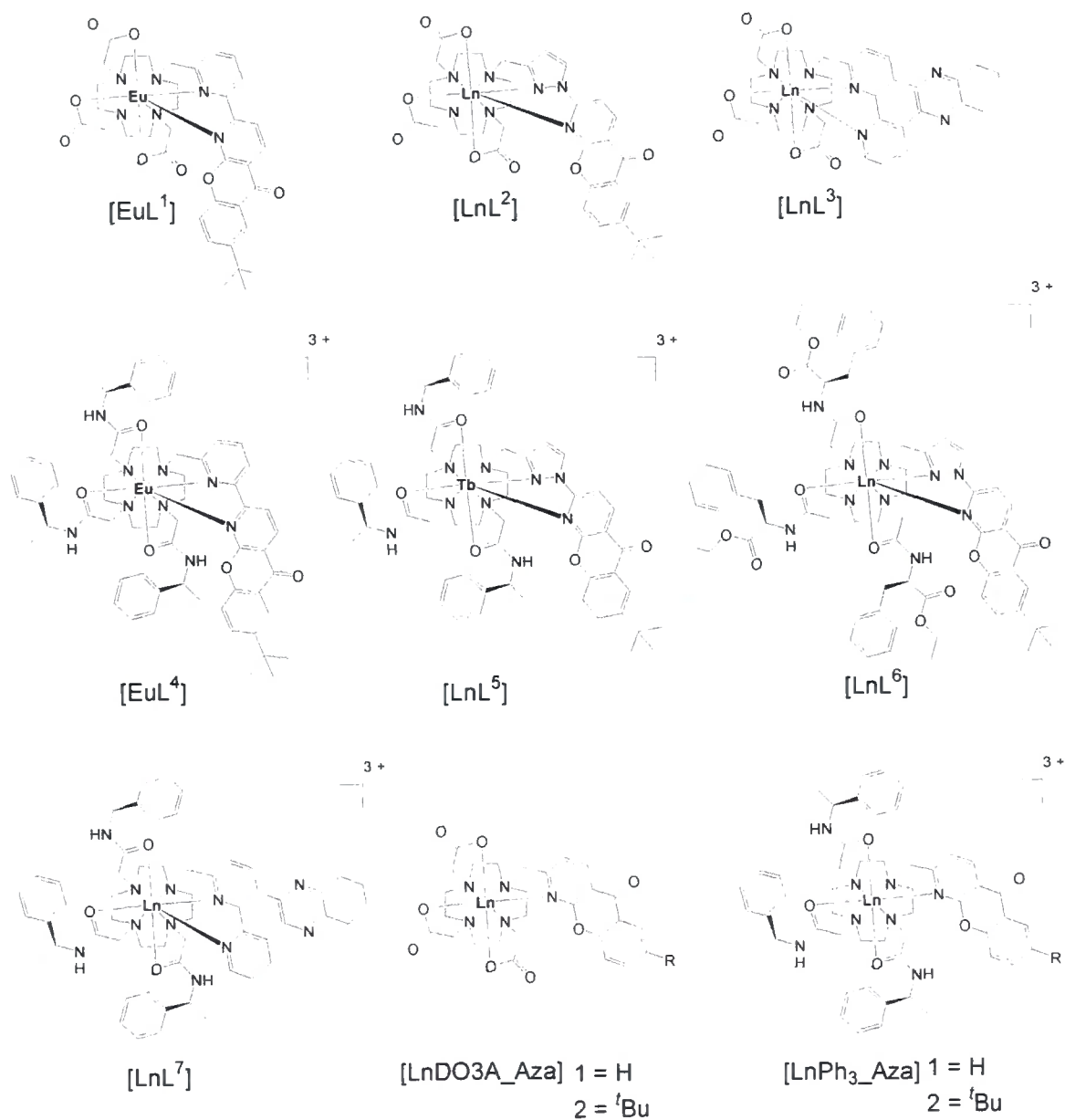


Figure 2.21: Lanthanide complexes incorporating the pyridyl-, pyrazoyl-azaxanthenes, *dpqC* and parent azaxanthenes

(all cationic complexes are as their respective chloride salts)

Complex	$\tau_{\text{H}_2\text{O}} / \text{ms}$	$\tau_{\text{D}_2\text{O}} / \text{ms}$	q
[EuL ¹]	1.00	1.34	0
[EuL ²]	0.70	1.76	0.73
[EuL ³]	1.04	1.59	0
[EuL ⁴]	1.00	1.34	0
[EuL ⁷]	1.04	1.59	0
[EuDO3A_Aza ¹]	0.57	2.02	1.2
[EuDO3A_Aza ²]	0.58	1.8	1
[EuPh ₃ _Aza ¹]	0.54	1.73	1
[EuPh ₃ _Aza ²]	0.60	1.86	1
[TbL ²]	2.24	2.65	0
[TbL ³]	1.56	1.72	0
[TbL ⁵]	2.00	2.38	0
[TbL ⁶]	2.25	2.48	0
[TbL ⁷]	1.56	1.72	0
[TbDO3A_Aza ¹]	1.82	2.73	0.60
[TbPh ₃ _Aza ¹]	1.65	2.89	1

Table 2.3: Lifetimes and q values (+/- 10 %) for complexes [EuL¹] – [LnL⁷]

The respective q values for complexes containing the pyridyl-azaxanthone show that the sensitising moiety binds in a bidentate fashion, through each pyridyl nitrogen atom. As a consequence, there are no directly bound water molecules, resulting in the long emissive lifetimes. For terbium pyrazoyl-azaxanthone complexes, q values of 0 are again consistent with bidentate binding in aqueous media. For complex [EuL²] a q value of 0.72 is consistent with pyridyl dissociation, leading to hydration of the lanthanide metal.

2.4.6 Luminescence Quantum Yields

Overall emission quantum yields, Φ_{em} (Equation 2.3), where Φ_{T} is the quantum yield of formation of the triplet state, η_{ET} is the efficiency of the energy transfer process, k_{o} is the natural radiative constant of the complex and τ_{obs} is the observed luminescence lifetime

of the lanthanide ion, (i.e. inverse of the radiative decay constant), were measured in water.

$$\Phi_{em} = \Phi_T \eta_{ET} k_0 \tau_{obs} \quad (2.3)$$

Measurements for complexes [EuL¹], [TbL²], [EuL⁴], [TbL⁵] and [TbL⁶] were made using an established integrated sphere method.²⁴ The remaining complexes have previously been determined relative to two standards: p-cresyl violet (in methanol) and rhodamine (in ethanol). Measurements were performed using an excitation wavelength corresponding to the lowest energy maximum in the absorption / excitation spectrum. These values are 365 nm for pyridyl-azaxanthone complexes, 355 nm for pyrazoyl-azaxanthone complexes and 348 nm for tetratriphenylene derivatives.

Complex	$\lambda_{exc} / \text{nm}$	Φ_{H_2O}
[EuL ¹]	375	15
[EuL ³]	348	18
[EuL ⁴]	375	25
[EuL ⁷]	348	16
[EuDO3A_Aza ¹]	336	7
[EuDO3A_Aza ²]	336	8
[EuPh ₃ _Aza ¹]	336	8
[EuPh ₃ _Aza ²]	336	9
[TbL ²]	355	15
[TbL ³]	348	33
[TbL ⁵]	355	46
[TbL ⁶]	355	54
[TbL ⁷]	348	40
[TbDO3A_Aza ¹]	336	24
[TbDO3A_Aza ²]	336	25
[TbPh ₃ _Aza ¹]	336	37
[TbPh ₃ _Aza ²]	336	28

Table 2.4: Emissive quantum yields (+/- 10 %) for complexes [EuL¹] – [LnL⁷]

The high quantum yields exhibited by complexes incorporating the dpqC chromophore are associated with a high quantum yield of formation of the triplet state and an efficient energy transfer step. For the analogous europium complexes, containing the pyridyl-azaxanthone, quantum yields are similar if not higher. For the DO3A complex $[\text{EuL}^1]$, emission is comparable; while in the cationic complex $[\text{EuL}^4]$ a higher efficiency is observed using a longer wavelength of excitation.

The pyrazoyl-azaxanthone chromophore is shown to exhibit strong terbium emission at pH 6.5 with quantum yields of 46 and 54 % for $[\text{TbL}^5]$ and $[\text{TbL}^6]$ respectively.

2.5 Conclusions

The pyridyl- and pyrazoyl-azaxanthenes allow long wavelengths of excitation and ligate to the lanthanide metal in a bidentate manner. For the pyrazoyl-azaxanthone systems, this binding has been shown to be sensitive to both pH and the presence of biological anions in aqueous solution. The pyridyl nitrogen atom possesses a pK_a of 6.5, and nitrogen dissociation leads to a dramatic decrease in lanthanide emission and subsequent increase in ligand fluorescence. Addition of endogenous bioactive anions to the analogous pyridyl-azaxanthone system results in a change in spectral form, with the formation of an intense $\Delta J = 2$ band, and the simplification of the $\Delta J = 4$ manifold.

Exclusion of directly bound water molecules in their respective complexes gives rise to long emissive lifetimes and high quantum yields. The pyridyl-azaxanthone only allows efficient europium sensitisation, while the pyrazoyl-azaxanthone systems give rise to emissive terbium complexes in aqueous medium. The impressive quantum yields of complexes $[\text{EuL}^4]$ (25 %) and $[\text{TbL}^5]$ (46 %) highlight these as suitable candidates with which to develop complexes suitable for conjugation (Chapter 7).

References

- 1.) R. B. Bates and S. T. Taylor, *J. Org. Chem.*, 1993, **58**, 4469.
- 2.) J. Lewis and T. D. O'Donoghue, *J. Chem. Soc. Dalton Trans.*, 1980, 736.
- 3.) P. Atkinson, K. S. Findlay, F. Kielar, R. Pal, D. Parker, R. A. Poole, H. Puschmann, S. L. Richardson, P. A. Stenson, A. L. Thompson and Y. Yu, *Org. Biomol. Chem.*, 2006, **4**, 1707.
- 4.) H. Adams, W. Z. Alsindi, G. M. Davies, M. B. Duriska, T. L. Easun, H. E. Fenton, J. M. Herrera, M. W. George, K. L. Ronayne, X. L. Sun, M. Towrie and M. D. Ward, *Dalton Trans.*, 2006, 39.
- 5.) A. Suzuki, *J. Organomet. Chem.*, 1999, **576**, 147.
- 6.) T. E. Barder, S. D. Walker, J. R. Martinelli and S. L. Buchwald, *J. Am. Chem. Soc.*, 2005, **127**, 4685.
- 7.) T. E. Barder and S. L. Buchwald, *Org. Lett.*, 2004, **6**, 2649.
- 8.) V. V. Grushin and H. Alper, *Chem. Rev.*, 1994, **94**, 1047.
- 9.) A. F. Littke and G. C. Fu, *Angew. Chem., Int. Edit.*, 2002, **41**, 4176.
- 10.) A. F. Littke, C. Dai and G. C. Fu, *J. Am. Chem. Soc.*, 2000, **122**, 4020.
- 11.) A. Lutzen and M. Hapke, *Eur. J. Org. Chem.*, 2002, 2292.
- 12.) J. R. Roppe, B. Wang, D. Huang, L. Tehrani, T. Kamenecka, E. J. Schweiger, J. J. Anderson, J. Brodtkin, X. Jiang, M. Cramer, J. Chung, G. Reyes-Manalo, B. Munoz and N. D. P. Cosford, *Bioorg. Med. Chem. Lett.*, 2004, **14**, 3993.
- 13.) G. Ulrich, S. Bedel, C. Picard and P. Tisnès, *Tetrahedron. Lett.*, 2001, **42**, 6113.
- 14.) U. S. Schubert, C. Eschbaumer and M. Heller., *Org. Lett.*, 2000, **2**, 3373.
- 15.) E. Brunet, O. Juanes, M. A. Rodriguez-Blasco, S. P. Vila-Nueva, D. Garayalde and J. C. Rodriguez-Ubis, *Tetrahedron. Lett.*, 2005, **46**, 78012.
- 16.) R. A. Poole, G. Bobba, M. J. Cann, J-C. Frias, D. Parker and R. D. Peacock, *Org. Biomol. Chem.*, 2005, **3**, 1013.
- 17.) J. C. Scaiano, D. Weldon, C. N. Pliva and L. J. Martinez, *J. Phys. Chem. A.*, 1998, **102**, 6898.
- 18.) L. J. Martinez and J. C. Scaiano, *J. Phys. Chem. A.*, 1999, **103**, 203.
- 19.) R. D. Shannon, *Acta. Crystallogr.*, 1976, **A32**, 751.
- 20.) R. S. Dickins, D. Parker, J. I. Bruce and D. J. Tozer, *Dalton. Trans.*, 2003, 1264.

- 21.) R. S. Dickins, S. Aime, A. S. Batsanov, A. Beeby, M. Botta, J. I. Bruce, J. A. K. Howard, C. S. Love, D. Parker, R. D. Peacock and H. Puschmann, *J. Am. Chem. Soc.*, 2002, **124**, 12697.
- 22.) R. S. Dickins, A. S. Batsanov, J. A. K. Howard, D. Parker, H. Puschmann and S. Salamano, *Dalton. Trans.*, 2004, 70.
- 23.) A. Beeby, I. M. Clarkson, R. S. Dickins, S. Faulkner, D. Parker, L. Royle, A.S. de Sousa, J. A. G. Williams and M. Woods, *J. Chem. Soc., Perkin Trans. 2.*, 1999, 493.
- 24.) L. Porrès, A. Holland, L-O. Pålsson, A. P. Monkman, C. Kemp and A. Beeby, *J. Fluoresc.*, 2006, **16**, 267.

CHAPTER THREE:

Dynamic Quenching Studies

Chapter Three: Dynamic Quenching Studies

Consideration of the mechanistic pathway that leads to sensitised lanthanide emission reveals three major processes for lanthanide excited state deactivation.¹

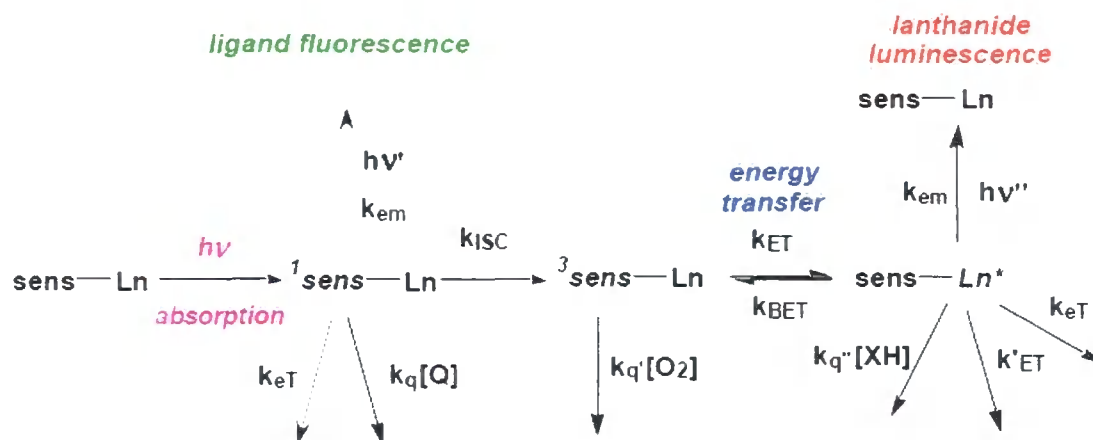


Figure 3.1: Photophysical processes during sensitised emission

The lanthanide excited state is prone to deactivation by vibrational energy transfer, involving energy matched X – H oscillators.² Of particular significance is the close proximity of O – H (water) and N – H (amine) groups. Quenching by energy transfer to an energy-matched acceptor group may also occur. Finally, lanthanide excited state deactivation may occur via *electron* or *charge transfer* processes. The following chapter describes a detailed study of dynamic quenching of macrocyclic complexes $[\text{EuL}^1]$ – $[\text{LnL}^7]$.

The terbium $^5\text{D}_4$ and europium $^5\text{D}_0$ excited states lie 244 and 206 kJ mol^{-1} above the ground state, and possess a natural lifetime of the order of milliseconds. As a result, this free energy may be harnessed to drive deactivation processes via an electron transfer process involving electron-rich species.³

The feasibility of such a quenching process can be assessed using the Rehm-Weller equation:⁴

$$n G_{\text{ET}} = nF [(E_{\text{ox}} - E_{\text{red}}) - E^{\text{Ln}^*} - e^2 / \epsilon r] \text{ J mol}^{-1} \quad (3.1)$$

where: E_{ox} is the oxidation potential of the electron donor (the quencher)

E_{red} is the reduction potential of the complex

E^{Ln*} is the energy of the lanthanide excited state (2.52 and 2.13 eV for Tb / Eu)

$e^2 / \epsilon r$ is a Coulombic attraction correction term correcting for formation of the transient charge-separated species and is usually < 0.2 eV

3.1 Cyclic Voltammetry

When considering the quenching mechanism involving electron transfer from a donor to a lanthanide complex, it is likely that charge or electron density will reside on the heterocyclic ligand rather than the lanthanide ion. In the limit, an electron-rich species may be fully oxidised and the metal complex, reduced. It is therefore important to consider the susceptibility of the pyridyl-, pyrazoyl-azaxanthenes and dpqC chromophores to accept electron density. The one-electron reduction potentials of pyridyl-azaxanthone, **8**, and pyrazoyl-azaxanthone, **11**, were measured by cyclic voltammetry. Measurements were performed in acetonitrile, containing 0.1 M $n\text{Bu}_4\text{NClO}_4$ as a supporting electrolyte and ferrocene / ferrocinium as an internal standard. The voltammograms for both the pyridyl and pyrazoyl-azaxanthone (**Figure 3.2**) chromophores are consistent with reversible reduction processes, occurring at $E_p = -1.78$ V and -1.92 V vs. Fc^+ / Fc respectively.

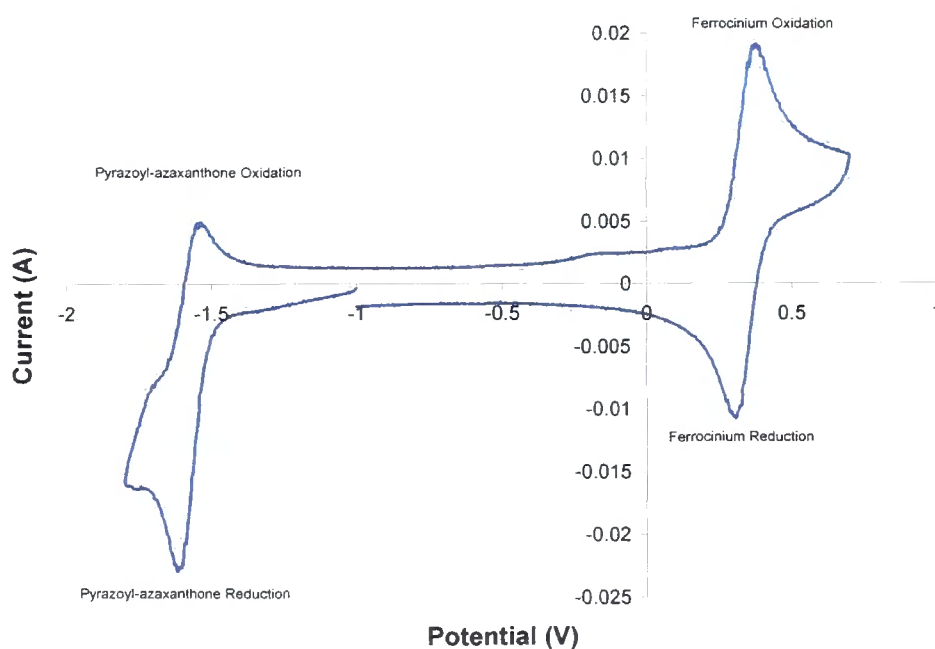


Figure 3.2: Cyclic voltammogram of pyrazoyl-azaxanthone, **11**, at 298 K in MeCN.
Scan rate of 50 mV/ s.

Chromophore	E_{red} vs Fc^+ / Fc	E_{red} vs NHE
2-Methyl-1-azaxanthone	- 2.00 V	~ - 1.60 V
7-tert-Butyl-2-methyl-1-azaxanthone	- 2.02 V	~ - 1.62 V
7-tert-Butyl-2-methylpyridyl-1-azaxanthone	- 1.78 V	~ - 1.38 V
7-tert-Butyl-2-methylpyrazoyl-1-azaxanthone	- 1.92 V	~ - 1.52 V
dpqC	n/d	~ - 1.07 V

Table 3.1: E_{red} potentials for derivatised azaxanthone chromophores

The reduction potential of the pyrazoyl-azaxanthone does not show significant difference from the parent azaxanthone moieties (i.e. $E_{red} \sim -1.60$ V vs ~ -1.52 V for NHE). The lower reduction potential for the pyridyl-azaxanthone suggests complexes incorporating this sensitiser may be slightly more susceptible to quenching by electron rich species.

It is important to emphasise that values for the reduction potential of the chromophores were measured in the ground state. In reality, the chromophore may accept an electron in the excited state of the complex. In addition, the reduction potential for Eu^{3+} (- 1.1 eV) is lower than that of the azaxanthone chromophores, suggesting that the lanthanide may be preferentially reduced. Therefore measurements of complex reduction potential are important to help clarify the actual electron transfer process.

3.2 Stern-Volmer Constants

A key issue in assessing the potential intracellular application of luminescent complexes is their sensitivity towards quenching by endogenous electron-rich species, either when free or protein bound (covalent or non-covalent). Studies have shown that it may be the extent to which the complexes are quenched in cellulo that limits their ability to be observed by fluorescence microscopy,⁵ as much as any preferential cellular uptake profile. For this reason, understanding and minimising intracellular quenching is extremely important in the development of emissive probes for biological media.

The anti-oxidants in the highest concentration within common cell types are ascorbate and urate. Each is typically found in the range of 0.1 to 0.2 mM concentration within most eukaryotic cells.⁵ Consequently, the quenching of complexes $[EuL^1] - [LnL^7]$, by

urate, ascorbate and the highly polarisable anion iodide, was studied. Stern-Volmer analysis was undertaken, where the Stern-Volmer quenching constant ($1/K_{sv}$ in mM) represents the concentration of quencher needed to reduce the observed lanthanide emission lifetime by 50 %. The Stern-Volmer equation is given below:

$$\tau_0 / \tau = 1 + k_q \tau_0 [Q] = 1 + k_{sv}[Q] \quad (3.2)$$

where the term τ_0 is the excited state lifetime in the absence of added quencher Q.

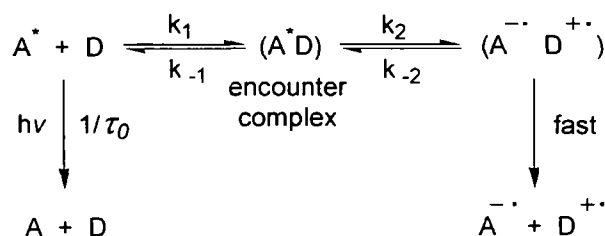
All measurements were made under standard conditions of 10 μ M complex at pH 7.4, with 0.1 M 4-(2-hydroxyethyl)-1-piperazineethanesulfonic acid (HEPES) and 10 mM NaCl at 298 K. The range of quencher concentration was selected carefully, in order for ideal Stern-Volmer behaviour to be observed (i.e. linear gradient). The ranges used were 1.0 – 5.0 mM for iodide, 0.1 – 0.5 mM for ascorbate, and 10 – 50 μ M for urate. These ranges were necessary to avoid curvature (i.e. limiting value), where the rate of change of τ_0 / τ versus concentration of quencher becomes constant.

Complex	Terbium K_{sv}^{-1} / mM	Europium K_{sv}^{-1} / mM
[LnL ²]	5.4	72
[LnL ³]	2.10	>10 ³
[LnL ⁵]	13.8	—
[LnL ⁷]	0.92	27
[LnDO3A_Aza ²]	53.5	125
[LnPh ₃ _Aza ¹]	9.2	278
[LnPh ₃ _Aza ²]	38.2	250

Table 3.2: Stern – Volmer quenching constants for iodide
(pH 7.4, 0.1 M HEPES, 10 mM NaCl, 298 K)

In examining these results, several conclusions can be drawn. Terbium complexes are much more sensitive to dynamic quenching than their europium analogues, coinciding with the greater ‘free’ energy of the terbium ⁵D₄ excited state. For complexes with a common chromophore, the cationic triamide complexes were quenched to a greater extent than their neutral DO3A comparators. This trend in sensitivity follows the favouring of collisional encounters by electrostatic attraction. For a common set of pendant cyclen arms, in which the nature of chromophore is varied, the sensitivity mirrors the reduction potential of the heterocyclic moiety. This is shown in the series of cationic complexes [TbPh₃_Aza¹], [TbL⁵] and [TbL⁷].

Iodide quenches lanthanide complexes such as those shown in **Figure 3.3**, in a classical collisional encounter model, first proposed by Rehm and Weller.^{6,7} The mechanism, which is shown in **Scheme 3.1**, involves reversible formation of an encounter complex, under diffusion control, is followed by electron transfer between the donor and the acceptor.



Scheme 3.1: Classical collisional quenching model

Quenching by this mechanistic pathway has been confirmed by performing quenching of iodide at varying temperatures and ionic strengths of NaCl. Studies showed that iodide quenching was highly dependent on each parameter. Such behaviour is consistent with a thermally activated collisional quenching model.³

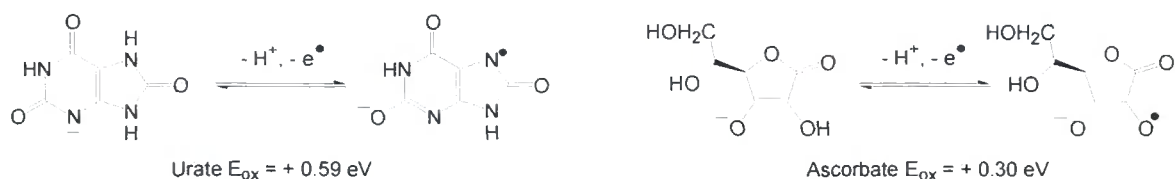
3.2.2 Quenching Studies with Ascorbate and Urate

Stern-Volmer quenching constants for complexes $[\text{EuL}^1]$ to $[\text{LnL}^7]$ by urate and ascorbate are collated in **Table 3.3**.

Tb Complex	Urate K_{sv}^{-1} / mM	Ascorbate K_{sv}^{-1} / mM
$[\text{TbL}^2]$	0.03	1.39
$[\text{TbL}^3]$	0.005	0.35
$[\text{TbL}^5]$	0.05	0.36
$[\text{TbL}^7]$	0.025	0.18
$[\text{TbDO3A_Aza}^2]$	0.012	0.57
$[\text{TbPh}_3\text{_Aza}^1]$	0.04	0.37
$[\text{TbPh}_3\text{_Aza}^2]$	0.02	0.30
$[\text{EuL}^2]$	0.45	8.43
$[\text{EuL}^3]$	0.11	2.92
$[\text{EuL}^7]$	0.07	0.39
$[\text{EuDO3A_Aza}^2]$	0.28	8.90
$[\text{EuPh}_3\text{_Aza}^1]$	0.60	1.50
$[\text{EuPh}_3\text{_Aza}^2]$	0.27	1.52

Table 3.3: Stern – Volmer quenching constants for urate and ascorbate
(pH 7.4, 0.1 M HEPES, 10 mM NaCl, 298 K)

As observed with iodide quenching, terbium complexes are quenched more strongly than their europium analogues. This behaviour is again consistent with a mechanism in which it is the excited state energy of the lanthanide that drives the quenching process. Interestingly, the complexes possess a high sensitivity towards urate quenching compared to ascorbate. Such behaviour does not correlate with the greater one oxidation potential of the latter ($E_{\text{ox}} = 0.30 \text{ eV}^8$ for ascorbate compared to $E_{\text{ox}} = + 0.59 \text{ eV}$ for urate).



Scheme 3.2: Half equations for urate (left) and ascorbate (right)

The apparent absence of correlation with Coulombic attraction indicates that urate and ascorbate quench by a mechanism where electrostatic encounter is not dominant. For example, urate is seen to quench the neutral DO3A complexes more strongly than their respective cationic analogues. Furthermore, urate quenching behaviour does not follow the typical one electron reduction potential of the heterocyclic chromophores, as observed with iodide. The most notable example is the reduced susceptibility of the pyrazoyl-azaxanthone complexes to quenching.

Evaluation of this behaviour, and the observation of non-linearity in urate and ascorbate quenching (e.g. **Figure 3.4**), suggests that these anions do not follow the classic Stern-Volmer model of quenching. This is further supported by the behaviour of urate quenching as a function of temperature and ionic strength.³ Given that a biomolecular association process is entropically unfavourable, higher temperatures should disfavour quenching, a trend which is the opposite of that expected for a purely collisionally controlled mechanism, for which the classical Stern – Volmer approximation holds.

$$\Delta G = \Delta H - T\Delta S \quad (3.3)$$

As the temperature was increased, quenching by urate became less apparent. In the case of iodide, a small positive activation energy, $E_a = +1.5 \text{ kJ mol}^{-1}$ was estimated, whereas for ascorbate and urate (-6.0 and -3.6 kJ mol^{-1} respectively) negative values were determined. The respective activation energies could then be calculated using Eyring's transition-state analysis. For urate and ascorbate, negative entropies of activation were estimated ($\Delta S = -260 \text{ J mol}^{-1} \text{ K}^{-1}$) in keeping with an associative process, rather than a collisional Stern – Volmer mechanism.

By considering the structure of urate, it is possible to postulate how it may form exciplex complexes. Urate is a mono anion, with an electron rich π -system where the charge is delocalised onto the nitrogen and amide oxygens. It is plausible to suggest that exciplex formation may involve a $\pi - \pi$ interaction between the electron poor chromophore and urate. Such a mechanism would be disfavoured by increased steric hindrance of the lanthanide complexes, thereby impeding the proximity of the urate anion. Analysis of the Stern-Volmer constants in **Table 3.3** indicates that steric inhibition created by the local ligand environment may well be a more influential factor than Coulombic interactions, in minimising urate quenching.

This hypothesis perhaps helps to explain the reduced tendency of the pyrazoyl-azaxanthone complexes to quenching. In this respect, the *tert*-butyl substituent of the azaxanthone moiety would be expected to provide some steric inhibition to the approach of a urate counter anion.

3.3 Non Covalent Protein Association and Inhibition of Quenching

Examination of complexes analogous to those in **Figure 3.3**, by either luminescence emission or gadolinium relaxivity titrations has highlighted the tendency of such complexes to bind reversibly with proteins.^{5,11,12} It is envisaged that if complexes exhibit an affinity towards a given protein, then if protein bound, they may exhibit a different sensitivity towards quenching. Serum albumins constitute the most common endogenous protein in mammalian cells. Therefore, the effect of protein binding on the susceptibility of complexes towards dynamic quenching is extremely appropriate in defining complexes suitable for cellular applications.

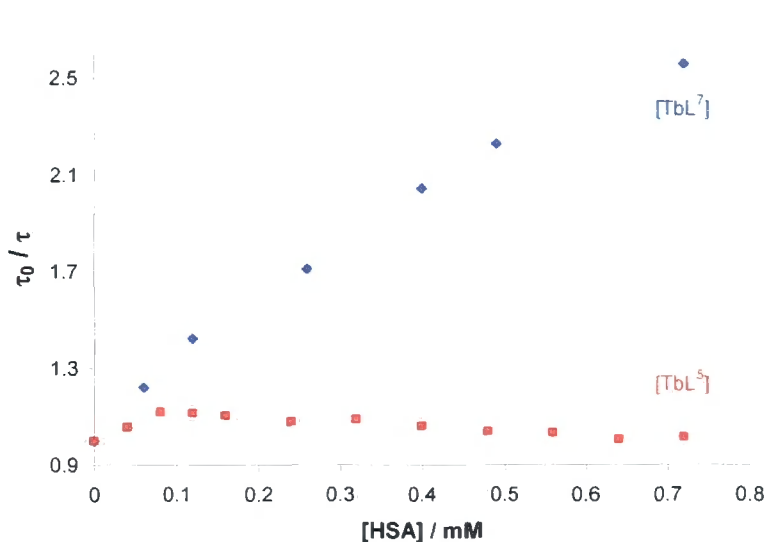


Figure 3.5: Plot of τ_0 / τ vs. [BSA] for [TbL⁵] and [TbL⁷]

Addition of bovine serum albumin to [EuL⁴] and [TbL⁵] resulted in less than a 10 % decrease in the respective europium and terbium emission lifetimes over the concentration range of 0.01 to 0.7 mM (Figure 3.5). It can therefore be concluded that non-covalent protein association does not quench the lanthanide excited states of complexes [EuL⁴] or [TbL⁵].¹³ However, the addition of BSA was shown to cause a reduction in the overall emission intensity of between 30 – 40 % for each complex. Such behaviour is consistent with a modest amount of quenching of the chromophore excited state, presumably via a charge transfer interaction with the pyridyl- / pyrazoyl-azaxanthenes.

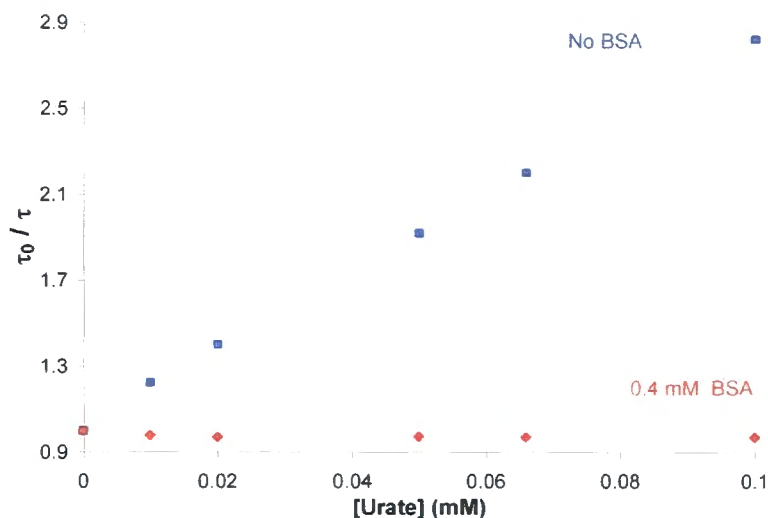


Figure 3.6: Plot of τ_0 / τ vs. $[\text{Urate}]$ for $[\text{TbL}^5]$ with and without 0.4 mM BSA

Interestingly, in the presence of 0.4 mM bovine serum albumin, 0.1 mM urate and 0.2 mM ascorbate, (pH 7.4, 298 K, 0.1 M HEPES), the emission lifetime of $[\text{TbL}^5]$ was within 10 % of its value in water, i.e. 2.1 ms, compared to 0.7 ms and 0.5 ms for $[\text{TbL}^7]$ and $[\text{TbPh}_3\text{Aza}^1]$ respectively, under the same conditions.¹³ Complex $[\text{EuL}^4]$ also exhibited similar behaviour (i.e. 1.00 ms in water, 0.89 ms in 0.4 mM BSA), thereby, demonstrating that non covalent protein association completely suppresses quenching of complexes $[\text{EuL}^4]$ and $[\text{TbL}^5]$ by endogeneous species (**Figure 3.6**). This characteristic augurs well for their application as cellular probes, and their ability to be observed and monitored by luminescence microscopy.

References

- 1.) R. A. Poole, G. Bobba, M. J. Cann, J-C. Frias, D. Parker and R. D. Peacock, *Org. Biomol. Chem.*, 2005, **3**, 1013.
- 2.) A. Beeby, I. M. Clarkson, R. S. Dickins, S. Faulkner, D. Parker, L. Royle, A. S. de Sousa, J. A. G. Williams and M. Woods, *J. Chem. Soc., Perkin Trans. 2.*, 1999, 493.
- 3.) F. Kielar, C. P. Montgomery, E. J. New, D. Parker, R. A. Poole, S. L. Richardson and P. A. Stenson, *Org. Biomol. Chem.*, 2007, **5**, 2975.
- 4.) A. Weller, *Pure Appl. Chem.*, 1968, **16**, 115.
- 5.) R. A. Poole, C. P. Montgomery, E. J. New, A. Congreve, D. Parker and M. Botta, *Org. Biomol. Chem.*, 2007, **5**, 2055.
- 6.) D. Rehm and A. Weller, *Ber. Bunsen. Phys. Chem.*, 1969, **73**, 834.
- 7.) D. Rehm and A. Weller, *Israel. J. Chem.*, 1970, **8**, 259.
- 8.) S. Steenken and P. Neta, *J. Phys. Chem.*, 1982, **86**, 3661.
- 9.) M. G. Kuzmin, *Pure Appl. Chem.*, 1993, **65**, 1653.
- 10.) M. Dossot, D. Burget, X. Allonas and P. Jacques, *New. J. Chem.*, 2001, **25**, 194.
- 11.) Y. Brettoniere, M. J. Cann, D. Parker and R. Slater, *Chem. Commun.*, 2002, 1930.
- 12.) J. Yu, D. Parker, R. Pal, R. A. Poole and M. J. Cann, *J. Am. Chem. Soc.*, 2006, **128**, 2294.
- 13.) C. P. Montgomery, D. Parker and L. Lamarque, *Chem. Commun.*, 2007, 3841.

CHAPTER FOUR:

Circularly Polarised Luminescence

Chapter Four: Circularly Polarised Luminescence (CPL)

In the series of cationic triamide complexes (e.g. $[\text{EuL}^4] - [\text{LnL}^7]$), the stereogenic centres at the carbon atoms are δ to the cyclen ring nitrogen atoms. As a result, lanthanide ions form pairs of stereoisomeric complexes of these ligands in aqueous solution. Investigation of this chirality is most conveniently signalled by optical methods, involving either differential absorption of left- or right-handed circularly polarised light (CD), or differential emission (CPL). Circularly dichroism (CD) probes the differential absorption of the ground state of the complex. However, the low molar absorption coefficients of lanthanide ions limit the utility of this technique. In contrast, circularly polarised luminescence probes the excited state structure of the complex, measuring the differential emission of left and right circularly polarised light. Since excitation of the complex is indirect (i.e. sensitised excitation) this technique does not suffer from the same limitations as CD.

CPL can provide a correlation between structural and electronic spectral information for lanthanide complexes in aqueous solution. Such data can give highly specific local information about the chiral environment of the lanthanide metal ion. Furthermore, changes in the circularly polarised luminescence from Eu (or Tb) excited states are sensitive to the nature (eg. Λ or Δ) and degree of local helicity, because this mixes the electric and magnetic dipole transition moments, enhancing the 'allowedness' (intensity) of a given transition.¹ Thus, conformational changes may, in principle, be signalled by changes in the form and polarisation of the CPL.²

4.1 Complex Conformational Studies

The lanthanide complexes of cyclen based systems may adopt a number of isomeric conformations. For example, upon complexation of 1,4,7,10-tetraazacyclododecane-tetra-acetate (or DOTA), four stereoisomeric complexes are formed. These systems exhibit two elements of chirality, defined as the torsion angles about the macrocyclic ring N-C-C-N (which may be $+60^\circ$ (δ) or -60° (λ)) and about the pendant arm N-C-C-O groups (which may be $+30^\circ$ (Δ) or -30° (Λ)). Consequently, two pairs of enantiomers exist, with a positive δ or negative λ torsion angle confirmation in the five-ring NLnN chelates, and a clockwise Δ or anticlockwise Λ layout of the four pendant arms (**Figure 4.1**).³

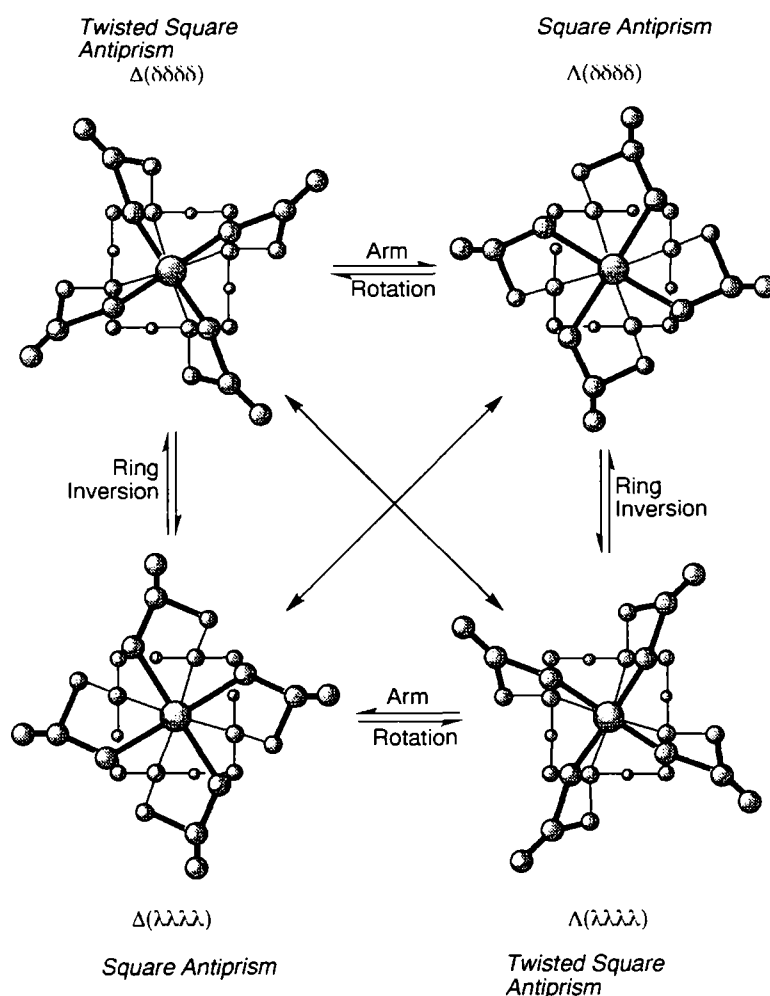


Figure 4.1: Four stereoisomers of Ln-DOTA complexes, showing ring inversion and pendant arm rotation⁴

The stereoisomers can adopt one of two geometries: $\Lambda(\delta\delta\delta\delta)$ and $\Delta(\lambda\lambda\lambda\lambda)$ each adopt a square antiprismatic (SAP) geometry, with a twist angle of approximately 40° between the oxygen and nitrogen planes, while $\Lambda(\lambda\lambda\lambda\lambda)$ and $\Delta(\delta\delta\delta\delta)$ adopt a twisted square antiprismatic (TSAP) geometry, with a twist angle of approximately 29° . In solution, the conformational mobility of the ligand allows intramolecular exchange between the Δ and Λ isomers. This may occur via ring inversion (δ / λ exchange) followed by independent reorientation of the ring pendant arms (Λ / Δ exchange), possibly via a tricapped trigonal prismatic intermediate. Such processes are often slow with respect to the timescale of NMR and luminescence emission, with the position of equilibrium between the two forms determined by their respective conformational free energies.

The introduction of a chromophore and more sterically demanding pendant arms onto cyclen can impart conformational rigidity. In such rigid, non-fluxional complexes, arm rotation becomes inhibited, and ring inversion slow, leading to preferential formation of one stereoisomer in solution.

4.2 CPL Spectra

The CPL spectra for $(SSS)\text{-[EuL}^7\text{]}$ and $(RRR)\text{-[EuL}^7\text{]}$ (and analogous terbium complexes), as their chloride salts in D_2O , revealed the expected mirror image behaviour (Figures 4.2 and 4.3).

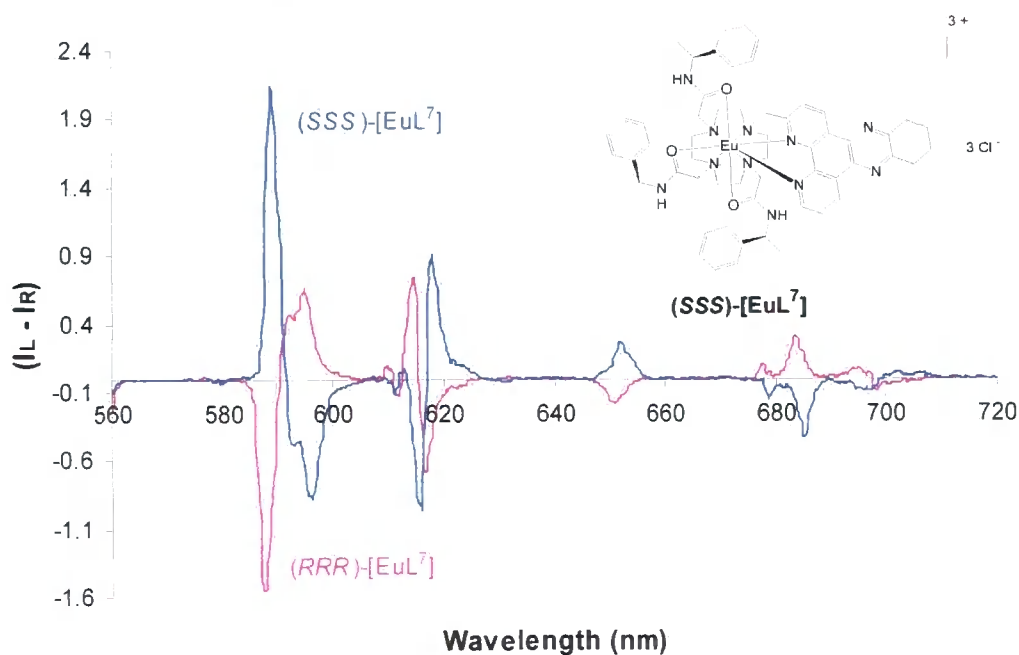


Figure 4.2: Mirror image CPL spectra for $(SSS)\text{-}\Delta\text{-[EuL}^7\text{]}$ (blue) and $(RRR)\text{-}\Delta\text{-[EuL}^7\text{]}$ (red) (295 K, D_2O , $15\mu\text{M}$)

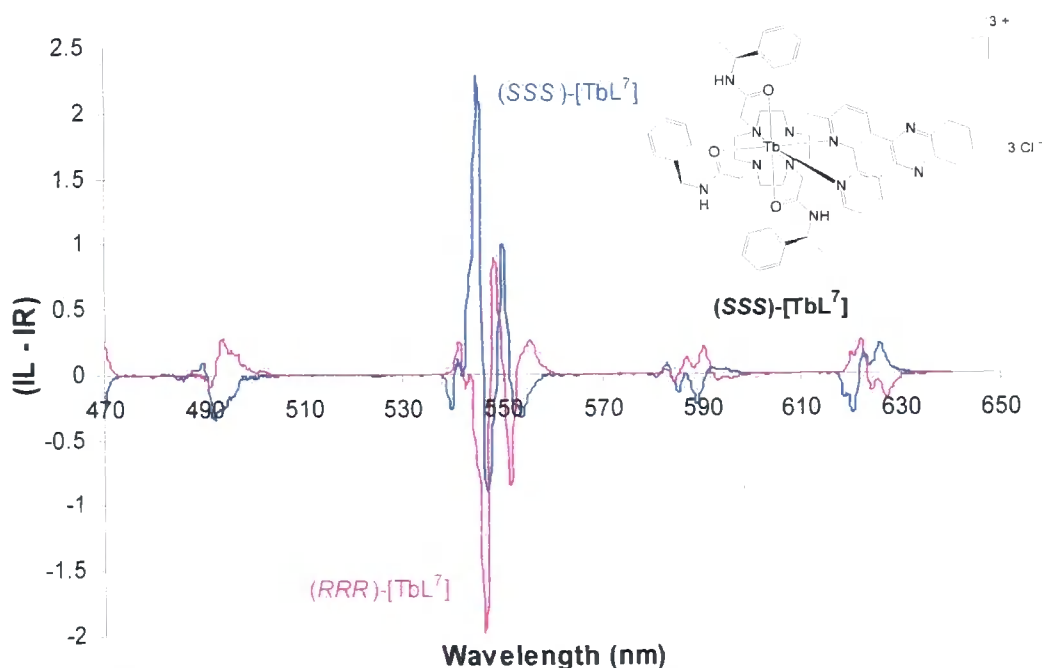
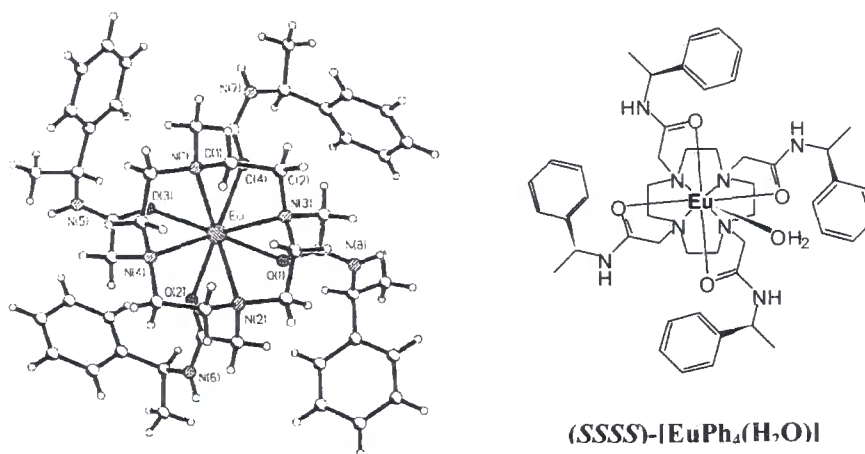


Figure 4.3: Mirror image CPL spectra for $(SSS)\text{-}\Delta\text{-[TbL}^7\text{]}$ (blue) and $(RRR)\text{-}\Delta\text{-[TbL}^7\text{]}$ (red) (295 K, D_2O , $15\mu M$)

The sign and sequence of the transitions observed in the CPL of $(SSS)\text{-[EuL}^7\text{]}$ (and $(SSS)\text{-[TbL}^7\text{]}$) are consistent to those observed for the related C_4 -symmetric tetraamide $(SSSS)\text{-[EuPh}_4\text{(H}_2\text{O)]}$ complex shown below:



The parent tetraamide $(SSSS)\text{-[EuPh}_4\text{(H}_2\text{O)]}$ has been shown to exist as one predominant isomer ($> 90\%$) in aqueous solution.⁵ The preferred isomer, whose absolute configuration has been verified by X-ray crystallography, is a regular monocapped square antiprismatic structure. It can be concluded that for the series $[\text{EuL}^7]$

and $[\text{TbL}^7]$, a similar square antiprismatic structure is adopted, whereby the (SSS) - $[\text{LnL}^7]$ complex possesses a Δ helicity and the (RRR) - $[\text{LnL}^7]$ complex a Λ helicity.

In contrast, examination of the CPL spectra for complexes (SSS) - $[\text{TbL}^5]$ and (RRR) - $[\text{TbL}^5]$ reveals quite different behaviour to $[\text{LnL}^7]$ (Figure 4.4). This opposing helicity around the lanthanide metal is most probably attributed to the sterically demanding chromophore, which appears to impose a twisted square antiprismatic geometry on the complexes. Consequently, (SSS) - $[\text{TbL}^5]$ can be assigned a Λ helicity, while (RRR) - $[\text{TbL}^5]$ possesses a Δ helicity.

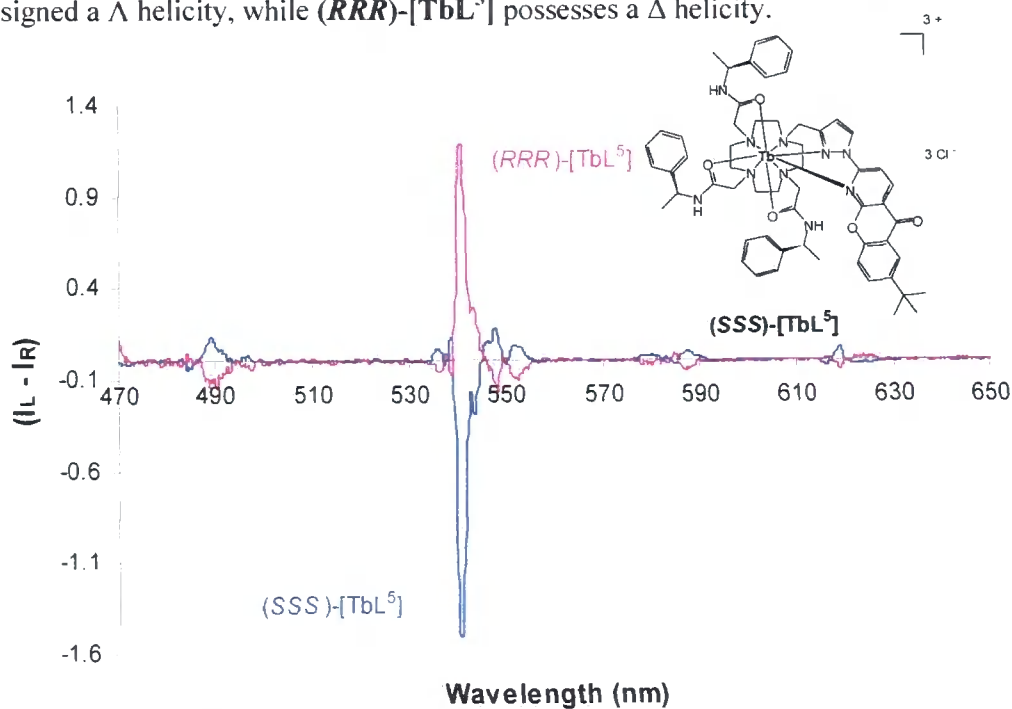


Figure 4.4: Mirror image CPL spectra for (SSS) - Λ - $[\text{TbL}^5]$ (blue) and (RRR) - Δ - $[\text{TbL}^5]$ (red) (295 K, D_2O , $15\mu M$)

4.3 Emission Dissymmetry Factors

In circularly polarised luminescence, the emission dissymmetry factor, g_{em} , measures the ‘degree of chirality’ sensed by an electronic transition. Dissymmetry factors are described by Equation 4.1:

$$g_{em} = 2(I_L - I_R) / (I_L + I_R) \quad (4.1)$$

where $I_{L(R)}$ is the intensity of the left (or right) circularly polarised luminescence component.

The largest dissymmetry factors are exhibited by transitions which are magnetic-dipole allowed and electric-dipole forbidden, whereas the most intense CPL transitions tend to be both magnetic and electric dipole allowed.³

Emission dissymmetry factors were determined for complexes (SSS)-[EuL⁴], (SSS)-[TbL⁵] and (SSS)-[LnL⁷] (Table 4.1).

Complex	$g_{em}^{\lambda} / \lambda$ (nm)		
	$\Delta J = 1$ (λ)	$\Delta J = 2$ (λ)	$\Delta J = 4$ (λ)
(SSSS)-[EuPh ₄ (H ₂ O)]	-0.09 (594)	+0.08 (614)	-0.10 (688)
(SSS)-[EuL ⁴]	-0.14 (596)	+0.03 (615)	-0.003 (688)
(SSS)-[EuL ⁷]	-0.16 (595)	-0.04 (614)	-0.08 (686)

Complex	$g_{em}^{\lambda} / \lambda$ (nm)		
	$\Delta J = 6$ (λ)	$\Delta J = 5$ (λ)	$\Delta J = 4$ (λ)
(SSSS)-[TbPh ₄ (H ₂ O)]	n/d	+0.12 (545)	n/d
(SSS)-[TbL ⁵]	+0.02 (489)	-0.13 (540)	+0.01 (583)
(SSS)-[TbL ⁷]	-0.03 (492)	+0.15 (544)	-0.05 (589)

Table 4.1: Emission dissymmetry factors for Tb and Eu complexes⁶

The magnitude of the observed emission dissymmetry factors for each complex is similar to (SSSS)-[EuPh₄(H₂O)], suggesting a similar degree of helical twist about the principal axis. The solution structures of each of the (SSS)-[EuL⁴] and (SSS)-[LnL⁷] enantiopure complexes possess a Δ -configuration, in a regular mono-capped square antiprismatic structure. In contrast, the (SSS)-[TbL⁵] pyrazoyl-azaxanthone is shown to have a different helicity around the metal centre, with the complex preferring a Λ configuration. Similar behaviour has been shown in nonadentate dpqC complexes, with (*S*)-phenylalanine pendant arms.⁷ Here, the (SSS) enantiopure complex was shown to possess a unique distorted structure, with an amide carbonyl oxygen occupying the capping apical site of the monocapped aquare-antiprismatic polyhedron. Thus, it can be concluded that the pyrazoyl-azaxanthone complex (SSS)-[TbL⁵] favours an alternative (and possibly distorted) geometry, compared to analogous pyridyl-azaxanthone and dpqC complexes.

4.4. Protein Association

Circularly polarised luminescence has previously been utilised to characterise reversible anion binding to lanthanide complexes.² In seeking to develop enantiopure emissive probes for cellular applications, it was necessary to study complexes $[\text{EuL}^4]$ to $[\text{LnL}^7]$ in a biological context. Non-covalent protein associations with complexes $[\text{EuL}^4]$ and $[\text{TbL}^5]$, (Chapter 3) can reduce their susceptibility towards charge or electron transfer quenching.^{8,9} Consequently, circularly polarised emission spectra were measured for each complex in the presence of human (or bovine) serum albumin.

With $(\text{SSS})\text{-}[\text{EuL}^4]$, no change in emission polarisation or spectral form was observed, over a protein concentration range of 0.03 – 0.3 mM (**Figure 4.5**).

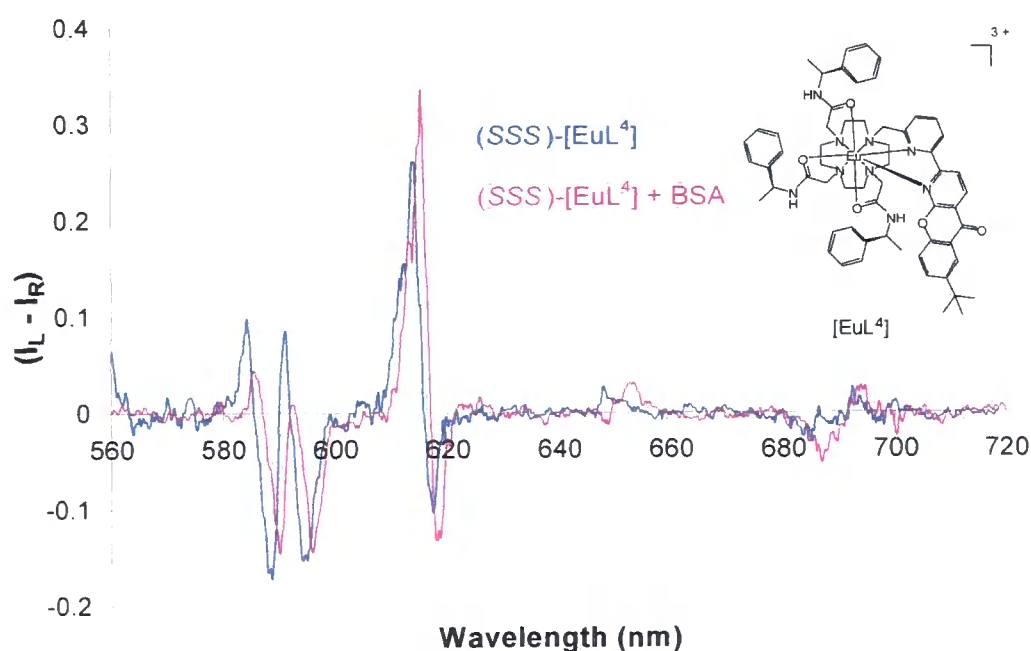


Figure 4.5: CPL spectra for $(\text{SSS})\text{-}[\text{EuL}^4]$; (295 K, D_2O , 15 μM) in the presence and absence of 10 equivalents of BSA (blue = without; red = with BSA)

For complexes $(\text{SSS})\text{-}\Lambda\text{-}[\text{TbL}^5]$ and $(\text{RRR})\text{-}\Delta\text{-}[\text{TbL}^5]$, addition of protein was accompanied by a large change in the $^5\text{D}_4 \rightarrow ^7\text{F}_5$ band, centred at 545 nm (**Figure 4.6**). In the absence of protein, a dominant single peak is observed, which becomes more structured upon protein addition.

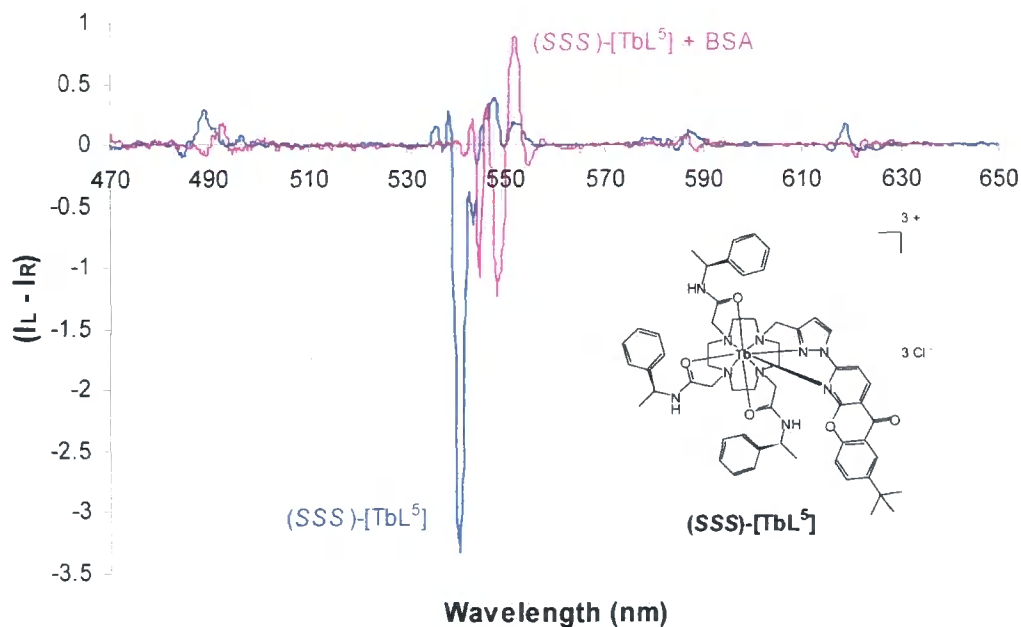


Figure 4.6: CPL spectra for $(SSS)\text{-[TbL}^5\text{]}$; (295 K, D_2O , $15\ \mu\text{M}$) in the presence and absence of 10 equivalents of BSA (blue = without; red = with BSA)

The most interesting behaviour was observed with the tetraazatriphenylene complexes $[\text{LnL}^7]$. The circular polarised luminescence spectra of $(SSS)\text{-}\Delta\text{-[TbL}^7\text{]}$ and $(RRR)\text{-}\Delta\text{-[TbL}^7\text{]}$ in the presence of $30\ \mu\text{M}$ BSA are shown in **Figures 4.7** and **4.8**.

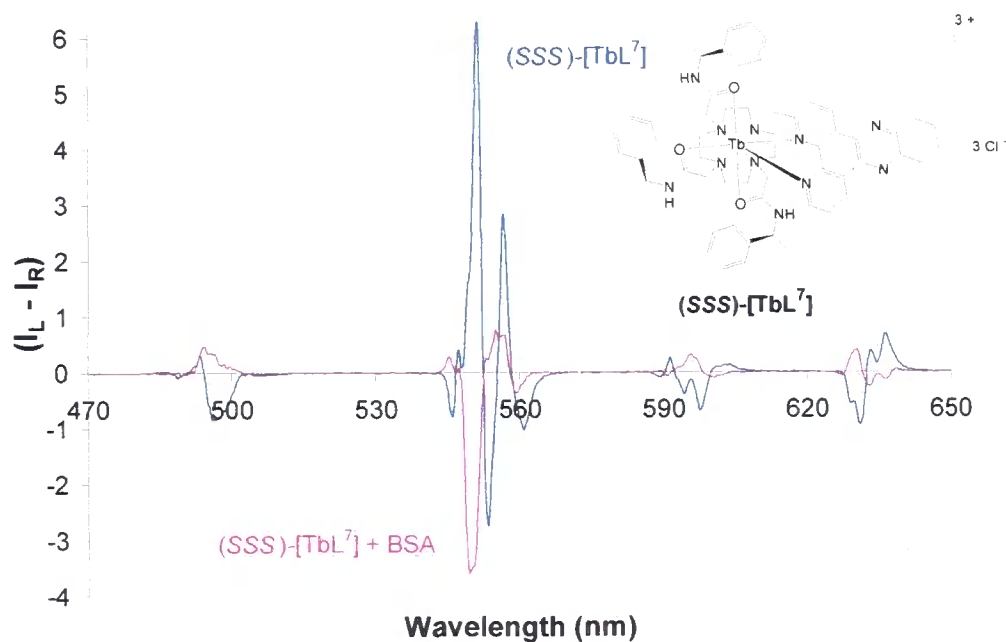


Figure 4.7: CPL spectra for $(SSS)\text{-[TbL}^7\text{]}$; (295 K, D_2O , $15\ \mu\text{M}$) in the presence and absence of 10 equivalents of BSA (blue = without; red = with BSA)

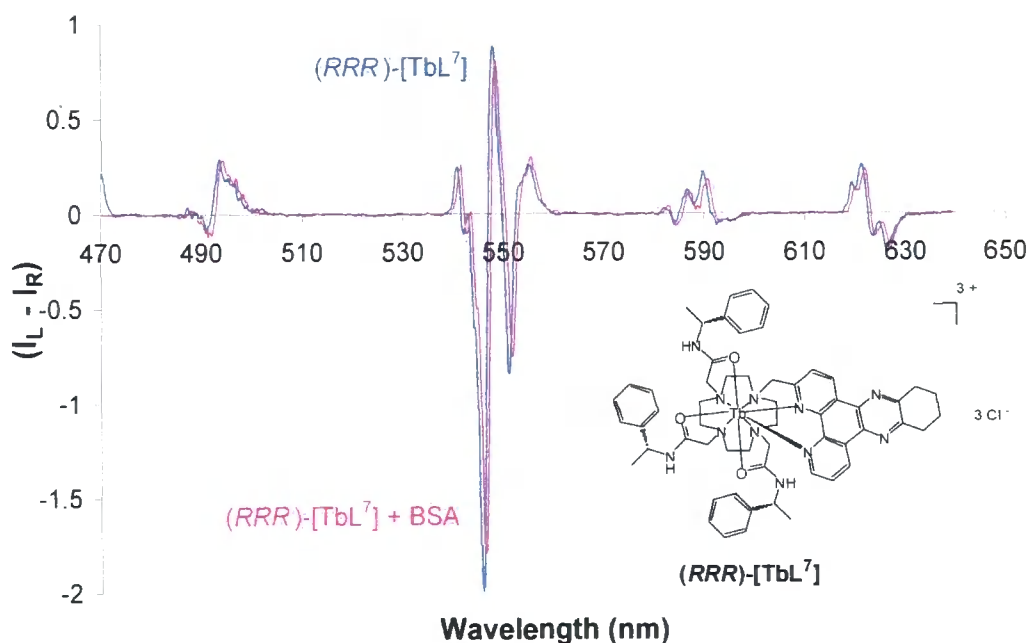


Figure 4.8: CPL spectra for $(RRR)\text{-[TbL}^7\text{]}$; (295 K, D_2O , $15\ \mu\text{M}$) in the presence and absence of 10 equivalents of BSA (blue = without; red = with BSA)

With the Λ isomer (**Figure 4.8**), addition of protein gave no change in emission polarisation or spectral form. Only an apparent reduction in signal intensity was evident, consistent with dynamic quenching of the terbium excited state by the protein. In contrast to the Λ isomer, the Δ isomer gave rise to very different behaviour (**Figure 4.7**). An inversion of the sign of the emission polarisation was observed, which was most well-defined in the magnetic dipole-allowed $^5D_4 \rightarrow ^7F_5$ transition around 545 nm. This behaviour is consistent with an inversion of the helicity of the complex in the protein bound form, for the Δ isomer only.¹⁰ This unique behaviour was not shown by structurally-related tetraazatriphenylene analogues, suggesting that the steric environment created by the cyclen pendant arms, in addition to the chromophore, plays a pivotal role in determining this complex – protein interaction.

Parallel experiments were performed with $(SSS)\text{-}\Delta\text{-[EuL}^7\text{]}$ and $(RRR)\text{-}\Lambda\text{-[EuL}^7\text{]}$. Again, protein addition led to a reduction in the overall emission intensity for each complex, with no change in CPL spectral form for the Λ isomer. The Δ isomer showed complementary behaviour to the terbium analogue, with dramatic changes in sign and form of the CPL spectrum (**Figure 4.9**). This behaviour suggests that upon protein association, complexes $(SSS)\text{-}\Delta\text{-[TbL}^7\text{]}$ and $(SSS)\text{-}\Delta\text{-[EuL}^7\text{]}$ undergo both

helicity inversion and changes in the relative orientation of ligand donors around the metal centre.^{10,11}

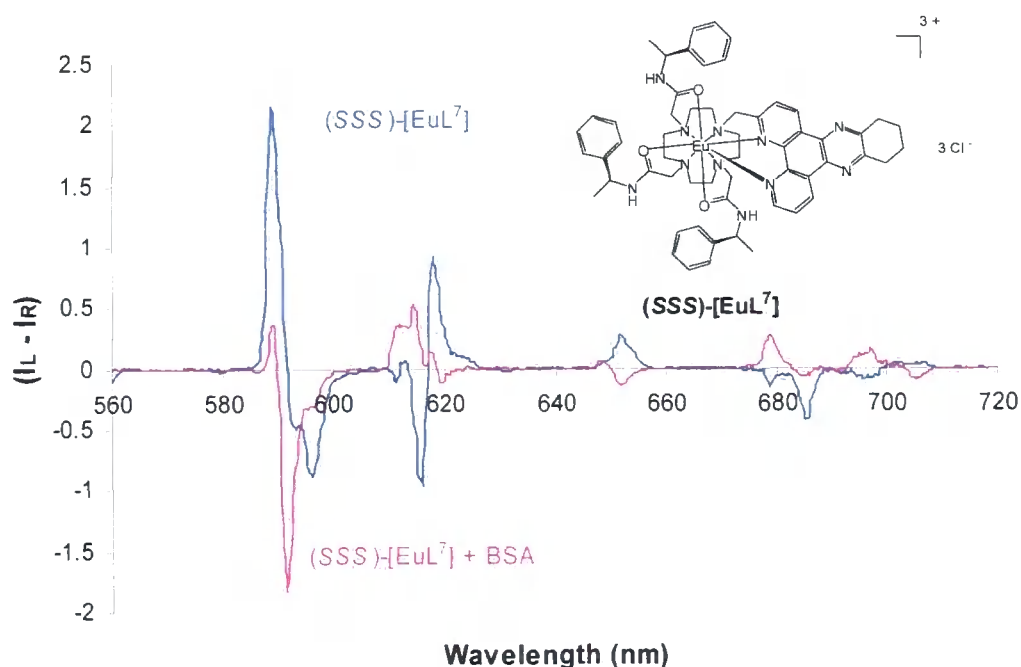
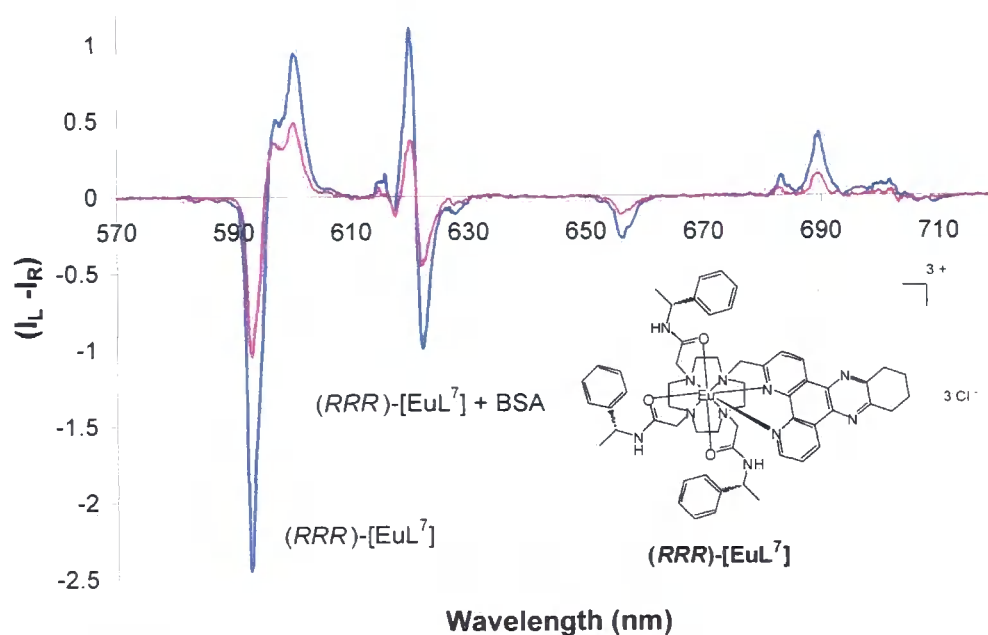


Figure 4.9: CPL spectra for (SSS) -[EuL⁷] (above) and (RRR) -[EuL⁷] (below); (295 K, D₂O, 15 μM) in the presence and absence of 10 equivalents of BSA (blue = without; red = with BSA)



The different enantiomeric behaviour of complexes (SSS) -[LnL⁷] and (RRR) -[LnL⁷] was mirrored in the reduction of both the intensity and lifetime of the

respective complexes after incremental addition of BSA. For $(SSS)\text{-}\Lambda\text{-[TbL}^7\text{]}$ a binding isotherm was interpreted in terms of an apparent 1 : 1 binding constant ($\log K = 5.1$, 298 K, pH 7.4, HEPES 0.1 M), while $(RRR)\text{-}\Lambda\text{-[TbL}^7\text{]}$ gave different behaviour, consistent with stepwise formation of various adducts of lower affinity (Figure 4.10). As discussed previously, addition of BSA or HSA to $(SSS)\text{-[EuL}^4\text{]}$ or $(SSS)\text{-[TbL}^5\text{]}$ is not accompanied by any significant changes in emission lifetimes (Figure 4.10).

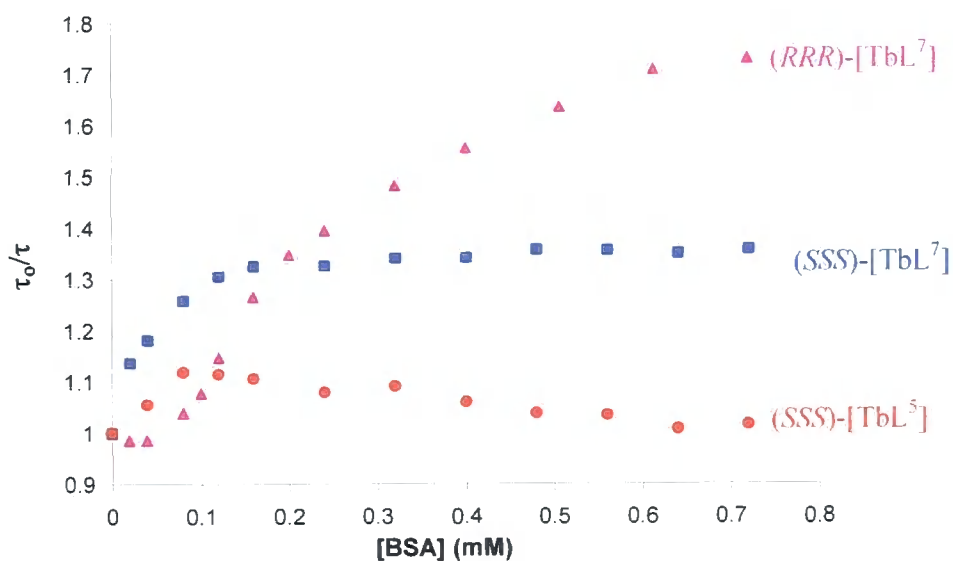


Figure 4.10: Quenching of the observed terbium emission lifetime, τ , (τ_0 – no added protein) as a function of added BSA for $(SSS)\text{-[TbL}^5\text{]}$ (red), $(SSS)\text{-[TbL}^7\text{]}$ (blue) and $(RRR)\text{-[TbL}^7\text{]}$ (pink) (298 K, pH 7.4, 10 mM NaCl, 0.1 M HEPES, 30 μM [complex])

4.5 HSA Binding Studies

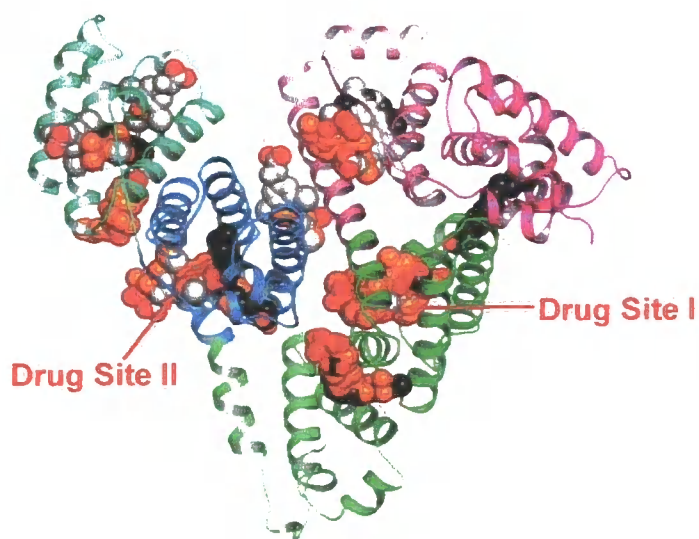


Figure 4.11: Summary of the ligand binding capacity of HSA as defined by crystallographic studies.¹²

Serum albumin contains two well defined drug binding sites, referred to as drug site I and II respectively.^{13,14} Warfarin (K_d 4 μM) is understood to probe drug site I, while *N*-dansylsarcosine (K_d 6 μM) is known to selectively bind drug site II.^{14,15} It was thought that these two compounds could be used as competitive probes to distinguish whether complexes $(SSS)\text{-}[\text{LnL}^7]$ have a preferential binding association with HSA. Crystallographic studies of complexes of HSA have suggested that ‘drug site II’ is the more stereo-differentiating binding site in serum albumin.¹²

An appropriate method for measuring protein binding is by examining changes in proton relaxivity of gadolinium complexes in aqueous solution. The proton relaxivity r_{1p} , of $(SSS)\text{-}\Delta\text{-}[\text{GdL}^7]$ and $(RRR)\text{-}\Lambda\text{-}[\text{GdL}^7]$ is 3.1 $\text{mM}^{-1} \text{s}^{-1}$ (60 MHz, 310 K), and increased to 13 $\text{mM}^{-1} \text{s}^{-1}$ in each case, in the presence of 0.4 mM human serum albumin. Incremental addition of warfarin (up to 3 mM) to solutions of $(SSS)\text{-}\Delta\text{-}[\text{GdL}^7]$ and $(RRR)\text{-}\Lambda\text{-}[\text{GdL}^7]$ containing protein caused less than a 10 % change in the observed relaxivity.

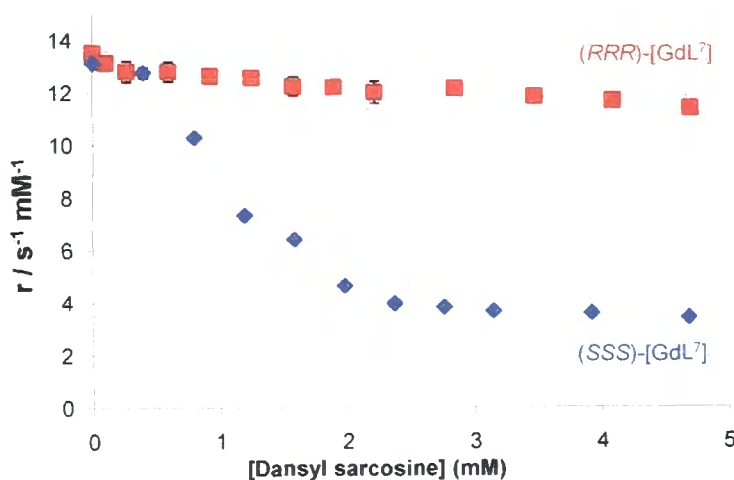


Figure 4.12: Variation of proton relaxivity (310 K, 60 MHz, 0.4 mM HSA, 1.7 mM $[\text{GdL}^7]$) as a function of added *N*-dansylsarcosine for $(\text{SSS})\text{-[GdL}^7]$ (blue diamonds) and $(\text{RRR})\text{-[GdL}^7]$ (red squares)

However, addition of *N*-dansylsarcosine over the same concentration range, resulted in a reduction of the r_{1p} of $(\text{SSS})\text{-}\Delta\text{-[GdL}^7]$ to its original unbound value ($3.1 \text{ mM}^{-1} \text{ s}^{-1}$). In contrast, addition of *N*-dansylsarcosine to the $(\text{RRR})\text{-}\Delta\text{-[GdL}^7]$ protein solution led to less than a 15 % reduction in r_{1p} (**Figure 4.12**). This set of experimental data is consistent with the selective reversible binding of $(\text{SSS})\text{-}\Delta\text{-[LnL}^7]$ complexes to ‘drug site II’ of serum albumin.¹⁰ During this process, the complex structure is altered and helicity reversed to enable efficient binding. This conclusion supports previous evidence suggesting ‘drug site II’ is the most stereo-differentiating binding site.¹² Future microscopic techniques may allow these complexes to be utilised for tracking protein association *in vitro* and in living cells, via circularly polarised luminescence measurements.

References

- 1.) E. Huskowska, C. L. Maupin, D. Parker, J. A. G. Williams and J. P. Riehl, *Enantiomer.*, 1997, **2**, 381.
- 2.) J. I. Bruce, R. S. Dickins, L. J. Govenlock, T. Gunnlaugsson, S. Lopinski, M. P. Lowe, D. Parker, R. D. Peacock, J. J. B. Perry, S. Aime and M. Botta, *J. Am. Chem. Soc.*, 2000, **122**, 9674.
- 3.) J. I. Bruce, D. Parker, S. Lopinski and R. D. Peacock, *Chirality.*, 2002, **14**, 562.
- 4.) R. S. Dickins, J. A. K. Howard, C. L. Maupin, J. M. Moloney, D. Parker, R. D. Peacock, J. P. Riehl and G. Siligardi, *New. J. Chem.*, 1998, **22**, 891.
- 5.) R. S. Dickins, J. A. K. Howard, C. L. Maupin, J. M. Moloney, J. P. Riehl, G. Gilligardi and J. A. G. Williams, *Chem. Eur. J.*, 1999, **5**, 1095.
- 6.) R. A. Poole, G. Bobba, M. J. Cann, J-C. Frias, D. Parker and R. D. Peacock, *Org. Biomol. Chem.*, 2005, **3**, 1013.
- 7.) E. J. New, D. Parker and R. D. Peacock, *Dalton Trans.*, *In Press*
- 8.) C. P. Montgomery, D. Parker and L. Lamarque, *Chem. Commun.*, 2007, **3841**.
- 9.) R. A. Poole, C. P. Montgomery, E. J. New, A. Congreve, D. Parker and M. Botta, *Org. Biomol. Chem.*, 2007, **5**, 2055.
- 10.) C. P. Montgomery, E. J. New, D. Parker and R. D. Peacock, *Chem. Commun.*, 2008, 4261.
- 11.) J. I. Bruce, R. S. Dickins, D. Parker and D. J. Tozer, *Dalton Trans.*, 2003, 1264.
- 12.) J. Ghuman, P. A. Zunszain, I. Petitpas, A. A. Bhattacharya, M. Otagiri and S. Curry, *J. Mol. Biol.*, 2005, **353**, 38.
- 13.) G. Sudlow, D. J. Birkett and D. N. Wade, *Mol. Pharmacol.*, 1975, **11**, 824.
- 14.) G. Sudlow, D. J. Birkett and D. N. Wade, *Mol. Pharmacol.*, 1976, **12**, 1052.
- 15.) P. Caravan, G. Parigi, J. M. Chasse, N. J. Cloutier, J. J. Ellison, R. B. Lauffer, C. Luchinat, S. A. McDermid, M. Spiller and T. J. McMurray, *Inorg. Chem.*, 2007, **46**, 6632.

CHAPTER FIVE:

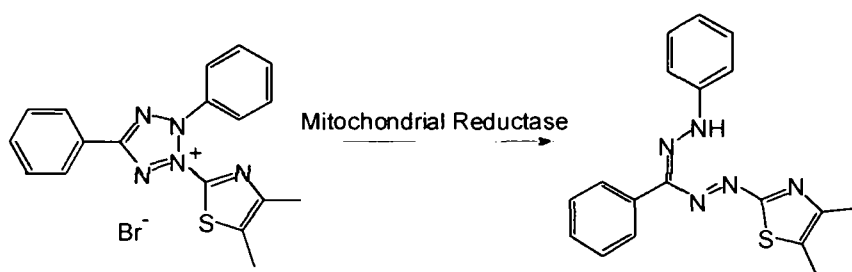
Cellular Studies

Chapter Five: Cellular Studies

In the rational development of lanthanide complexes as cellular probes, it is important to understand their mechanisms of cell entry. In addition, a link must be established between the structure of the complex and its compartmentalisation profile, cytotoxicity and any observed intracellular trafficking. The following chapter describes aspects of the biological analysis of complexes $[\text{EuL}^4]$ and $[\text{TbL}^5]$ as potential cellular probes.

5.1 Cellular Cytotoxicity Profiles

The relative cytotoxicity of complexes was assessed in mouse skin fibroblast (NIH-3T3) cells using an established MTT assay.¹ This spectroscopic technique relies on the conversion of 3-(4,5-dimethylthiazol-3-yl)-2,5-diphenyltetrazolium bromide to a purple 'formazan' product by mitochondrial dehydrogenase enzymes within viable cells.



Scheme 5.1: Formation of purple 'formazan' used in MTT assays

Following a 24 h incubation of at least 10,000 cells with varying concentrations of complex, the insoluble 'formazan' was dissolved in DMSO and quantified spectrophotometrically in a 96-well plate reader to yield an IC_{50} value. This IC_{50} value was defined as the complex concentration required to reduce the absorbance to 50 % of that in the untreated control. The procedures were repeated at least three times for each complex, and averaged to provide the respective IC_{50} values.

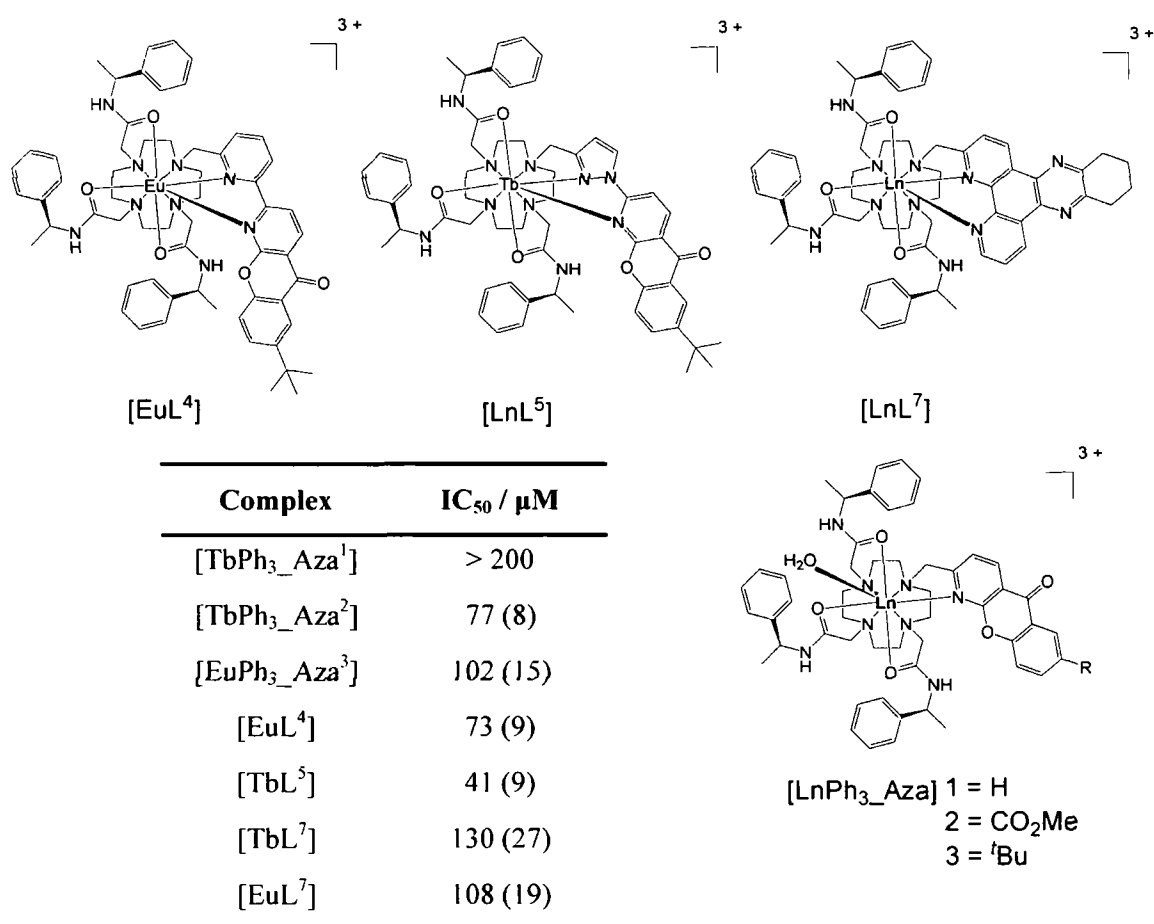


Table 5.1: IC₅₀ values for a range of triamide cationic lanthanide complexes ²

Examination of the IC₅₀ values in **Table 5.1** shows complexes possessing a *tert*-butyl substituent exhibit the highest degree of toxicity. For example, complexes [EuL⁴], [TbL⁵] and [EuPh₃_Aza³] show higher IC₅₀ values than analogous unsubstituted azaxanthone and tetraazatriphenylene complexes.

Flow cytometry experiments with the complexes [EuL⁴] and [TbL⁵] were performed to help distinguish the mechanism by which these complexes impose cell death (i.e. necrosis or apoptosis).³ Apoptosis is a form of programmed cell death, triggered by a series of biochemical events. This mechanism is signalled by an increase in surface phospho-serine residues which lead to changes in cell morphology and eventual cell death. In contrast, necrosis is a form of traumatic cell death characterised by loss of outer and nuclear membrane integrity, resulting from acute cellular injury.⁴

Each complex was studied in Chinese hamster ovarian (CHO) and NIH-3T3 cells. Results were compared to an untreated control and to controls for necrosis (0 °C, 70 % EtOH, 3 h) and apoptosis (1 μM staurosporine, 3 h). Interestingly, despite possessing similar structures, in which only the ‘linkage’ heterocyclic ring has changed, complexes [EuL⁴] and [TbL⁵] showed different behaviour (**Figure 5.1**).

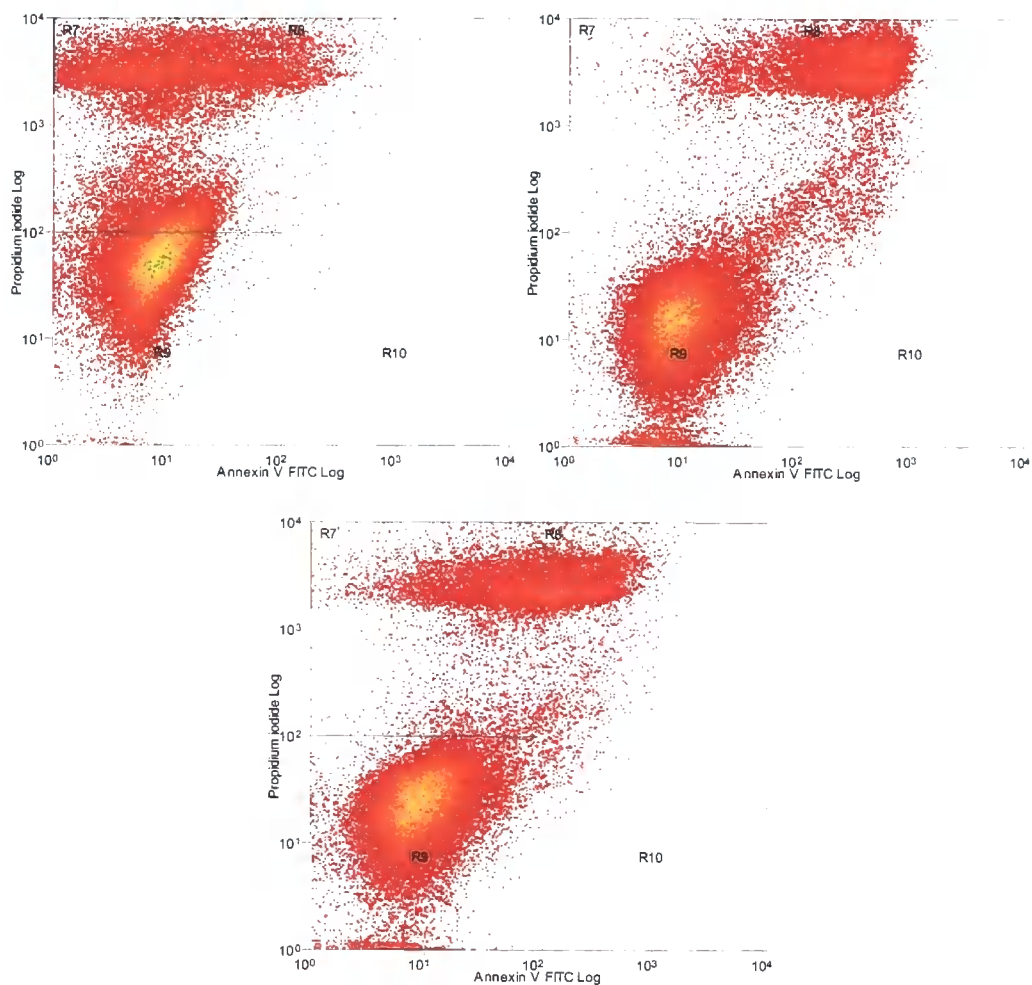


Figure 5.1: *Left: Flow cytometry plot of cells, 24 h after incubation with [TbL⁵] (200 μM); right: plot of cells after 24 h incubation with [TbPh₃_Aza³] (200 μM); middle: plot of cells after 24 h incubation with [EuL⁴] (200 μM). (In each case flow cytometry ‘dot images’ correlate fluorescence of an Annexin-FITC conjugate (apoptosis marker) on the x-axis, with propidium iodide fluorescence (necrosis marker) on the y-axis; apoptosis is then revealed in the north east quadrant and necrosis in the north west).*



The complex **[TbPh₃Aza³]** clearly exhibits apoptosis, while the analogous pyrazoyl-azaxanthone complex, **[TbL⁵]**, showed necrosis. In contrast, the ‘dot plot’ for **[EuL⁴]** was inconsistent, with no distinct correlation to suggest necrosis or apoptosis. These results indicate that the manner in which the azaxanthone moiety is attached to the cyclen macrocycle (i.e. CH₂ or pyridyl / pyrazoyl heterocycles) plays an important role in determining how these complexes interact within a cell. In addition, this behaviour indicates that the inclusion of the *tert*-butyl group does not in itself give rise to cell death by a consistent mechanism.

5.2 Luminescence Microscopy Studies

Preliminary cell uptake studies with over sixty emissive europium and terbium complexes have been performed within the Parker group. Results have shown that uptake and compartmentalisation profiles are dependent upon the nature and mode of linkage of the heterocyclic sensitising moiety, rather than complex charge or lipophilicity.^{2,5,6,7}

Three main classes of behaviour have been observed to date. The majority of complexes examined (~ 80 %) are taken up relatively quickly and exhibit an endosomal – lysosomal profile.⁸ A second class of complexes localise in protein dense organelles, such as ribosomes and nucleoli. These complexes tend to differ from the latter, by showing relatively slow uptake and egress behaviour.^{6,9} The final class of complexes reveal very fast uptake and slow egress, showing intracellular shuttling between mitochondria and the endosomal / lysosomal compartments. This time dependent behaviour has been confirmed by co-staining with Mitotracker GreenTM and LysoTracker GreenTM.⁷

The cellular uptake and localisation profiles of complexes **[EuL⁴]** and **[TbL⁵]** were examined in Chinese hamster ovarian and mouse skin fibroblast cells using fluorescence microscopy. Cultured cells were exposed to a growth medium with complex concentrations varying from 10 to 100 μM. The living cells were then examined by fluorescence microscopy at time intervals in the range of 20 min to 24 h. Following excitation of the chromophore and by using appropriate filter sets, europium **[EuL⁴]** and terbium **[TbL⁵]** emission was readily detected. Optical sections throughout the cells were taken to ensure the complex was internalised rather than simply associated with the cell membrane.

For [EuL⁴], within 20 minutes of incubation of a 50 μ M solution, complex was observed that was consistent with mitochondrial localisation. Co-localisation studies at 2 h incubation with Mitotracker GreenTM confirmed this compartmentalisation, with merged images showing good correspondence (Figure 5.2).

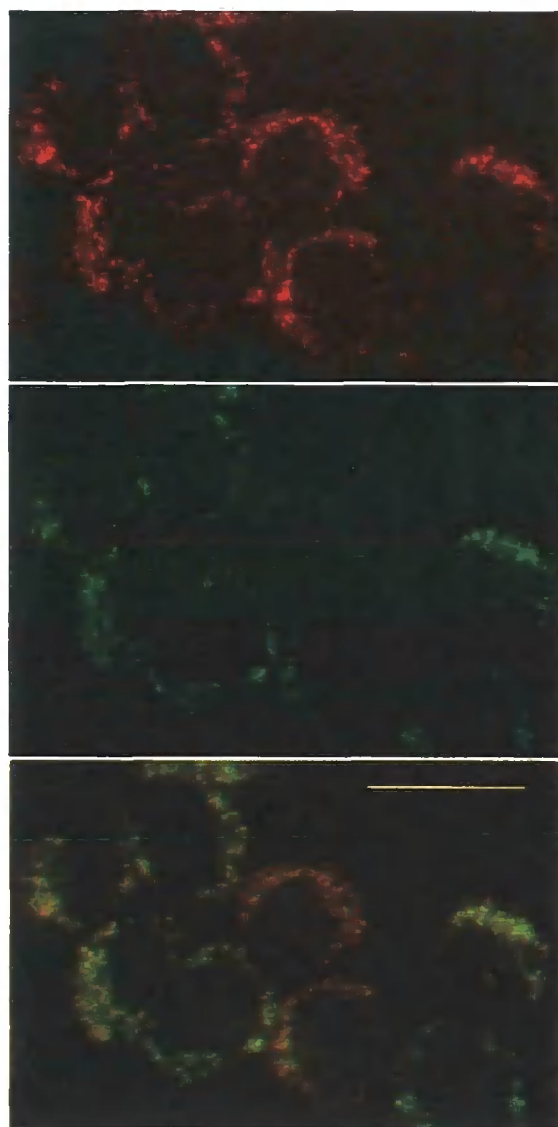


Figure 5.2: *Fluorescence microscopy images for [EuL⁴] (50 μ M complex, 2 h incubation) showing a mitochondrial localisation profile as revealed by co-localisation experiments with Mitotracker GreenTM: upper: [EuL⁴], middle: Mitotracker GreenTM, lower: merged image (scale bar 20 microns)*

At longer incubation periods (> 4 h), merged images between the complex and Mitotracker GreenTM started to show inconsistencies (**Figure 5.3**).

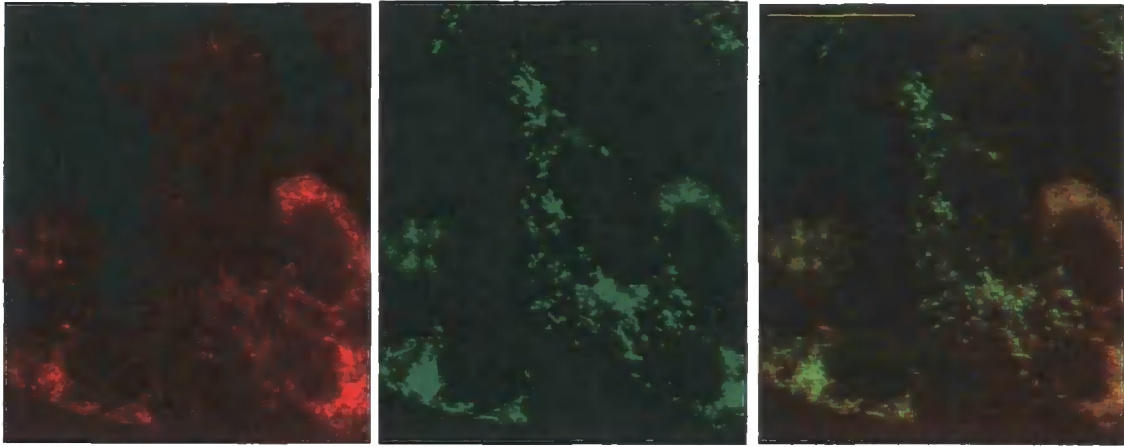


Figure 5.3: *Fluorescence microscopy images for [EuL⁴] (50 μ M complex, 4 h incubation) showing a partial mitochondrial localisation profile as revealed by co-localisation experiments with Mitotracker GreenTM: left: [EuL⁴], middle: Mitotracker GreenTM, right: merged image (scale bar 20 microns)*

In prolonging the incubation period to > 12 h, the complex appeared to migrate from the mitochondria to perinuclear endosomes and lysosomes. This hypothesis was confirmed by co-staining with commercially available Lysotracker GreenTM (**Figure 5.4**). It has been hypothesised that the rate of intracellular trafficking of these complexes to recycling vesicles may be associated with their ability to bind reversibly to a given carrier protein.



Figure 5.4: Fluorescence microscopy images for $[\text{EuL}^4]$ ($50 \mu\text{M}$ complex, 24 h incubation) showing a lysosomal localisation profile as revealed by co-localisation experiments with Lysotracker GreenTM: left: $[\text{EuL}^4]$, middle: Lysotracker GreenTM, right: merged image (scale bar 20 microns)

Like $[\text{EuL}^4]$, complex $[\text{TbL}^5]$ exhibited time-dependent intracellular trafficking between mitochondrial and endosomal / lysosomal compartments. No change in the localisation behaviour was observed upon changing the chirality of the cyclen pendant arms (i.e. (RRR) - $[\text{TbL}^5]$). This suggests intracellular shuttling occurs via a process in which chirality of the complex is not pivotal.

No differentiation in cell localisation could be distinguished between complexes $[\text{TbL}^5]$ and $[\text{TbL}^6]$ (Figure 5.5). These complexes differ only in the structure of the pendant arms, therefore the behaviour of these complexes suggests that the pendant arm structure does not play a significant role in either localisation profile or intracellular shuttling processes. Similar conclusions have been independently reached by examining six sets of Eu / Tb complexes with a common dpqC sensitising moiety.¹⁰ Taken together, these observations support the theory that it is the constitution of the sensitising moiety that influences the complexes uptake and trafficking behaviour. These condensed aromatic groups are most likely to be recognised in protein association, which presumably must be a key recognition process in the intracellular trafficking that may involve recycling vesicles.

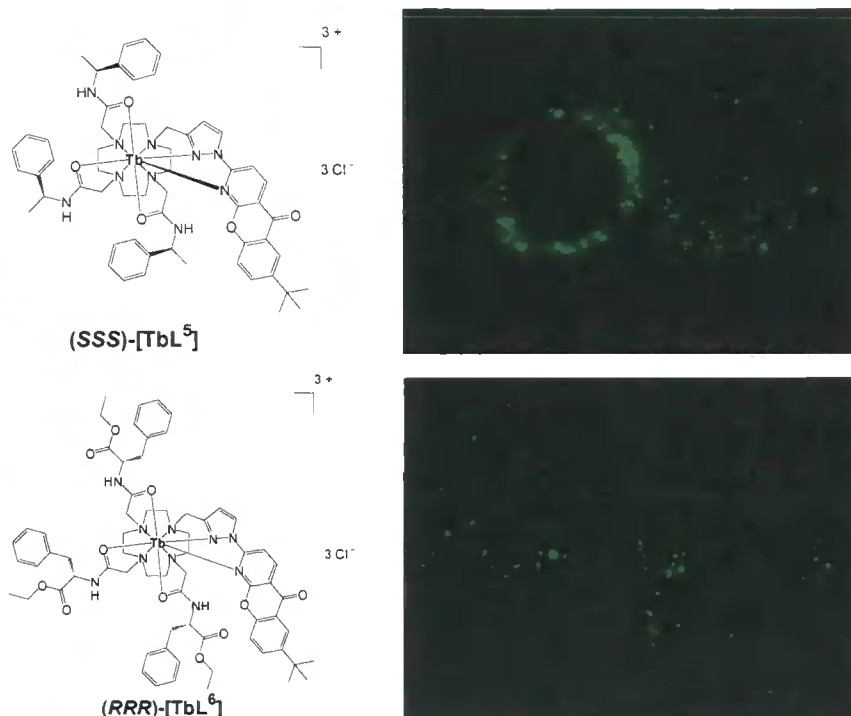


Figure 5.5: Fluorescence microscopy images for (SSS)-[TbL⁵] and (RRR)-[TbL⁶] (50 μ M complex, 24 h incubation) showing similar localisation profiles

5.3 Cellular Uptake Mechanism

Complexes [EuL⁴] and [TbL⁵] have been used in recent research to address the mechanism of complex cellular uptake.¹¹ Using microscope image intensity and ICP-MS analysis, an array of established inhibitors and promoters has been examined, to observe their effect on intracellular uptake. Suppressed uptake was seen at 4 °C, consistent with an energy dependent process (i.e. endocytosis),¹² while effects of inhibitors and promoters were consistent with an uptake mechanism of macropinocytosis. This was confirmed by suppressed uptake using both wortmannin (blocking PI-3 kinase)¹³ and amiloride (blocking the Na⁺ / H⁺ pump).¹⁴

Macropinocytosis involves the formation of endocytotic vesicles generated by the invagination of the plasma membrane. This mode of cell uptake is attractive, as macropinosomes are regarded as leakier vesicles than other endosomes.¹⁵ Therefore, the lanthanide complexes can escape from encapsulation more readily than from other components, and hence be transferred to other organelles.

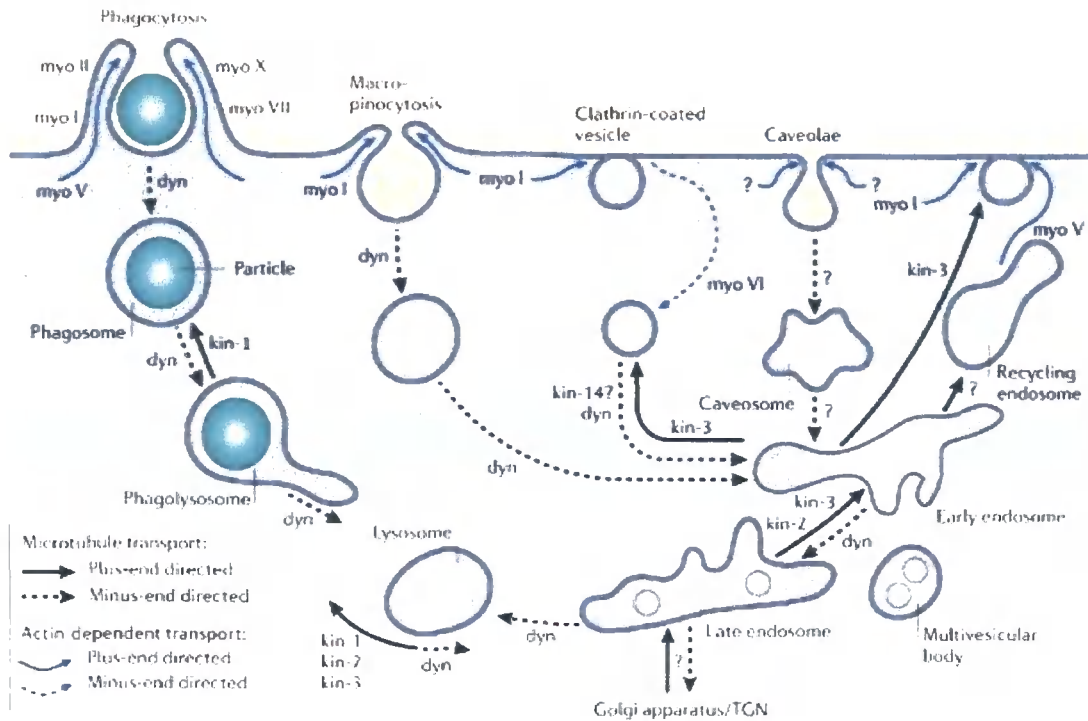


Figure 5.6: Endocytotic cellular uptake mechanisms¹⁶

5.4 Conclusions

The cellular localisation studies of complexes [EuL⁴] and [TbL⁵] highlights the need for further investigation into potential cellular applications. The pH sensitivity (Chapter 2, section 2.4.3) and time-dependent localisation of [TbL⁵] may allow the real time monitoring of pH change within ageing lysosomes. A change in pH could be followed ratiometrically using the terbium $\Delta J = 5$ band and residual ligand fluorescence, with pH estimated using a calibration curve.

References

- 1.) J. Carmichael, W. G. DeGraff, A. F. Gazdar, J. D. Mina and J. B. Mitchell, *Cancer Res.*, 1987, **47**, 936.
- 2.) F. Kielar, G-L. Law, E. J. New and D. Parker, *Org. Biomol. Chem.*, 2008, **6**, 2256.
- 3.) M. van Engeland, L. J. W. Nieland, F. C. S. Ramakers, B. Schutte and C. P. M. Reutilingsperger, *Cytometry.*, 1998, **31**, 1.
- 4.) C. P. Montgomery, B. S. Murray, E. J. New, R. Pal and D. Parker, *Acc. Chem. Res.*, 2009, *In press*.
- 5.) R. A. Poole, G. Bobba, M. J. Cann, J-C. Frias, D. Parker and R. D. Peacock, *Org. Biomol. Chem.*, 2005, **3**, 1013.
- 6.) J. Yu, D. Parker, R. Pal, R. A. Poole and M. J. Cann, *J. Am. Chem. Soc.*, 2006, **128**, 2294.
- 7.) B. S. Murray, E. J. New, R. Pal and D. Parker, *Org. Biomol. Chem.*, 2008, **6**, 2085.
- 8.) Y. Bretonnière, M. J. Cann, D. Parker and R. Slater, *Org. Biomol. Chem.*, 2004, **2**, 1624.
- 9.) R. Pal and D. Parker, *Chem. Commun.*, 2007, 474.
- 10.) E. J. New, D. Parker and R. D. Peacock, *Dalton Trans.*, *In Press*.
- 11.) E. J. New and D. Parker, *Chem. Commun.*, *Submitted*
- 12.) S. Kessner, A. Kronise, U. Rothe and G. Bendas, *Biochim. Biophys. Acta*, 2001, **1514**, 177.
- 13.) A. Arcaro and M. P. Wymann, *Biochem. J.*, 1993, **295**, 297.
- 14.) P. R. Hoffmann, A. M. de Cathelineau, C. A. Ogden, Y. Leverrier, D. L. Bratton, D. L. Dalecke, A. J. Ridley, V. A. Fathok and P. M. Henson, *J. Cell. Biol.*, 2001, **155**, 649.
- 15.) I. A. Khalil, K. Kogure, H. Akita, H. Harashima, *Pharmacol. Rev.*, 2006, **58**, 32.
- 16.) T. Soldati and M. Schliwa, *Nat. Rev. Mol. Cell. Bio.*, 2006, **7**, 897.

CHAPTER SIX:

Conjugate Complexes

Chapter Six: Conjugate Complexes

The high luminescent quantum yields, long emissive lifetimes and cellular profiles associated with complexes $[\text{EuL}^4]$, $[\text{TbL}^5]$ and $[\text{LnL}^7]$ augur well for their application as biological emissive probes. In addition, the tendency for the collisional quenching of $[\text{EuL}^4]$ and $[\text{TbL}^5]$ to be completely inhibited by the presence of serum albumin at concentrations typically found in cells (0.2 – 0.7 mM), becomes vitally important in identifying and selecting complexes to be developed for potential cellular probes or HTRF bio-assays components.

In order for complexes to be applicable in HTRF (homogeneous time resolved fluorescence), it is imperative that they possess a point of potential conjugation, through which the complex can be linked to an appropriate ‘tag’ or ‘acceptor’. Research has previously been undertaken in which a sensitising azaxanthone chromophore has been functionalised to an activated NHS ester to allow conjugation (**Figure 6.1**).¹

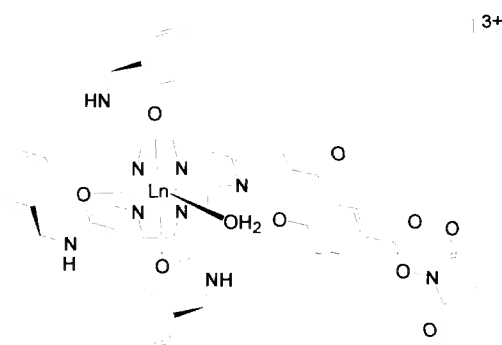


Figure 6.1: Complex $[\text{LnPh}_3\text{-AzaNHS}]$, containing an azaxanthone activated NHS ester

The introduction of different substituents at the azaxanthone 7 position was shown to strongly influence the intracellular uptake and distribution profile of the respective complexes.² This route was deemed inappropriate for the pyridyl- and pyrazoyl-azaxanthone derivatives due to the presence of the *tert*-butyl group which was required to enhance solubility. With the dpqC chromophore, there is no obvious point of conjugation directly associated with the chromophore. Consequently, linkage through the trans pendant arm on the macrocyclic ring was investigated. This position provided the most feasible alternative, without compromising the photophysical properties of the complexes. Complexes such as $[\text{TbPh}_2\text{-NH}_2]$ (**Figure 6.2**) have previously been

synthesised in an attempt to utilise this lanthanide complex linkage point. However, the structure of the linkable pendant NH_2 arm resulted in the observation of numerous stereoisomers by HPLC analysis.³

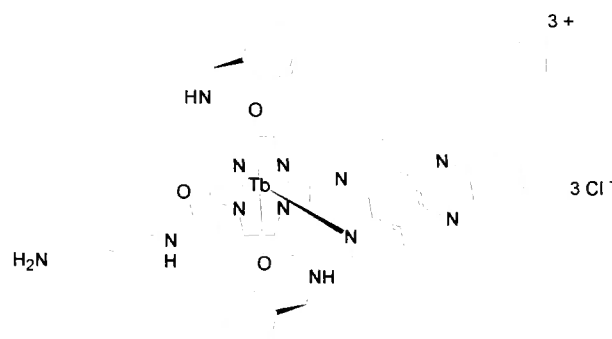
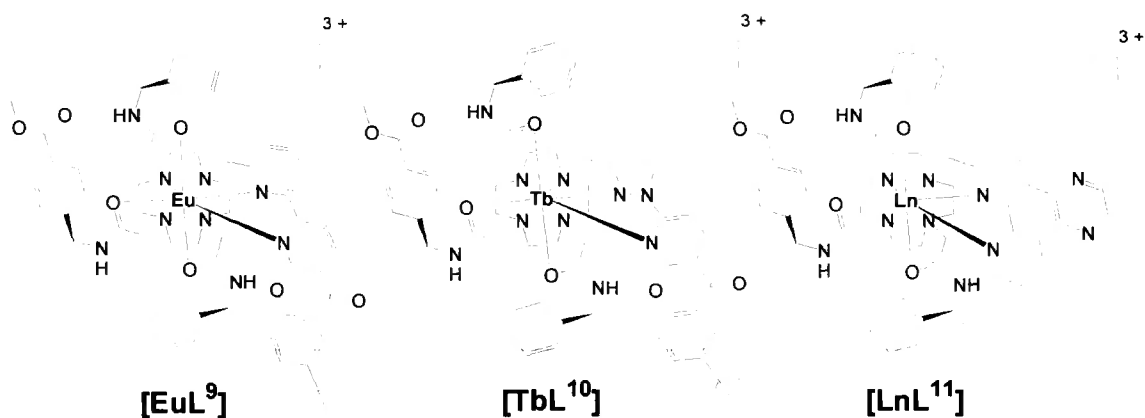


Figure 6.2: Conjugatable *dpqC* complex $[\text{TbPh}_2\text{-NH}_2]$

For complexes to be applicable as HTRF components they should preferably exist as a single stereoisomer. Therefore, to eradicate this problem, new targets were designed, in which the linkage pendant arm resembles the other ring N-substituents. The target complexes are shown below:

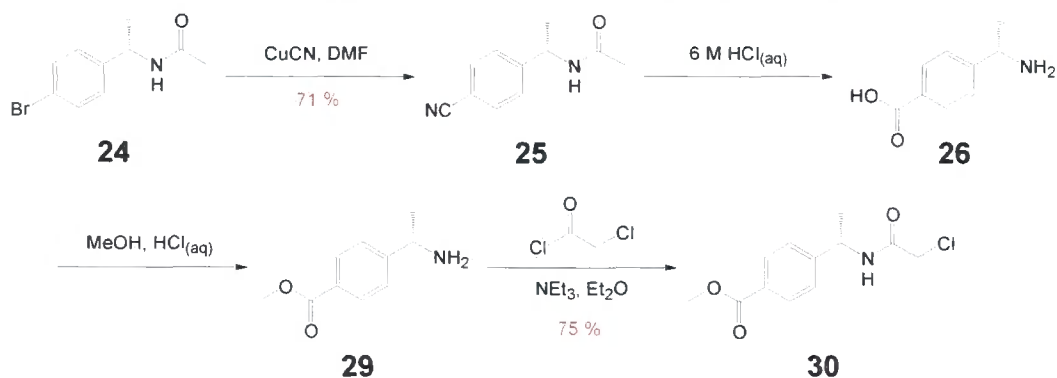


6.1 Amide Conjugate Ligand and Complex Synthesis

6.1.1 Trans Pendant Arm Synthesis

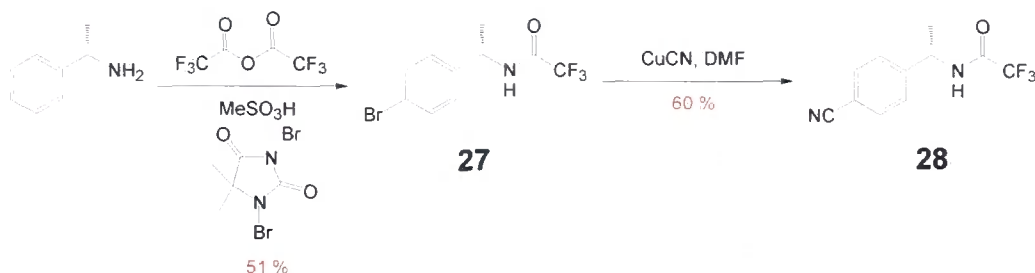
4-[(*S*)-1-(2-Chloro-acetylamino)-ethyl]-benzoic acid methyl ester **28** was synthesised from commercially available (*S*)-1-(4-bromophenyl)ethylamine in a five step process (**Scheme 6.1**).⁴ Reaction of (*S*)-1-(4-bromophenyl)ethylamine with acetyl chloride selectively protected the amine group, allowing conversion of the para-substituted

bromide into a cyano group (**25**) in 71 % yield, using Cu(I)CN. Subsequent acid hydrolysis using 1 M HCl_(aq) yielded the acid **26** in quantitative yield.



Scheme 6.1: Synthesis of 4-[(*S*)-1-(2-chloro-acetyl-amino)-ethyl]-benzoic acid methyl ester **30**

The acid, **26**, was also synthesised from the more readily available (*S*)-(-)- α -methylbenzylamine as shown in **Scheme 6.2**.⁵ Reaction of (*S*)-(-)- α -methylbenzylamine with trifluoroacetic acid, followed by treatment with methanesulfonic acid and 1,3-dibromo-5,5-dimethylhydantoin afforded **27**, in 51 % yield. Cyanation with Cu(I)CN in dimethylformamide yielded the cyano derivative **28**, which was subsequently converted into **26** by acid hydrolysis in 1 M HCl_(aq). Finally, esterification and reaction with chloroacetyl chloride afforded the functionalised arm **30**.



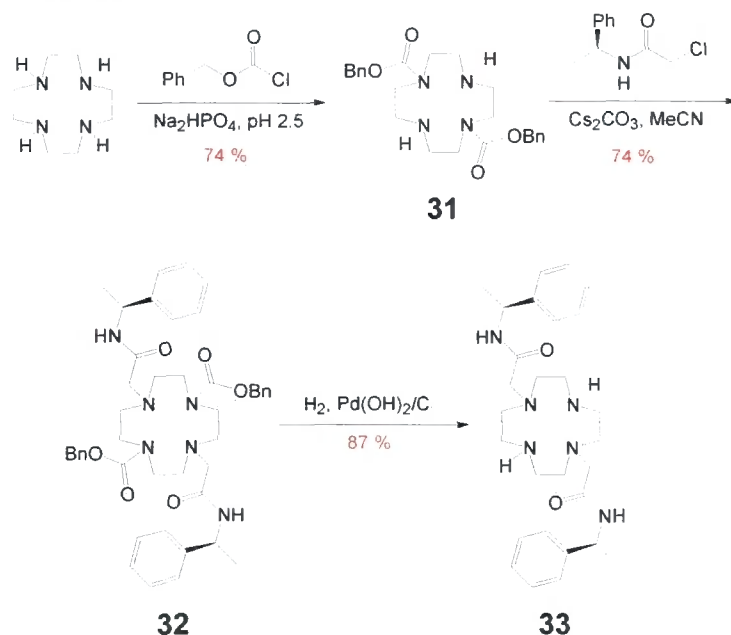
Scheme 6.2: Synthesis of intermediate **28**

6.1.2 Functionalisation of Cyclen

The use of appropriate protecting group strategies enabled the synthesis of the tri-substituted mono-alkylated cyclen ligands [**L**⁸], [**L**¹⁰] and [**L**¹¹].

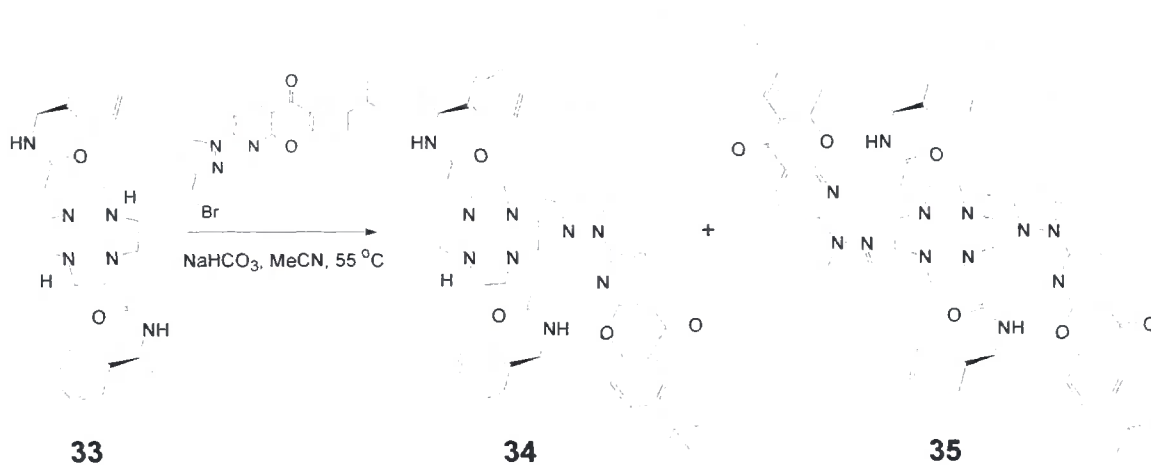
The synthesis of the trans-bis(benzylcarbamate) protected cyclen, **31**, was undertaken following established literature procedures,⁶ using pH control to ensure selective trans-disubstitution (**Scheme 6.3**). Purification was achieved through selective extraction

using diethyl ether and dichloromethane to afford the product in 74 % yield. Alkylation of **31** under S_N2 conditions (CS_2CO_3 , MeCN) using (*S*)-*N*-2-chloroethanoyl-2-phenylethylamine proceeded to give the tetrasubstituted cyclen **32**, which was reacted under standard hydrogenation conditions (40 psi, $Pd(OH)_2/C$, $CH_3OH - H_2O$) to remove the Cbz protecting groups (**33**).



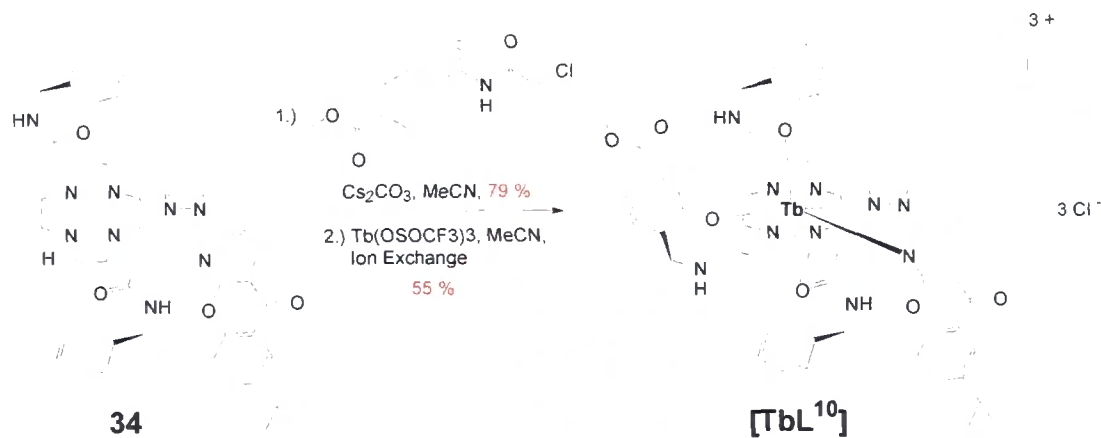
Scheme 6.3: Synthesis of disubstituted cyclen **33**

Attempts to synthesise the desired pyrazoyl-azaxanthone ligand [**L**¹⁰] centred around the mono-alkylation of di-substituted cyclen **33** (**Scheme 6.4**). Despite using mild alkylating conditions ($NaHCO_3$, MeCN, 55 °C) using an excess of cyclen **33**, both the mono and di-alkylated derivatives were apparent by mass spectrometry (**34**; MS (ES^+) $m/z = 1067.7$, $[M + Na]^+$, **35**; MS (ES^+) $m/z = 1179.6$, $[M + Na]^+$). Similar R_F values for compounds **34** and **35** meant that purification by column chromatography on neutral alumina was extremely difficult.



Scheme 6.4: Alkylation of cyclen **33** with bromopyrazoyl-azaxanthone, **12**.

Consequently, the crude material of **34** (~ 85 % pure by NMR analysis) was alkylated with the methyl carboxylate arm derivative **30** under S_N2 conditions to yield [L¹⁰], which was purified by column chromatography on neutral alumina. Complexation was performed using Tb(CF₃SO₃)₃ in acetonitrile, followed by anion exchange chromatography to yield the corresponding water soluble chloride salt [TbL¹⁰] (**Scheme 6.5**).



Scheme 6.5: Synthesis of complex [TbL¹⁰]

The water solubility of [TbL¹⁰] enabled discrimination between the complex and the di-alkylated ligand by-product **35**. HPLC purification was avoided by simple syringe filtration in aqueous solution, leading to isolation of [TbL¹⁰] as a single species, as revealed by analytical HPLC (**Figure 6.3**).

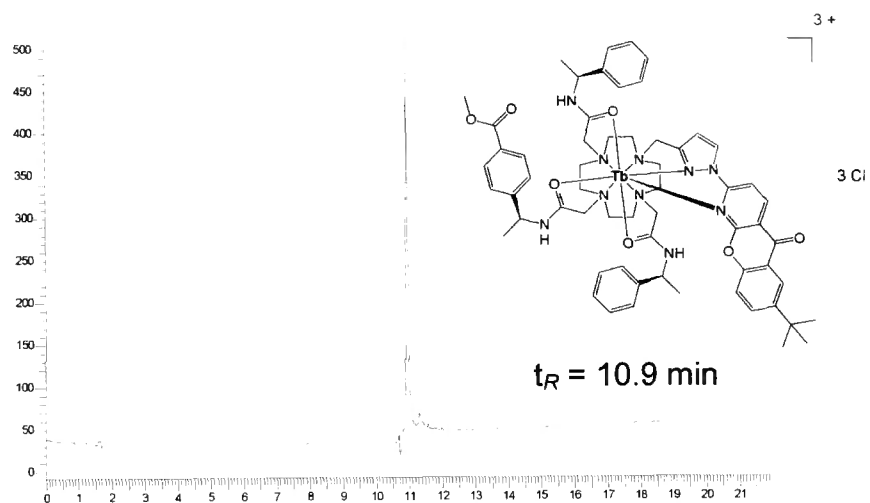


Figure 6.3: Reverse phase analytical HPLC analysis of $[\text{TbL}^{10}]$

(Chromolith performance RP18e column; Method A; $\lambda_{exc} = 355 \text{ nm}$, $\lambda_{em} = 355 / 516 \text{ nm}$)

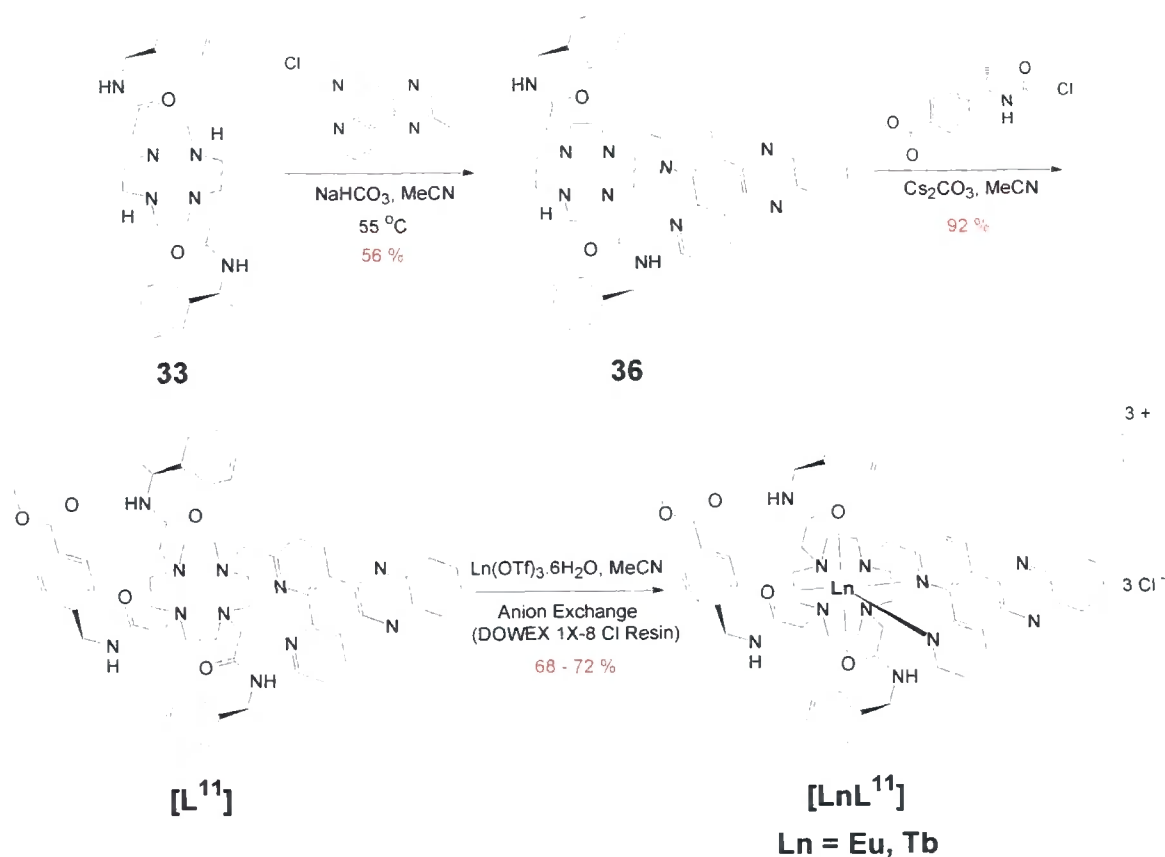
The problem of di-alkylation observed with bromopyrazoyl-azaxanthone (**Scheme 6.4**) was not apparent with the analogous dpqC intermediate, **15** (below).



15

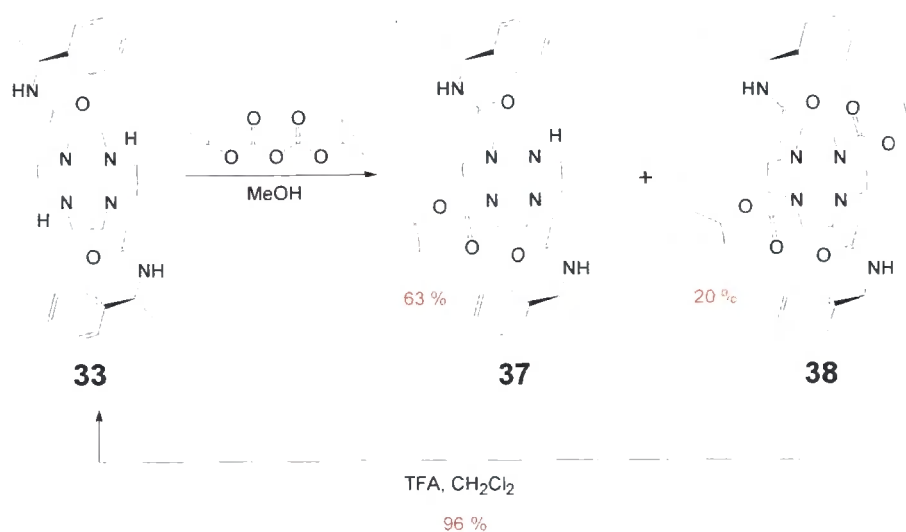
This observation is consistent with the lower reactivity of benzyl chlorides, with respect to benzyl bromides. This enabled the mono-alkylated cyclen **36** to be synthesised from di-substituted cyclen **33** under mild conditions (NaHCO_3 , acetonitrile, $55 \text{ }^\circ\text{C}$) (**Scheme 6.6**). Following purification by column chromatography on neutral alumina, alkylation with 4-[(*S*)-1-(2-chloro-acetylamino)-ethyl]-benzoic acid methyl ester **30** gave $[\text{L}^{11}]$ after purification by column chromatography on neutral alumina. Complexation of the ligand was achieved in acetonitrile using $\text{Ln}(\text{CF}_3\text{SO}_3)_3$, followed by anion exchange chromatography to yield the water soluble cationic complexes, $[\text{EuL}^{11}]$ and $[\text{TbL}^{11}]$, as their chloride salts (**Scheme 6.6**).

ⁱ For HPLC solvents and gradients see Chapter 7: Experimental



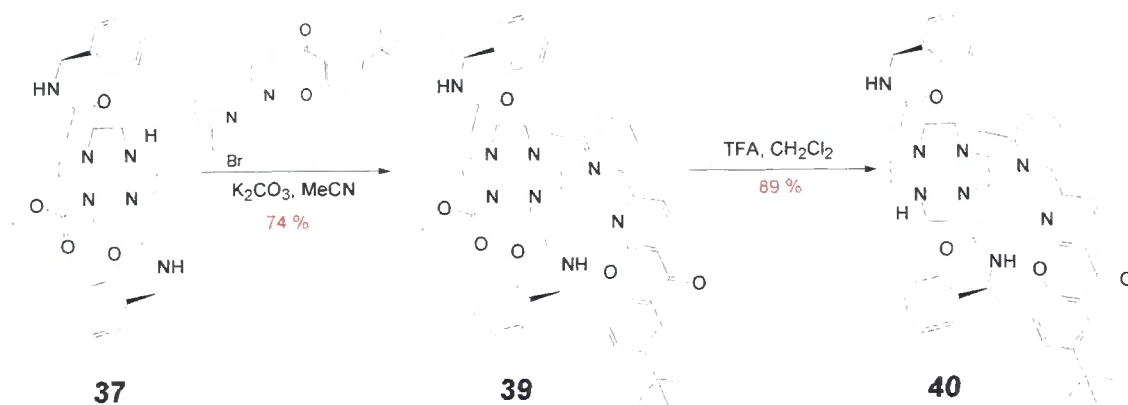
Scheme 6.6: Synthesis of complexes $[\text{LnL}^{11}]$ from disubstituted cyclen, **33**.

A different approach was undertaken for the synthesis of ligand $[\text{L}^9]$. In considering the problems associated with the bromopyrazoyl-azaxanthone system, it was deemed appropriate to use suitable protecting groups to ensure only mono-alkylation of cyclen **33**. Reaction of di-substituted cyclen **33** with di-*tert*-butyl dicarbonate in anhydrous MeOH led to the formation of the mono and di-BOC protected derivatives **37** and **38** (**Scheme 6.7**).⁷ Separation of the compounds was achieved using column chromatography on silica. The di-BOC alkylated species was then deprotected ($\text{CF}_3\text{COOH} - \text{CH}_2\text{Cl}_2$) to recover the cyclen start material **33**, after appropriate washing.



Scheme 6.7: Synthesis of mono-BOC alkylated cyclen, **37**.

Alkylation of mono-BOC alkylated cyclen **37** with bromopyridyl-azaxanthone, followed by deprotection with CF₃CO₂H – CH₂Cl₂, yielded the mono-alkylated species **40** (Scheme 6.8). The ¹H NMR (Figure 6.4) and HPLC analyses of ligand **40** indicated that the BOC protecting group had successfully prevented any di-alkylation.



Scheme 6.8: Synthesis of mono-pyridyl-azaxanthone cyclen, **40**.

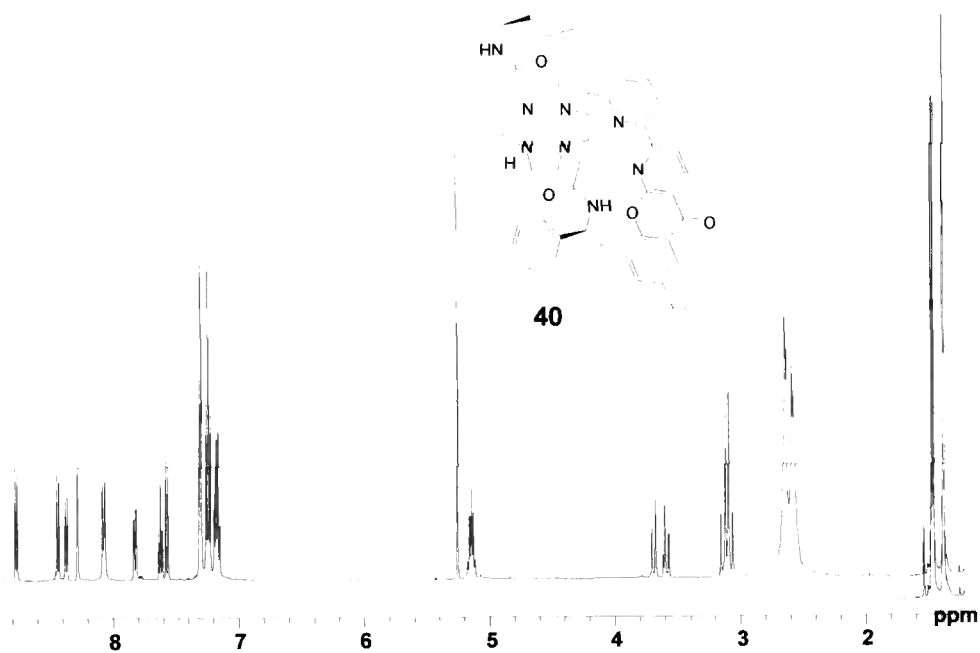
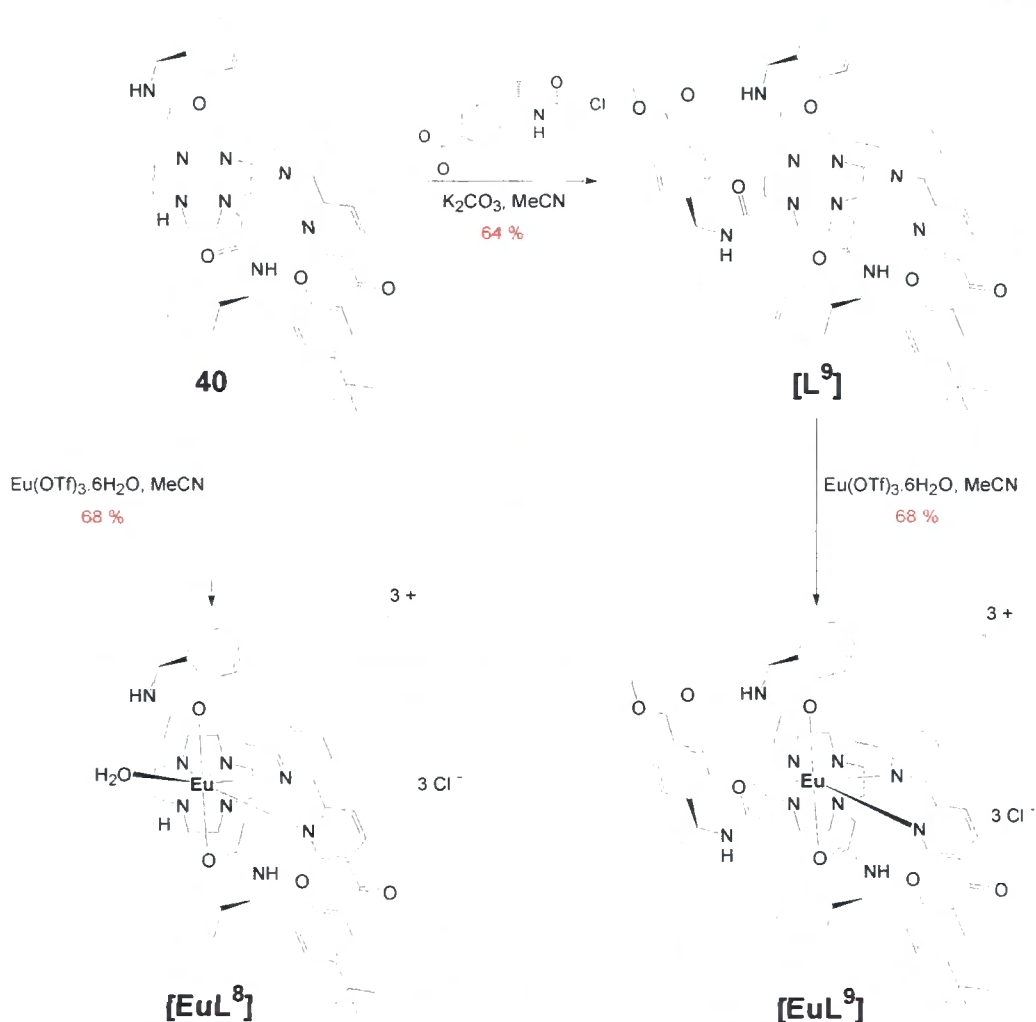


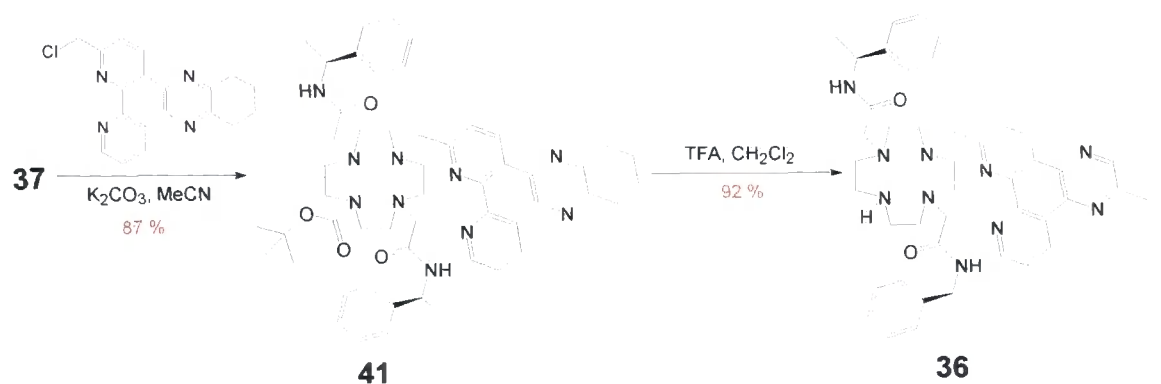
Figure 6.4: ¹H NMR spectrum of pyridyl-azaxanthone alkylated cyclen, **40**, (CDCl₃, 700 MHz).

Complexation of ligand **40** was undertaken to examine any potential anion sensitivity of the octadentate complex, [EuL⁸] (**Scheme 6.9**). Alkylation of ligand **40** with 4-[(*S*)-1-(2-chloro-acetylamino)-ethyl]-benzoic acid methyl ester **30**, followed by complexation in acetonitrile with Eu(CF₃SO₃)₃, yielded the complex [EuL⁹] (**Scheme 6.9**).



Scheme 6.9: Synthesis of complexes $[\text{EuL}^8]$ and $[\text{EuL}^9]$

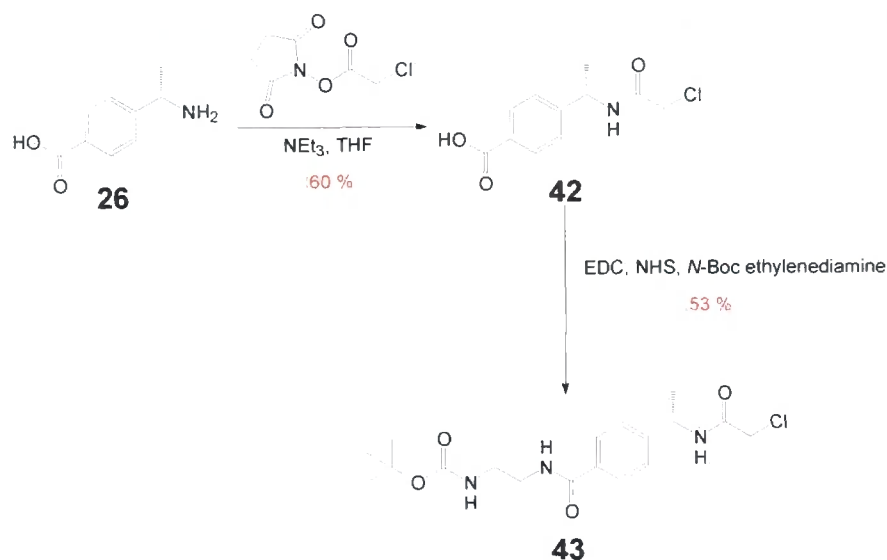
The selectively protected intermediate **37** was also utilised at a later stage for the synthesis of $[\text{LnL}^{11}]$. The BOC protecting group enabled a less cautious alkylation approach, using strong $\text{S}_{\text{N}}2$ conditions to couple dpqC (**Scheme 6.10**). Finally, deprotection using $\text{CF}_3\text{CO}_2\text{H} - \text{CH}_2\text{Cl}_2$ yielded the desired mono-alkylated compound **36**, which was converted into $[\text{LnL}^{11}]$ using the procedures outlined previously in **Scheme 6.6**.



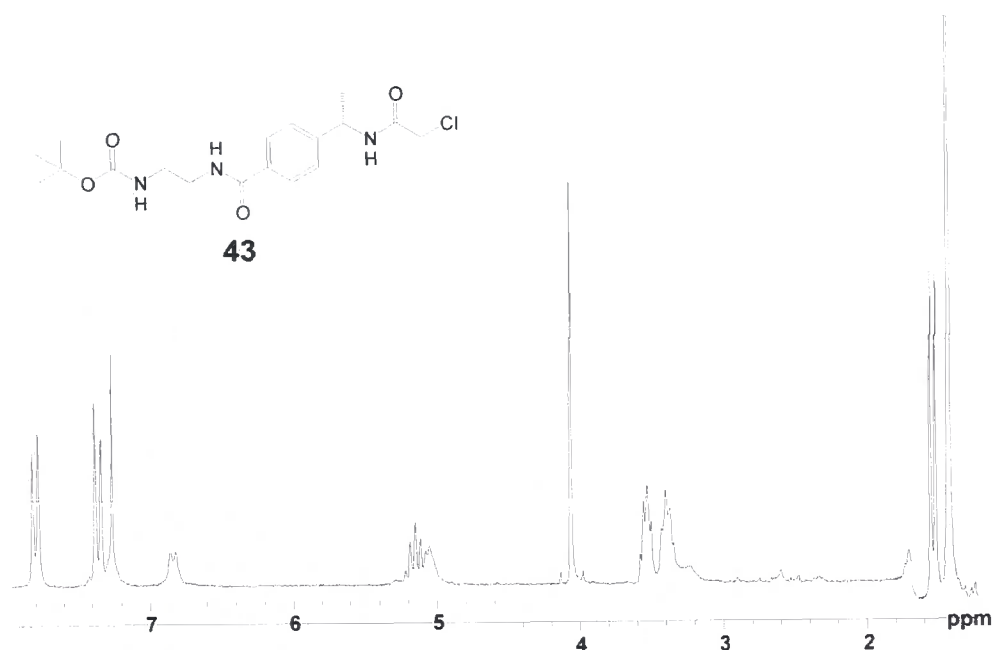
Scheme 6.10: Synthesis of mono-alkylated dpqC cyclen **36**

Complexes $[EuL^9]$, $[TbL^{10}]$ and $[LnL^{11}]$ provide carboxylate functional groups through which to perform conjugation. An attempt to transform these functional groups into primary amine derivatives was investigated. This would provide an alternative group through which to conjugate appropriate ‘tags’ or ‘acceptors’. Direct reaction of $[TbL^{10}]$ with ethylenediamine as both a reagent and solvent led to the formation of numerous products, including decomplexation. An attempt to react $[L^{10}]$ with ethylenediamine at 80 °C (in DMF) also proved unsuccessful. It was concluded that although the methoxy ester is conjugated to an aromatic group, it was not sufficiently activated to undergo nucleophilic substitution under conditions compatible with the stability of the complex. Consequently, the synthesis of a primary amine conjugate arm was undertaken.

Reaction of *N*-hydroxysuccinimide and chloroacetic acid in the presence of EDC, afforded 1-(2-chloroacetyl)pyrrolidine-2,5-dione⁸ in 41 % yield after chromatographic purification on silica. Selective acylation of intermediate (*S*)-4-(1-aminoethyl)benzoic acid **26** was achieved using 1-(2-chloroacetyl)pyrrolidine-2,5-dione and anhydrous triethylamine to yield compound **42**, in 60 % yield. Subsequent in situ generation of an NHS active ester, followed by reaction with commercially available *N*-Boc ethylenediamine yielded the functionalised arm **43** (**Scheme 6.11**).



Scheme 6.11: Synthesis of functionalised arm 43

Figure 6.5: ^1H NMR spectrum of functionalised arm, 43, (CDCl_3 , 500 MHz).

Preliminary attempts to alkylate the dpqC cyclen intermediate **36** with pendant arm **43** proved difficult, with the compounds proving unreactive (Cs_2CO_3 , MeCN, 80°C). This behaviour may be due to the steric hindrance created by the *tert*-butyl group. Consequently, any further investigations into the use of this compound may require utilisation of less sterically demanding cyclen substrates.

6.2 Complex Characterisation

Photophysical characterisation of the conjugate complexes $[\text{EuL}^9]$ and $[\text{LnL}^{11}]$ unsurprisingly resembled that of the analogous triamide derivatives $[\text{EuL}^4]$ and $[\text{LnL}^7]$ respectively. However, the total emission spectrum of $[\text{TbL}^{10}]$ (Figure 6.7) showed reduced ligand fluorescence compared to the triamide $[\text{TbL}^5]$. This observed increase in intersystem crossing efficiency is accompanied by an increase in the overall emissive quantum yield ($\Phi_{\text{Tb}} = 61\%$, measured at 355 nm using an integrated sphere).

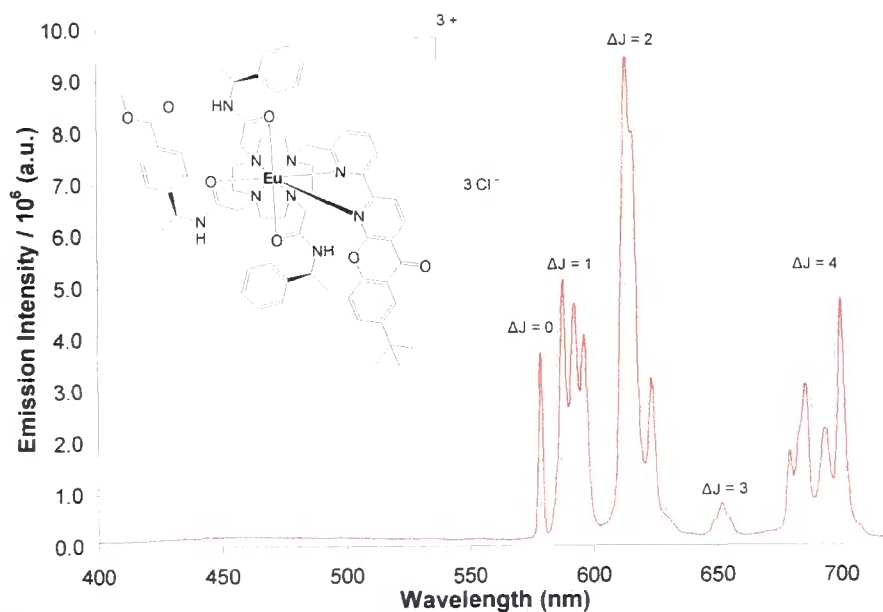


Figure 6.6: Total emission spectrum of $[\text{EuL}^9]$ (aerated water, 295 K, λ_{exc} 355 nm).

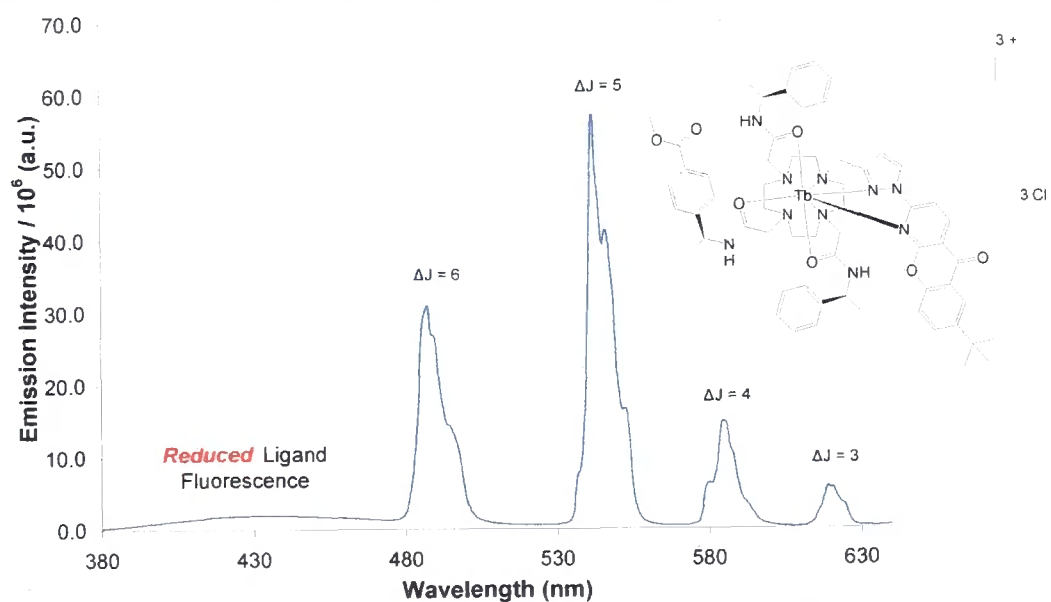


Figure 6.7: Total emission spectrum of $[\text{TbL}^{10}]$ (aerated water, 295 K, λ_{exc} 355 nm).

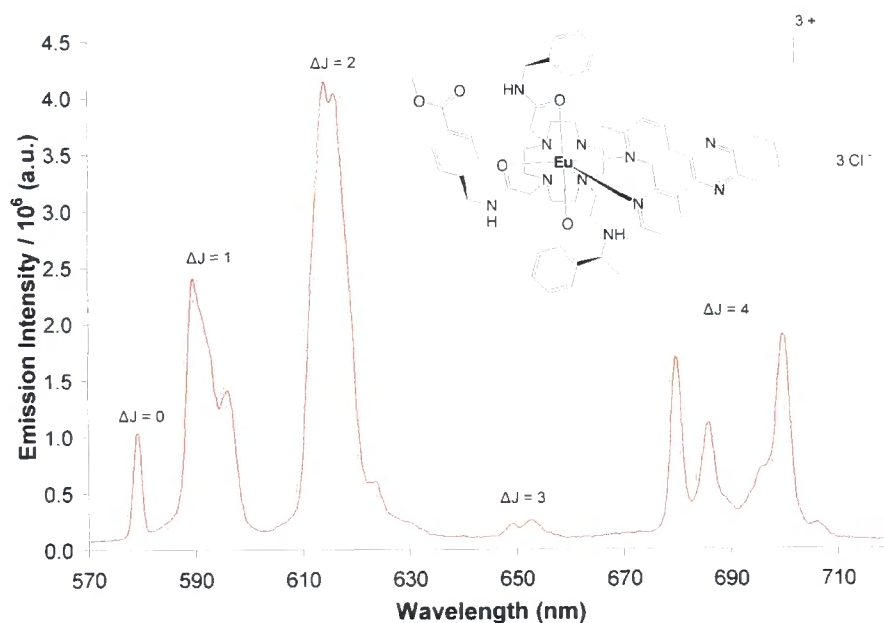


Figure 6.8: Total emission spectrum of $[\text{EuL}^{11}]$ (aerated water, 295 K, λ_{exc} 348 nm).

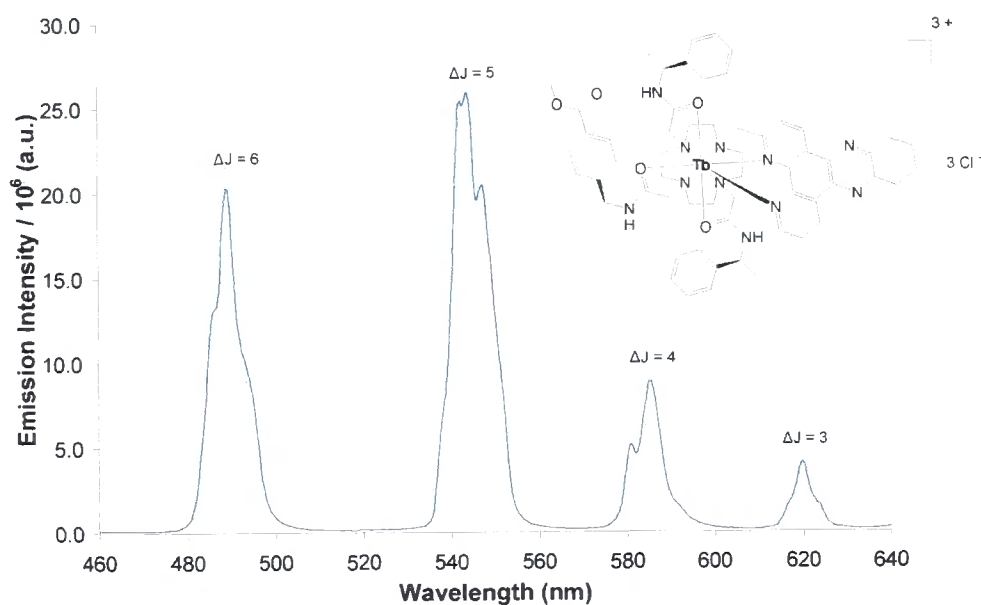


Figure 6.9: Total emission spectrum of $[\text{TbL}^{11}]$ (aerated water, 295 K, λ_{exc} 348 nm).

6.3 Anion Sensitivity of $[\text{EuL}^8]$

The complex $[\text{EuL}^8]$ was synthesised to examine its potential as a responsive cellular probe. In developing responsive optical probes, it is important that the lanthanide emission encodes information about the chemical composition of the local environment through either modulation of spectral form or lifetime. Such complexes must operate

under cellular conditions, (i.e. in the presence of protein, oxygen and variable concentration of competing ions and quenching species) and report on the target analyte by ratiometric analysis.

For these reasons, europium complexes constitute suitable candidates as emissive probes. The relative simplicity of the europium spectral emission profile has been correlated to the speciation of the metal ion. In particular, the nature and polarisability of the group occupying a position on or close to the principal axis of the complex, primarily determine the magnitude of the second order crystal field coefficient. The magnitude of this coefficient determines the degree of splitting in the $\Delta J = 1$ manifold.⁹ For cyclen derivatives, this is typically the 'axial' ligand occupying the ninth site, which caps the square anti-prismatic polyhedron. The more polarisable the axial donor atom, the greater the relative intensity of the hypersensitive and electric-dipole allowed $\Delta J = 2$ emission band. Thus, changes in the coordination environment of the Eu(III) ion can give rise to large changes in the $\Delta J = 2 / 1$ intensity ratio and in the overall spectral form.

The binding affinity of the octadentate complex $[\text{EuL}^8]$ to four bio-active oxy-anions (lactate, citrate, HCO_3^- and HPO_4^{2-}) was examined by monitoring changes of both intensity and form in the europium emission. The emission spectrum of $[\text{EuL}^8]$ in water (**Figure 6.10**) shows both ligand fluorescence and metal based emission. Measurements of the radiative lifetimes in H_2O and D_2O gave an estimated q value (number of bound water molecules) of 1.¹⁰

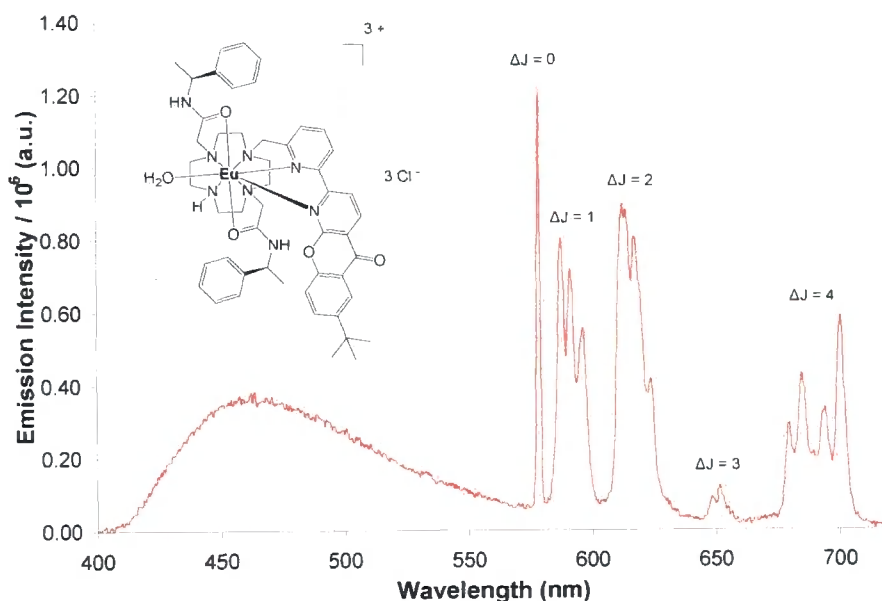


Figure 6.10: Total emission spectrum (aerated water, 295 K, λ_{exc} 355 nm) for $[\text{EuL}]^3+$

For each oxy-anion, the europium spectral form was recorded as a function of anion concentration. With lactate, HCO_3^- and HPO_4^{2-} , changes in the spectral form were not very significant, but were still sufficient to allow ratiometric analysis of the intensity of two emission bands (616 nm / 687 nm). By plotting these intensity ratios as a function of anion concentration, it was possible to calculate apparent affinity constants (**Table 6.1**). The observation of only minor changes in spectral form and relative intensity after the addition of lactate, HCO_3^- and HPO_4^{2-} , suggests that the nature of the axial donor is conserved.

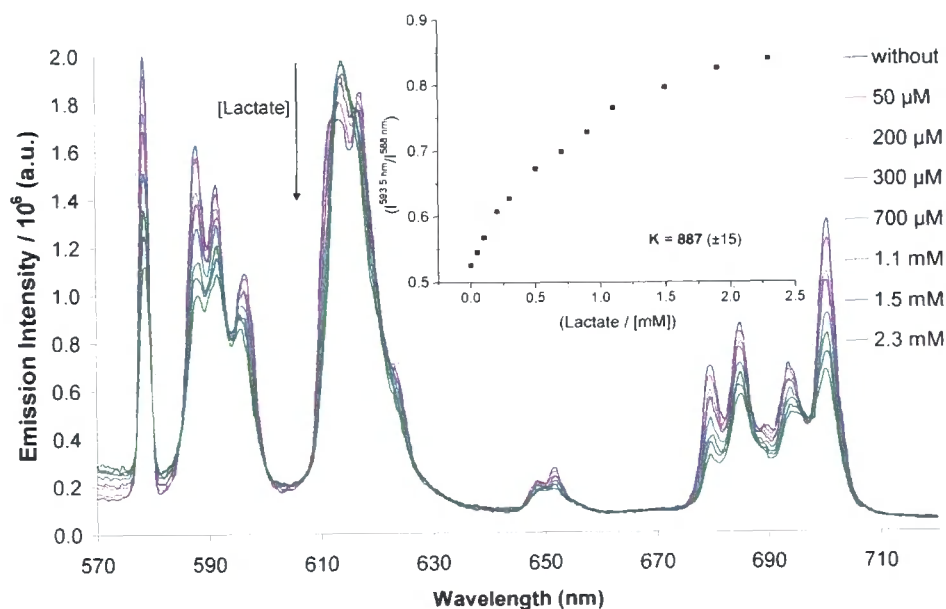


Figure 6.11: Total emission spectrum of $[\text{EuL}^8]$ as a function of lactate concentration (aerated water, 295 K, λ_{exc} 355 nm)

Complex	Lactate (pH 6.0)	HCO_3^- (pH 7.4)	HPO_4^{2-} (pH 7.4)	Citrate (pH 7.4)
$[\text{EuL}^8]$	2.83 (1.05)	3.57 (1.15)	3.26 (1.38)	5.26

Table 6.1: Affinity constants of $[\text{EuL}^8]$ for selected anions (298 K, 0.1 M NaCl)

The most distinctive changes in europium emission were observed following incremental addition of citrate (**Figure 6.12**), which gave rise to a large change in the intensity of the $\Delta J = 2 / 1$ ratio. Changes in lifetime measurements were consistent with the formation of a ternary adduct with no bound water molecules ($q = 0$).

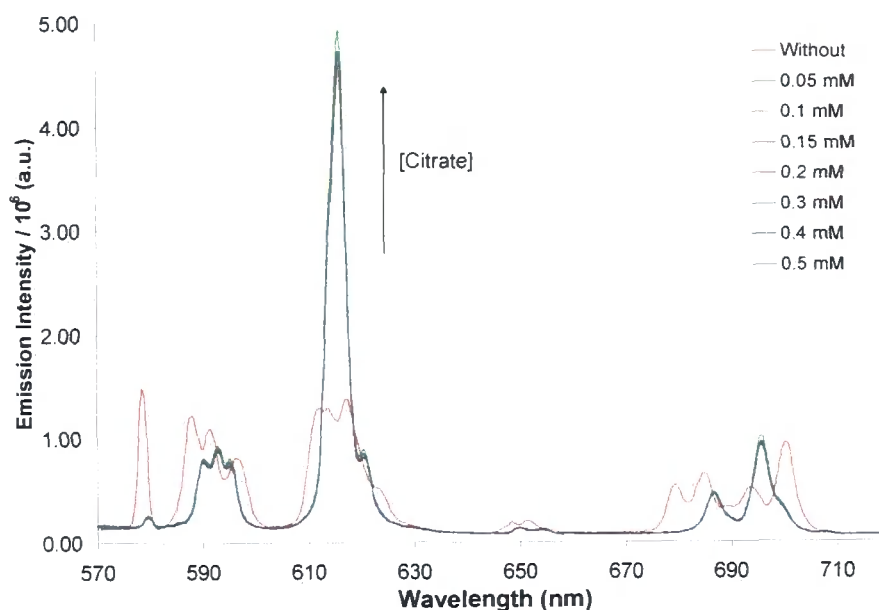


Figure 6.12: Total emission spectrum of $[\text{EuL}^8]$ as a function of citrate concentration (aerated water, 295 K, λ_{exc} 355 nm)

The affinity of $[\text{EuL}^8]$ to citrate anions probably makes the complex unsuitable for ‘in cellulo’ anion sensing. In the presence of only 0.05 mM citrate, a complete change in the emission spectral profile is observed. This spectral form does not alter despite further addition of citrate. Consequently, ratiometric measurement of putative biological concentrations (0 – 0.13 mM citrate) is not applicable with this complex.

6.4 HTRF

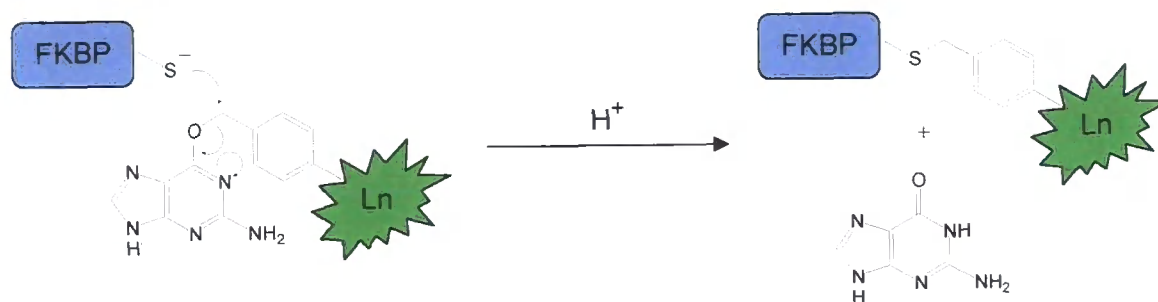
Homogeneous time resolved fluorescence (HTRF) is based on fluorescence resonance energy transfer (FRET) between two interacting components. One of the constituents is labelled with a donor fluorophore and the other is labelled with an acceptor fluorophore. Energy transfer from the excited donor to the acceptor is only seen when the two fluorophores are in close proximity, typically below 10 nm. This distance dependence ($1/r^6$) of FRET allows HTRF systems to address molecular interactions on the 1 – 10 nm scale.¹¹

A common problem with the majority of resonance energy transfer techniques is a low signal-to-noise ratio.¹² These problems are often encountered due to the intrinsic fluorescence of proteins and the overlap between the emission spectra of the FRET

donors and acceptors. HTRF technology alleviates this problem by using long-lived donor fluorophores such as europium cryptates. These complexes allow the use of time gated detection to enhance the signal-to-noise ratio. In addition, acceptors such as Alexa Fluor 647 and d2 (a fluorophore developed by Cisbio International) have very limited emission at 665 nm, and therefore provide an accurate emission parameter with which to measure FRET interactions.

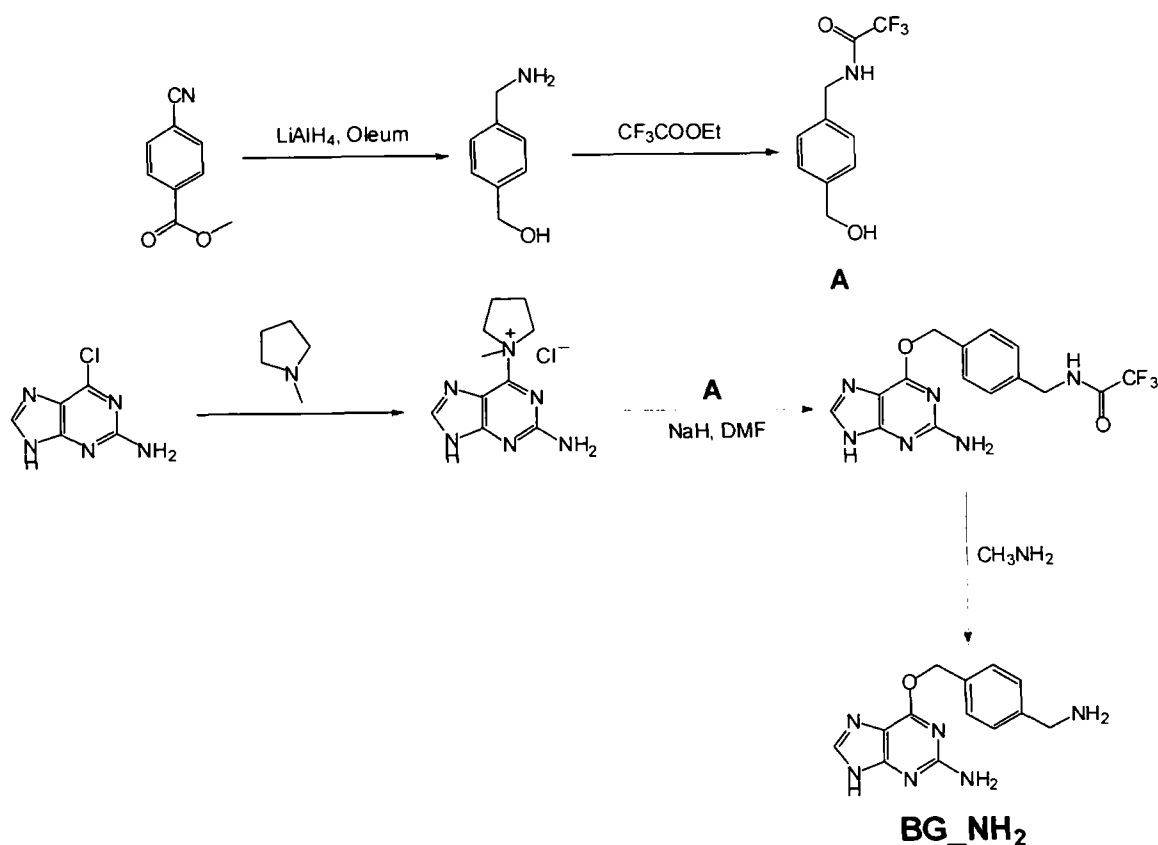
For HTRF to occur, the two components must interact with one another. To date, various strategies have been employed to achieve this interaction, with one common method being the use of protein antibodies. Although it increases the assay complexity, this technique is a widely employed approach despite the large molecular volumes (150 kDa, 160 Å in length) and multiple labelling characteristics of protein antibodies.¹¹

SNAP-tag technology provides an alternative labelling approach which eliminates the need for antibodies and reduces the assay complexity. Developed by Covalys, the SNAP-tag method allows the covalent labelling of proteins (acceptors) with compatible donor fluorophores, labelled with benzyl guanine moieties. SNAP-tag is a mutant DNA repair enzyme, human O⁶-alkylguanine-DNA alkyltransferase (hAGT),¹² which irreversibly and specifically reacts with O⁶-alkylguanine (BG) derivatives to form a thioether bond and release free guanine (**Scheme 6.12**). The labelled synthetic probe of the BG derivative is then transferred to a reactive cysteine residue.^{13,14}



Scheme 6.12: Mechanism of SNAP-TAG activation with BG

For the conjugate complexes [EuL⁹], [TbL¹⁰] and [LnL¹¹] to be applicable as HTRF assay donors, it was necessary to establish a method of conjugation that allows the covalent linkage of the BG 'tag' BG_NH₂. A synthetic preparation of BG_NH₂ is shown in **Scheme 6.13**.¹⁵

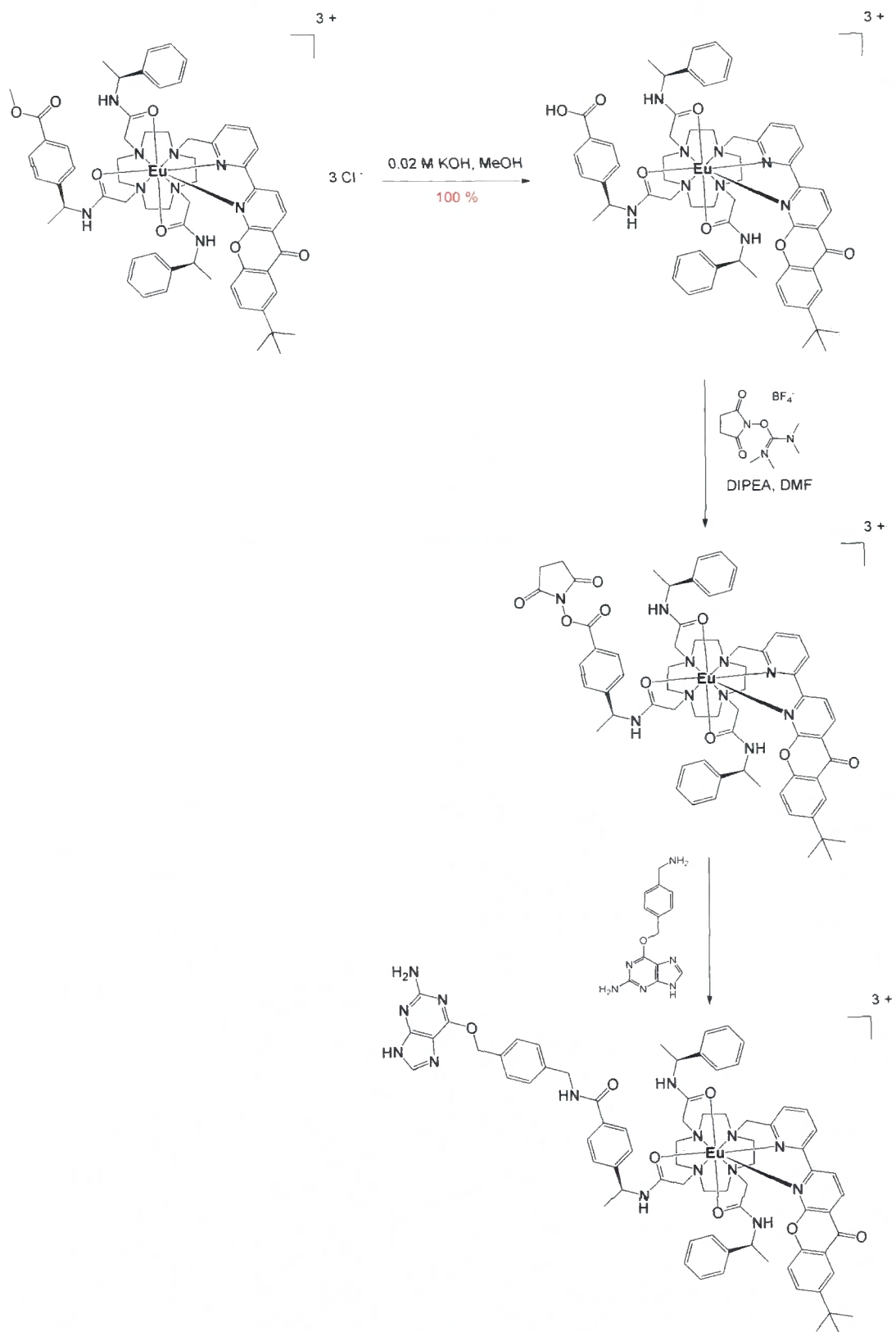


Scheme 6.13: One synthetic route to **BG_NH₂**¹⁵

6.4.1 Complex Activation and Conjugation

Hydrolysis of the methyl ester functionalities within $[\text{EuL}^9]$, $[\text{TbL}^{10}]$ and $[\text{LnL}^{11}]$ was achieved under basic conditions (0.02 M KOH, pH 10), at ambient temperature. A mixture of 0.02 M KOH – MeOH (1:1, 4 ml) drove the reactions to completion (10 mg complex) within 2 h. Neutralisation to pH 7 and evaporation of the solvents yielded the acid derivatives (as salts) in quantitative yield. The acid complexes were then activated to the corresponding *N*-hydroxysuccinimide esters without any further purification. To avoid the use of two activating agents (e.g. DCC or EDCI.HCl with *N*-hydroxysuccinimide), the coupling agent TSTU was utilised. Subsequently, activation was achieved by incremental addition of DIPEA and TSTU to a solution of the complex in anhydrous DMF. The reaction was monitored by reverse phase HPLC. Following completion, semi-preparative HPLC was performed to purify the respective NHS derivatives. However, after purification, the separated materials were shown by analytical

HPLC to be composed of the NHS and acid derivatives. This highlighted the instability of the NHS esters in aqueous solutions. Consequently, following formation of the NHS derivatives, the material was either coupled directly without isolation, or the solution dropped onto diethyl ether to induce precipitation of the complex. This material could then be stored in a freezer without any apparent hydrolysis. Reaction of the *in situ* NHS derivatives proceeded quickly following the introduction of excess **BG-NH₂** (3 equivalents). Purification of the complexes was achieved by preparative reverse phase HPLC using a Chromolith performance RP-18e column. The BG-derivatives were then characterised by HPLC, absorption and emission spectroscopy and electrospray mass spectrometry before being screened in an HTRF assay.



Scheme 6.11: Activation and conjugation of complex $[\text{EuL}^{11}]$

Photophysical characterisation of the conjugate complexes resembled that observed for the parent systems (i.e. $[\text{EuL}^9]$, $[\text{TbL}^{10}]$, $[\text{LnL}^{11}]$). For example, the total emission spectrum of $[\text{EuL}^9\text{-BG}]$ (Figure 6.13) shows 3 bands in the $\Delta J = 1$ band, indicating one chiral species. This was confirmed by reverse phase HPLC analysis. The europium emission lifetime was found to be 1.00 ms in water (compared to 1.02 ms for $[\text{EuL}^9]$), suggesting that the aromatic BG vector does not quench the lanthanide excited state.

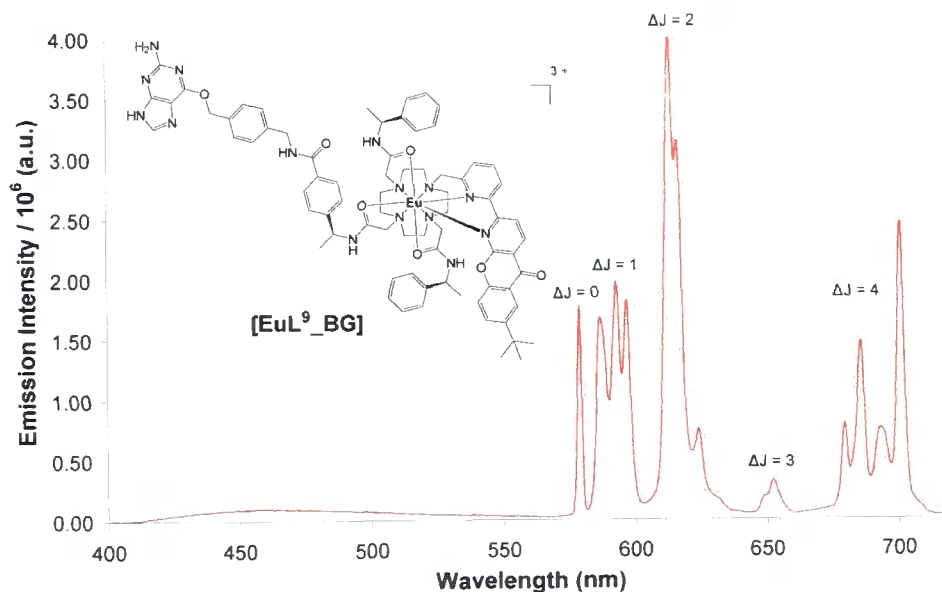


Figure 6.13: Total emission spectrum of $[\text{EuL}^9\text{-BG}]$ (aerated water, 295 K, λ_{exc} 355 nm).

6.4.2 HTRF Application and Screening

The complex $[\text{EuL}^9\text{-BG}]$, and analogous complexes $[\text{TbL}^{10}\text{-BG}]$ and $[\text{LnL}^{11}\text{-BG}]$, will be examined by Cisbio International to determine their performance as components in homogeneous time resolved fluorescence (HTRF) assays. The assay format is comprised of a BG labelled complex (e.g. $[\text{EuL}^9\text{-BG}]$), and the protein FRB. This protein is coupled with the FRET acceptor, d2, and the protein FKBP-SNAPTAG when in the presence of rapamycin. Addition of the respective lanthanide donor results in FRET, which can be monitored as a function of concentration. This allows the calculation of a FRET efficiency as a function of BG concentration. Figure 6.14 shows the components present in a HTRF assay.

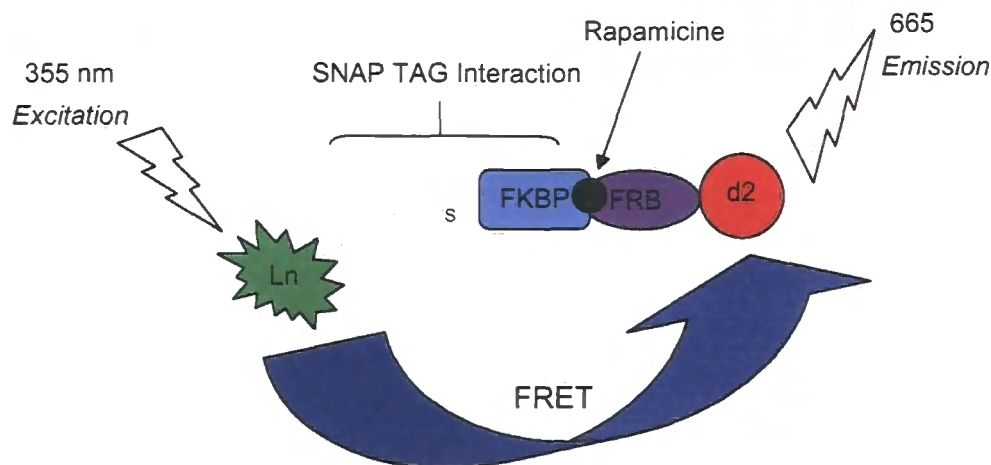


Figure 6.14: Diagram representing the components present for successful FRET during a HTRF assay

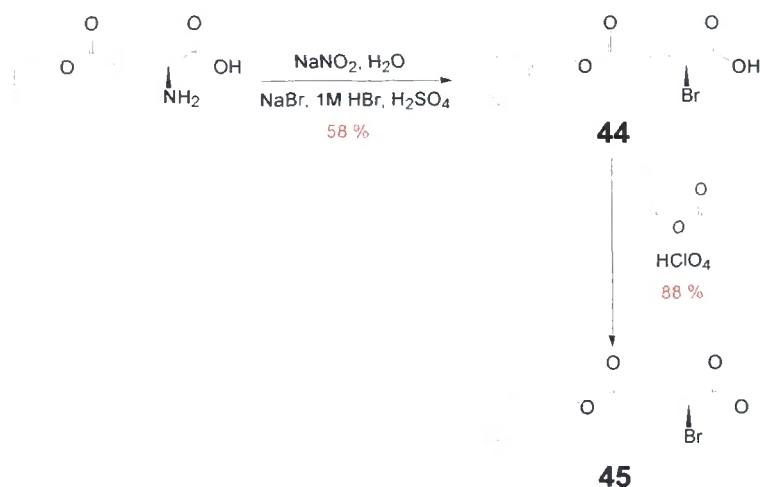
6.5 Alternative Conjugation Complexes

The cationic nature of the complexes $[\text{EuL}^9]$, $[\text{TbL}^{10}]$ and $[\text{LnL}^{11}]$ results in a high degree of electrostatic adhesion. To alleviate this property, the synthesis of a neutral carboxylate conjugate complex was also pursued.

6.5.1 Carboxylate Conjugate Complex Synthesis

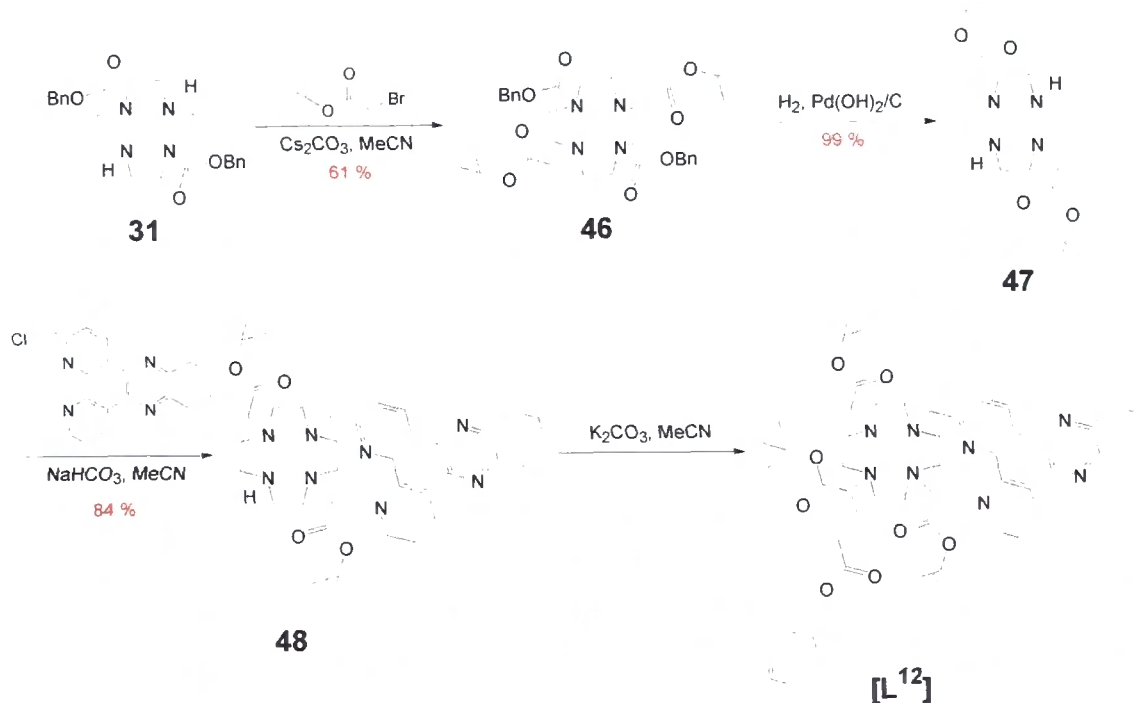
In exploring the possibility of synthesising a carboxylate conjugate complex, it was important to identify a chiral compound that would resemble the remaining cyclen pendant arms. Compound **45** (**Scheme 6.12**) was deemed appropriate, as it could be attached to cyclen through alkylation with the bromine atom, while deprotection of the BOC group would enable coordination to the lanthanide ion. Finally, removal of the Cbz group would provide a carboxylate group through which to conjugate, in a similar manner to those described previously in **Scheme 6.11**.

The synthesis of the (*S*)-2-bromo-pentanedioic acid 5-benzyl ester 1-*tert*-butyl ester, **45**, is outlined in **Scheme 6.12**. Reaction of (*S*)-glutamic acid 5-benzyl ester with sodium nitrite, followed by treatment with 1 M HBr led to the formation of (*S*)-2-bromo-pentanedioic acid 5-benzyl ester, **44**, in 58 % after chromatographic purification.¹⁶ Finally, conversion to the *tert*-butyl ester, **45**, was achieved using *tert*-butyl acetate and HClO_4 to afford the product in 88 % yield.



Scheme 6.12: Synthesis of derivatised carboxylate arm **45**

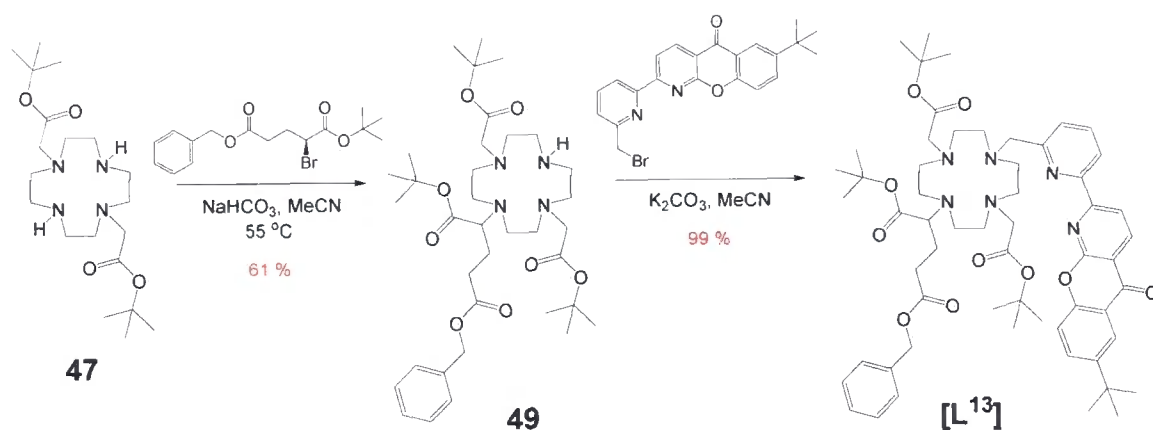
Using the previously synthesised di-Cbz protected cyclen **31**, it was possible to incorporate **45** selectively onto cyclen (**Scheme 6.13**). Alkylation of the protected cyclen **31** with *tert*-butyl bromoacetate (Cs_2CO_3 , MeCN), followed by removal of the Cbz protecting groups, under standard hydrogenation conditions (40 psi, $\text{Pd}(\text{OH})_2/\text{C}$), yielded cyclen DO2A, **47**, in 61 % overall yield.



Scheme 6.13: Synthesis of DO2A **47**, and *dpqC* ligand [L¹²].

Reaction of DO2A cyclen, **47**, with dpqC (NaHCO₃, 60 °C, MeCN) gave the mono-alkylated dpqC ligand, **48**, in 84 % yield following column chromatography of neutral alumina. Analysis of the product by reverse phase analytical HPLC showed that the material was free of any ligand and comprised only one species in solution (> 98 % pure). Alkylation of **48** with a large excess of (*S*)-2-bromo-pentanedioic acid 5-benzyl ester 1-*tert*-butyl ester (**45**) was shown by mass spectrometry to form some of the desired product [**L**¹²]. However, the reaction did not run to completion despite using forceful conditions (100 °C, DMF). It was concluded that ligand **48** is too sterically demanding for efficient coupling with the bulky substrate, **45**. Attempts to purify the two materials by column chromatography proved unsuccessful, with both materials showing a tendency to elute together. HPLC analysis confirmed that the isolated material was composed of compounds **48** and [**L**¹²].

In attempting to overcome this unreactivity, it was decided to utilise the apparent steric demand of (*S*)-2-bromo-pentanedioic acid 5-benzyl ester 1-*tert*-butyl ester **45**. Reaction of **45** with DO2A cyclen (**47**) using mild alkylation conditions enabled the synthesis of the mono-alkylated derivative **49** in 60 % yield after chromatographic purification (**Scheme 6.14**). Finally, reaction with bromomethylpyridyl-azaxanthone, **9**, (K₂CO₃, MeCN) yielded [**L**¹³] after chromatographic purification.



Scheme 6.14: Synthesis of ligand [**L**¹³] from DO2A cyclen, **47**.

Analysis of ligand [**L**¹³] by reverse phase analytical HPLC showed that the material was free of any starting materials and was comprised of only one species in solution

(Figure 6.15). ^1H NMR and mass spectrometry (MS (ES^+) m/z 1019.6 (100 %, $[\text{M} + \text{H}]^+$)) confirmed the structure.

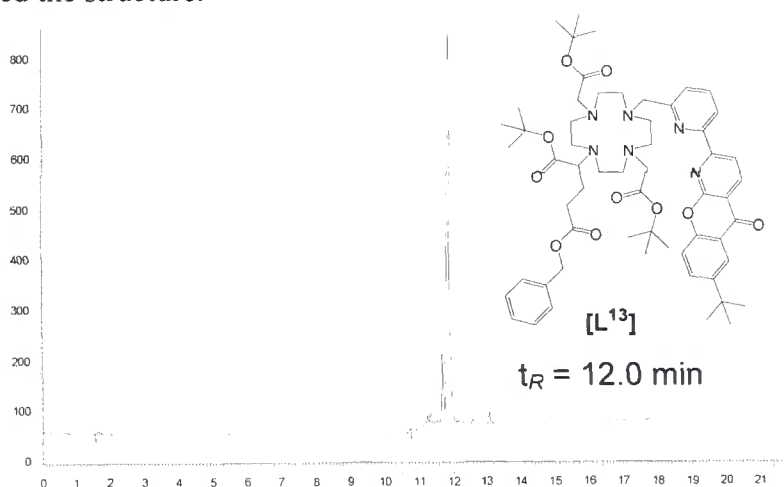
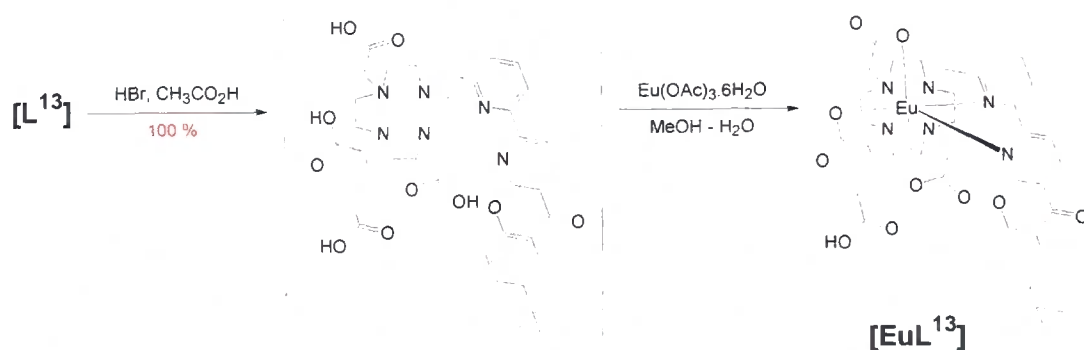


Figure 6.15: Reverse phase analytical HPLC analysis of $[\text{L}^{13}]$

(Chromolith performance RP18e column; Method A;ⁱⁱ $\lambda_{\text{exc}} = 355 \text{ nm}$, $\lambda_{\text{em}} = 355 \text{ nm}$)

Literature precedent has demonstrated the potential to deprotect Cbz and BOC protecting groups in a one pot reaction.¹⁷ Consequently, $[\text{L}^{13}]$ was stirred in neat HBr / acetic acid at 40°C for 4 h (**Scheme 6.15**). Examination of the reaction mixture by ^1H NMR showed the disappearance of both the characteristic benzyl CH_2 (Cbz) and *tert*-butyl (Boc) signals, suggesting complete deprotection. Analysis of the material by HPLC showed the formation of a new single product, exhibiting a significant shift in retention time (t_{R} (SM) = 12.0 min; t_{R} (Prod) = 10.8 min). Complexation of the crude reaction product was performed in MeOH – H_2O (1:1 v/v) at pH 5.5 using $\text{Eu}(\text{OAc})_3 \cdot 6\text{H}_2\text{O}$. Finally, removal of excess lanthanide was achieved by precipitation of $\text{Eu}(\text{OH})_3$ at pH 10.



Scheme 6.15: Reaction of $[\text{L}^{12}]$ with HBr / acetic acid and subsequent complexation

ⁱⁱ For HPLC solvents and gradients see Chapter 7: Experimental

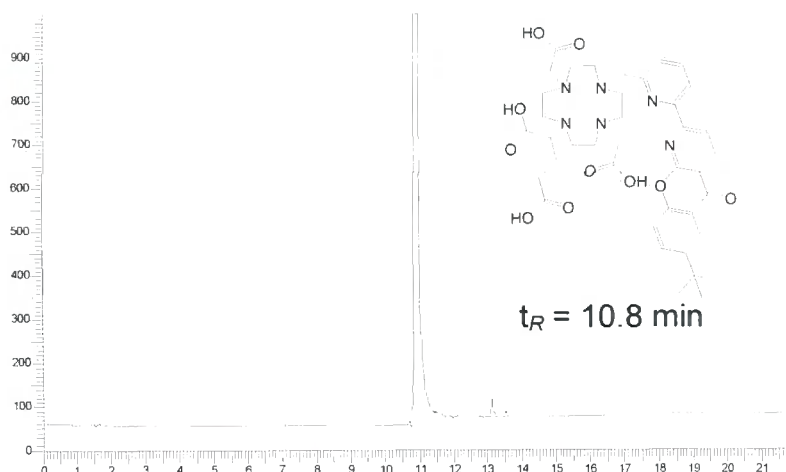


Figure 6.16: Reverse phase analytical HPLC analysis of $[L^{13}]$ following HBr / acetic acid deprotection

6.5.2 Carboxylate Conjugate Complex Characterisation

Photophysical characterisation of the carboxylate conjugate complex $[L^{13}]$ resembled that of the analogous DO3A complex $[EuL^1]$. Examination of the total emission spectrum showed both azaxanthone fluorescence and the Eu spectral fingerprint from the 5D_0 emissive state. The luminescent lifetime was determined as 0.90 ms in H_2O , with the complex exhibiting a q value of 0 in aqueous media. Although the ligand-based emission ($\Phi_{em}^f = \sim 20\%$) lowers the europium quantum yield when compared to the tri-amide derivative, $[EuL^9]$, the presence of a distinct $\Delta J = 2$ band provides an observable parameter through which the complex can be monitored in an HTRF assay. Future work will involve analogous synthesis of the BG conjugate complex to that described for $[EuL^9]$.

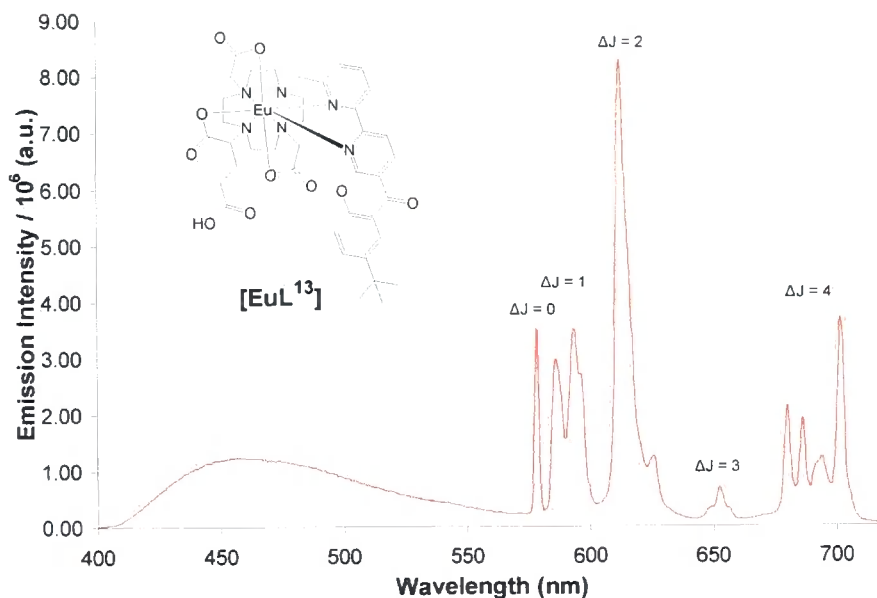


Figure 6.17: Total emission spectrum of $[\text{EuL}^{13}]$ (aerated water, 295 K, λ_{exc} 355 nm).

6.6 Conclusions

Para-methoxy functionalised cationic amide complexes incorporating the pyridyl-, pyrazoyl-azaxanthone and dpqC chromophore have been synthesised. A convenient and reproducible method of activation via a *N*-hydroxysuccinimide ester has enabled the conjugation of a benzyl guanine vector. The respective complexes will be examined under HTRF assay conditions to determine their FRET efficiencies.

A neutral carboxylate conjugate complex has been synthesised to alleviate the high electrostatic adhesion of complexes $[\text{EuL}^9]$, $[\text{TbL}^{10}]$ and $[\text{LnL}^{11}]$. This complex is amenable to conjugation via a carboxylate function, and will be assessed for potential HTRF application by Cisbio International.

Future Work

6.7 Chromophore Optimisation

Coupling of 2-chloro-azaxanthone with commercially available pyrazoles was undertaken to investigate the effect of substituents on the chromophores extinction coefficient and triplet energy (T_1). Preliminary findings show that the inclusion of a carboxylic acid group was accompanied by a large increase in the molar extinction coefficient, without comprising other photophysical attributes (**Table 6.2**). In addition to providing favourable photophysical characteristics, a carboxylate group provides a means of conjugation.

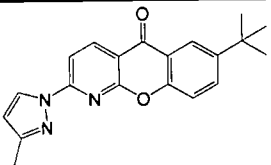
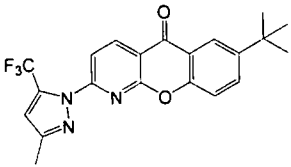
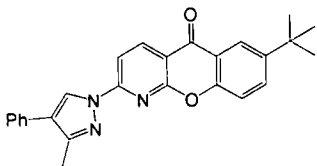
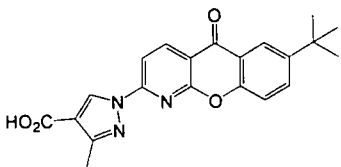
Chromophore	λ_{\max} (nm) ^a	ϵ (dm ³ mol ⁻¹ cm ⁻¹) ^a	E_T (cm ⁻¹) ^{b iii}
	346	15,380	23,470
	330	10,090	23,800
	353	20,000	23,500
	350	25,000	23,300

Table 6.2: Photophysical properties of selected sensitising chromophores

^a MeOH, 295 K; ^b 77K in an Et₂O-isopentane-ethanol (EPA) frozen glass)

ⁱⁱⁱ For phosphorescence emission spectra see Chapter 7: Experimental appendix

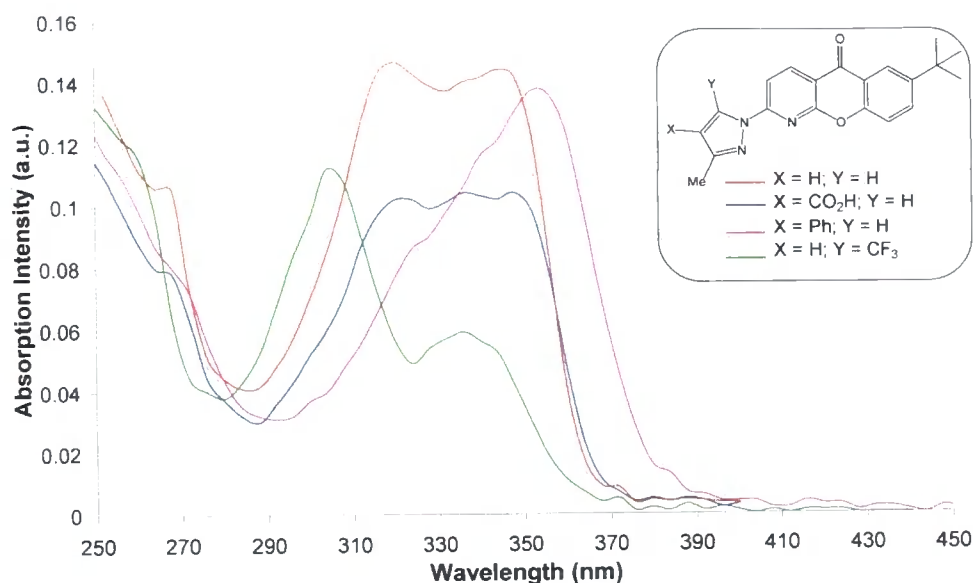


Figure 6.19: Absorption spectra of functionalised pyrazoyl-azaxanthenes (298 K, MeOH)

The commercial availability of 2-bromo-6-methyl-isonicotinic acid could also allow the investigation of a carboxylate functionalised pyridyl-azaxanthone and its potential conjugation.

6.8 Phosphinate Conjugate Complexes

An attractive alternative to carboxylic acid donor groups are phosphinic acid derivatives. Tri-phosphinic acid cyclen derivatives incorporating dpqC or azaxanthone chromophores have been shown to form kinetically stable and emissive complexes in aqueous solutions.³ The pentavalency of phosphorus means that an alkyl, aryl or other functionalities may be introduced readily, permitting not only control over complex lipophilicity but also providing a potential route of conjugation. By using selective protection and deprotection strategies, the synthesis of phosphinate conjugate complexes could be investigated. Literature precedents show synthetic procedures for synthesising two different phosphinate linkers.^{18,19} The two compounds provide contrasting functionalities (i.e. CO₂H and NH₂) with which to conjugate appropriate vectors.

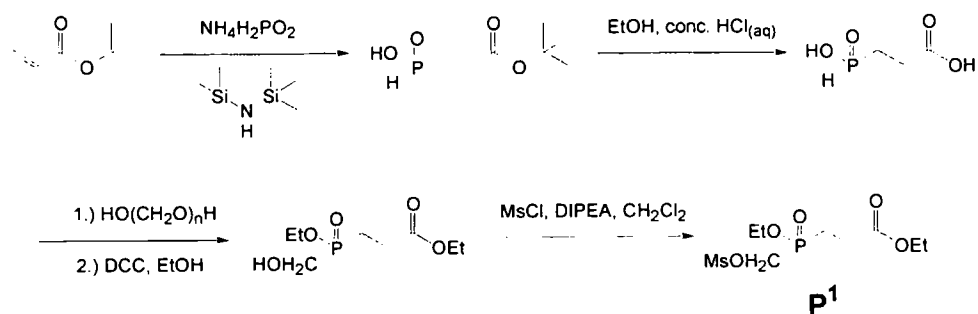
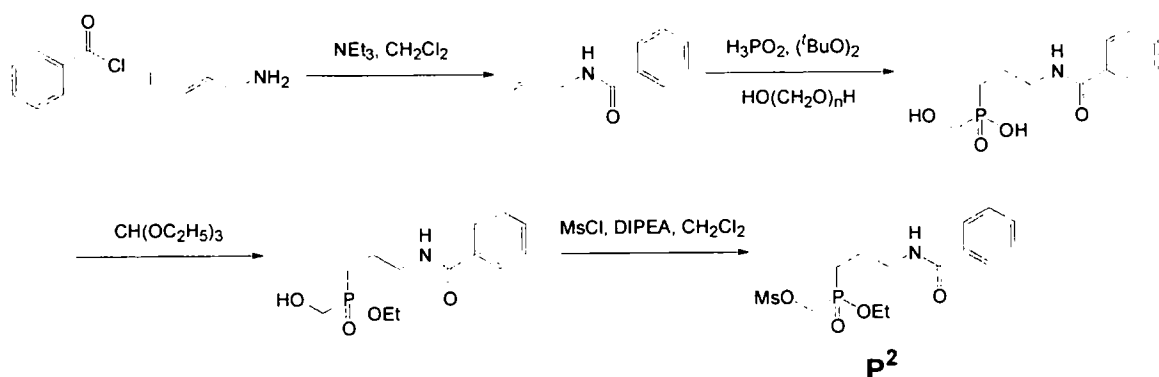
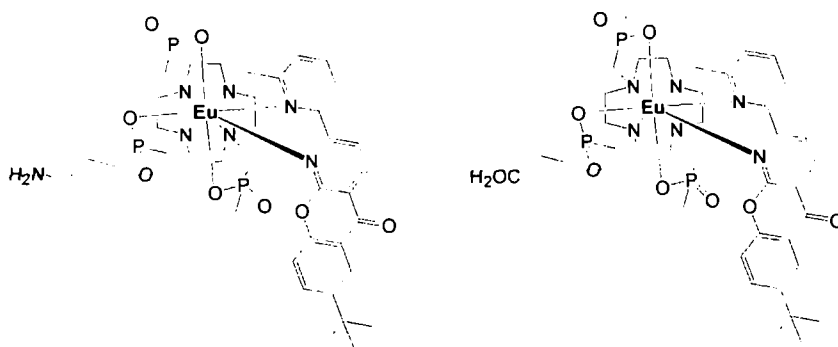
Scheme 6.17: Synthesis of the *o*-mesyl phosphinate **P¹**Scheme 6.18: Synthesis of the *o*-mesyl phosphinate **P²**

Figure 6.20: Structures of potential conjugate phosphinate complexes

Initial alkylation reactions of the mesylate derivatives **P¹** and **P²** highlighted the lack of reactivity of these compounds towards sterically demanding cyclen derivatives. Consequently, attempts to incorporate these moieties onto cyclen should be performed earlier in the synthetic route, and on a non-sterically demanding cyclen compound.

References

- 1.) F. Kielar, A. Congreve, G-L. Law, E. J. New, D. Parker, K-L. Wong, P. Castreño and J. de Mendoza, *Chem. Commun.*, 2008, 2435.
- 2.) F. Kielar, G-L. Law, E. J. New and D. Parker, *Org. Biomol. Chem.*, 2008, **6**, 2256.
- 3.) R. A. Poole, *Luminescent Lanthanide Complexes for Cellular Applications*, PhD Thesis, Department of Chemistry, University of Durham, 2006.
- 4.) R. S. Dickins, J. A. K. Howard, C. L. Maupin, J. M. Moloney, D. Parker, J. P. Riehl, G. Siligardi and J. A. G. Williams, *Chem. Eur. J.*, 1999, **5**, 1095.
- 5.) B. B. Shankar, B. J. Lavey, G. Zhou, J. A. Spitler, L. Tong, R. Rizvi, D-Y. Yang, R. Wolin, J. A. Kozlowski, N-Y. Shih, J. Wu, R. W. Hipkin, W. Gonsiorek and C. A. Lunn, *Bioorg. Med. Chem. Lett.*, 2005, **15**, 4417.
- 6.) Z. Kovacs and A. D. Sherry, *J. Chem. Soc., Chem. Commun.*, 1995, **2**, 185
- 7.) L-O. Pålsson, R. Pal, B. S. Murray, D. Parker and A. Beeby, *Dalton Trans.*, 2007, 5726.
- 8.) M. Woods and A. D. Sherry, *Inorg. Chim. Acta.*, 2003, **351**, 395.
- 9.) J. I. Bruce, R. S. Dickins, D. Parker and D. J. Tozer, *Dalton Trans.*, 2003, 1264.
- 10.) A. Beeby, I. M. Clarkson, R. S. Dickins, S. Faulkner, D. Parker, L. Royle, A.S. de Sousa, J. A. G. Williams and M. Woods, *J. Chem. Soc. Perkin Trans. 2.*, 1999, 493.
- 11.) M. Schwab, T. Gibbs and A. Brecht, *Genet. Eng. News.*, 2005, **25**, 21.
- 12.) D. Maurel, L. Comps-Agrar, C. Brock, M-L. Rives, E. Bourrier, M. A. Ayoub, H. Bazin, N. Tinel, T. Durroux, L. Prézeau, E. Trinquet and J-P. Pin, *Nat. Methods.*, *In Press*
- 13.) A. Keppler, S. Gendreizig, T. Gronemeyer, H. Pick, H. Vogel and K. Johnsson, *Nat. Biotechnol.*, 2003, **21**, 86.
- 14.) A. Keppler, H. Pick, C. Arrivoli, H. Vogel and K. Johnsson, *P. Natl. Acad. Sci. USA.*, 2004, **101**, 9955.
- 15.) A. Keppler, M. Kindermann, S. Gendreizig, H. Pick, H. Vogel and K. Johnsson, *Methods*, 2004, **32**, 437.
- 16.) K-P. Eisenwiener, P. Powell and H. R. Mäcke, *Bioorg. Med. Chem. Lett.*, 2000, **10**, 2133.
- 17.) C. Schmuck and P. Wich, *Angew. Chem. Int. Ed.*, 2006, **45**, 4277.

18.) C. J. Broan, E. Cole, K. J. Jankowski, D. Parker, K. Pulukkody, B. A. Boyce, N. R. A. Beeley, K. Millar and A. T. Millican, *Synthesis*, 1992, 63.

19.) P. Rězanka, V. Kubíček, P. Herman and I. Lukeš, *Synthesis.*, 2008, 1431.

CHAPTER SEVEN:

Experimental

Chapter 7: Experimental

General Procedures

Reagents and Solvents

All commercially available reagents were used as received, from their respective suppliers. Solvents were dried using an appropriate drying agent when required. Reactions requiring anhydrous conditions were carried out using Schlenk-line techniques under an atmosphere of dry argon. Water and H₂O refer to high purity water with conductivity $\leq 0.04 \mu\text{S cm}^{-1}$ obtained from the 'Purite_{STILL} plus' purification system.

Chromatography

Thin-layer chromatography was carried out on neutral alumina plates (Merck Art 5550) or silica plates (Merck 5554) and visualised under UV (254 nm / 365 nm) or by staining with iodine. Preparative column chromatography was carried out using neutral alumina (Merck Aluminium Oxide 90, activity II-III, 70-230 mesh), pre-soaked in ethyl acetate, or silica (Merck Silica Gel 60, 230-400 mesh).

Spectroscopy

¹H and ¹³C NMR spectra were recorded on a Varian Mercury 200 (¹H at 199.98 MHz, ¹³C at 50.29 MHz), Varian Unity 300 (¹H at 299.91 MHz, ¹³C at 75.41 MHz), Varian VXR 400 (¹H at 399.97 MHz, ¹³C at 100.57 MHz), Bruker AMX 500 (¹H at 499.76 MHz, ¹³C at 125.66 MHz) or Varian Unity 700 spectrometer (¹H at 699.73 MHz, ¹³C at 175.94 MHz). Spectra were referenced internally to the residual protio-solvent resonances and are reported relative to TMS. Chemical shifts are reported as ppm and coupling constants in Hz. Splitting patterns are described as singlet (s), doublet (d), triplet (t), quartet (q) or multiplet (m).

Electrospray mass spectra were recorded on a VG Platform II (Fisons instrument), operating in positive or negative ion mode as stated, with methanol as the carrier solvent.

Accurate mass spectra were recorded using a Thermo Finnigan LTQ FT mass spectrometer.

UV/Vis absorbance spectra were recorded on a Perkin Elmer Lambda 900 UV/Vis/NIR spectrometer. Samples were contained in quartz cuvettes with a path length of 1 cm and measurements obtained relative to a reference of pure solvent contained in a matched cell.

Emission Spectra were recorded at 298 K using a Fluorolog 3-11 spectrometer using DataMax v 2.1 for Windows. Luminescence spectra of the europium (III) and terbium (III) complexes were recorded using a 420 nm cut-off filter, following indirect excitation of the lanthanide (III) ion, via the pyridyl-, pyrazoyl-azaxanthone or dpqC at 355 nm or 348 nm respectively, except where stated. An integration time of 0.5 seconds, increment of 0.5 nm and excitation and emission slit widths of 2 and 1 nm, respectively, were employed throughout.

Circularly Polarised Luminescence (CPL) measurements were made using a home-built (Glasgow University, UK) CPL spectrometer based on a Spex Fluopomax-2-spectrofluorimeter with the assistance of Dr. R. D. Peacock. Samples were run using D₂O as a solvent.

Relaxivity measurements were performed at 37 °C and 60 MHz on a Bruker Minispec mq60 instrument. The mean value of three separate measurements was recorded and an average taken.

Melting points were recorded using a Köfler block and are uncorrected

pH Measurements

pH measurements were performed using a Jenway 3020 or a Jenway 3320 pH meter attached to an Aldrich Chemical Company micro-pH combination electrode. Calibration was achieved using pH 4.01, pH 7.00 and pH 10.03 buffer solutions supplied by Aldrich.

Triplet Energy Measurements

Low temperature phosphorescence spectra were performed using an Oxford Instruments optical cryostat operating at 77 K. Samples were dissolved in EPA (diethyl ether – isopentane – ethanol (2 : 5 : 5 : v/v)) and contained in 10 mm cuvettes. The triplet energy was obtained from the extrapolation of the highest energy phosphorescence band, corresponding to the 0 – 0 transition, using time-gated detection.

Europium and Terbium Lifetime Measurements

Emissive lifetimes were recorded at 298 K using a Perkin Elmer LS55 luminescence spectrometer using FL Winlab software. The lifetimes of the Eu and Tb complexes were measured by exciting the sample using a short pulse of light, followed by the monitoring of the integrated intensity of light (545 nm for terbium, 620 nm for europium) emitted during a fixed gate time, t_g , after a delay time, t_d . At least 20 delay times were used covering 3 or more lifetimes. A gate time of 0.1 ms was employed, and the excitation and emission slits set to bandpass of 10 nm. The obtained exponential decay curves were fitted to the equation below

$$I = A_0 + A_1 \exp(-kt)$$

where:

I = intensity at time t after the flash

A_0 = intensity after the decay has finished

A_1 = pre-exponential factor

k = rate constant for decay of the excited state.

The excited state lifetime, τ , is the inverse of the rate constant, k .

Quantum Yield Measurements ⁱ

The Photoluminescence Quantum Yields (PLQY) were determined using a method based upon that originally developed by de Mello et al.ⁱⁱ In this approach the PLQY (Φ_{PL}) is given by:

$$\phi_{PL} = \frac{E_{in}(\lambda) - (1 - \alpha)E_{out}(\lambda)}{X_{empty}(\lambda)\alpha}$$

with

$$\alpha = \frac{X_{out}(\lambda) - X_{in}(\lambda)}{X_{out}(\lambda)}$$

where:

$E_{in}(\lambda)$ is the integrated luminescence from direct excitation of the film

$E_{out}(\lambda)$ is the integrated luminescence from secondary excitation

$X_{empty}(\lambda)$ is the integrated excitation profile with the empty sphere

α is the film absorptance (Absorptance, α , is the fraction of light absorbed, equal to one minus the transmittance, which is obtained by measuring the integrated excitation bands

$X_{in}(\lambda)$ is the integrated excitation when the sample lies directly in the excitation path

$X_{out}(\lambda)$ is the integrated excitation when the excitation light first hits the sphere wall

Measurements were performed at 298 K using solutions with absorption of less than 0.15 at the chosen excitation wavelength (in a 1 cm pathlength cuvette). The samples were measured in a homemade cylindrical optical quartz cuvette with a diameter of 8 mm, equipped with a homemade Teflon stopper. A HORIBA Jobin-Yvon Fluorolog 3-22 Tau-3 fluorimeter was used, incorporating a Labsphere® optical Spectralon integrating sphere (diameter 100 mm, reflectance > 99 % over 400 – 1500 nm range).

ⁱ L. Porrès, A. Holland, L-O. Pålsson, A. P. Monkman, C. Kemp and A. Beeby, *J. Fluorescence*, 2006, **16**, 267.

ⁱⁱ J. C. de Mello, H. F. Wittmann and R. H. Friend, *Adv. Mater.*, 1997, **9**, 230.

HPLC Analysis***Durham***

Analytical reverse phase HPLC analysis were performed at 298 K on a Perkin Elmer system comprising of Perkin Elmer Series 200 Pump, Perkin Elmer Series 200 Autosampler, Perkin Elmer Series 200 Diode array detector and Perkin Elmer Series 200 Fluorescence detector.

All analysis was performed using a Chromolith performance RP18e 100 x 4.6 mm column, using a flow rate of 1 ml / min and solvent Method A.

Method A:

Time (min)	H₂O + 0.1 % HCO₂H	CH₃CN + 0.1 % HCO₂H
0	95	5
2	95	5
15	0	100
17	0	100
22	95	5

Cisbio International, France

Analytical and semi-preparative HPLC were performed at 298 K using a Waters HPLC system equipped with a diode array detector.

Analytical HPLC was performed using a Chromolith performance RP18e 100 x 4.6 mm column, using a flow rate of 3 ml / min and one of the selected methods shown below;

Method B:

Time (min)	H₂O + 0.1 % HCO₂H	CH₃CN + 0.1 % HCO₂H
0	95	5
1	95	5
8	35	65
10	0	100
11	85	15
13	95	5

Method C:

Time (min)	H₂O + 0.1 % HCO₂H	CH₃CN + 0.1 % HCO₂H
0	85	15
1	85	15
10	0	100
11	85	15
13	85	15

Method D:

Time (min)	H₂O + 0.1 % HCO₂H	CH₃CN + 0.1 % HCO₂H
0	90	10
1	90	10
11	30	70
12	0	100
14	0	100
15	90	10
17	90	10

Semi-preparative HPLC was performed using a Chromolith performance RP18e 100 x 10 mm column, using a flow rate of 14.1 ml / min and one of the selected methods shown below;

Method E:

Time (min)	H₂O + 0.1 % HCO₂H	CH₃CN + 0.1 % HCO₂H
0	80	20
1	80	20
8	45	55
10	0	100
11	0	100
12	80	20
13	80	20

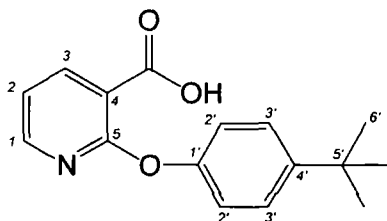
Method F:

Time (min)	H₂O + 0.1 % HCO₂H	CH₃CN + 0.1 % HCO₂H
0	85	15
3	85	15
30	0	100
33	0	100
36	85	15
40	85	15

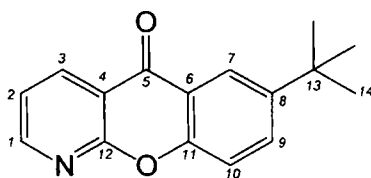
Ligand and Complex Synthesis

7.1 Sensitising Chromophores

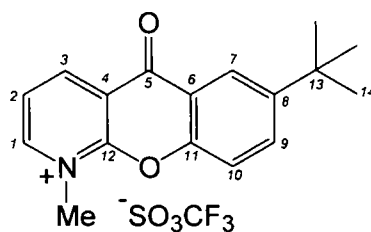
2-(4-*tert*-Butylphenoxy)-nicotinic acid **1** (1)



4-*tert*-Butylphenol (15.2 g, 101 mmol) was added to a stirred solution of sodium metal (1.02 g, 44.4 mmol) in *anhydrous* CH₃OH (25 ml) to form a thick cream coloured solution. The solvent was removed under reduced pressure to afford a cream coloured residue. 2-Chloronicotinic acid (3.31 g, 21.0 mmol) was added to the residue and the resulting mixture heated at 190 °C, with stirring, for 20 h. The reaction mixture was allowed to cool to 100 °C, then poured into H₂O (200 ml). The aqueous solution was extracted with diethyl ether (2 x 150 ml), and acidified to pH 5 by the addition of glacial acetic acid to afford a fine precipitate. The precipitate was filtered, washed with H₂O (100 ml) and dried under vacuum to yield the *title compound 1* as a colourless crystalline solid (4.89 g, 18.0 mmol, 86 %); m.p. 180-181 °C {lit. 179-181 °C}; ¹H NMR (CDCl₃, 500 MHz) δ 1.37 (9H, s, *t*Bu CH₃), 7.14 (2H, d, *J* = 8.5 Hz, H^{2'}), 7.20 (1H, dd, *J* = 7.5; 5.0 Hz, H²), 7.49 (2H, d, *J* = 9.0 Hz, H^{3'}), 8.35 (1H, dd, *J* = 4.5; 2.0 Hz, H¹), 8.55 (1H, dd, *J* = 8.0; 2.0 Hz, H³); ¹³C NMR (CDCl₃, 125 MHz, ¹H decoupled 500 MHz) δ 31.7 (3C, C^{6'}), 34.8 (1C, C^{5'}), 113.5 (1C, C⁴), 119.7 (1C, C²), 121.4 (1C, C^{2'}), 127.1 (1C, C^{3'}), 143.8 (1C, C³), 149.3 (1C, C^{4'}), 149.8 (1C, C^{1'}), 152.4 (1C, C¹), 161.5 (1C, C⁵), 164.9 (1C, C=O); MS (ES⁻) *m/z* 270.2 (100 %, [M - H]⁻); HRMS (ES⁻) *m/z* found 270.1135 [M - H]⁻ C₁₆H₁₆O₃N₁ requires 270.1135; C₁₆H₁₇N₂O (%): calcd C 70.83, H 6.32, N 5.16; found C 70.54, H 6.20, N 4.91.

6-*tert*-Butyl-9-oxa-1-aza-anthracen-10-one ¹ (2)

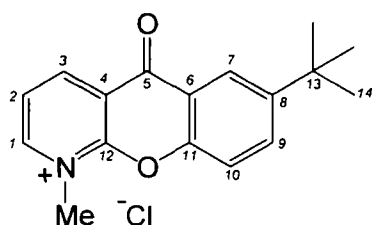
A stirred mixture of polyphosphoric acid (70 g) and 2-(4-*tert*-butyl-phenoxy)-nicotinic acid **1** (2.15 g, 7.93 mmol), was heated at 120 °C, for 16 h. The brown reaction mixture was allowed to cool to rt, before being poured onto iced water (400 ml) to afford a pale yellow solution. The pH of the aqueous solution was adjusted to pH 7 by the addition of conc. NaOH_(aq). The aqueous solution was then extracted with diethyl ether (3 x 300 ml). The organic extracts were combined, dried over MgSO₄, filtered and the solvent removed under reduced pressure to yield the *title compound 2* as a yellow coloured solid (1.79 g, 7.08 mmol, 89 %); m.p. 97-98 °C {lit. 98-100 °C}; ¹H NMR (CDCl₃, 500 MHz) δ 1.42 (9H, s, ^tBu CH₃), 7.45 (1H, dd, *J* = 7.5; 4.5 Hz, H²), 7.58 (1H, d, *J* = 8.5 Hz, H¹⁰), 7.86 (1H, dd, *J* = 9.0; 3.0 Hz, H⁹), 8.30 (1H, d, *J* = 2.5 Hz, H⁷), 8.73 (1H, d, *J* = 7.5 Hz, H¹), 8.76 (1H, d, *J* = 7.5 Hz, H³); ¹³C NMR (CDCl₃, 125 MHz, ¹H decoupled 500 MHz) δ 31.6 (3C, C¹⁴), 35.1 (1C, C¹³), 117.0 (1C, C⁴), 118.4 (1C, C¹⁰), 121.1 (1C, C²), 121.1 (1C, C¹), 122.7 (1C, C⁷), 133.9 (1C, C⁹), 137.6 (1C, C³), 148.2 (1C, C⁶), 154.1 (1C, C⁸), 154.3 (1C, C¹²), 160.6 (1C, C¹¹), 178.1 (1C, C⁵); MS (ES⁺) *m/z* 254.2 (100 %, [M + H]⁺); HRMS (ES⁺) *m/z* found 254.1177 [M + H]⁺ C₁₆H₁₆O₂N₁ requires 254.1176; C₁₆H₁₅NO₂ (%): calcd C 75.87, H 5.97, N 5.53; found C 75.80, H 5.91, N 5.61.

6-*tert*-Butyl-1-methyl-9-oxa-1-aza-anthracen-10-one trifluoromethylsulfonate (3)

A solution of 6-*tert*-butyl-9-oxa-1-aza-anthracen-10-one **2** (1.00 g, 3.95 mmol) in *anhydrous* toluene (20 ml) was stirred at 0 °C, under an atmosphere of argon. Methyl trifluoromethanesulfonate (6 ml, 8.70 g, 53.0 mmol) was added to the solution dropwise

over 10 min. The solution was stirred at 0 °C for 1 h, to afford a fine precipitate. The precipitate was filtered and dried under vacuum to afford the *title compound 3* as a colourless solid (1.49 g, 3.58 mmol, 91 %); ^1H NMR (CD_3OD , 400 MHz) δ 1.43 (9H, s, ^tBu CH_3), 4.51 (3H, s, CH_3), 7.84 (1H, d, $J = 9.0$ Hz, H^{10}), 7.99 (1H, dd, $J = 8.0$; 6.0 Hz, H^2), 8.15 (1H, dd, $J = 9.0$; 2.5 Hz, H^9), 8.33 (1H, d, $J = 2.5$ Hz, H^7), 9.14 (1H, dd, $J = 6.0$; 2.0 Hz, H^1), 9.30 (1H, dd, $J = 8.0$; 2.0 Hz, H^3); ^{13}C NMR (CD_3OD , 100 MHz, ^1H decoupled 400 MHz) δ 30.3 (3C, C^{14}), 34.8 (1C, C^{13}), 41.7 (1C, CH_3), 118.2 (1C, C^{10}), 120.4 (1C, C^4), 120.8 (1C, C^6), 121.2 (1C, C^2), 122.6 (1C, C^7), 135.4 (1C, C^9), 145.9 (1C, C^3), 149.1 (1C, C^1), 151.1 (1C, C^8), 152.4 (1C, C^{11}), 156.3 (1C, C^{12}), 173.8 (1C, C^5); ^{19}F NMR (CD_3OD , 188 MHz, ^1H decoupled 400 MHz) δ 80.5 (s, CF_3); MS (ES^+) m/z 268.2 (100 %, $[\text{M}]^+$); HRMS (ES^+) m/z found 268.1332 $[\text{M}]^+$ $\text{C}_{17}\text{H}_{18}\text{O}_2\text{N}_1$ requires 268.1332.

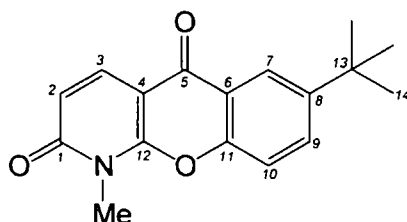
6-*tert*-Butyl-1-methyl-9-oxa-1-aza-anthracen-10-one chloride (4)



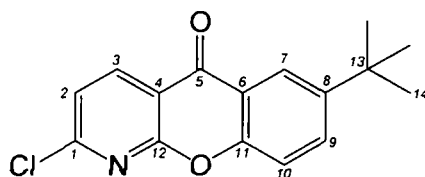
Ion exchange of 6-*tert*-butyl-1-methyl-9-oxa-1-aza-anthracen-10-one trifluoromethylsulfonate **3** to the corresponding chloride salt was performed to enhance water solubility. DOWEX 1x8 200-400 mesh Cl ion exchange resin was refluxed in CH_3OH overnight, followed by washing with H_2O (500 ml), then 0.1 M HCl (200 ml) and finally H_2O until the eluted solvent was of neutral pH. 6-*tert*-Butyl-1-methyl-9-oxa-1-aza-anthracen-10-one trifluoromethylsulfonate (1.00 g, 2.40 mmol) was dissolved in a mixture of H_2O and CH_3OH (1:1, v/v 20 ml) and added to an excess of prepared DOWEX resin (0.5 g). The mixture was stirred at rt for 2 h, filtered and the solvent removed under reduced pressure to yield the corresponding chloride salt **4** in quantitative yield; ^1H NMR (CD_3OD , 500 MHz) δ 1.46 (9H, s, ^tBu CH_3), 4.55 (3H, s, CH_3), 7.88 (1H, d, $J = 9.0$ Hz, H^{10}), 8.03 (1H, t, $J = 6.5$ Hz, H^2), 8.18 (1H, dd, $J = 9.0$; 2.0 Hz, H^9), 8.36 (1H, d, $J = 2.0$ Hz, H^7), 9.22 (1H, d, $J = 6.5$ Hz, H^1), 9.33 (1H, d, $J = 7.5$ Hz, H^3); ^{13}C NMR (CD_3OD , 125 MHz, ^1H decoupled 500 MHz) δ 30.4 (3C, C^{14}), 34.8 (1C, C^{13}), 41.8 (1C, CH_3), 118.2 (1C, C^{10}), 120.5 (1C, C^4), 120.8 (1C, C^6), 121.2 (1C, C^2), 122.6 (1C,

C⁷), 135.4 (1C, C⁹), 145.9 (1C, C³), 149.1 (1C, C¹), 151.1 (1C, C⁸), 152.4 (1C, C¹¹), 156.3 (1C, C¹²), 173.8 (1C, C⁵).

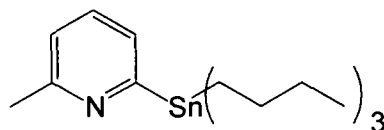
6-*tert*-Butyl-1-methyl-1H-9-oxa-1-aza-anthracene-2,10-dione (5)



A solution of 6-*tert*-butyl-1-methyl-9-oxa-1-aza-anthracen-10-one chloride **4** (0.361 g, 1.18 mmol) in H₂O (10 ml) was added dropwise over 30 min, to a stirred solution of potassium hexacyanoferrate (III) (1.16 g, 3.54 mmol) in H₂O (6 ml), at 0 °C. This was followed by the dropwise addition of a solution of NaOH (0.850 g, 21.2 mmol) in H₂O (10 ml) to the stirred solution over 30 min. The solution was allowed to warm to rt and stirred for 8 h. The solution was acidified to pH 3 by the addition of conc. H₂SO₄ (aq) to afford a green precipitate. The precipitate was filtered, dissolved in CHCl₃ (50 ml) and washed with H₂O (2 x 50 ml). The organic phase was separated, dried over MgSO₄, filtered and the solvent removed under reduced pressure to yield the *title compound 5* as a red coloured solid (0.251 g, 0.872 mmol, 74 %); m.p. 243-244 °C; ¹H NMR (CDCl₃, 500 MHz) δ 1.41 (9H, s, *t*Bu CH₃), 3.76 (3H, s, CH₃), 6.54 (1H, d, *J* = 9.5 Hz, H²), 7.47 (1H, d, *J* = 8.5 Hz, H¹⁰), 7.79 (1H, dd, *J* = 9.0; 2.0 Hz, H⁹), 8.21 (1H, d, *J* = 9.5 Hz, H³), 8.29 (1H, d, *J* = 2.0 Hz, H⁷); ¹³C NMR (CDCl₃, 125 MHz, ¹H decoupled 500 MHz) δ 28.5 (1C, CH₃), 31.6 (3C, C¹⁴), 35.2 (1C, C¹³), 102.8 (1C, C⁴), 116.0 (1C, C²), 117.3 (1C, C¹⁰), 121.6 (1C, C⁶), 122.9 (1C, C⁷), 132.3 (1C, C⁹), 135.7 (1C, C³), 149.7 (1C, C⁸), 152.0 (1C, C¹¹), 156.5 (1C, C¹²), 162.3 (1C, C¹), 174.2 (1C, C⁵); MS (ES⁺) *m/z* 284.3 (100 %, [M + H]⁺); HRMS (ES⁺) *m/z* found 284.1281 [M + H]⁺ C₁₇H₁₈O₃N₁ requires 284.1281; C₁₇H₁₇NO₃ (%): calcd C 72.07, H 6.05, N 4.94; found C 72.02, H 5.99, N 4.90.

6-tert-Butyl-2-chloro-9-oxa-1-aza-anthracen-10-one (6)

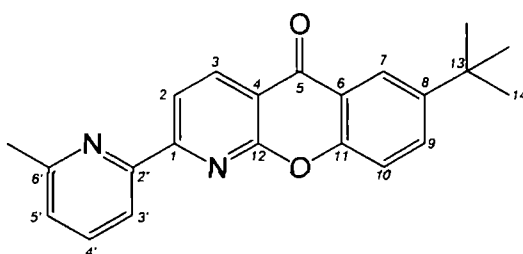
A stirred solution of 6-*tert*-butyl-1-methyl-1H-9-oxa-1-aza-anthracene-2,10-dione **5** (0.180 g, 0.636 mmol) in POCl_3 (10 ml) and *N,N*-dimethylaniline (0.30 ml, 0.313 g, 2.59 mmol) was heated at reflux, for 18 h. The mixture was allowed to cool to rt and slowly added dropwise to iced water (300 ml) in a well ventilated fumehood. The aqueous solution was extracted with CH_2Cl_2 (2 x 200 ml) and the organic phases combined. The organic phase was washed with 0.1 M K_2CO_3 (aq) (100 ml), dried over K_2CO_3 , filtered and the solvent removed under reduced pressure. The residue was dried onto silica and purified by column chromatography on silica (gradient elution: Hexane to 10 % EtOAc : Hexane, utilising 1 % EtOAc increments) to yield the *title compound 6* as a pink coloured solid (0.090 g, 0.313 mmol, 49 %); $R_F = 0.33$ (Silica, Hexane – EtOAc, 9 : 1 v/v); m.p. 132-133 °C; ^1H NMR (CDCl_3 , 500 MHz) δ 1.41 (9H, s, *t*Bu CH_3), 7.43 (1H, d, $J = 8.0$ Hz, H^2), 7.54 (1H, d, $J = 9.0$ Hz, H^{10}), 7.86 (1H, dd, $J = 9.0; 2.5$ Hz, H^9), 8.27 (1H, d, $J = 2.5$ Hz, H^7), 8.65 (1H, d, $J = 8.0$ Hz, H^3); ^{13}C NMR (CDCl_3 , 125 MHz, ^1H decoupled 500 MHz) δ 31.5 (3C, C^{14}), 35.1 (1C, C^{13}), 115.6 (1C, C^4), 118.4 (1C, C^{10}), 121.1 (1C, C^6), 121.9 (1C, C^2), 122.7 (1C, C^7), 134.1 (1C, C^9), 139.9 (1C, C^3), 148.8 (1C, C^8), 153.8 (1C, C^{11}), 155.6 (1C, C^{12}), 159.7 (1C, C^1), 177.2 (1C, C^5).

7.1.1 Pyridyl-azaxanthone**2-Methyl-6-tributylstannanyl-pyridine ² (7)**

n-Butyllithium (1.94 ml, 3.13 mmol, 1.6 M in hexane) was added dropwise to a stirred solution of 2-bromo-6-methylpyridine (0.50 g, 0.33 ml, 2.90 mmol) in *anhydrous* THF (15 ml), at -78 °C. After stirring the solution at -78 °C for 2 h, tributyltinchloride (0.94 ml, 3.49 mmol) was added dropwise, and the mixture stirred while allowed to warm to rt.

H₂O (20 ml) was poured into the reaction mixture and the phases separated. The aqueous phase was extracted with diethyl ether (2 x 20 ml). The combined organic extracts were dried over MgSO₄, filtered, and the solvent removed under reduced pressure to yield the crude *title compound 7*. The material was used directly without any further purification.

6-*tert*-Butyl-2-(6-methyl-pyridin-2-yl)-9-oxa-1-aza-anthracen-10-one (8)



Procedure A; Stille Cross-Coupling

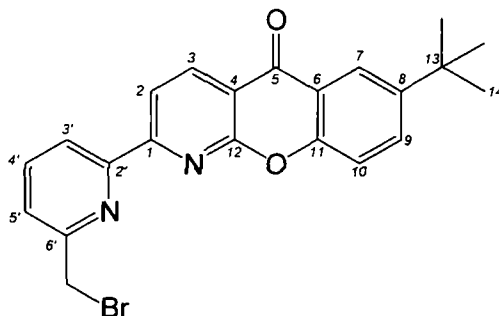
6-*tert*-Butyl-2-chloro-9-oxa-anthracen-10-one **6** (0.201 g, 0.696 mmol) and 6-methyl-2-(tributylstannyl)pyridine **7** (0.293 g, 0.766 mmol) were added to a Schlenk tube which was evacuated and back filled with argon three times. Degassed toluene (5 ml) was added to the vessel which was then evacuated and back filled with argon five times. Tetrakis(triphenylphosphine)palladium (0) (0.040 g, 0.034 mmol) was added to the solution under an atmosphere of argon. The reaction mixture was stirred and heated at reflux, under argon, for 16 h. The reaction mixture was allowed to cool to rt, filtered, and the solute concentrated under reduced pressure to afford a residual brown oil. The crude material was triturated with diethyl ether (10 ml) to yield a fine precipitate in red solute. The solvent was decanted and the solid dried under vacuum to yield the *title compound 8* as a colourless solid (0.145 g, 0.422 mmol, 61 %); m.p. 191-192 °C; ¹H NMR (CDCl₃, 700 MHz) δ 1.37 (9H, s, ^tBu CH₃), 2.60 (3H, s, CH₃), 7.18 (1H, d, *J* = 8.0 Hz, H^{5'}), 7.53 (1H, d, *J* = 8.0 Hz, H¹⁰), 7.69 (1H, t, *J* = 8.0 Hz, H^{4'}), 7.79 (1H, dd, *J* = 8.0; 2.0 Hz, H⁹), 8.26 (1H, d, *J* = 2.0 Hz, H⁷), 8.29 (1H, d, *J* = 8.0 Hz, H^{3'}), 8.54 (1H, d, *J* = 8.5 Hz, H²), 8.74 (1H, d, *J* = 8.5 Hz, H³); ¹³C NMR (CDCl₃, 176 MHz, ¹H decoupled 700 MHz) δ 24.8 (1C, CH₃), 31.5 (3C, C¹⁴), 35.0 (1C, C¹³), 116.4 (1C, C⁴), 118.3 (1C, C¹⁰), 118.5 (1C, C²), 119.7 (1C, C⁵), 121.3 (1C, C⁶), 122.7 (1C, C⁷), 124.9 (1C, C^{2'}), 133.6 (1C, C⁹), 137.4 (1C, C^{4'}), 138.2 (1C, C³), 148.0 (1C, C⁸), 153.6 (1C, C^{1'}), 154.2 (1C, C¹¹), 158.6

(1C, C⁶), 160.2 (1C, C¹), 160.6 (1C, C¹²), 177.8 (1C, C⁵); MS (ES⁺) m/z 345.2 (100 %, [M + H]⁺); HRMS (ES⁺) m/z found 345.1596, C₂₂H₂₁O₂N₂ requires 345.1597, [M + H]⁺.

Procedure B; Suzuki-Miyaura Cross-Coupling

6-*tert*-Butyl-2-chloro-9-oxa-anthracen-10-one **6** (0.040 g, 0.14 mmol), 6-methyl-2-pyridineboronic acid *N*-phenyldiethanolamine ester (0.047 g, 0.17 mmol) and Cs₂CO₃ (0.054 g, 0.17 mmol) were added to a Schlenk tube which was evacuated and back filled with argon three times. Degassed 1,4-dioxane (4 ml) was added to the vessel, which was evacuated and back filled with argon three times. Pd₂(dba)₃ (2 mg, 1.5 % mol) and P(*t*Bu)₃ (1 mg, 3.6 % mol) were added to the reaction mixture, which was stirred and heated at 85 °C, under argon, for 18 h. After 18 h a further addition of Pd₂(dba)₃ (2 mg, 1.5 % mol) and P(*t*Bu)₃ (1 mg, 3.6 % mol) were introduced to the vessel, with heating continued at 85 °C for a further 24 h. The reaction mixture was allowed cool to rt and the solvent removed under reduced pressure. The residue was dissolved in diethyl ether (50 ml) and washed with H₂O (50 ml), followed by brine (50 ml). The organic phase was dried over K₂CO₃, filtered and the solvent removed under reduced pressure. The crude material was purified by column chromatography on silica (gradient elution: CH₂Cl₂ to 8 % CH₃OH:CH₂Cl₂, utilising 0.1 % CH₃OH increments). The product was recrystallised from warm EtOH and dried under vacuum to yield the *title compound* **8** as a colourless solid (0.008 g, 0.015 mmol, 16 %); R_F = 0.38 (Silica, CH₃OH – CH₂Cl₂, 9 : 1 v/v).
Characterisation as reported in procedure A.

2-(6-Bromomethyl-pyridin-2-yl)-6-*tert*-butyl-9-oxa-1-aza-anthracen-10-one (**9**)



Procedure A:

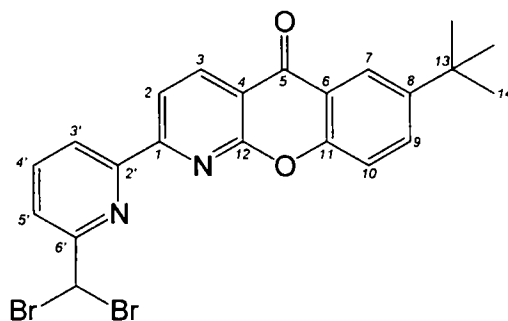
A stirred mixture of 6-*tert*-butyl-2-(6-methyl-pyridin-2-yl)-9-oxa-1-aza-anthracen-10-one **8** (0.200 g, 0.581 mmol), *N*-bromosuccinimide (0.129 g, 0.725 mmol) and benzoyl peroxide (0.010 g, 0.041 mmol) in CCl₄ (5 ml) was heated at reflux, for 16 h. The reaction progress was monitored by ¹H NMR analysis. After 8 h, *N*-bromosuccinimide (0.100 g, 0.562 mmol) and dibenzoyl peroxide (0.010 g, 0.041 mmol) were added to the reaction mixture, which was heated at reflux for a further 16 h. The reaction mixture was allowed to cool to rt, filtered and the solvent removed under reduced pressure to yield a yellow residue. The crude material was purified by column chromatography on silica (using 100 % CH₂Cl₂ elution) to yield the *title compound* **9** as a colourless solid (0.101 g, 0.406 mmol, 41 %); *R*_F = 0.35 (Silica, CH₂Cl₂, 100 v); m.p. 186-187 °C; ¹H NMR (CDCl₃, 500 MHz) δ 1.42 (9H, s, ^tBu CH₃), 4.66 (2H, s, CH₂Br), 7.56 (1H, d, *J* = 7.5 Hz, H⁵), 7.60 (1H, d, *J* = 9.0 Hz, H¹⁰), 7.85 (1H, dd, *J* = 8.5; 2.5 Hz, H⁹), 7.90 (1H, t, *J* = 8.0 Hz, H⁴), 8.32 (1H, d, *J* = 2.5 Hz, H⁷), 8.48 (1H, d, *J* = 8.0 Hz, H³), 8.63 (1H, d, *J* = 8.0 Hz, H²), 8.82 (1H, d, *J* = 8.0 Hz, H³); ¹³C NMR (CDCl₃, 126 MHz, ¹H decoupled 500 MHz) δ 31.6 (3C, C¹⁴), 34.0 (1C, CH₂Br), 35.1 (1C, C¹³), 116.8 (1C, C⁴), 118.3 (1C, C¹⁰), 118.7 (1C, C²), 121.3 (1C, C⁶), 121.8 (1C, C⁵), 122.8 (1C, C⁷), 125.1 (1C, C³), 133.8 (1C, C⁹), 138.4 (1C, C⁴), 138.6 (1C, C³), 148.2 (1C, C⁸), 154.0 (1C, C¹), 154.2 (1C, C¹¹), 157.0 (1C, C⁶), 160.0 (1C, C¹), 160.2 (1C, C¹²), 177.9 (1C, C⁵); MS (ES⁺) *m/z* 423.2 (100 %, [M + H]⁺); HRMS (ES⁺) *m/z* found 423.0700, C₂₂H₂₀O₂N₂⁷⁹Br₁ requires 423.0702, [M + H]⁺.

Procedure B:

A solution of 6-*tert*-butyl-2-(6-dibromomethyl-pyridin-2-yl)-9-oxa-1-aza-anthracen-10-one **10** (0.060 g, 0.120 mmol), ^tPr₂NEt (0.062 g, 0.084 ml, 0.480 mmol) and diethyl phosphite (0.066 g, 0.062 ml, 0.478 mmol) in *anhydrous* THF (5 ml), was stirred at rt, for 16 h. The solvent was removed under reduced pressure and the residue partitioned between CHCl₃ (10 ml) and H₂O (10 ml). The organic phase was separated and concentrated under reduced pressure to afford a residual oil. The crude material was purified by column chromatography on silica (using 100 % CH₂Cl₂ elution), to yield the

title compound 9 as a colourless solid (0.042 g, 0.095 mmol, 79 %). Characterisation as reported in procedure A.

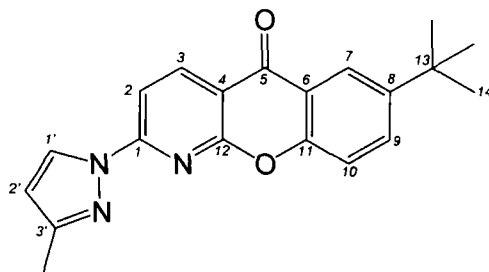
6-*tert*-Butyl-2-(6-dibromomethyl-pyridin-2-yl)-9-oxa-1-aza-anthracen-10-one (10)



6-*tert*-Butyl-2-(6-dibromomethyl-pyridin-2-yl)-9-oxa-1-aza-anthracen-10-one **10** was isolated using an identical procedure to that described for 2-(6-bromomethyl-pyridin-2-yl)-6-*tert*-butyl-9-oxa-1-aza-anthracen-10-one **9**. The procedure yielded the *title compound 10* as a colourless solid (0.061 g, 0.119 mmol, 33 %); $R_f = 0.71$ (Silica, CH_2Cl_2 , 100 v); ^1H NMR (CDCl_3 , 500 MHz) δ 1.41 (9H, s, *t*Bu CH_3), 6.78 (1H, s, CHBr_2), 7.58 (1H, d, $J = 8.5$ Hz, H^{10}), 7.84 (1H, dd, $J = 9.0; 2.5$ Hz, H^9), 7.92 (1H, d, $J = 8.0$ Hz, $\text{H}^{5'}$), 7.98 (1H, t, $J = 8.0$ Hz, $\text{H}^{4'}$), 8.30 (1H, d, $J = 2.5$ Hz, H^7), 8.50 (1H, d, $J = 7.5$ Hz, $\text{H}^{3'}$), 8.59 (1H, d, $J = 8.0$ Hz, H^2), 8.81 (1H, d, $J = 8.0$ Hz, H^3); ^{13}C NMR (CDCl_3 , 126 MHz, ^1H decoupled 500 MHz) δ 31.6 (3C, C^{14}), 35.1 (1C, C^{13}), 41.6 (1C, CHBr_2), 116.9 (1C, C^4), 118.3 (1C, C^{10}), 118.7 (1C, C^2), 121.3 (1C, C^6), 122.8 (1C, C^7), 122.9 (1C, C^3), 123.6 (1C, $\text{C}^{5'}$), 133.9 (1C, C^9), 138.7 (1C, C^3), 139.1 (1C, C^4), 148.3 (1C, C^8), 152.7 (1C, $\text{C}^{2'}$), 154.2 (1C, C^{11}), 159.0 (1C, C^6), 159.1 (1C, C^1), 160.2 (1C, C^{12}), 177.8 (1C, C^5); MS (ES^+) m/z 503.2 (100 %, $[\text{M} + \text{H}]^+$).

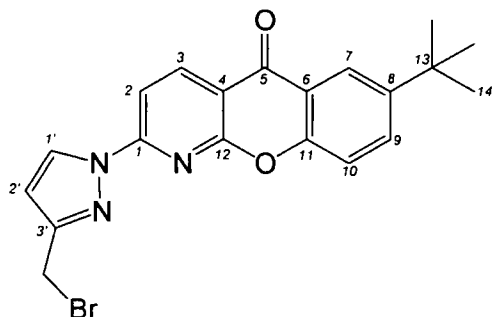
7.1.2 Pyrazoyl-azaxanthone

6-*tert*-Butyl-2-(3-methyl-pyrazol-1-yl)-9-oxa-1-aza-anthracen-10-one (11)



Sodium hydride (0.030 g, 1.25 mmol) was added to a stirred solution of 3-methylpyrazole (0.880 g, 1.07 mmol) in *anhydrous* THF (5 ml), under an atmosphere of argon. A solution of 6-*tert*-butyl-2-chloro-9-oxa-anthracen-10-one **6** (0.281 g, 0.972 mmol) in *anhydrous* THF (5 ml) was added to the reaction mixture, which was heated at 65 °C, for 16 h. The reaction mixture was allowed to cool to rt and H₂O (10 ml) added to the solution to induce precipitation. The precipitate was collected via centrifugation and the resultant solid triturated with a minimum volume of diethyl ether (10 ml). The solvent was decanted and the solid dried under vacuum to yield the *title compound* **11** as a colourless solid (0.294 g, 0.882 mmol, 90 %); m.p. 128-130 °C; ¹H NMR (CDCl₃, 400 MHz) δ 1.39 (9H, s, *t*Bu CH₃), 2.37 (3H, s, CH₃), 6.31 (1H, d, *J* = 3.0 Hz, H^{2'}), 7.51 (1H, d, *J* = 9.0 Hz, H¹⁰), 7.80 (1H, dd, *J* = 9.0; 3.0 Hz, H⁹), 7.99 (1H, d, *J* = 8.5 Hz, H²), 8.27 (1H, d, *J* = 3.0 Hz, H⁷), 8.51 (1H, d, *J* = 3.0 Hz, H^{1'}), 8.72 (1H, d, *J* = 8.5 Hz, H³); ¹³C NMR (CDCl₃, 100 MHz, ¹H decoupled 400 MHz) δ 14.2 (1C, CH₃), 31.6 (3C, C¹⁴), 35.1 (1C, C¹³), 109.7 (1C, C²), 110.1 (1C, C^{2'}), 113.9 (1C, C⁴), 118.1 (1C, C¹⁰), 121.4 (1C, C⁶), 122.7 (1C, C⁷), 129.0 (1C, C¹), 133.4 (1C, C⁹), 140.1 (1C, C³), 148.3 (1C, C⁸), 153.7 (1C, C¹¹), 153.9 (1C, C¹²), 154.0 (1C, C³), 160.0 (1C, C¹), 177.0 (1C, C⁵); MS (ES⁺) *m/z* 334.1 (100 %, [M + H]⁺); HRMS (ES⁺) *m/z* found 334.1551 [M + H]⁺ C₂₀H₂₀O₂N₃ requires 334.1550.

2-(3-Bromomethyl-pyrazol-1-yl)-6-*tert*-butyl-9-oxa-1-aza-anthracen-10-one
(12)



Procedure A:

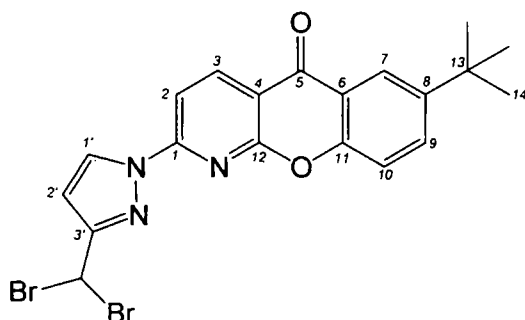
A stirred mixture of 6-*tert*-butyl-2-(3-methyl-pyrazol-1-yl)-9-oxa-1-aza-anthracen-10-one **11** (0.212 g, 0.636 mmol), *N*-bromosuccinimide (0.113 g, 0.635 mmol) and benzoyl peroxide (0.010 g, 0.041 mmol) in CCl₄ (15 ml) was heated at reflux, for 16 h. The reaction mixture was allowed to cool to rt, filtered and the solvent removed under reduced pressure to afford a residual yellow oil. The crude material was purified by column chromatography on silica (using 100 % CH₂Cl₂ elution) to yield the *title compound* **12** as a colourless solid (0.148 g, 0.362 mmol, 56 %); *R*_F = 0.28 (Silica, CH₂Cl₂, 100 v); m.p. 184-185 °C; ¹H NMR (CDCl₃, 500 MHz) δ 1.42 (9H, s, ^tBu CH₃), 4.56 (2H, s, CH₂Br), 6.62 (1H, d, *J* = 2.5 Hz, H²), 7.56 (1H, d, *J* = 9.0 Hz, H¹⁰), 7.85 (1H, dd, *J* = 9.0; 2.5 Hz, H⁹), 8.06 (1H, d, *J* = 8.0 Hz, H²), 8.31 (1H, d, *J* = 2.5 Hz, H⁷), 8.63 (1H, d, *J* = 2.5 Hz, H¹), 8.80 (1H, d, *J* = 8.5 Hz, H³); ¹³C NMR (CDCl₃, 125 MHz, ¹H decoupled 500 MHz) δ 24.6 (1C, CH₂Br), 31.6 (3C, C¹⁴), 35.1 (1C, C¹³), 109.7 (1C, C²), 110.0 (1C, C²), 114.6 (1C, C⁴), 118.1 (1C, C¹⁰), 121.4 (1C, C⁶), 122.8 (1C, C⁷), 129.8 (1C, C¹), 133.6 (1C, C⁹), 140.5 (1C, C³), 148.6 (1C, C⁸), 153.3 (1C, C¹¹), 153.7 (1C, C³), 153.9 (1C, C¹²), 159.9 (1C, C¹), 177.0 (1C, C⁵); MS (ES⁺) *m/z* 409.3 (100 %, [M + H]⁺); HRMS (ES⁺) *m/z* found 434.0475 [M + Na]⁺ C₂₀H₁₈O₂N₃⁷⁹Br₁²³Na₁ requires 434.0475.

Procedure B:

A solution of 6-*tert*-butyl-2-(3-dibromomethyl-pyrazol-1-yl)-9-oxa-1-aza-anthracen-10-one **13** (0.150 g, 0.307 mmol), ^tPr₂NEt (0.157 g, 0.211 ml, 1.22 mmol) and diethyl phosphite (0.168 g, 0.157 ml, 1.22 mmol) in *anhydrous* THF (10 ml) was stirred at rt, for

16 h. The solvent was removed under reduced pressure and the residue partitioned between CHCl_3 (10 ml) and H_2O (10 ml). The organic phase was separated and concentrated under reduced pressure. The crude material was purified by column chromatography on silica (using 100 % CH_2Cl_2 elution) to yield the *title compound* **12** as a colourless solid (0.085 g, 0.208 mmol, 67 %). *Characterisation as reported in procedure A.*

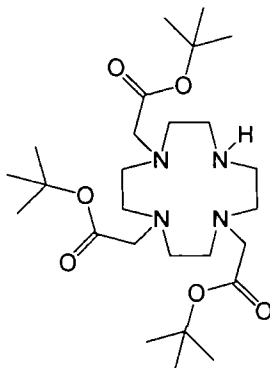
6-*tert*-Butyl-2-(3-dibromomethyl-pyrazol-1-yl)-9-oxa-1-aza-anthracen-10-one (13)



6-*tert*-Butyl-2-(3-dibromomethyl-pyrazol-1-yl)-9-oxa-1-aza-anthracen-10-one **13** was isolated using an identical procedure to that described for 2-(3-bromomethyl-pyrazol-1-yl)-6-*tert*-butyl-9-oxa-1-aza-anthracen-10-one **12**. The procedure yielded the *title compound* **13** as a colourless solid (0.970 g, 0.199 mmol, 31 %); $R_F = 0.33$ (Silica, CH_2Cl_2 , 100 v); ^1H NMR (CDCl_3 , 500 MHz) δ 1.42 (9H, s, ^tBu CH_3), 6.79 (1H, s, CHBr_2), 6.89 (1H, d, $J = 2.5$ Hz, $\text{H}^{2'}$), 7.56 (1H, d, $J = 8.5$ Hz, H^{10}), 7.85 (1H, dd, $J = 8.5$; 2.5 Hz, H^9), 8.03 (1H, d, $J = 8.5$ Hz, H^2), 8.31 (1H, d, $J = 2.5$ Hz, H^7), 8.67 (1H, d, $J = 2.5$ Hz, H^3), 8.81 (1H, d, $J = 8.5$ Hz, H^3); ^{13}C NMR (CDCl_3 , 125 MHz, ^1H decoupled 500 MHz) δ 31.0 (1C, CHBr_2), 31.6 (3C, C^{14}), 35.1 (1C, C^{13}), 108.8 (1C, C^2), 110.0 (1C, C^2), 114.9 (1C, C^4), 118.1 (1C, C^{10}), 121.3 (1C, C^6), 122.8 (1C, C^7), 130.1 (1C, C^3), 133.8 (1C, C^9), 140.6 (1C, C^3), 148.6 (1C, C^8), 153.1 (1C, C^{12}), 153.9 (1C, C^{11}), 157.0 (1C, C^1), 159.8 (1C, C^1), 177.0 (1C, C^5); MS (ES^+) m/z 486.3 (100 %, $[\text{M} + \text{H}]^+$).

7.2 DO3A Complexes

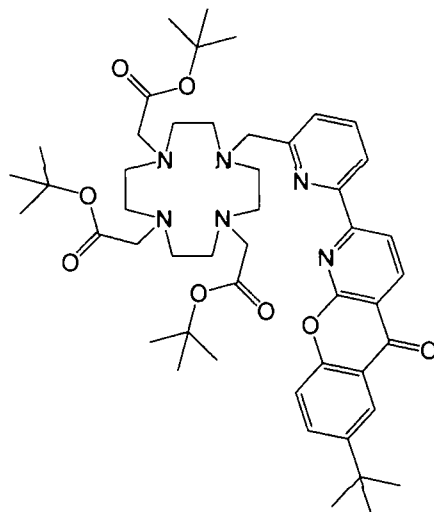
(4,7-bis-*tert*-Butoxycarbonylmethyl-1,4,7,10-tetraaza-cyclododec-1-yl)-acetic acid *tert* butyl ester³ (16)



A mixture of cyclen (2.54 g, 14.7 mmol), *tert*-butyl bromoacetate (8.67 g, 44.2 mmol) and NaHCO₃ (3.72 g, 44.2 mmol) in *anhydrous* CH₃CN (75 ml) was stirred at rt, under argon, for 24 h. The solution was filtered and the filtrate concentrated under reduced pressure to afford a residual orange oil, which crystallised upon standing. The crude material was purified by column chromatography on silica (gradient elution: CH₂Cl₂ to 5 % CH₃OH : CH₂Cl₂, utilising 0.1 % CH₃OH increments) to yield the *title compound* **16** as a colourless crystalline solid (2.41 g, 4.68 mmol, 32 %); m.p. 179-181 °C; ¹H NMR (CDCl₃, 500 MHz) δ 1.47 (27H, s, 'Boc CH₃), 2.88 (12H, br s, cyclen CH₂), 3.11 (4H, br s, cyclen CH₂), 3.30 (2H, s, CH₂CO₂'Bu), 3.39 (4H, s, CH₂CO₂'Bu), 10.04 (1H, br s, NH); ¹³C NMR (CDCl₃, 125 MHz, ¹H decoupled 500 MHz) δ 28.4 (9C, 'Boc CH₃), 30.6-31.2 (6C, cyclen CH₂), 47.8 (1C, cyclen CH₂), 49.4 (2C, CH₂CO), 51.4 (1C, cyclen CH₂), 58.5 (1C, CH₂CO), 81.9 (2C, 'Boc_(q)), 82.1(1C, 'Boc_(q)), 169.9 (2C, C = O), 170.8 (1C, C = O); MS (ES⁺) *m/z* 515.6 (100 %, [M + H]⁺).

7.2.1 Pyridyl-azaxanthone DO3A Complexes

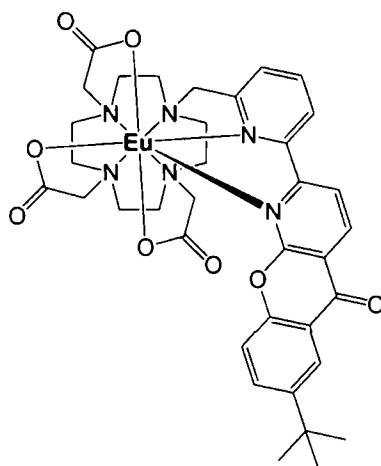
{4,7-bis-*tert*-Butoxycarbonylmethyl-10-[6-(6-*tert*-butyl-10-oxo-10*H*-9-oxa-1-aza-anthracen-2-yl)-pyridin-2-ylmethyl]-1,4,7,10-tetraaza-cyclododec-1-yl}-acetic acid *tert*-butyl ester ([L¹])



A stirred mixture of (4,7-bis-*tert*-butoxycarbonylmethyl-1,4,7,10-tetraaza-cyclododec-1-yl)-acetic acid *tert* butyl ester **16** (0.032 g, 0.062 mmol), 2-(6-bromomethyl-pyridin-2-yl)-6-*tert*-butyl-9-oxa-1-aza-anthracen-10-one **9** (0.024 g, 0.057 mmol) and Cs₂CO₃ (0.026 g, 0.080 mmol) in *anhydrous* CH₃CN (5 ml), was heated at reflux, under argon, for 16 h. The mixture was allowed to cool to rt, syringe filtered and the filtrate concentrated under reduced pressure to afford a residual yellow oil. The crude material was purified by column chromatography on alumina (gradient elution; CH₂Cl₂ to 2 % CH₃OH : CH₂Cl₂, utilising 0.1 % CH₃OH increments) to yield the *title compound* [L¹] as a pale yellow crystalline solid (0.035 g, 0.042 mmol, 74 %); *R*_F = 0.22 (Alumina, CH₂Cl₂ – CH₃OH, 19 : 1 v/v); ¹H NMR (CDCl₃, 700 MHz) δ 1.29 (9H, s, ^tBu CH₃), 1.32 (18H, br s, ^tBoc CH₃), 1.35 (9H, br s, ^tBoc CH₃), 2.71 (8H, br s, cyclen CH₂), 3.24 (8H, br s, cyclen CH₂), 3.50 (4H, br s, CH₂CO₂^tBu), 3.55 (2H, br s, CH₂CO₂^tBu), 3.69 (2H, s, CH₂ pyridine), 7.25 (1H, d, *J* = 8.0 Hz, H⁵), 7.45 (1H, d, *J* = 8.5 Hz, H¹⁰), 7.69 (1H, t, *J* = 8.0 Hz, H⁴), 7.71 (1H, dd, *J* = 9.0; 3.0 Hz, H⁹), 8.17 (1H, d, *J* = 3.0 Hz, H⁷), 8.32 (1H, d, *J* = 8.0 Hz, H³), 8.36 (1H, d, *J* = 7.0 Hz, H²), 8.64 (1H, d, *J* = 8.0 Hz, H³); ¹³C NMR (CDCl₃, 176 MHz, ¹H decoupled 700 MHz) δ 28.3 (3C, C¹⁴), 31.5 (6C, ^tBoc CH₃), 35.1 (3C, ^tBoc CH₃), 50.6 (2C, cyclen CH₂), 51.8 (2C, cyclen CH₂), 56.1 (2C, cyclen CH₂), 56.7 (2C, cyclen CH₂),

57.1 (1C, CH₂ pyridine), 82.4 (4C, C^tBu), 116.4 (1C, C⁴), 118.2 (1C, C¹⁰), 118.3 (1C, C²), 121.0 (1C, C³), 121.2 (1C, C⁶), 122.6 (1C, C⁷), 126.2 (1C, C⁵), 133.6 (1C, C⁹), 137.4 (1C, C⁴), 138.2 (1C, C³), 148.0 (1C, C⁸), 153.6 (1C, C¹), 154.2 (1C, C¹¹), 158.6 (1C, C⁶), 160.2 (1C, C¹), 160.6 (1C, C¹²), 177.8 (1C, C⁵); MS (ES⁺) *m/z* 857.5 (100 %, [M + H]⁺); HRMS (ES⁺) *m/z* found 857.5176 [M + H]⁺ C₄₈H₆₉O₈N₆ requires 857.5171.

[EuL¹]



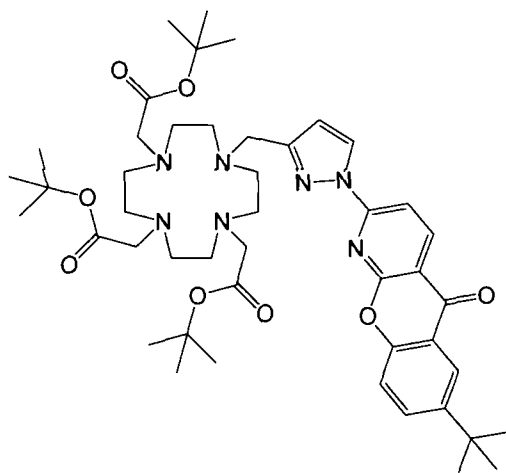
A solution of {4,7-bis-*tert*-butoxycarbonylmethyl-10-[6-(6-*tert*-butyl-10-oxo-10*H*-9-oxa-1-aza-anthracen-2-yl)-pyridin-2-ylmethyl]-1,4,7,10-tetraaza-cyclododec-1-yl}-acetic acid *tert*-butyl ester [L¹] (0.035 g, 0.0419 mmol) in CH₂Cl₂ – TFA (1 : 1 v/v, 2 ml) was stirred at rt, in a sealed flask, for 16 h to afford an orange solution. The solvent was removed under reduced pressure to yield a glassy solid. The crude material was repeatedly (x 3) dissolved in CH₂Cl₂ (5 ml) and the solvent removed under reduced pressure to facilitate elimination of excess acid and *tert*-butyl alcohol. The desired ligand, as its TFA salt, was examined by ¹H NMR to ensure complete ester hydrolysis, with the material used immediately for complexation.

The hydrolysed ligand was dissolved in CH₃OH – H₂O (1:1 v/v, 4 ml) and Eu(OAc)₃·6H₂O (0.017 g, 0.039 mmol) added to the mixture. The pH of the solution was raised to 5.5 by the addition of 1 M KOH (aq), then stirred and heated at 80 °C, for 15 h. The reaction mixture was allowed to cool to rt before raising the pH of the solution to 10.0 using dilute KOH (aq). The reaction mixture was stirred for 1 h to allow precipitation of excess Eu metal as its hydroxide salt, Eu(OH)₃. The solid precipitate was removed by syringe filtration and the pH of the colourless aqueous filtrate lowered to pH 5.5 using a

solution of 1 M HCl_(aq). The solvent was removed under reduced pressure using a freeze-drier to yield a colourless solid. The material was purified by column chromatography on neutral alumina (elution; CH₂Cl₂ : CH₃OH, 8 : 2 v/v) to yield the *title complex* [EuL¹] as a colourless solid (0.024 g, 0.028 mmol, 68 %); $R_F = 0.41$ (Alumina, CH₂Cl₂ – CH₃OH, 7 : 3 v/v); λ_{\max} (H₂O) = 356 nm; τ (H₂O) = 1.00 ms; τ (D₂O) = 1.34 ms; ϕ_{Eu} (H₂O; pH 7.4; λ_{exc} 365 nm) = 14 %.

7.2.2 Pyrazoyl-azaxanthone DO3A Complexes

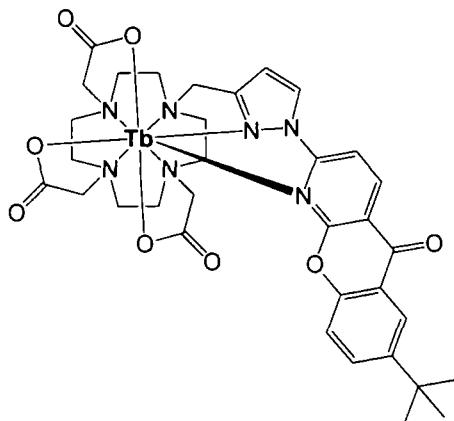
{4,7-bis-*tert*-Butoxycarbonylmethyl-10-[1-(6-*tert*-butyl-10-oxo-10*H*-9-oxa-1-aza-anthracen-2-yl)-1*H*-pyrazol-3-ylmethyl]-1,4,7,10-tetraaza-cyclododec-1-yl]-acetic acid *tert*-butyl ester ([L²])



A stirred mixture of (4,7-bis-*tert*-butoxycarbonylmethyl-1,4,7,10-tetraaza-cyclododec-1-yl)-acetic acid *tert* butyl ester **16** (0.075 g, 0.146 mmol), 2-(3-bromomethyl-pyrazol-1-yl)-6-*tert*-butyl-9-oxa-1-aza-anthracen-10-one **12** (0.060 g, 0.146 mmol) and Cs₂CO₃ (0.050 g, 0.153 mmol) in *anhydrous* CH₃CN (5 ml) was heated at reflux, under argon, for 16 h. The reaction mixture was allowed to cool to rt, syringe filtered and the filtrate concentrated under reduced pressure to afford a residual yellow oil. The crude material was purified by column chromatography on silica (gradient elution; CH₂Cl₂ to 8 % CH₃OH : CH₂Cl₂, utilising 0.1 % CH₃OH increments) to yield the *title compound* [L²] as a pale yellow coloured solid (0.090 g, 0.106 mmol, 73 %); $R_F = 0.36$ (Silica, CH₂Cl₂ – CH₃OH, 19 : 1 v/v); ¹H NMR (CDCl₃, 500 MHz) δ 1.40 (9H, s, ^tBu CH₃), 1.51 (27H, br

s, 'Boc CH₃), 2.67 (8H, br s, cyclen CH₂), 3.27 (8H, br s, cyclen CH₂), 3.44 (4H, br s, CH₂CO₂'Bu), 3.51 (2H, br s, CH₂CO₂'Bu), 3.55 (2H, s, CH₂-pyrazole), 6.57 (1H, d, $J = 2.5$ Hz, H²), 7.56 (1H, d, $J = 8.0$ Hz, H¹⁰), 7.86 (1H, dd, $J = 9.0; 2.5$ Hz, H⁹), 8.23 (1H, d, $J = 8.0$ Hz, H²), 8.27 (1H, d, $J = 2.5$ Hz, H⁷), 8.57 (1H, d, $J = 2.5$ Hz, H¹), 8.62 (1H, d, $J = 8.5$ Hz, H³); ¹³C NMR (CDCl₃, 125 MHz, ¹H decoupled 500 Mz) δ 28.3 (3C, C¹⁴), 31.5 (6C, 'Bu CH₃), 35.1 (3C, C'Bu), 50.6 (2C, cyclen CH₂), 51.8 (2C, cyclen CH₂), 56.1 (2C, cyclen CH₂), 56.7 (3C, cyclen CH₂; CH₂_PyAza), 82.4 (4C, C'Bu), 110.8 (1C, C²), 110.9 (1C, C²), 114.3 (1C, C⁴), 118.2 (1C, C¹⁰), 121.1(1C, C⁶), 122.7 (1C, C⁷), 129.6 (1C, C¹), 133.9 (1C, C⁹), 140.1 (1C, C³), 148.7 (1C, C⁸), 153.6 (1C, C¹¹), 153.9 (1C, C¹²), 155.3 (1C, C³), 159.8 (1C, C¹), 172.9 (3C, C=O_{ester}), 176.9 (1C, C⁵); MS (ES⁺) m/z 846.5 (100 %, [M + H]⁺).

[TbL²]



A solution of {4,7-bis-*tert*-butoxycarbonylmethyl-10-[1-(6-*tert*-butyl-10-oxo-10*H*-9-oxa-1-aza-anthracen-2-yl)-1*H*-pyrazol-3-ylmethyl]-1,4,7,10-tetraaza-cyclododec-1-yl}-acetic acid *tert*-butyl ester [L²] (0.045 g, 0.053 mmol) in CH₂Cl₂ – TFA (2 : 1 v/v, 3 ml) was stirred at rt, in a sealed flask, for 16 h. The solvent was removed under reduced pressure to yield a glassy solid. The crude material was repeatedly (x 3) dissolved in CH₂Cl₂ (5 ml) and the solvent removed under reduced pressure to facilitate elimination of excess acid and *tert*-butyl alcohol. The desired ligand, as its TFA salt, was examined by ¹H NMR to ensure complete ester hydrolysis, with the material used immediately for complexation.

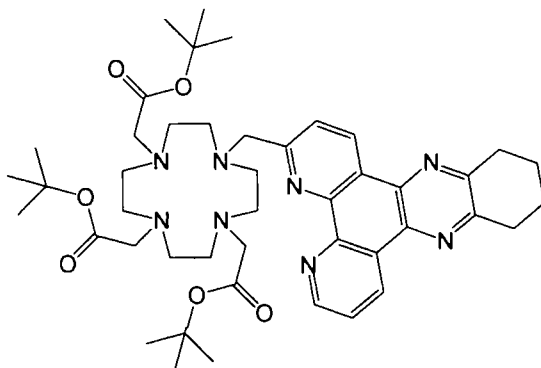
The deprotected ligand was dissolved in CH₃OH – H₂O (2 : 3 v/v, 5 ml) and TbCl₃.6H₂O (0.010 g, 0.028 mmol) added to the solution. The pH of the solution was raised to 5.4 by the addition of 1 M KOH_(aq), then stirred and heated at 90 °C, for 14 h. Over this period the pH of the solution lowered to 3.4. The pH was adjusted to 5.4 and the solution stirred and heated at 90 °C, for a further 16 h. The reaction mixture was allowed to cool to rt before raising the pH of the solution to 10.0 using dilute KOH_(aq). The reaction mixture was stirred for 1 h to allow precipitation of excess Tb metal as its hydroxide salt, Tb(OH)₃. The solid precipitate was removed by syringe filtration and the pH of the colourless aqueous filtrate reduced to pH 5.5 using a solution of 1 M HCl_(aq). The solvent was removed under reduced pressure using a freeze-drier to yield an off-white solid. The material was purified by column chromatography on neutral alumina (elution; CH₂Cl₂ : CH₃OH, 8 : 2 v/v) to yield the *title complex* [TbL²] as a colourless solid (0.026 g, 0.032 mmol, 61 %); $R_F = 0.39$ (Alumina, CH₂Cl₂ – CH₃OH, 7 : 3 v/v); λ_{\max} (H₂O) = 350 nm; τ (H₂O) = 2.24 ms; τ (D₂O) = 2.65 ms; ϕ_{Tb} (H₂O; pH 6.0; λ_{exc} 355 nm) = 15 %.

[EuL²]

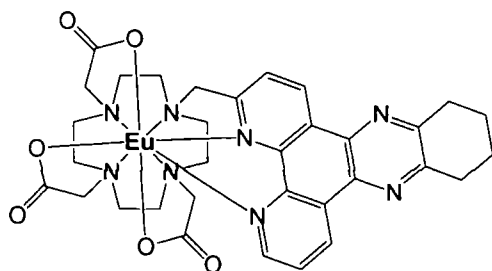
An analogous procedure to that described for [TbL²] was followed using {4,7-bis-*tert*-butoxycarbonylmethyl-10-[1-(6-*tert*-butyl-10-oxo-10*H*-9-oxa-1-aza-anthracen-2-yl)-1*H*-pyrazol-3-ylmethyl]-1,4,7,10-tetraaza-cyclododec-1-yl}-acetic acid *tert*-butyl ester [L²] (0.024 g, 0.035 mmol) and EuCl₃.6H₂O (0.014 g, 0.038 mmol) in CH₃OH – H₂O (1 : 1 v/v, 6 ml). The procedure yielded the *title complex* [EuL²] as a colourless solid (0.015 g, 0.018 mmol, 52 %); λ_{\max} (H₂O) = 350 nm; τ (H₂O) = 0.70 ms; τ (D₂O) = 1.76 ms.

7.2.3 Tetraazatriphenylene DO3A Complexes

1-(3-Methyl-10,11,12,13-tetrahydrodipyrido[3,2-a:2',3'-c]phenazine)-4,7,10-tris-*tert*-butoxycarbonylmethyl-1,4,7,10-tetraazacyclododecane ⁴ ([L³])



A stirred mixture of (4,7-bis-*tert*-butoxycarbonylmethyl-1,4,7,10-tetraaza-cyclododec-1-yl)-acetic acid *tert* butyl ester **16** (0.150 g, 0.290 mmol), 3-chloromethyl-10,11,12,13-tetrahydrodipyrido-[3,2a:2',3'-c] phenazine (0.112 g, 0.290 mmol) and K₂CO₃ (0.201 g, 1.45 mmol) in *anhydrous* CH₃CN, was heated at reflux, under argon, for 16 h. The reaction mixture was allowed to cool to rt, syringe filtered and the filtrate concentrated under reduced pressure. The crude material was purified by column chromatography on silica (gradient elution: CH₂Cl₂ to 3.5 % CH₃OH : CH₂Cl₂, utilising 0.1 % CH₃OH increments) to yield the *title compound* as a yellow coloured solid (0.169 g, 0.209 mmol, 72 %); R_F = 0.47 (Silica, CH₂Cl₂ – CH₃OH, 9 : 1 v/v); m.p. 137–139 °C; ¹H NMR (CDCl₃, 500 MHz) δ 1.08 (18H, s, ^tBoc CH₃), 1.41 (9H, s, ^tBoc CH₃), 2.05 (4H, m, H¹⁰; H¹³), 2.25–3.58 (28H, br m, cyclen CH₂; H¹¹; H¹²), 7.65 (1H, m, H⁷), 7.75 (1H, m, H²), 8.76 (1H, dd, *J* = 4.5; 1.5 Hz, H⁶), 9.42 (1H, m, H¹), 9.48 (1H, m, H⁸); ¹³C NMR (CDCl₃, 125 MHz, ¹H decoupled at 500 MHz) δ 27.9 (9C, ^tBoc CH₃), 50.9–60.4 (8C, cyclen CH₂), 81.6–82.7 (3C, CH₂CO), 123.6 (1C, C²), 123.9 (1C, Ar), 126.2 (1C, C Ar), 127.7 (1C, Ar), 133.5 (1C, Ar), 133.9 (1C, Ar), 137.2 (1C, C⁸), 137.5 (1C, C¹), 145.8 (1C, C Ar), 146.4 (1C, Ar), 151.0 (1C, C⁶), 154.2 (1C, Ar), 154.5 (1C, Ar), 160.4 (1C, Ar), 172.5 (2C, C = O), 172.9 (1C, C = O); MS (ES⁺) *m/z* 836.4 (100 %, [M + Na]⁺).

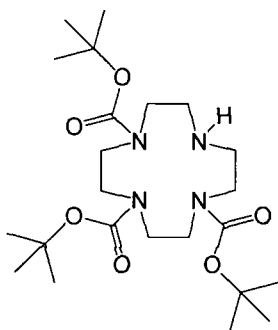
[EuL³]⁴

A solution of 1-(3-methyl-10,11,12,13-tetrahydrodipyrido[3,2-a:2',3'-c]phenazine)-4,7,10-tris-*tert*-butoxycarbonylmethyl-1,4,7,10-tetraazacyclododecane [L³] (0.037 g, 0.045 mmol) in CH₂Cl₂ – TFA (2 : 1 v/v, 3ml) was stirred at rt, in a sealed flask, for 8 h to afford a red coloured solution. The solvent was removed under reduced pressure to yield a glassy solid. The crude material was repeatedly (x 3) dissolved in CH₂Cl₂ (5 ml) and the solvent removed under reduced pressure to facilitate elimination of excess acid and *tert*-butyl alcohol. The desired ligand, as its TFA salt, was examined by ¹H NMR analysis to ensure complete ester hydrolysis, with the material used immediately for complexation.

The deprotected ligand was dissolved in CH₃OH – H₂O (1:1 v/v, 2 ml) and Eu(OAc)₃.6H₂O (0.021 g, 0.049 mmol) added to the solution. The pH of the solution was raised to 5.5 by the addition of 1 M KOH (aq), then stirred and heated at 90 °C, for 22 h. The reaction mixture was allowed to cool to room temperature before raising the pH of the solution to 10.0 using dilute KOH (aq). The reaction mixture was stirred for 1 h to allow precipitation of excess Eu metal as its hydroxide salt, Eu(OH)₃. The solid precipitate was removed by syringe filtration and the pH of the colourless aqueous filtrate reduced to pH 5.5 using a solution of 1 M HCl (aq). The solvent was removed under reduced pressure using a freeze-drier to yield an off-white solid, which was purified by column chromatography on neutral alumina (elution; CH₂Cl₂ : CH₃OH, 8 : 2 v/v) to yield the *title complex* [EuL³] as a colourless solid (0.020 g, 0.025 mmol, 56 %); *R*_F = 0.33 (Alumina, CH₂Cl₂ – CH₃OH, 7 : 3 v/v); λ_{max} (H₂O) = 348 nm; τ (H₂O) = 1.08 ms; φ_{Eu} (H₂O; pH 7.4; λ_{exc} 348 nm) = 18 %.

[GdL³]

An analogous procedure to that described for [EuL³] was followed using 1-(3-methyl-10,11,12,13-tetrahydrodipyrido[3,2-a:2',3'-c]phenazine)-4,7,10-tris-*tert*-butoxycarbonylmethyl-1,4,7,10-tetraazacyclododecane [L³] (0.043 g, 0.067 mmol) and Gd(OAc)₃.6H₂O (0.025 g, 0.067 mmol) in CH₃OH – H₂O (1:1 v/v, 2 ml). The procedure yielded the *title complex* [GdL³] as a pale yellow coloured solid (0.012 g, 0.015 mmol, 22 %); *R*_F = 0.33 (Alumina, CH₂Cl₂ – CH₃OH, 7 : 3 v/v); λ_{max} (H₂O) = 348 nm; MS (ES⁺) *m/z* 822.3 (100 %, [M + Na]⁺).

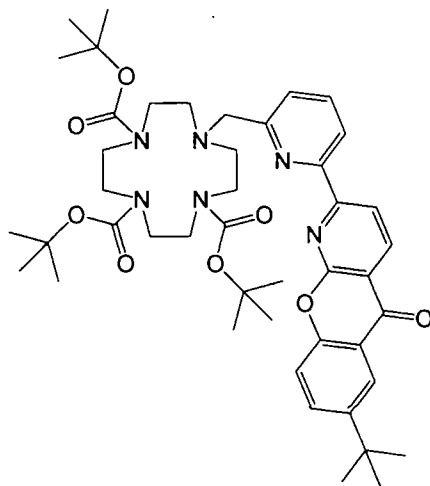
7.3 Triamide Complexes**1,4,7-Tetraaza-cyclododecane-1,4,7-tricarboxylic acid tri-*tert*-butyl ester⁵**
(17)

A solution of di-*tert*-butyl dicarbonate (6.08 g, 27.8 mmol) in *anhydrous* CH₂Cl₂ (100 ml) was added dropwise to a stirred solution of cyclen (2.00 g, 11.61 mmol) in *anhydrous* CH₂Cl₂ (300 ml). The reaction mixture was stirred at rt, for 18 h. The solvent was removed under reduced pressure to afford a transparent oil. The crude material was purified by column chromatography on silica (gradient elution: CH₂Cl₂ to 5 % CH₃OH : CH₂Cl₂, utilising 0.1 % CH₃OH increments) to yield the *title compound* 17 as a colourless crystalline solid (3.08 g, 6.51 mmol, 56 %); *R*_F = 0.29 (Silica, CH₂Cl₂ – CH₃OH, 9 : 1, v/v); ¹H NMR (CDCl₃, 500 MHz) δ 1.42 (18H, s, 'Boc CH₃), 1.44 (9H, s, 'Boc CH₃), 2.81 (4H, br s, cyclen CH₂), 3.28 (8H, br s, cyclen CH₂), 3.60 (4H, br s, cyclen CH₂); ¹³C NMR (CDCl₃, 125 MHz, ¹H decoupled 500 MHz) δ 28.9 (6C, 'Boc CH₃), 29.0 (3C, 'Boc CH₃), 46.1 (2C, cyclen CH₂), 49.9 (2C, cyclen CH₂), 51.2 (4C, cyclen CH₂), 79.4 (2C, 'Boc_(q)), 79.6 (1C, 'Boc_(q)), 155.8 (2C, 'Boc C = O), 156.0 (1C,

¹Boc C = O); MS (ES⁺) *m/z* 473.3 (100 %, [M + H]⁺); HRMS (ES⁺) *m/z* found 473.3330 [M + H]⁺ C₂₃H₄₅O₆N₄ requires 473.3333.

7.3.1 Pyridyl-azaxanthone Triamide Complexes

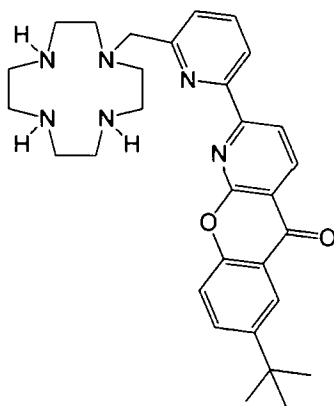
10-[6-(6-*tert*-Butyl-10-oxo-10*H*-9-oxa-1-aza-anthracen-2-yl)-pyridin-2-ylmethyl]-1,4,7,10-tetraaza-cyclododecane-1,4,7-tricarboxylic acid tri-*tert*-butyl ester (18)



A stirred mixture of 1,4,7-tetraaza-cyclododecane-1,4,7-tricarboxylic acid tri-*tert*-butyl ester **17** (0.117 g, 0.248 mmol), 2-(6-bromomethyl-pyridin-2-yl)-6-*tert*-butyl-9-oxa-1-aza-anthracen-10-one **9** (0.100 g, 0.236 mmol) and K₂CO₃ (0.049 g, 0.354 mmol) in *anhydrous* CH₃CN (4 ml), was heated at reflux, under argon, for 16 h. The reaction mixture was allowed to cool to rt, syringe filtered and the filtrate concentrated under reduced pressure to afford a residual yellow oil. The crude material was purified by column chromatography on silica (gradient elution: CH₂Cl₂ to 3 % CH₃OH : CH₂Cl₂, utilising 0.1 % CH₃OH increments) to yield the *title compound* **18** as a pale yellow coloured solid (0.173 g, 0.212 mmol, 90 %); *R*_F = 0.70 (Silica, CH₂Cl₂ – CH₃OH, 49 : 1, v/v); ¹H NMR (CDCl₃, 700 MHz) δ 1.29 (9H, s, ^tBu CH₃), 1.32 (9H, s, ^tBoc CH₃), 1.35 (18H, br s, ^tBoc CH₃), 2.71 (4H, br s, cyclen CH₂), 3.24 (8H, br s, cyclen CH₂), 3.50 (4H, br s, cyclen CH₂), 3.87 (2H, s, CH₂ pyridine), 7.25 (1H, d, *J* = 8.0 Hz, H⁵), 7.45 (1H, d, *J* = 8.5 Hz, H¹⁰), 7.69 (1H, t, *J* = 8.0 Hz, H⁴), 7.71 (1H, dd, *J* = 9.0; 3.0 Hz, H⁹), 8.17 (1H, d, *J* = 3.0 Hz, H⁷), 8.32 (1H, d, *J* = 8.0 Hz, H³), 8.36 (1H, d, *J* = 7.0 Hz, H²), 8.64 (1H, d,

$J = 8.0$ Hz, H^3); ^{13}C NMR ($CDCl_3$, 176 MHz, 1H decoupled 700 MHz) δ 28.6 (9C, 'Boc CH_3), 31.5 (3C, C^{14}), 35.0 (1C, C^{13}), 47.3 (1C, cyclen CH_2), 47.7 (1C, cyclen CH_2), 48.0 (1C, cyclen CH_2), 48.4 (1C, cyclen CH_2), 50.1 (1C, cyclen CH_2), 51.1 (1C, cyclen CH_2), 54.4 (1C, cyclen CH_2), 55.2 (1C, cyclen CH_2), 57.1 (1C, CH_2 pyridine), 79.5 (4C, 'Boc_(q); C^{14}), 116.4 (1C, C^4), 118.2 (1C, C^{10}), 118.3 (1C, C^2), 121.0 (1C, C^3), 121.2 (1C, C^6), 122.6 (1C, C^7), 126.2 (1C, C^5), 133.6 (1C, C^9), 137.4 (1C, C^4), 138.2 (1C, C^3), 148.0 (1C, C^8), 153.6 (1C, C^1), 154.2 (1C, C^{11}), 155.9 (3C, Boc C = O), 158.6 (1C, C^6), 160.2 (1C, C^1), 160.6 (1C, C^{12}), 177.8 (1C, C^5); MS (ES^+) m/z 815.4 (100 %, $[M + H]^+$); HRMS (ES^+) m/z found 815.4710 $[M + H]^+$ $C_{45}H_{63}O_8N_6$ requires 815.4710.

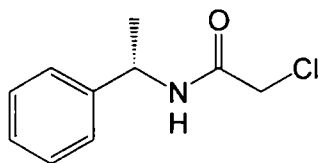
6-*tert*-Butyl-2-[6-(1,4,7,10-tetraaza-cyclododec-1-ylmethyl)-pyridin-2-yl]-9-oxa-1-aza-anthracen-10-one (19)



A solution of 10-[6-(6-*tert*-butyl-10-oxo-10*H*-9-oxa-1-aza-anthracen-2-yl)-pyridin-2-ylmethyl]-1,4,7,10-tetraaza-cyclododecane-1,4,7-tricarboxylic acid tri-*tert*-butyl ester **18** (0.173 g, 0.212 mmol) in CH_2Cl_2 – TFA (2 : 1 v/v, 3 ml) was stirred at rt, in a sealed flask, for 6 h, to afford an orange solution. The solvent was removed under reduced pressure to yield a glassy orange solid. The crude material was repeatedly (x 3) dissolved in CH_2Cl_2 (5 ml) and the solvent removed under reduced pressure to facilitate elimination of excess acid and *tert*-butyl alcohol. The residue was finally taken into $KOH_{(aq)}$ (1 M, 10 ml) and extracted with CH_2Cl_2 (3 x 5 ml). The organic extracts were combined, dried over K_2CO_3 , filtered and the filtrate concentrated under reduced pressure to yield the *title compound* **19** as an orange coloured crystalline solid (0.065 g, 0.129 mmol, 94 %); 1H NMR ($CDCl_3$, 500 MHz) δ 1.36 (9H, s, 'Bu CH_3), 2.54 (4H, s, cyclen CH_2), 2.68 (8H, s,

cyclen CH₂), 2.77 (4H, s, cyclen CH₂), 3.85 (2H, s, CH₂ pyridine), 7.44 (1H, d, $J = 7.5$ Hz, H⁵), 7.54 (1H, d, $J = 9.0$ Hz, H¹⁰), 7.79 (1H, dd, $J = 8.5; 2.5$ Hz, H⁴), 7.81 (1H, t, $J = 7.5$ Hz, H⁹), 8.26 (1H, d, $J = 2.5$ Hz, H⁷), 8.38 (1H, d, $J = 7.5$ Hz, H³), 8.62 (1H, d, $J = 8.0$ Hz, H²), 8.73 (1H, d, $J = 8.0$ Hz, H³); ¹³C NMR (CDCl₃, 126 MHz, ¹H decoupled 500 MHz) δ 31.5 (3C, C¹⁴), 35.0 (1C, C¹³), 45.3 (2C, cyclen CH₂), 46.6 (2C, cyclen CH₂), 47.4 (2C, cyclen CH₂), 51.8 (2C, cyclen CH₂), 60.8 (1C, CH₂ pyridine), 116.4 (1C, C⁴), 118.2 (1C, C¹⁰), 118.6 (1C, C²), 121.0 (1C, C⁵), 121.3 (1C, C⁶), 122.6 (1C, C⁷), 124.6 (1C, C²), 133.7 (1C, C⁹), 137.8 (1C, C⁴), 138.1 (1C, C³), 148.1 (1C, C⁸), 153.5 (1C, C¹), 154.2 (1C, C¹¹), 159.7 (1C, C⁶), 160.2 (1C, C¹), 160.6 (1C, C¹²), 178.0 (1C, C⁵); MS (ES⁺) m/z 289.4 (100 %, [M + Zn]²⁺); HRMS (ES⁺) m/z found 515.3130 [M + H]⁺; C₃₀H₃₉O₂N₆ requires 515.3129.

(S)-N-2-Chloroethanoyl-2-phenylethylamine ⁶

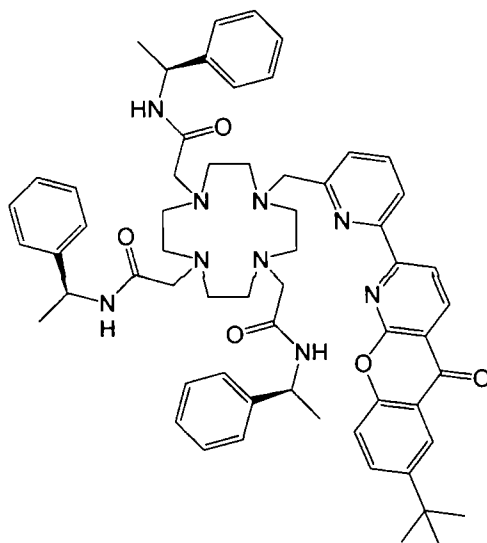


Chloroacetyl chloride (10.5 g, 7.40 ml, 93.0 mmol) was added dropwise to a stirring solution of (S)-1-phenylethylamine (9.40 g, 10.0 ml, 77.50 mmol) and *anhydrous* NEt₃ (13.0 ml, 93.00 mmol) in *anhydrous* diethyl ether (70 ml) at -10 °C, under argon. The solution was allowed to warm to room temperature then stir for a further 3 h. The reaction mixture was washed with H₂O (150 ml) followed by HCl_(aq) (0.1 M, 150 ml). The organic phase was separated, dried over Na₂SO₄, filtered and the filtrate concentrated under reduced pressure to afford a colourless solid. Recrystallisation from warm diethyl ether yielded the *title compound* as colourless needle-like crystals (10.46 g, 53.09 mmol, 69 %); m.p. 95-96 °C; ¹H NMR (CDCl₃, 500 MHz) δ 1.56 (3H, d, $J = 6.5$ Hz, CH₃), 4.05 (2H, dd, $J = 15.5; 8.0$ Hz, CH₂), 5.15 (1H, q, $J = 7.5$ Hz, CH), 6.83 (1H, br s, NH), 7.34-7.39 (5H, m, Ph); ¹³C NMR (CDCl₃, 125 MHz, ¹H decoupled 500 MHz) δ 21.9 (1C, CH₃), 42.9 (1C, CH₂), 49.5 (1C, CH), 126.4 (2C, Ph_(o)), 127.9 (1C, Ph_(p)), 129.1 (2C, Ph_(m)), 142.6 (1C, Ph_(q)), 165.2 (1C, C = O); C₁₀H₁₂ClNO (%): calcd C 60.80, H 6.12, N 7.08; found C 60.06, H 6.15, N 6.94.

(R)-N-2-Chloroethanoyl-2-phenylethylamine

An analogous procedure to that described for 2-chloro-*N*-[(*S*)-methylbenzyl]ethanamide was followed using chloroacetyl chloride (5.25 g, 3.70 ml, 46.5 mmol) and a stirring solution of (*R*)-1-phenylethylamine (4.70 g, 5.00 ml, 38.8 mmol) and *anhydrous* NEt₃ (6.51 ml, 46.52 mmol) in *anhydrous* diethyl ether (100 ml) at – 10 °C. The procedure yielded the *title compound* as colourless needle-like crystals (3.71 g, 18.83 mmol, 49 %). *Characterisation was identical to that reported for 2-chloro-N-[(S)-methylbenzyl]ethanamide.*

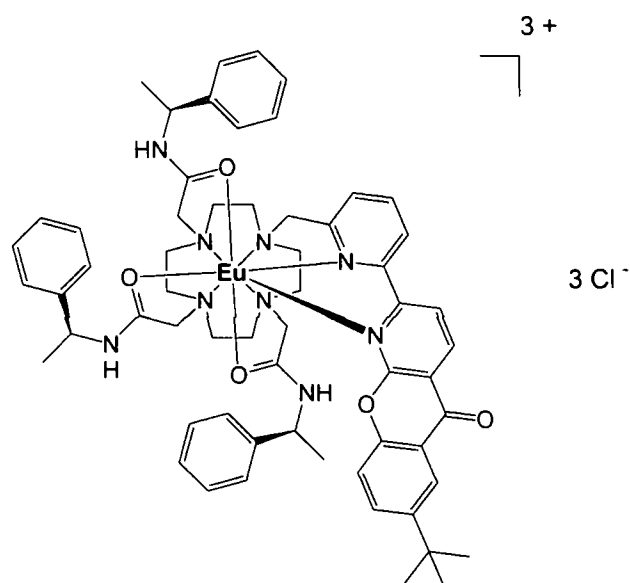
2-{4-[6-(6-*tert*-Butyl-10-oxo-10*H*-9-oxa-1-aza-anthracen-2-yl)-pyridin-2-ylmethyl]-7,10-bis-(((*S*)-1-phenyl-ethylcarbamoyl)-methyl)-1,4,7,10-tetraaza-cyclododec-1-yl}-*N*-((*S*)-1-phenyl-ethyl)-acetamide ([L⁴])



A stirred mixture of 6-*tert*-butyl-2-[6-(1,4,7,10-tetraaza-cyclododec-1-ylmethyl)-pyridin-2-yl]-9-oxa-1-aza-anthracen-10-one **19** (0.060 g, 0.116 mmol), (*S*)-*N*-2-chloroethanoyl-2-phenylethylamine (0.080 g, 0.408 mmol) and K₂CO₃ (0.064 g, 0.466 mmol) in *anhydrous* CH₃CN (5 ml), was heated at reflux, under argon, for 16 h. The resultant mixture was allowed to cool to rt, syringe filtered and the filtrate concentrated under reduced pressure to afford a residual yellow oil. The crude material was purified by column chromatography on neutral alumina (gradient elution: CH₂Cl₂ to 2 % CH₃OH : CH₂Cl₂, utilising 0.1 % CH₃OH increments) to yield the *title compound* [L⁴] as a free flowing pale yellow coloured solid (0.074 g, 0.0741 mmol, 64 %); *R*_F = 0.21 (Alumina, CH₂Cl₂ –

CH₃OH, 19 : 1, v/v); ¹H NMR (CDCl₃, 700 MHz) δ 1.38 (9H, s, ^tBu CH₃), 1.45 (9H, br s, CH₃), 2.60 (8H, br s, cyclen CH₂), 2.92 (8H, br s, cyclen CH₂), 3.06 (2H, br s, CH₂CO), 3.54 (2H, br s, CH₂CO), 3.67 (2H, br s, CH₂CO), 3.96 (2H, br s, CH₂ pyridine), 4.96 (1H, q, CH), 5.11 (2H, q, CH), 7.11-7.30 (15H, m, Ph), 7.45 (1H, br s, H⁵), 7.58 (1H, d, *J* = 9.0 Hz, H¹⁰), 7.70 (1H, br s, H⁴), 7.82 (1H, dd, *J* = 9.0; 2.0 Hz, H⁹), 8.28 (1H, d, *J* = 3.0 Hz, H⁷), 8.43 (1H, br s, H³), 8.62 (1H, d, *J* = 8.5 Hz, H²), 8.77 (1H, d, *J* = 8.5 Hz, H³); MS (ES⁺) *m/z* 998.6 (100 %, [M + H]⁺); HRMS (ES⁺) *m/z* found 998.5667 [M + H]⁺; C₆₀H₇₂O₅N₉ requires 998.5651.

[EuL⁴]

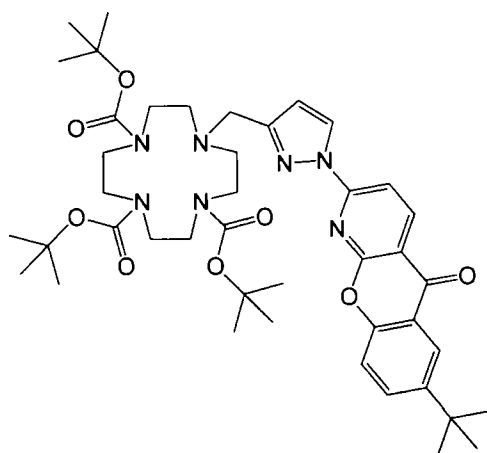


A solution of 2-{4-[6-(6-*tert*-butyl-10-oxo-10*H*-9-oxa-1-aza-anthracen-2-yl)-pyridin-2-ylmethyl]-7,10-bis-[(*S*)-1-phenyl-ethylcarbamoyl]-methyl]-1,4,7,10-tetraaza-cyclododec-1-yl}-*N*-[(*S*)-1-phenyl-ethyl]-acetamide [**L⁴**] (0.040 g, 0.040 mmol) and Eu(OTf)₃·6H₂O (0.034 g, 0.041 mmol) in *anhydrous* CH₃CN (1 ml) was heated at reflux, under argon, for 18 h. The resultant solution was allowed to cool to rt followed by the removal of solvent under reduced pressure to afford a glassy orange solid. CH₂Cl₂ (10 ml) was added to the solid, and the mixture sonicated for 10 min. The solvent was then decanted and the solid material dissolved in a minimum volume of CH₃CN (0.5 ml). The solution was added dropwise onto diethyl ether (25 ml) to induce precipitation. The solid material was isolated by centrifugation, and the process of induced precipitation repeated twice more

to yield the complex as its triflate salt. The off white solid was made water soluble by the exchange of triflate anions for chloride anions using ‘DOWEX 1 x 8 200-400 mesh Cl’ resin. The solid material was dissolved in a mixture of H₂O – CH₃OH (1:1 v/v, 16 ml) and 0.8 g of prepared resin added to the solution, which was stirred at room temperature, for 3 h. The resin was removed by filtration, and the filtrate concentrated under reduced pressure to yield the *title complex [EuL⁴]* (0.034 g, 0.027 mmol, 68 %); λ_{\max} (H₂O) = 356 nm; τ (H₂O) = 1.00 ms; τ (D₂O) = 1.34 ms; ϕ (H₂O; pH 7.4; λ_{exc} 365 nm) = 24 %; HPLC (Method A) t_R = 10.9 min.

7.3.2 Pyrazoyl-azaxanthone Triamide Complexes

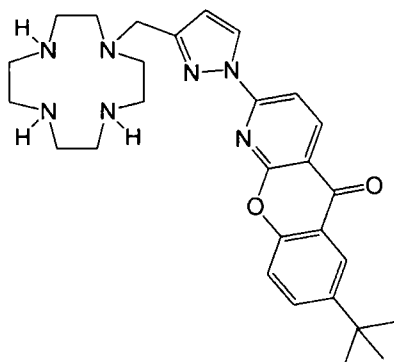
10-[1-(6-*tert*-Butyl-10-oxo-10*H*-9-oxa-1-aza-anthracen-2-yl)-1*H*-pyrazol-3-ylmethyl]-1,4,7,10-tetraaza-cyclododecane-1,4,7-tricarboxylic acid tri-*tert*-butyl ester (**20**)



A stirred mixture of 1,4,7-tetraaza-cyclododecane-1,4,7-tricarboxylic acid tri-*tert*-butyl ester **17** (0.045 g, 0.109 mmol), 2-(3-bromomethyl-pyrazol-1-yl)-6-*tert*-butyl-9-oxa-1-aza-anthracen-10-one **12** (0.057 g, 0.119 mmol), K₂CO₃ (0.019 g, 0.131 mmol) and a catalytic amount of KI (2 mg) in *anhydrous* CH₃CN – CH₂Cl₂ (1 : 1, v/v, 5 ml), was heated at reflux, under argon, for 16 h. The reaction mixture was allowed to cool to rt, syringe filtered and the filtrate concentrated under reduced pressure to afford a residual oil. The crude material was purified by chromatography on silica (gradient elution: CH₂Cl₂ to 3 % CH₃OH : CH₂Cl₂, utilising 0.1 % CH₃OH increments) to yield the *title compound 20* as a pale yellow coloured solid (0.075 g, 0.093 mmol, 85 %); R_F = 0.41

(Silica, CH₂Cl₂ – CH₃OH, 24 : 1, v/v); ¹H NMR (CDCl₃, 500 MHz) δ 1.44 (36H, br s, 3 'Boc CH₃; 'Bu CH₃), 2.78 (4H, br s, cyclen CH₂), 3.39 (8H, br, cyclen CH₂), 3.59 (4H, s, cyclen CH₂), 3.89 (2H, s, CH₂ pyrazole), 6.44 (1H, d, *J* = 3.0 Hz, H^{2'}), 7.56 (1H, d, *J* = 8.5 Hz, H¹⁰), 7.86 (1H, dd, *J* = 9.0; 2.5 Hz, H⁹), 8.04 (1H, d, *J* = 8.5 Hz, H²), 8.30 (1H, d, *J* = 2.5 Hz, H⁷), 8.60 (1H, d, *J* = 2.0 Hz, H¹), 8.78 (1H, d, *J* = 8.5 Hz, H³); ¹³C NMR (CDCl₃, 125 MHz, ¹H decoupled 500 MHz) δ 28.7 (9C, 'Boc CH₃), 31.5 (3C, C¹⁴), 35.5 (1C, C¹³), 47.5 (1C, cyclen CH₂), 47.9 (1C, cyclen CH₂), 48.4 (2C, cyclen CH₂), 50.1 (2C, cyclen CH₂), 53.6 (1C, cyclen CH₂), 54.0 (1C, cyclen CH₂), 55.3 (1C, CH₂ pyrazole), 79.5 (3C, 'Boc_(q)), 109.9 (1C, C²), 110.8 (1C, C^{2'}), 114.2 (1C, C⁴), 118.1 (1C, C¹⁰), 121.4 (1C, C⁶), 122.8 (1C, C⁷), 129.0 (1C, C¹), 133.6 (1C, C⁹), 140.3 (1C, C³), 148.5 (1C, C⁸), 153.6 (1C, C¹¹), 153.9 (1C, C¹²), 155.6 (1C, C³), 155.9 (3C, 'Boc C = O), 159.9 (1C, C¹), 177.0 (1C, C⁵). MS (ES⁺) *m/z* 804.3 (100 %, [M + H]⁺).

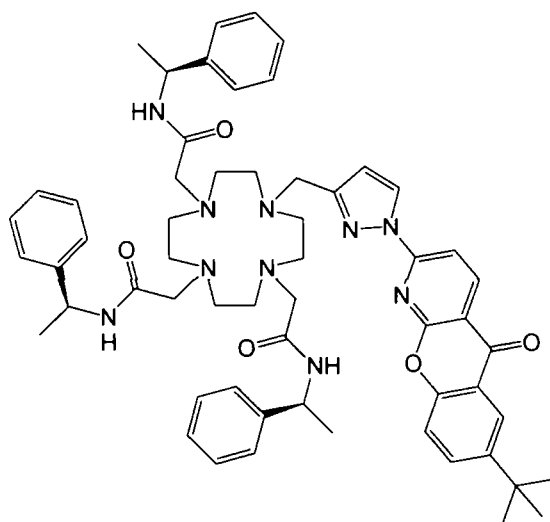
6-*tert*-Butyl-2-[3-(1,4,7,10-tetraaza-cyclododec-1-ylmethyl)-pyrazol-1-yl]-9-oxa-1-aza-anthracen-10-one (21)



A solution of 10-[1-(6-*tert*-butyl-10-oxo-10*H*-9-oxa-1-aza-anthracen-2-yl)-1*H*-pyrazol-3-ylmethyl]-1,4,7,10-tetraaza-cyclododecane-1,4,7-tricarboxylic acid tri-*tert*-butyl ester **20** (0.110 g, 0.137 mmol) in CH₂Cl₂ – TFA (2 : 1 v/v, 3 ml) was stirred at rt, in a sealed flask, for 16 h, to afford a red solution. The solvent was removed under reduced pressure to yield an orange glassy solid. The crude material was repeatedly (x 3) dissolved in CH₂Cl₂ (5 ml) and the solvent removed under reduced pressure to facilitate elimination of excess acid and *tert*-butyl alcohol. The residue was taken into 1 M KOH_(aq) (15 ml) and extracted with CH₂Cl₂ (3 x 15 ml). The organic extracts were combined, dried over K₂CO₃, filtered and the filtrate concentrated under reduced pressure to yield the *title*

compound 21 as an orange coloured solid (0.065 g, 0.129 mmol, 94 %); $^1\text{H NMR}$ (CDCl_3 , 200 MHz) δ 1.39 (9H, s, $t\text{-Bu CH}_3$), 2.70 (4H, br s, cyclen CH_2), 2.80 (8H, br s, cyclen CH_2), 2.85 (4H, br s, cyclen CH_2), 3.83 (2H, s, CH_2^*), 6.51 (1H, d, $J = 3.0$ Hz, $\text{H}^{2'}$), 7.54 (1H, d, $J = 8.5$ Hz, H^{10}), 7.82 (1H, dd, $J = 9.0; 2.0$ Hz, H^9), 8.04 (1H, d, $J = 8.5$ Hz, H^2), 8.28 (1H, d, $J = 2.0$ Hz, H^7), 8.58 (1H, d, $J = 2.0$ Hz, $\text{H}^{1'}$), 8.74 (1H, d, $J = 8.5$ Hz, H^3).

2-{7-[1-(6-*tert*-Butyl-10-oxo-10*H*-9-oxa-1-aza-anthracen-2-yl)-1*H*-pyrazol-3-ylmethyl]-4,10-bis-[(*S*)-1-phenyl-ethylcarbamoyl]-methyl]-1,4,7,10-tetraaza-cyclododec-1-yl}-*N*-[(*S*)-1-phenyl-ethyl]-acetamide ($[\text{L}^5]$)



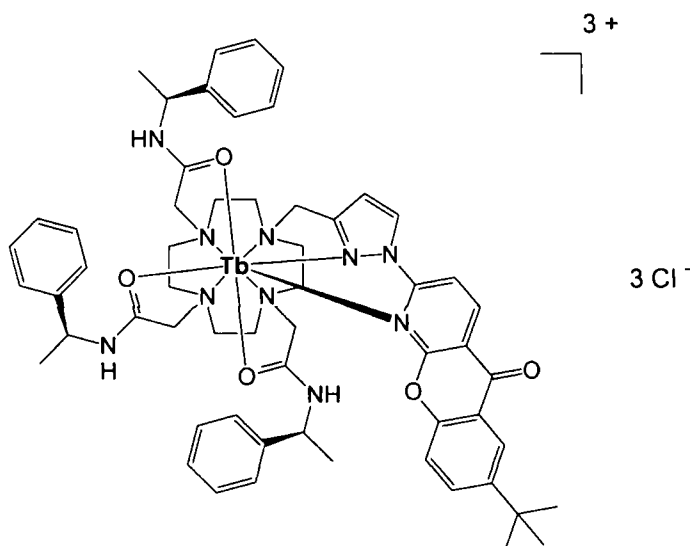
A stirred mixture of 6-*tert*-butyl-2-[3-(1,4,7,10-tetraaza-cyclododec-1-ylmethyl)-pyrazol-1-yl]-9-oxa-1-aza-anthracen-10-one **21** (0.039 g, 0.078 mmol), (*S*)-*N*-2-chloroethanoyl-2-phenylethylamine (0.050 g, 0.250 mmol) and Cs_2CO_3 (0.081 g, 0.251 mmol) in *anhydrous* CH_3CN (5 ml), was heated at reflux, under argon, for 16 h. The reaction mixture was allowed to cool to rt, syringe filtered and the filtrate concentrated under reduced pressure to afford an orange glassy solid. The crude material was sonicated in diethyl ether (15 ml) to yield a fine pale yellow precipitate which was isolated via centrifugation. The material was sonicated in diethyl ether and centrifuged twice more to yield the *title compound* $[\text{L}^5]$ as a free flowing pale yellow solid (0.062 g, 0.063 mmol, 81 %); $^1\text{H NMR}$ (CDCl_3 , 500 MHz) δ 1.41 (9H, s, $t\text{-Bu CH}_3$), 1.52 (9H, br, CH_3), 2.48-3.12 (20H, br m, cyclen CH_2 ; CH_2CONH), 3.77 (2H, s, CH_2), 4.05 (2H, s, CH_2 pyrazole), 5.01 (3H, m, 3 x CH), 6.38 (1H, br s, $\text{H}^{2'}$), 7.03-7.19 (15H, br m, 3 x Ph), 7.54 (1H, d, $J =$

8.0 Hz, H¹⁰), 7.84 (1H, dd, $J = 8.0 ; 2.0$ Hz, H⁹), 7.96 (1H, d, $J = 8.0$ Hz, H²), 8.30 (1H, d, $J = 2.5$ Hz, H⁷), 8.60 (1H, d, $J = 2.0$ Hz, H¹), 8.81 (1H, d, $J = 8.0$ Hz, H³); MS (ES⁺) m/z 998.4 (100 %, [M + H]⁺).

2-{7-[1-(6-*tert*-Butyl-10-oxo-10*H*-9-oxa-1-aza-anthracen-2-yl)-1*H*-pyrazol-3-ylmethyl]-4,10-bis-(((*R*)-1-phenyl-ethylcarbamoyl)-methyl)-1,4,7,10-tetraaza-cyclododec-1-yl}-*N*-((*R*)-1-phenyl-ethyl)-acetamide

An analogous procedure to that described for 2-{7-[1-(6-*tert*-butyl-10-oxo-10*H*-9-oxa-1-aza-anthracen-2-yl)-1*H*-pyrazol-3-ylmethyl]-4,10-bis-(((*S*)-1-phenyl-ethylcarbamoyl)-methyl)-1,4,7,10-tetraaza-cyclododec-1-yl}-*N*-((*S*)-1-phenyl-ethyl)-acetamide [**L**⁵] was followed using 6-*tert*-butyl-2-[3-(1,4,7,10-tetraaza-cyclododec-1-ylmethyl)-pyrazol-1-yl]-9-oxa-1-aza-anthracen-10-one **21** (0.026 g, 0.052 mmol), (*R*)-*N*-2-chloroethanoyl-2-phenylethylamine (0.033 g, 0.165 mmol) and Cs₂CO₃ (0.054 g, 0.167 mmol) in *anhydrous* CH₃CN (5 ml). The procedure yielded the *title compound* as a free flowing pale yellow solid (0.037 g, 0.038 mmol, 74 %). *Characterisation was identical to that reported for 2-{7-[1-(6-tert-butyl-10-oxo-10*H*-9-oxa-1-aza-anthracen-2-yl)-1*H*-pyrazol-3-ylmethyl]-4,10-bis-(((*S*)-1-phenyl-ethylcarbamoyl)-methyl)-1,4,7,10-tetraaza-cyclododec-1-yl}-*N*-((*S*)-1-phenyl-ethyl)-acetamide [**L**⁵].*

(*SSS*)-[TbL⁵]



A stirred mixture of 2-{7-[1-(6-*tert*-butyl-10-oxo-10*H*-9-oxa-1-aza-anthracen-2-yl)-1*H*-pyrazol-3-ylmethyl]-4,10-bis-(((S)-1-phenyl-ethylcarbamoyl)-methyl)-1,4,7,10-tetraaza-cyclododec-1-yl}-*N*-((S)-1-phenyl-ethyl)-acetamide [**L**⁵] (0.044 g, 0.044 mmol) and Tb(OTf)₃·6H₂O (0.030 g, 0.049 mmol) in *anhydrous* CH₃CN (1 ml) was heated at reflux, under argon, for 16 h. The resultant solution was allowed to cool to rt followed by the removal of solvent under reduced pressure to afford a glassy orange solid. CH₂Cl₂ (5 ml) was added to the solid, and the mixture sonicated for 10 min. The solvent was then decanted and the solid material dissolved in a minimum volume of CH₃CN (0.4 ml). The solution was added dropwise onto diethyl ether (15 ml) to induce precipitation. The solid material was isolated by centrifugation, and the process of induced precipitation repeated twice more to yield the complex as its triflate salt. The off white solid was made water soluble by the exchange of triflate anions for chloride anions using ‘DOWEX 1 x 8 200-400 mesh Cl’ resin. The solid material was dissolved in a mixture of H₂O – CH₃OH (1:1 v/v, 10 ml) and 0.5 g of prepared resin added to the solution, which was stirred at room temperature, for 3 h. The resin was removed by filtration, and the filtrate concentrated under reduced pressure to yield the *title complex* (**SSS**)-[**TbL**⁵] as a colourless solid (0.040 g, 0.030 mmol, 69 %); λ_{max} (H₂O) = 348 nm; τ (H₂O) = 2.00 ms; τ (D₂O) = 2.38 ms; φ_{Tb} (H₂O; pH 6.0; λ_{exc} 355 nm) = 46 %; HPLC (Method A) *t*_R = 11.0 min.

(**SSS**)-[**EuL**⁵]

An analogous procedure to that described for (**SSS**)-[**TbL**⁵] was followed using 2-{7-[1-(6-*tert*-butyl-10-oxo-10*H*-9-oxa-1-aza-anthracen-2-yl)-1*H*-pyrazol-3-ylmethyl]-4,10-bis-(((S)-1-phenyl-ethylcarbamoyl)-methyl)-1,4,7,10-tetraaza-cyclododec-1-yl}-*N*-((S)-1-phenyl-ethyl)-acetamide [**L**⁵] (0.042 g, 0.042 mmol) and Eu(OTf)₃·6H₂O (0.033 g, 0.046 mmol) in *anhydrous* CH₃CN (1 ml). Following anion exchange, the procedure yielded the *title complex* (**SSS**)-[**EuL**⁵] as a colourless solid (0.027 g, 0.022 mmol, 54 %); λ_{max} (H₂O) = 348 nm.

(**RRR**)-[**TbL**⁵]

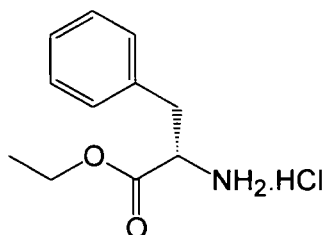
An analogous procedure to that described for (**SSS**)-[**TbL**⁵] was followed using 2-{7-[1-(6-*tert*-butyl-10-oxo-10*H*-9-oxa-1-aza-anthracen-2-yl)-1*H*-pyrazol-3-ylmethyl]-4,10-bis-

[[*(R)*-1-phenyl-ethylcarbamoyl]-methyl]-1,4,7,10-tetraaza-cyclododec-1-yl}-*N*-[[*(R)*-1-phenyl-ethyl]-acetamide (0.021 g, 0.021 mmol) and Tb(OTf)₃·6H₂O (0.014 g, 0.023 mmol) in *anhydrous* CH₃CN (1 ml). Following anion exchange, the procedure yielded the *title complex* (***RRR***)-[TbL⁵] as a colourless solid (0.017 g, 0.013 mmol, 60 %). *Photophysical characterisation was identical to that reported for* (***SSS***)-[TbL⁵].

(***RRR***)-[EuL⁵]

An analogous procedure to that described for (***SSS***)-[TbL⁵] was followed using 2-{7-[1-(6-*tert*-butyl-10-oxo-10*H*-9-oxa-1-aza-anthracen-2-yl)-1*H*-pyrazol-3-ylmethyl]-4,10-bis-[[*(R)*-1-phenyl-ethylcarbamoyl]-methyl]-1,4,7,10-tetraaza-cyclododec-1-yl}-*N*-[[*(R)*-1-phenyl-ethyl]-acetamide (0.011 g, 0.011 mmol) and Eu(OTf)₃·6H₂O (0.008 g, 0.012 mmol) in *anhydrous* CH₃CN (1 ml). Following anion exchange, the procedure yielded the *title complex* (***RRR***)-[EuL⁵] as a colourless solid (0.008 g, 0.007 mmol, 66 %). *Photophysical characterisation was identical to that reported for* (***SSS***)-[EuL⁵].

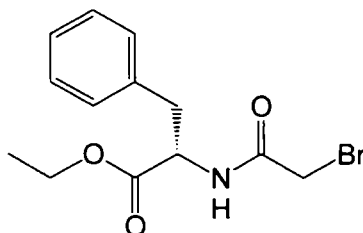
(***S***)-2-Amino-3-phenyl-propionic acid ethyl ester ⁷



HCl_(g), generated *in situ* by dropping conc. H₂SO₄ into a solution of conc. HCl / NaCl, was bubbled through a stirred mixture of (*S*)-phenylalanine (0.500 g, 3.03 mmol) in *anhydrous* ethanol (30 ml), under argon, for 1 h. The solution was then stirred and heated at reflux, under argon, for 24 h. The solution was allowed to cool to rt followed by the removal of solvent removed under reduced pressure to yield the hydrochloride salt of the *title compound*, as a colourless crystalline solid, in quantitative yield. ¹H NMR (CD₃OD, 500 MHz) δ 1.24 (3H, t, *J* = 7.0 Hz, CH₃), 3.24 (2H, t, *J* = 7.0 Hz, CHCH₂), 4.24 (2H, q, *J* = 7.0 Hz, OCH₂), 4.30 (1H, t, *J* = 7.0 Hz, CH), 7.15-7.24 (5H, m, Ph); ¹³C NMR (CD₃OD, 125 MHz, ¹H decoupled 500 MHz) δ 13.1 (1C, CH₃), 36.3 (1C, CH₂), 54.1 (1C,

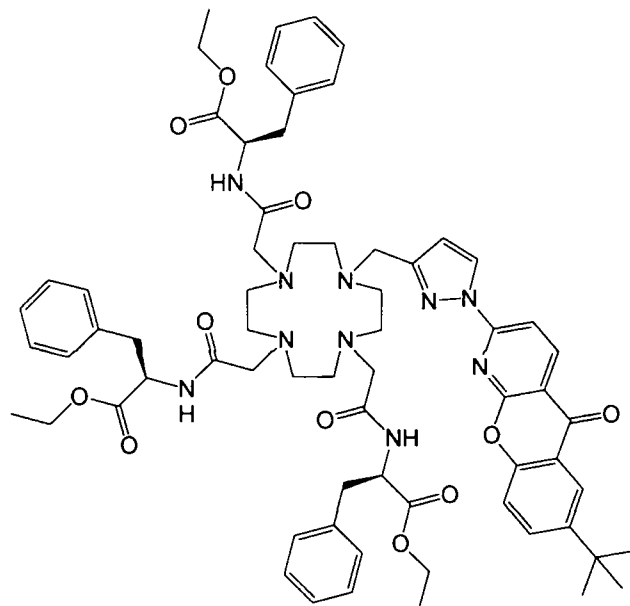
CH), 62.4 (1C, OCH₂), 127.8 (1C, Ph_(p)), 129.0 (2C, Ph_(o/m)), 129.3 (2C, Ph_(o/m)), 134.2 (1C, Ph_(q)), 168.9 (1C, C = O).

(S)-2-(2-Bromo-acetylamino)-3-phenyl-propionic acid ethyl ester⁷



A solution of (*S*)-2-amino-3-phenyl-propionic acid ethyl ester (0.500 g, 2.18 mmol), *anhydrous* NEt₃ (0.305 ml, 2.18 mmol) and bromoacetyl bromide (0.482 g, 0.208 ml, 2.40 mmol) in *anhydrous* THF, was stirred at - 5 °C, under argon, for 16 h. The solvent was removed under reduced pressure and the residue dissolved in CH₂Cl₂ (15 ml). The organic phase was washed with H₂O (20 ml), followed by 1 M HCl_(aq) (20 ml). The organic phase was then concentrated under reduced pressure to yield *the title compound* as a colourless solid (0.505 g, 1.61 mmol, 74 %); m.p. 32-33 °C; ¹H NMR (CDCl₃, 500 MHz) δ 1.26 (3H, *J* = 7.0 Hz, CH₂CH₃), 3.15 (2H, m, CH₂Ph), 3.84 (2H, s, CH₂Br), 4.18 (2H, q, *J* = 7.0 Hz, CH₂CH₃), 4.83 (1H, q, *J* = 7.0 Hz, CH), 6.93 (1H, br s, NH), 7.19-7.28 (5H, m, Ph); ¹³C NMR (CDCl₃, 125 MHz, ¹H decoupled 500 MHz) δ 14.3 (1C, CH₃), 28.9 (1C, CH₂Br), 38.0 (1C, CH₂Ph), 54.0 (1C, CH), 62.1 (1C, CH₂CH₃), 127.5 (1C, Ph_(p)), 128.9 (2C, Ph_(o/m)), 129.6 (2C, Ph_(o/m)), 135.6 (1C, Ph_(q)), 165.5 (1C, C = O), 171.1 (1C, ester C = O); MS (ES⁺) 313.9 (100 %, [M + H]⁺).

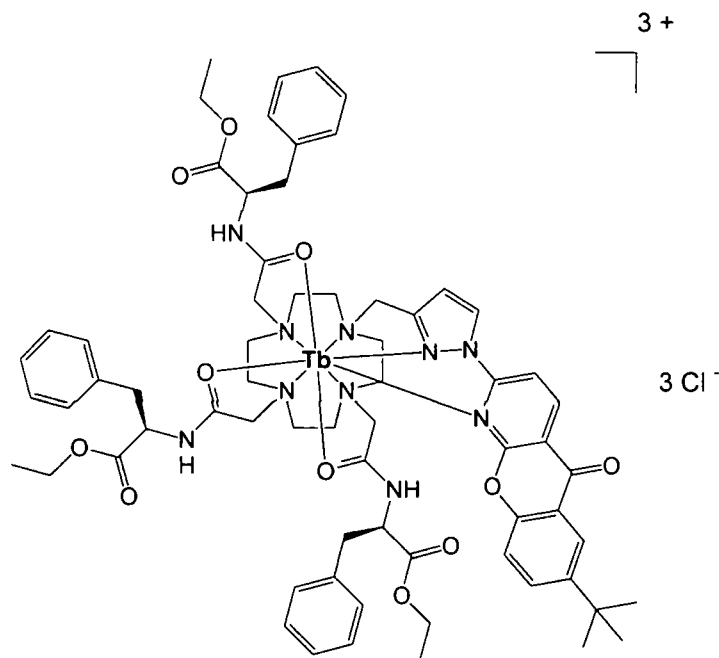
(S)-2-(2-{4-[1-(6-*tert*-Butyl-10-oxo-10*H*-9-oxa-1-aza-anthracen-2-yl)-1*H*-pyrazol-3-ylmethyl]-7,10-bis-[(*S*)-1-ethoxycarbonyl-2-phenyl-ethyl carbamoyl]-methyl]-1,4,7,10-tetraaza-cyclododec-1-yl}-acetylamino)-3-phenyl-propionic acid ethyl ester ([L⁶])



A stirred mixture of 6-*tert*-butyl-2-[3-(1,4,7,10-tetraaza-cyclododec-1-ylmethyl)-pyrazol-1-yl]-9-oxa-1-aza-anthracen-10-one **21** (0.033 g, 0.065 mmol), (*S*)-2-(2-bromoacetylamino)-3-phenyl-propionic acid ethyl ester (0.064 g, 0.206 mmol) and Cs₂CO₃ (0.073 g, 0.231 mmol) in *anhydrous* CH₃CN (7 ml) was heated at reflux, under argon, for 16 h. The resultant mixture was allowed to cool to room temperature, syringe filtered, and the filtrate concentrated under reduced pressure to afford an orange glassy solid. The crude material was sonicated in diethyl ether (15 ml) to yield a fine pale yellow precipitate which was isolated via centrifugation. The material was sonicated in diethyl ether and centrifuged twice more to yield the *title compound* [L⁶] as a free flowing pale yellow solid (0.028 g, 0.023 mmol, 36 %); ¹H NMR (CDCl₃, 400 MHz) δ 1.13 (9H, t, *J* = 6.0 Hz, OCH₂CH₃), 1.35 (9H, s, *t*-Bu CH₃), 2.41-2.60 (12H, br m, cyclen CH₂), 2.68-3.08 (14H, br m, cyclen CH₂; CH₂CO; CH₂Ph), 4.02 (2H, s, CH₂ pyrazole), 4.06 (6H, t, *J* = 6.0 Hz, OCH₂CH₃), 4.76 (3H, q, CH), 6.38 (1H, br s, H²), 7.03-7.19 (15H, br m, Ph), 7.50 (1H, d, *J* = 8.0 Hz, H¹⁰), 7.77 (1H, dd, *J* = 8.0 ; 2.0 Hz, H⁹), 7.94 (1H, d, *J* = 8.0 Hz, H²), 8.24 (1H, d, *J* = 2.5 Hz, H⁷), 8.52 (1H, d, *J* = 2.0 Hz, H¹), 8.92 (1H, d, *J* = 8.0 Hz,

H^3); MS (ES^+) m/z 1203.6 (100 %, $[M + H]^+$); HRMS (ES^+) m/z found 1203.6241 $[M + H]^+$ $C_{67}H_{83}N_{10}O_{11}$ requires 1203.6237.

[TbL⁶]



A stirred solution of (S)-2-(2-{4-[1-(6-*tert*-butyl)-10-oxo-10*H*-9-oxa-1-aza-anthracen-2-yl]-1*H*-pyrazol-3-ylmethyl]-7,10-bis-[(S)-1-ethoxycarbonyl-2-phenyl-ethylcarbamoyl]-methyl]-1,4,7,10-tetraaza-cyclododec-1-yl}-acetyl-amino)-3-phenyl-propionic acid ethyl ester [**L⁶**] (0.013 g, 0.011 mmol) and Tb(OTf)₃·6H₂O (0.007 g, 0.012 mmol) in *anhydrous* CH₃CN (1 ml) was heated at reflux, under argon, for 16 h. The solution was allowed to cool to room temperature followed by the removal of solvent under reduced pressure to afford a glassy orange solid. CH₂Cl₂ (5 ml) was added to the solid, and the mixture sonicated for 10 min. The solvent was then decanted and the solid material dissolved in a minimum volume of CH₃CN (0.4 ml). The solution was added dropwise onto diethyl ether (15 ml) to induce precipitation. The solid material was isolated by centrifugation, and the process of induced precipitation repeated twice more to yield the complex as its triflate salt. The off white solid was made water soluble by the exchange of triflate anions for chloride anions using ‘DOWEX 1 x 8 200-400 mesh Cl’ resin. The solid material was dissolved in a mixture of H₂O – CH₃OH (1:1 v/v, 10 ml) and 0.5 g of prepared resin added to the solution, which was stirred at room temperature, for 3 h. The

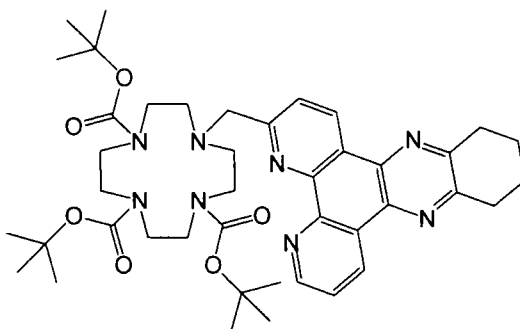
resin was removed by filtration, and the filtrate concentrated under reduced pressure to yield the *title complex* [TbL⁶] as a colourless solid (0.008 g, 0.006 mmol, 56 %); λ_{\max} (H₂O) = 348 nm, τ (H₂O) = 2.25 ms; ϕ_{fb} (H₂O; pH 6.0; λ_{exc} 355 nm) = 54 %; HPLC (Method A) t_{R} = 11.2 min.

[EuL⁶]

An analogous procedure to that described for [TbL⁶] was followed using (*S*)-2-(2-{4-[1-(6-*tert*-butyl-10-oxo-10*H*-9-oxa-1-aza-anthracen-2-yl)-1*H*-pyrazol-3-yl]methyl}-7,10-bis-[(*S*)-1-ethoxycarbonyl-2-phenyl-ethylcarbamoyl]-methyl]-1,4,7,10-tetraaza-cyclododecane-1-yl}-acetyl-amino)-3-phenyl-propionic acid ethyl ester [L⁶] (0.011 g, 0.009 mmol) and Eu(OTf)₃·6H₂O (0.008 g, 0.012 mmol) in *anhydrous* CH₃CN (1 ml). Following anion exchange, the procedure yielded the *title complex* [EuL⁶] as colourless solid (0.008 g, 0.007 mmol, 78 %).

7.3.3 Tetraazatriphenylene Triamide Complexes

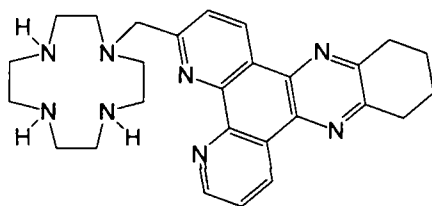
10-(10,11,12,13-Tetrahydro-4,5,9,14-tetraaza-benzo[*b*]triphenylen-6-ylmethyl)-1,4,7,10-tetraaza-cyclododecane-1,4,7-tricarboxylic acid tri-*tert*-butyl ester ⁴ (22)



A stirred mixture of 1,4,7-tetraaza-cyclododecane-1,4,7-tricarboxylic acid tri-*tert*-butyl ester **17** (0.400 g, 0.848 mmol), 3-chloromethyl-10,11,12,13-tetrahydrodipyrido-[3,2*a*:2',3'-*c*]-phenazine (0.300 g, 0.901 mmol) and K₂CO₃ (0.625 g, 4.56 mmol) in *anhydrous* CH₃CN – CH₂Cl₂ (1:1, 10 ml) was heated at reflux, under argon, for 16 h. The resultant mixture was allowed to cool to rt, syringe filtered and the filtrate concentrated under reduced pressure to afford a residual yellow oil. The crude material was purified by

column chromatography on silica gel (gradient elution: CH₂Cl₂ to 2.5 % CH₃OH : CH₂Cl₂), utilising 0.1 % CH₃OH increments) to yield the *title compound* as an orange crystalline solid (0.55 g, 0.65 mmol, 77 %); $R_F = 0.44$ (Silica, CH₂Cl₂ – CH₃OH, 9 : 1 v/v); m.p. 114-116 °C; ¹H NMR (CDCl₃, 300 MHz) δ 0.71 (27H, br s, ^tBoc CH₃), 2.04 (4H, m, H¹⁰; H¹³), 2.62 (4H, br s, cyclen CH₂), 2.75 (8H, br s, cyclen CH₂), 2.86 (4H, br s, cyclen CH₂), 3.23 (4H, br s, H¹¹; H¹²), 4.24 (2H, s, CH₂ dpqC), 7.67 (1H, dd, $J = 8.0$; 4.5 Hz, H⁷), 7.72 (1H, br s, H²), 9.71 (1H, br s, H⁶), 9.26 (2H, br m, H⁸; H¹); MS (ES⁺) m/z 793.4 (100 %, [M + Na]⁺); HRMS (ES⁺) m/z found 793.4379 [M + Na]⁺ C₄₂H₅₈O₆N₈Na requires 793.4377.

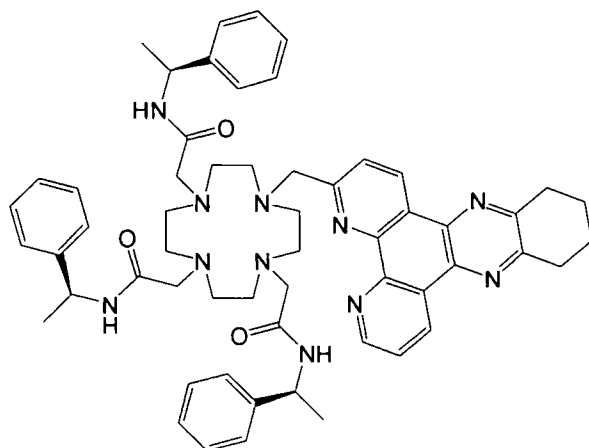
6-(1,4,7,10-Tetraaza-cyclododec-1-ylmethyl)-10,11,12,13-tetrahydro-4,5,9,14-tetraaza-benzo[*b*]triphenylene ⁴ (23)



A solution of 10-(10,11,12,13-tetrahydro-4,5,9,14-tetraaza-benzo[*b*]triphenylen-6-ylmethyl)-1,4,7,10-tetraaza-cyclododecane-1,4,7-tricarboxylic acid tri-*tert*-butyl ester **22** (0.090 g, 0.122 mmol) in CH₂Cl₂ – TFA (2 : 1 v/v, 3 ml) was stirred at rt, in a sealed flask, for 24 h, to afford an orange solution. The solvent was removed under reduced pressure to yield a glassy orange solid. The crude material was repeatedly (x 3) dissolved in CH₂Cl₂ (5 ml) and the solvent removed under reduced pressure to facilitate elimination of excess acid and *tert*-butyl alcohol. The residue was finally taken into 1 M KOH (aq) (10 ml) and extracted with CH₂Cl₂ (3 x 15 ml). The organic extracts were combined, dried over K₂CO₃, filtered and the filtrate concentrated under reduced pressure to yield the *title compound* **23** as an orange coloured crystalline solid (0.053 g, 0.111 mmol, 96 %); ¹H NMR (CDCl₃, 500 MHz) δ 2.08 (4H, br s, H¹⁰; H¹³), 2.62 (4H, br s, cyclen CH₂), 2.75 (8H, br s, cyclen CH₂), 2.86 (4H, br s, cyclen CH₂), 3.23 (4H, br s, H¹¹; H¹²), 4.24 (2H, s, CH₂ dpqC), 7.73 (1H, d, $J = 8.0$ Hz, H¹), 8.05 (1H, d, $J = 8.0$ Hz, H⁷), 9.26 (1H, d, $J = 8.0$ Hz, H⁶), 9.45 (2H, d, $J = 8.0$ Hz, H¹/H⁸); ¹³C NMR (CDCl₃, 125 MHz, ¹H decoupled 500 MHz) δ 22.6 (1C, CH₂), 32.6 (1C, CH₂), 45.2 (2C, cyclen CH₂), 46.3 (2C, cyclen CH₂),

47.1 (2C, cyclen CH₂), 52.0 (2C, cyclen CH₂), 61.7 (1C, CH₂ dpqC), 122.8 (1C, C⁷), 123.2 (1C, C²), 125.9 (1C, Ar_(q)), 127.0 (1C, Ar_(q)), 132.7 (1C, C⁸), 133.5 (1C, C¹), 137.1 (1C, Ar_(q)), 146.0 (1C, Ar_(q)), 146.8 (1C, Ar_(q)), 151.3 (1C, C⁶), 153.3 (1C, Ar_(q)), 153.6 (1C, Ar_(q)), 162.3 (1C, Ar_(q)).

2-[4,7-Bis-(((S)-1-phenyl-ethylcarbamoyl)-methyl)-10-(10,11,12,13-tetrahydro-4,5,9,14-tetraaza-benzo[*b*]triphenylen-6-ylmethyl)-1,4,7,10-tetraaza-cyclododec-1-yl]-*N*-((S)-1-phenyl-ethyl)-acetamide ⁴ ([L⁷])

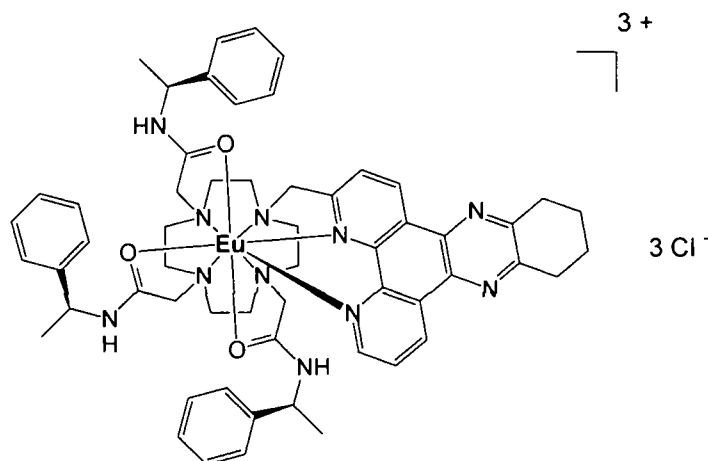


A stirred mixture of 6-(1,4,7,10-tetraaza-cyclododec-1-ylmethyl)-10,11,12,13-tetrahydro-4,5,9,14-tetraaza-benzo[*b*]triphenylene **23** (0.050 g, 0.104 mmol), (*S*)-*N*-2-chloroethanoyl-2-phenylethylamine (0.066 g, 0.332 mmol) and Cs₂CO₃ (0.108 g, 0.332 mmol) in *anhydrous* CH₃CN (5 ml) was heated at reflux, under argon, for 16 h. The reaction mixture was allowed to cool to rt, syringe filtered and the filtrate concentrated under reduced pressure to afford a residual yellow oil. The crude material was purified by column chromatography on neutral alumina (gradient elution: CH₂Cl₂ to 2 % CH₃OH : CH₂Cl₂, utilising 0.1 % CH₃OH increments) to yield the *title compound* [L⁷] as a pale yellow coloured solid (0.075 g, 0.079 mmol, 76 %); *R*_F = 0.57 (Alumina, CH₂Cl₂ – CH₃OH, 99 : 1, v/v); ¹H NMR (CDCl₃, 500 MHz) δ 1.44 (3H, d, *J* = 2.5 Hz, CH₃), 1.46 (6H, d, *J* = 2.5 Hz, CH₃), 2.10 (4H, br s, H¹⁰: H¹³), 2.43-2.62 (16 H, br m, cyclen CH₂), 2.94 (6H, br s, CH₂C(O)), 3.25 (4H, br s, H¹¹: H¹²), 4.05 (2H, s, CH₂ dpqC), 5.12 (3H, q, *J* = 7.0 Hz, CH), 7.16-7.29 (15H, br s, Ph), 7.74 (1H, dd, *J* = 8.0 Hz, H²), 7.82 (1H, d, *J* = 8.0 Hz, H⁷), 9.20 (1H, dd, *J* = 8.0; 2.0 Hz, H⁶), 9.33 (1H, d, *J* = 8.0 Hz, H¹), 9.48 (1H, dd,

$J = 8.0; 2.0$ Hz, H^8); ^{13}C NMR ($CDCl_3$, 125 MHz, 1H decoupled 500 MHz) δ 22.2 (1C, CH_3), 22.7 (2C, C^{10} , C^{13}), 22.8 (2C, CH_3), 32.7 (2C, C^{11} , C^{12}), 49.5 (3C, CH), 49.8-52.4 (11C, cyclen CH_2 ; CH_2CO), 60.4 (CH_2 dpqC), 123.4 (1C, C^2), 125.1 (1C, C^7), 126.3 (1C, $Ar_{(q)}$), 126.4 (1C, $Ar_{(q)}$), 126.8 (1C, $Ar_{(q)}$), 126.9 (1C, $Ar_{(q)}$), 127.4 (1C, $Ar_{(q)}$), 128.1 (1C, $Ar_{(q)}$), 128.2 (1C, $Ar_{(q)}$), 128.4 (1C, $Ar_{(q)}$), 133.2 (1C, C^8), 134.1 (1C, C^1), 137.0 (1C, $Ar_{(q)}$), 137.5 (1C, Ar), 143.5 (1C, Ar), 144.2 (1C, Ar), 145.6 (1C, Ar), 146.2 (1C, Ar), 153.6 (1C, Ar), 153.9 (1C, Ar), 154.1 (1C, Ar), 159.9 (1C, Ar), 169.1 (1C, C=O), 170.7 (2C, C=O); MS (ES^+) m/z 954.5 (100 %, $[M + H]^+$); HRMS (ES^+) m/z found 954.5505 $[M + H]^+$ $C_{57}H_{68}N_{11}O_3$ requires 954.5506.

2-[4,7-Bis-(((*R*)-1-phenyl-ethylcarbamoyl)-methyl)-10-(10,11,12,13-tetrahydro-4,5,9,14-tetraaza-benzo[*b*]triphenylen-6-ylmethyl)-1,4,7,10-tetraaza-cyclododec-1-yl]-*N*-((*R*)-1-phenyl-ethyl)-acetamide

An analogous procedure to that described for 2-[4,7-bis-(((*S*)-1-phenyl-ethylcarbamoyl)-methyl)-10-(10,11,12,13-tetrahydro-4,5,9,14-tetraaza-benzo[*b*]triphenylen-6-ylmethyl)-1,4,7,10-tetraaza-cyclododec-1-yl]-*N*-((*S*)-1-phenyl-ethyl)-acetamide [**L**⁷] was followed using 6-(1,4,7,10-tetraaza-cyclododec-1-ylmethyl)-10,11,12,13-tetrahydro-4,5,9,14-tetraaza-benzo[*b*]triphenylene **23** (0.085 g, 0.177 mmol), (*R*)-*N*-2-chloroethanoyl-2-phenylethylamine (0.112 g, 0.564 mmol) and CS_2CO_3 (0.183 g, 0.564 mmol) in *anhydrous* CH_3CN (5 ml). The procedure yielded the *title compound* as a free flowing pale yellow solid (0.117 g, 0.124 mmol, 70 %). *Characterisation was identical to that reported for 2-[4,7-bis-(((S)-1-phenyl-ethylcarbamoyl)-methyl)-10-(10,11,12,13-tetrahydro-4,5,9,14-tetraaza-benzo[*b*]triphenylen-6-ylmethyl)-1,4,7,10-tetraaza-cyclododec-1-yl]-*N*-((S)-1-phenyl-ethyl)-acetamide [**L**⁷].*

(SSS)-[EuL⁷]⁴⁺

A solution of 2-[4,7-bis-[[*(S)*-1-phenyl-ethylcarbamoyl]-methyl]-10-(10,11,12,13-tetrahydro-4,5,9,14-tetraaza-benzo[*b*]triphenylen-6-ylmethyl)-1,4,7,10-tetraaza-cyclododec-1-yl]-*N*-[*(S)*-1-phenyl-ethyl]-acetamide [**L⁷**] (0.070 g, 0.073 mmol) and Eu(OTf)₃·6H₂O (0.044 g, 0.073 mmol) in *anhydrous* CH₃CN (1 ml) was heated at reflux, under argon, for 18 h. The solution was allowed to cool to rt followed by the removal of solvent under reduced pressure to afford a glassy orange solid. CH₂Cl₂ (10 ml) was added to the solid, and the mixture sonicated for 10 min. The solvent was then decanted and the solid material dissolved in a minimum volume of CH₃CN (0.5 ml). The solution was added dropwise onto diethyl ether (25 ml) to induce precipitation. The solid material was isolated by centrifugation, and the process of induced precipitation repeated twice more to yield the complex as its triflate salt. The yellow solid was made water soluble by the exchange of triflate anions for chloride anions using ‘DOWEX 1 x 8 200-400 mesh Cl⁻’ resin. The solid material was dissolved in a mixture of H₂O – CH₃OH (1:1 v/v, 20 ml) and 1.0 g of prepared resin added to the solution, which was stirred at room temperature, for 6 h. The resin was removed by filtration, and the filtrate concentrated under reduced pressure to yield the *title complex* **(SSS)-[EuL⁷]** as a pale yellow coloured solid (0.064 g, 0.053 mmol, 72 %); MS (ES⁺) *m/z* 368.1 (100 %, [M]³⁺); HRMS (ES⁺) *m/z* found 368.1541 [M]³⁺ C₅₇H₆₇O₃N₁₁Eu requires 368.1537; λ_{max} (H₂O) = 348 nm; τ (H₂O) = 1.04 ms; τ (D₂O) = 1.59 ms; φ_{Eu} (H₂O; pH 7.4; λ_{exc} 348 nm) = 16 %; HPLC (Method A) *t_R* = 10.8 min.

(SSS)-[TbL⁷]

An analogous procedure to that described for **(SSS)-[EuL⁷]** was followed using 2-[4,7-bis-(((S)-1-phenyl-ethylcarbamoyl)-methyl)-10-(10,11,12,13-tetrahydro-4,5,9,14-tetraaza-benzo[*b*]triphenylen-6-ylmethyl)-1,4,7,10-tetraaza-cyclododec-1-yl]-*N*-((S)-1-phenyl-ethyl)-acetamide [**L⁷**] (0.075 g, 0.079 mmol) and Tb(OTf)₃·6H₂O (0.056 g, 0.081 mmol) in *anhydrous* CH₃CN (1 ml). Following anion exchange, the procedure yielded the *title complex* **(SSS)-[TbL⁷]** as colourless solid (0.062 g, 0.051 mmol, 64 %); MS (ES⁺) *m/z* 370.0 (100 %, [M]³⁺); HRMS (ES⁺) *m/z* found 370.8226 [M]³⁺ C₅₇H₆₇O₃N₁₁Tb requires 370.8222; λ_{max} (H₂O) = 348 nm; τ (H₂O) = 1.56 ms; τ (D₂O) = 1.72 ms; φ_{Tb} (H₂O; pH 7.4; λ_{exc} 348 nm) = 40 %.

(SSS)-[GdL⁷]

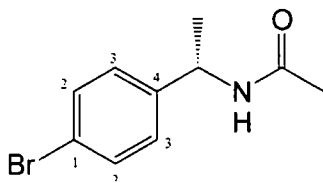
An analogous procedure to that described for **(SSS)-[EuL⁷]** was followed using 2-[4,7-bis-(((S)-1-phenyl-ethylcarbamoyl)-methyl)-10-(10,11,12,13-tetrahydro-4,5,9,14-tetraaza-benzo[*b*]triphenylen-6-ylmethyl)-1,4,7,10-tetraaza-cyclododec-1-yl]-*N*-((S)-1-phenyl-ethyl)-acetamide [**L⁷**] (0.020 g, 0.021 mmol) and Gd(OAc)₃·6H₂O (0.008 g, 0.025 mmol) in *anhydrous* CH₃CN (1 ml). Following anion exchange, the procedure yielded the *title complex* **(SSS)-[GdL⁷]** as colourless solid (0.013 g, 0.011 mmol, 54 %); MS (ES⁺) *m/z* 1109.4 (100 %, [M - 2H]⁺); HRMS (ES⁺) found 1109.4517 [M - 2H]⁺ C₅₇H₆₅O₃N₁₁Gd requires 1109.4513; λ_{max} (H₂O) = 348 nm.

(RRR)-[EuL⁷]

An analogous procedure to that described for **(SSS)-[EuL⁷]** was followed using 2-[4,7-bis-(((S)-1-phenyl-ethylcarbamoyl)-methyl)-10-(10,11,12,13-tetrahydro-4,5,9,14-tetraaza-benzo[*b*]triphenylen-6-ylmethyl)-1,4,7,10-tetraaza-cyclododec-1-yl]-*N*-((S)-1-phenyl-ethyl)-acetamide [**L⁷**] (0.016 g, 0.017 mmol) and Eu(OTf)₃·6H₂O (0.010 g, 0.017 mmol) in *anhydrous* CH₃CN (1 ml). Following anion exchange, the procedure yielded the *title complex* **(RRR)-[EuL⁷]** as colourless solid (0.015 g, 0.013 mmol, 73 %); *Photophysical characterisation was identical to that reported for (SSS)-[EuL⁷].*

(SSS)-[TbL⁷]

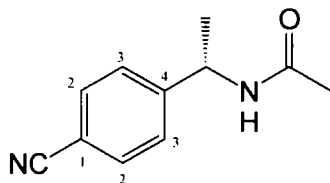
An analogous procedure to that described for **(SSS)-[EuL⁷]** was followed using 2-[4,7-bis-(((S)-1-phenyl-ethylcarbamoyl)-methyl)-10-(10,11,12,13-tetrahydro-4,5,9,14-tetraaza-benzo[*b*]triphenylen-6-ylmethyl)-1,4,7,10-tetraaza-cyclododec-1-yl]-*N*-((S)-1-phenyl-ethyl)-acetamide **[L⁷]** (0.016 g, 0.017 mmol) and Eu(OTf)₃·6H₂O (0.010 g, 0.017 mmol) in *anhydrous* CH₃CN (1 ml). Following anion exchange, the procedure yielded the *title complex* **(RRR)-[TbL⁷]** as colourless solid (0.014 g, 0.012 mmol, 66 %); *Photophysical characterisation was identical to that reported for (SSS)-[TbL⁷]*.

7.4 Amide Conjugate Complexes**7.4.1 Conjugate Amide Pendant Arm****(S)-*N*-Ethanoyl-1-(4-bromophenyl)ethylamine⁶ (24)**

Acetyl chloride (2.40 ml, 30.0 mmol) was added dropwise to a stirring solution of (*S*)-1-(4-bromophenyl)ethylamine (5.00 g, 24.99 mmol) and *anhydrous* NEt₃ (4.40 ml, 31.0 mmol) in *anhydrous* diethyl ether (300 ml) at -10 °C. The solution was allowed to warm to rt then stir for a further 3 h. The reaction mixture was washed with H₂O (150 ml) and then 0.1 M HCl_(aq) (150 ml). The organic phase was separated, dried over Na₂SO₄, filtered and the filtrate concentrated under reduced pressure to afford a colourless solid. Recrystallisation from warm diethyl ether yielded the *title compound* **24** as colourless needle-like crystals (4.56 g, 18.8 mmol, 76 %). m.p. 127-129 °C; ¹H NMR (CDCl₃, 500 MHz) δ 1.47 (3H, d, *J* = 7.0 Hz, CH₃), 2.00 (3H, s, C(O)CH₃), 5.08 (1H, q, *J* = 7.0 Hz, CH), 5.71 (1H, br s, NH), 7.20 (2H, d, *J* = 8.5 Hz, H²), 7.46 (2H, d, *J* = 8.5 Hz, H³); ¹³C NMR (CDCl₃, 125 MHz, 1H decoupled 500 MHz) δ 21.9 (1C, CH₃), 23.7 (1C, C(O)CH₃), 48.5 (1C, CH), 121.4 (1C, C¹), 128.2 (2C, C³), 132.0 (2C, C²), 142.5 (1C, C⁴), 169.3 (1C, C = O); MS (ES⁺) *m/z* 263.9 (100 %, [M + Na]⁺); HRMS (ES⁺) *m/z* found

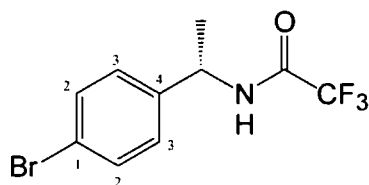
263.9994 $[M + Na]^+$ $C_{10}H_{12}ON^{79}Br^{23}Na$ requires 263.9995; $C_{10}H_{12}BrNO$ (%): calcd C 49.61, H 5.00, N 5.79; found C 49.48, H 4.98, N 5.52.

(S)-N-Ethanoyl-1-(4-cyanophenyl)ethylamine ⁶ (25)



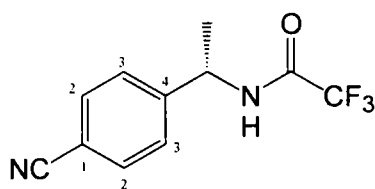
A stirred solution of (*S*)-*N*-ethanoyl-1-(4-bromophenyl)ethylamine **24** (4.00 g, 16.5 mmol) and CuCN (1.55 g, 17.3 mmol) in *anhydrous*, degassed DMF (40 ml) was heated at 180 °C, for 78 h. The resultant dark green solution was allowed to cool to rt followed by the removal of solvent under reduced pressure. The residue was taken up into 6 M HCl_(aq) (50 ml) in a well ventilated fumehood and the resulting aqueous solution extracted with CH₂Cl₂ (3 x 50 ml). The organic extracts were combined, washed with H₂O (100 ml), separated and the solvent removed under reduced pressure to yield the *title compound* **25** as a yellow crystalline solid (2.20 g, 11.7 mmol, 71 %); m.p. 188-190 °C; ¹H NMR (CDCl₃, 500 MHz) δ 1.47 (3H, d, *J* = 7.0 Hz, CH₃), 2.00 (3H, s, C(O)CH₃), 5.12 (1H, q, *J* = 7.0 Hz, CH), 6.02 (1H, d, *J* = 6.5 Hz, NH), 7.43 (2H, d, *J* = 8.0 Hz, H²), 7.63 (2H, d, *J* = 8.0 Hz, H³); ¹³C NMR (CDCl₃, 125 MHz, ¹H decoupled 500 MHz) δ 22.0 (1C, CH₃), 23.5 (1C, C(O)CH₃), 48.9 (1C, CH), 111.2 (1C, CN), 119.0 (1C, C⁴), 127.1 (2C, C³), 132.7 (2C, C²), 149.2 (1C, C¹), 169.7 (1C, C = O); MS (ES⁺) *m/z* 189.1 (100 %, [M + H]⁺); HRMS (ES⁺) *m/z* found 189.1023 [M + H]⁺ $C_{11}H_{13}ON_2$ requires 189.1022; $C_{11}H_{12}N_2O$ (%): calcd C 70.19, H 6.43, N 14.88; found C 70.05, H 6.49, N 15.00.

***N*-[(*S*)-1-(4-Bromo-phenyl)-ethyl]-2,2,2-trifluoro-acetamide ⁸ (27)**



A solution of (*S*)-(-)- α -methylbenzylamine (7.81 g, 39.1 mmol) in *anhydrous* CH₂Cl₂ (20 ml) was added dropwise to a stirring solution of trifluoroacetic anhydride (14.0 g, 9.27 ml, 66.7 mmol) in *anhydrous* CH₂Cl₂ (35 ml), under argon, at 0 °C. The solution was allowed to warm to rt then stir for a further 3 h. The solution was cooled to -10 °C for the addition of 70 % methanesulfonic acid (16.3 g, 11.0 ml, 169 mmol) followed by 1,3-dibromo-5,5-dimethylhydantoin (9.00 g, 31.6 mmol). The suspension was allowed to warm to rt then stir for 16 h. 1 M NaHSO_{3(aq)} (100 ml) was introduced into the reaction mixture and the organic phase washed with H₂O (200 ml). The organic phase was separated, dried over MgSO₄, filtered and the filtrate concentrated under reduced pressure to afford a crude colourless solid. The crude material was recrystallised from diethyl ether to yield the *title compound 27* as colourless needle-like crystals (5.80 g, 19.7 mmol, 51 %); m.p. 154-156 °C; ¹H NMR (CDCl₃, 500 MHz) δ 1.57 (3H, d, *J* = 7.0 Hz, CH₃), 5.10 (1H, q, *J* = 7.0 Hz, CH), 6.57 (1H, br s, NH), 7.20 (2H, d, *J* = 8.0 Hz, H³), 7.51 (2H, d, *J* = 8.0 Hz, H²); ¹³C NMR (CDCl₃, 125 MHz, ¹H decoupled 500 MHz) δ 21.2 (1C, CH₃), 49.5 (1C, CH), 122.3 (1C, C¹), 128.1 (2C, C³), 132.4 (2C, C²), 140.2 (1C, C⁴), 156.7 (1C, C = O); ¹⁹F NMR (CDCl₃, 470 MHz, ¹H decoupled 500 MHz) δ -76.2 (3F, s, CF₃); MS (ES⁺) *m/z* 318.1 (100 %, [M + Na]⁺); HRMS (ES⁺) *m/z* found 317.9713 [M + Na]⁺ C₁₀H₉ON⁷⁹BrF₃²³Na requires 317.9712; C₁₀H₉BrF₃NO (%): calcd C 40.57, H 3.06, N 4.73; found C 40.47, H 3.03, N 4.67.

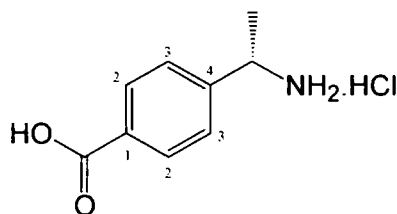
***N*-[(*S*)-1-(4-Cyano-phenyl)-ethyl]-2,2,2-trifluoro-acetamide ⁸ (28)**



A stirring solution of *N*-[(*S*)-1-(4-bromo-phenyl)-ethyl]-2,2,2-trifluoro-acetamide **27** (5.80 g, 19.7 mmol) and CuCN (2.12 g, 23.7 mmol) in *anhydrous*, degassed DMF (30 ml) was heated at 180 °C, under argon, for 48 h. The resultant dark green solution was allowed to cool to rt followed by the removal of the solvent under reduced pressure. The residue was taken up into 6 M HCl_(aq) (50 ml) in a well ventilated fumehood and the resulting aqueous solution extracted with CH₂Cl₂ (3 x 50 ml). The combined organic

extracts were combined and concentrated under reduced pressure to afford a brown solid. The crude material was purified by column chromatography on silica (using 100 % CH₂Cl₂ elution) to yield the *title compound 28* as a colourless solid (2.86 g, 11.8 mmol, 60 %); $R_F = 0.34$ (Silica, CH₂Cl₂, 100 v); m.p. 98-99 °C; ¹H NMR (CDCl₃, 500 MHz) δ 1.53 (3H, d, $J = 7.5$ Hz, CH₃), 5.10 (1H, q, $J = 7.0$ Hz, CH), 7.36 (1H, d, $J = 7.5$ Hz, NH), 7.41 (2H, d, $J = 8.0$ Hz, H²), 7.60 (2H, d, $J = 8.0$ Hz, H³); ¹³C NMR (CDCl₃, 125 MHz, ¹H decoupled 500 MHz) δ 21.3 (1C, CH₃), 49.9 (1C, CH), 111.7 (1C, C¹), 118.7 (1C, CN), 127.1 (2C, C³), 132.9 (2C, C²), 147.1 (1C, C⁴), 156.9 (1C, C = O); ¹⁹F NMR (CDCl₃, 470 MHz, ¹H decoupled 500 MHz) δ -75.7 (3F, s, CF₃); MS (ES⁻) m/z 241.2 (100 %, [M - H]⁻); HRMS (ES⁻) m/z found 241.0591 [M - H]⁻ C₁₁H₈ON₂F₃ requires 241.0594; C₁₁H₉F₃N₂O (%): calcd C 54.55, H 3.75, N 11.57; found C 54.48, H 3.85, N 11.65.

(S)-4-(1-Aminoethyl)benzoic acid ⁶ (26)

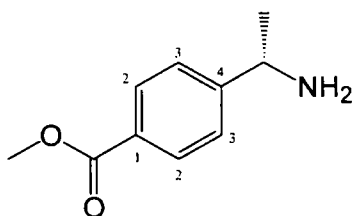


Procedure A:

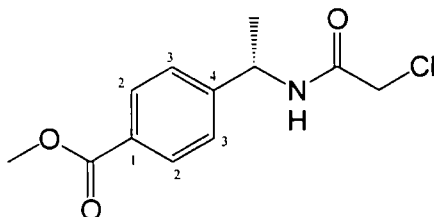
A solution of (*S*)-*N*-ethanoyl-1-(4-cyanophenyl)ethylamine **25** (2.00 g, 10.6 mmol) in 6 M HCl_(aq) (35 ml) was heated at reflux, for 72 h. The solution was allowed to cool to rt followed by the removal of solvent under reduced pressure to yield the hydrochloride salt of the *title compound 26*, as a colourless crystalline solid, in quantitative yield. ¹H NMR (D₂O, 500 MHz) δ 1.52 (3H, d, $J = 7.0$ Hz, CH₃), 4.48 (1H, q, $J = 7.0$ Hz, CH), 7.37 (2H, dd, $J = 6.5; 1.5$ Hz, H³), 7.86 (2H, dd, $J = 7.0; 2.0$ Hz, H²); ¹³C NMR (D₂O, 125 MHz, ¹H decoupled 500 MHz) δ 19.4 (1C, CH₃), 50.8 (1C, CH), 126.9 (2C, C³), 130.6 (2C, C²), 132.3 (1C, C¹), 143.1 (1C, C⁴), 170.2 (1C, C = O); MS (ES⁻) m/z 164.4 (100 %, [M - H]⁻); HRMS (ES⁻) m/z found 164.0715 [M - H]⁻ C₉H₁₀O₂N requires 164.0717.

Procedure B:

An analogous procedure to that described in *procedure A* was followed using *N*-[(*S*)-1-(4-cyano-phenyl)-ethyl]-2,2,2-trifluoro-acetamide **28** (2.67 g, 11.0 mmol) in 6 M HCl_(aq) (50 ml) for 72 h. The procedure yielded the hydrochloride salt of (*S*)-4-(1-aminoethyl)benzoic acid **26**, as a colourless crystalline solid, in quantitative yield. *Characterisation was identical to that reported in procedure A.*

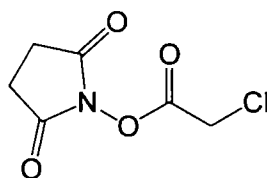
(*S*)-Methyl-4-(1-aminoethyl)benzoate ⁶ (29)

Concentrated HCl_(aq) (12 M, 2.00 ml) was added to a stirring solution of (*S*)-4-(1-aminoethyl)benzoic acid **26** (2.60 g, 11.9 mmol) in *anhydrous* CH₃OH (30 ml) and the solution heated at reflux, under argon, for 48 h. The solution was allowed to cool to rt followed by the removal of the solvent under reduced pressure to yield the hydrochloride salt of the *title compound* **29**, as a bright yellow crystalline solid, in quantitative yield. ¹H NMR (CH₃OD, 500 MHz) δ 1.66 (3H, d, *J* = 7.0 Hz, CH₃), 3.93 (3H, s, CO₂CH₃), 4.58 (1H, q, *J* = 7.0 Hz, CH), 7.61 (2H, d, *J* = 8.5 Hz, H³), 8.10 (2H, d, *J* = 8.5 Hz, H²); ¹³C NMR (CH₃OD, 125 MHz, ¹H decoupled 500 MHz) δ 19.5 (1C, CH₃), 50.8 (1C, CH), 51.7 (1C, CO₂CH₃), 126.9 (2C, C³), 130.2 (2C, C²), 133.0 (1C, C¹), 143.5 (1C, C⁴), 166.7 (1C, C = O); MS (ES⁺) *m/z* 180.0 (100 %, [M + H]⁺); HRMS (ES⁺) *m/z* found 180.1019 [M + H]⁺ C₁₀H₁₄NO₂ requires 180.1019.

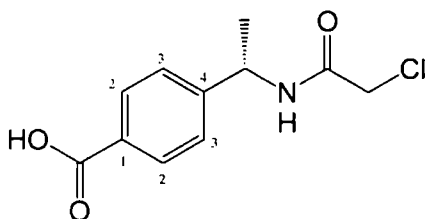
4-[(*S*)-1-(2-Chloro-acetylamino)-ethyl]-benzoic acid methyl ester ⁶ (30)

Chloroacetyl chloride (0.540 g, 0.380 ml, 4.78 mmol) was added dropwise to a stirring solution of (*S*)-methyl-4-(1-aminoethyl)benzoate **29** (0.791 g, 3.68 mmol) and *anhydrous* NEt₃ (1.43 ml, 10.1 mmol) in *anhydrous* diethyl ether (100 ml) at – 10 °C. The solution was allowed to warm to rt then stir for a further 4 h. The reaction mixture was washed with H₂O (150 ml) and then 0.1 M HCl (aq) (150 ml). The organic phase was separated, dried over K₂CO₃, filtered and the filtrate concentrated under reduced pressure to afford a crude solid. Recrystallisation from warm diethyl ether yielded the *title compound* **30** as colourless solid (0.704 g, 2.76 mmol, 75 %); ¹H NMR (CDCl₃, 500 MHz) δ 1.55 (3H, d, *J* = 7.5 Hz, CH₃), 3.92 (3H, s, CO₂CH₃), 4.08 (2H, dd, *J* = 15; 6.5 Hz, CH₂), 5.18 (1H, q, *J* = 7.0 Hz, CH), 6.85 (1H, d, *J* = 6.0 Hz, NH), 7.39 (2H, d, *J* = 8.5 Hz, H³), 8.03 (2H, d, *J* = 8.0 Hz, H²); ¹³C NMR (CDCl₃, 125 MHz, ¹H decoupled 500 MHz) δ 22.0 (1C, CH₃), 42.8 (1C, CH₂), 49.3 (1C, CH), 52.4 (1C, CO₂CH₃), 126.3 (2C, C³), 129.7 (1C, C⁴), 130.4 (2C, C²), 147.7 (1C, C¹), 165.4 (1C, C(O)CH₂), 167.0 (1C, C(O)CH₃); MS (ES⁺) *m/z* 256.0 (100 %, [M + H]⁺); HRMS (ES⁺) *m/z* found 256.0735 [M + H]⁺ C₁₂H₁₅O₃N₁³⁵Cl₁ requires 256.0735.

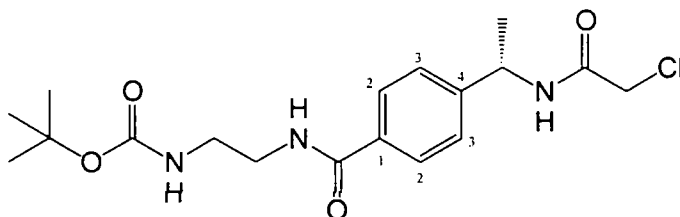
1-(2-Chloroacetyl)pyrrolidine-2,5-dione ⁹



A mixture of *N*-hydroxysuccinimide (4.86 g, 42.3 mmol), chloroacetic acid (4.00 g, 42.6 mmol) and *N*-(3-dimethylaminopropyl)-*N*-ethylcarbodiimide (8.10 g, 52.3 mmol) in *anhydrous* CH₂Cl₂ (200 ml) was stirred at rt, for 16 h. The solvent was removed under reduced pressure to afford a residual orange oil. The crude material was purified by column chromatography on silica (using 100 % EtOAc elution) to yield the *title compound* as a colourless crystalline solid (3.30 g, 17.3 mmol, 41 %); *R*_F = 0.51 (Silica, EtOAc, 100 v); m.p. 102-104 °C; ¹H NMR (CDCl₃, 500 MHz) δ 2.89 (4H, s, CH₂), 4.38 (2H, d, *J* = 4.0 Hz, CH₂); ¹³C NMR (CDCl₃, 125 MHz, ¹H decoupled 500 MHz) δ 25.8 (2C, CH₂), 38.1 (1C, CH₂), 163.4 (1C, C(O)CH₂Cl), 168.7 (2C, C=O).

4-[(S)-1-(2-Chloro-acetyl-amino)-ethyl]benzoic acid (42)

A solution of (*S*)-4-(1-aminoethyl)benzoic acid **26** (0.152 g, 0.901 mmol), 1-(2-chloroacetyl)pyrrolidine-2,5-dione (0.302 g, 1.57 mmol) and *anhydrous* NEt₃ (2 ml) in *anhydrous* THF (15 ml) was stirred at rt, for 16 h. The solvent was removed under reduced pressure and the residue partitioned between diethyl ether (15 ml) and H₂O (10 ml). The organic phase was separated, washed with 0.2 M HCl_(aq) (10 ml) and then concentrated under reduced pressure to yield the *title compound* **42** as a colourless solid (0.130 g, 0.541 mmol, 60 %); ¹H NMR (CD₃OD, 200 MHz) δ 1.48 (3H, d, *J* = 7.0 Hz, CH₃), 4.06 (2H, s, CH₂), 5.04 (1H, q, *J* = 7.0 Hz, CH), 7.43 (2H, d, *J* = 8.0 Hz, H³), 7.96 (2H, d, *J* = 8.0 Hz, H²), 8.79 (1H, d, *J* = 8.0 Hz, NH).

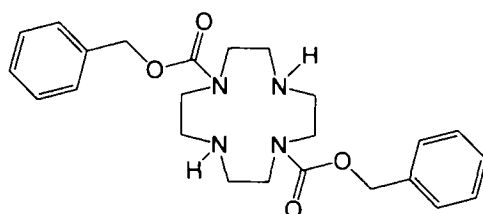
(2-(4-[(S)-1-(2-Chloro-acetyl-amino)-ethyl]-benzoylamino)-ethyl)-carbamic acid *tert*-butyl ester (43)

A mixture of 4-[(*S*)-1-(2-chloro-acetyl-amino)-ethyl]benzoic acid **42** (0.080 g, 0.331 mmol), *N*-(3-dimethylaminopropyl)-*N'*-ethylcarbodiimide (0.060 g, 0.382 mmol) and *N*-hydroxysuccinimide (0.044 g, 0.382 mmol) in *anhydrous* THF (10 ml) was stirred, under argon, at 0 °C. The mixture was stirred at 0 °C for 30 min, after which *N*-Boc-ethylenediamine (0.060 ml, 0.382 mmol) was added to the solution. The reaction mixture was then stirred, at rt, for 4 h. The solvent was removed under reduced pressure and the residue partitioned between diethyl ether (15 ml) and H₂O (15 ml). The organic layer was separated and the solvent removed under reduced pressure to yield the *title compound* **43** as a colourless solid (0.067 g, 0.168 mmol, 53 %); ¹H NMR (CDCl₃, 400 MHz) δ 1.42

(9H, s, 'Boc CH₃), 1.54 (3H, d, $J = 7.0$ Hz, CH₃), 3.40 (2H, m, NHCH₂), 3.52 (2H, m, NHCH₂), 4.05 (2H, s, CH₂Cl), 5.08 (1H, br s, NH), 5.15 (1H, q, CH), 6.84 (1H, d, $J = 7.0$ Hz, NH), 7.33 (2H, d, $J = 8.0$ Hz, H³), 7.78 (2H, d, $J = 8.0$ Hz, H²); MS (ES⁺) m/z 406.2 (100 %, [M + Na]⁺).

7.4.2 Cyclen Intermediates

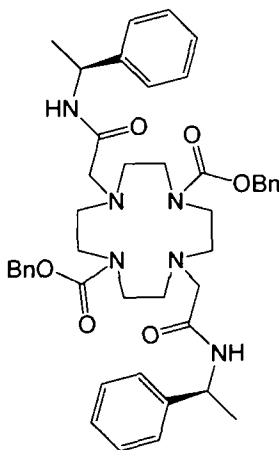
1,4,7,10-Tetraaza-cyclododecane-1,7-dicarboxylic acid dibenzyl ester ¹⁰ (31)



Disodium hydrogen phosphate (14.0 g, 98.6 mmol) was added to a solution of cyclen (5.00 g, 29.0 mmol) in H₂O – 1,4-dioxane (50 : 20 v/v, 70 ml) and the pH adjusted to pH 2.5 by the addition of conc. HCl_(aq) (12 M). Benzyl chloroformate (10.0 ml, 70.1 mmol) in dioxane (20 ml) was added dropwise to the stirred solution at rt, over 2 h, followed by stirring for a further 18 h to afford a colourless solution containing a white precipitate. The solvent was removed under reduced pressure and the residue dissolved in H₂O (100 ml). The pH of the aqueous phase was then raised to pH 7 by the addition of 1 M KOH_(aq). The aqueous phase was then extracted with diethyl ether (2 x 100 ml), followed by CH₂Cl₂ (2 x 100 ml). The CH₂Cl₂ extracts were combined, dried over MgSO₄, filtered and the filtrate concentrated under reduced pressure to afford a colourless oil. The material was repeatedly washed with diethyl ether and concentrated under reduced pressure (3 x 50 ml) to yield the *title compound* **31** as a colourless crystalline solid (9.47 g, 21.5 mmol, 74 %); m.p. 113-116 °C; ¹H NMR (CDCl₃, 500 MHz) δ 2.05 (2H, br s, NH), 2.86–3.12 (8H, br m, cyclen CH₂), 3.47–3.79 (8H, br m, cyclen CH₂), 5.18 (4H, s, Cbz CH₂), 7.33–7.40 (10H, m, Ph); ¹³C NMR (CDCl₃, 125 MHz, ¹H decoupled 500 MHz) δ 49.2 (1C, cyclen CH₂), 49.4 (1C, cyclen CH₂), 49.9 (1C, cyclen CH₂), 50.1 (1C, cyclen CH₂), 50.5 (1C, cyclen CH₂), 50.7 (1C, cyclen CH₂), 50.9 (1C, cyclen CH₂), 68.1 (2C, Cbz CH₂), 68.2 (1C, cyclen CH₂), 128.3 (2C, Ph), 128.4 (2C, Ph), 128.7 (2C, Ph),

128.8 (2C, Ph), 129.0 (2C, Ph), 129.1 (2C, Ph), 136.1 (2C, Ph_(q)), 136.2, 156.4 (1C, C = O), 156.5 (1C, C = O); MS (ES⁺) *m/z* 441.4 (100 %, [M + H]⁺).

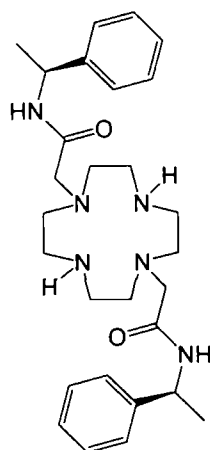
4,10-bis-(((S)-1-Phenyl-ethylcarbamoyl)-methyl)-1,4,7,10-tetraaza-cyclododecane-1,7-dicarboxylic acid dibenzyl ester (32)



A stirred mixture of 1,4,7,10-tetraaza-cyclododecane-1,7-dicarboxylic acid dibenzyl ester **31** (1.34 g, 3.05 mmol), (*S*)-*N*-2-chloroethanoyl-2-phenylethylamine (1.31 g, 6.65 mmol), Cs₂CO₃ (1.97 g, 6.06 mmol) and KI (0.010 g) in *anhydrous* CH₃CN (50 ml) was heated at reflux, under argon, for 24 h. The resulting orange solution was allowed to cool to room temperature, followed by the removal of the solvent under reduced pressure. The residual oil was dissolved in CH₂Cl₂ (20 ml) and washed with H₂O (2 x 20 ml). The organic layer was concentrated under reduced pressure to afford a residual oil which was then sonicated in diethyl ether (2 x 50 ml). The solid precipitate was collected by centrifugation, dissolved in CH₂Cl₂ and then dried under reduced pressure to yield the *title compound* **32** as a colourless crystalline solid (1.72 g, 2.26 mmol, 74 %); m.p. 64-66 °C; ¹H NMR (CDCl₃, 500 MHz) δ 1.45 (6H, br s, CH₃), 2.75 (8H, br s, cyclen CH₂), 3.16 (4H, br s, CH₂CO), 3.43 (8H, br s, cyclen CH₂), 4.96 (4H, br s, Cbz CH₂), 5.11 (2H, m, CH), 7.22-7.39 (20H, m, Ph), 7.59 (2H, br s, NH); ¹³C NMR (CDCl₃, 125 MHz, ¹H decoupled 500 MHz) δ 22.0 (2C, CH₃), 48.1 (1C, CH), 48.7 (1C, CH), 55.0 - 56.4 (4C, br s, cyclen CH₂), 59.3 (2C, CH₂CO), 67.6 (2C, Cbz CH₂), 126.3 (2C, Ph), 126.6 (2C, Ph), 127.4 (2C, Ph), 128.5 (2C, Ph), 128.6 (2C, Ph), 136.5 (2C, Cbz Ph_(q)), 143.8 (2C, amide

arm Ph_(q)), 157.1 (2C, C(O)OBn), 170.2 (2C, NHCO); MS (ES⁺) m/z 763.0 (100 %, [M + H]⁺); HRMS (ES⁺) m/z found 763.4187 [M + H]⁺ C₄₄H₅₅N₆O₆ requires 763.4178.

***N*-((*S*)-1-Phenyl-ethyl)-2-(7-(((*S*)-1-phenyl-ethylcarbamoyl)-methyl)-1,4,7,10-tetraaza-cyclododec-1-yl)-acetamide (**33**)**



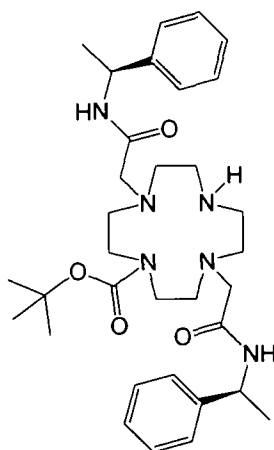
Procedure A:

4,10-bis-(((*S*)-1-Phenyl-ethylcarbamoyl)-methyl)-1,4,7,10-tetraaza-cyclododecane-1,7-dicarboxylic acid dibenzyl ester **32** (3.14 g, 4.12 mmol) in CH₃OH – H₂O (40 : 20 v/v, 60 ml) was shaken in a Parr hydrogenation flask at 40 psi H₂ over Pd(OH)₂/C (0.35 g) for 48 h. The resulting mixture was filtered through celite to afford a colourless solution which was concentrated under reduced pressure to yield the *title compound* **33** as a colourless crystalline solid (1.77 g, 3.58 mmol, 87 %); m.p. 140-143 °C; ¹H NMR (CD₃OD, 500 MHz) δ 1.46 (6H, d, J = 7.0 Hz, CH₃), 2.88-3.18 (16H, br m, cyclen CH₂), 3.41 (2H, d, J = 16.5 Hz, CHCO), 3.54 (2H, d, J = 17.0 Hz, CHCO), 5.04 (2H, m, CH), 7.21-7.28 (10H, m, Ph); ¹³C NMR (CDCl₃, 125 MHz, ¹H decoupled 500 MHz) δ 23.5 (2C, CH₃), 45.2 (4C, cyclen CH₂), 50.7 (2C, cyclen CH₂), 51.1 (2C, cyclen CH₂), 52.4 (2C, CH), 57.2 (2C, CH₂CO), 128.0 (4C, Ph_(o/m)), 129.0 (4C, Ph_(o/m)), 130.5 (2C, Ph_(p)), 145.8 (2C, Ph_(q)), 172.7 (2C, C = O); MS (ES⁺) m/z 495.3 (100 %, [M + H]⁺); HRMS (ES⁺) m/z found 495.3447 [M + H]⁺ C₂₈H₄₃N₆O₂ requires 495.3442.

Procedure B:

A solution of 4,10-bis-[[*(S)*-1-phenyl-ethylcarbamoyl]-methyl]-1,4,7,10-tetraaza-cyclododecane-1,7-dicarboxylic acid di-*tert*-butyl ester **38** (0.150 g, 0.216 mmol) in CH_2Cl_2 – TFA (2 : 1 v/v, 3 ml) was stirred at rt, in a sealed flask, for 12 h, to afford a yellow solution. The solvent was removed under reduced pressure to yield a glassy solid. The crude material was repeatedly (x 3) dissolved in CH_2Cl_2 (5 ml) and the solvent removed under reduced pressure to facilitate elimination of excess acid and *tert*-butyl alcohol. The residue was finally taken into 1 M $\text{KOH}_{(\text{aq})}$ (10 ml) and extracted with CH_2Cl_2 (3 x 15 ml). The organic extracts were combined, dried over K_2CO_3 , filtered and the filtrate concentrated under reduced pressure to yield the *title compound* **33** as a colourless crystalline solid (0.105 g, 0.211 mmol, 98 %); *Characterisation was indentical to that reported in procedure A.*

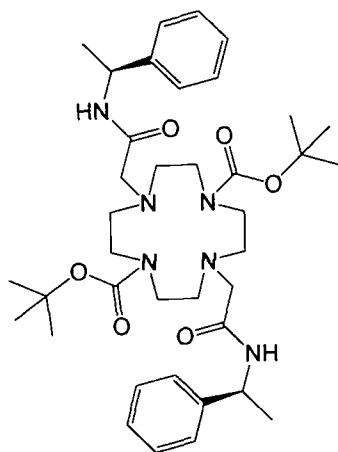
4,10-bis-[[*(S)*-1-Phenyl-ethylcarbamoyl]-methyl]-1,4,7,10-tetraaza-cyclododecane-1-carboxylic acid *tert*-butyl ester¹¹ (37**)**



A solution of di-*tert*-butyl dicarbonate (0.205 g, 0.940 mmol) in *anhydrous* CH_3OH (25 ml) was added dropwise over 3 h, at rt, to a stirring solution of N-[[*(S)*-1-phenyl-ethyl]-2-(7-[[*(S)*-1-phenyl-ethylcarbamoyl]-methyl]-1,4,7,10-tetraaza-cyclododecane-1-yl)-acetamide **33** (0.664 g, 1.34 mmol) in *anhydrous* CH_3OH (200 ml). The reaction mixture was left to stir for 16 h, then concentrated under reduced pressure to afford a residual yellow viscous oil. The crude material was purified by column chromatography on neutral alumina (gradient elution; CH_2Cl_2 to 2 % CH_3OH : CH_2Cl_2 , utilising 0.1 %

CH₃OH increments) to yield the *title compound 37* as a glassy colourless solid (0.354 g, 0.596 mmol, 63 %); $R_F = 0.46$ (Alumina, CH₂Cl₂ – CH₃OH, 49 : 1 v/v); m.p. 98-101 °C; ¹H NMR (CDCl₃, 500 MHz) δ 1.39 (9H, s, ^tBoc CH₃), 1.51 (6H, d, $J = 7.0$ Hz, CH₃), 2.61 (8H, br s, cyclen CH₂), 2.86 (4H, br s, cyclen CH₂), 2.94 (4H, br s, cyclen CH₂), 3.09 (4H, br s, CH₂CO), 4.95 (2H, q, CH), 7.17-7.23 (10H, m, Ph), 8.34 (1H, d, $J = 5.5$ Hz, NH); ¹³C NMR (CDCl₃, 125 MHz, ¹H decoupled 500 MHz) δ 22.0 (2C, CH₃), 28.8 (3C, ^tBoc CH₃), 48.7 (2C, CH), 49.0-53.8 (8C, br m, cyclen CH₂), 59.6 (2C, CH₂CO), 80.3 (1C, C^tBu), 126.8 (4C, Ph_(o/m)), 127.5 (4C, Ph_(o/m)), 128.8 (2C, Ph_(p)), 143.8 (2C, Ph_(q)), 156.7 (1C, ^tBoc C=O), 170.5 (2C, amide C=O); MS (ES⁺) m/z 595.4 (100 %, [M + H]⁺); HRMS (ES⁺) m/z found 595.3972 [M + H]⁺ C₃₃H₅₁O₄N₆ requires 595.3966.

4,10-bis-(((S)-1-Phenyl-ethylcarbamoyl)-methyl)-1,4,7,10-tetraaza-cyclododecane-1,7-dicarboxylic acid di-*tert*-butyl ester (38)

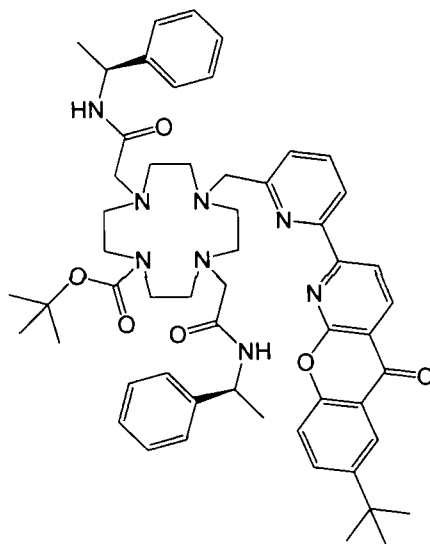


4,10-bis-(((S)-1-Phenyl-ethylcarbamoyl)-methyl)-1,4,7,10-tetraaza-cyclododecane-1,7-dicarboxylic acid di-*tert*-butyl ester **38** was isolated using an identical procedure to that described for 4,10-bis-(((S)-1-phenyl-ethylcarbamoyl)-methyl)-1,4,7,10-tetraaza-cyclododecane-1-carboxylic acid *tert* butyl ester **37**. The procedure yielded the *title compound 38* as a colourless solid (0.131 g, 0.188 mmol, 20 %); $R_F = 0.58$ (Alumina, CH₂Cl₂ – CH₃OH, 49 : 1 v/v); m.p. 65-68 °C; ¹H NMR (CDCl₃, 500 MHz) δ 1.39 (18H, s, ^tBoc CH₃), 1.51 (6H, d, $J = 7.0$ Hz, CH₃), 2.61 (8H, br s, cyclen CH₂), 2.86 (4H, br s, cyclen CH₂), 2.94 (6H, br s, cyclen CH₂; CH₂CO), 3.09 (4H, br s, CH₂CO), 4.95 (2H, q,

CH), 7.17-7.23 (10H, m, Ph); MS (ES⁺) m/z 695.0 (100 %, [M + H]⁺); HRMS (ES⁺) m/z found 695.4488 [M + H]⁺ C₃₈H₅₉O₆N₆ requires 695.4490.

7.4.3 Pyridyl-azaxanthone Amide Conjugate Complex

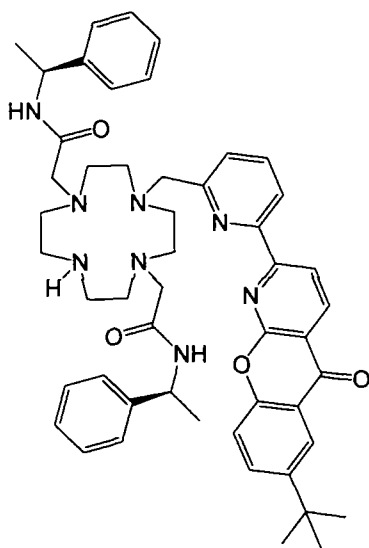
7-[6-(6-*tert*-Butyl-10-oxo-10*H*-9-oxa-1-aza-anthracen-2-yl)-pyridin-2-ylmethyl]-4,10-bis-[[*(S)*-1-phenyl-ethylcarbamoyl]-methyl]-1,4,7,10-tetraaza-cyclododecane-1-carboxylic acid *tert*-butyl ester (**39**)



A stirring mixture of 4,10-bis-[[*(S)*-1-phenyl-ethylcarbamoyl]-methyl]-1,4,7,10-tetraaza-cyclododecane-1-carboxylic acid *tert*-butyl ester **33** (0.325 g, 0.547 mmol), 2-(6-bromomethyl-pyridin-2-yl)-6-*tert*-butyl-9-oxa-1-aza-anthracen-10-one **9** (0.254 g, 0.601 mmol) and K₂CO₃ (0.113 g, 0.821 mmol) in *anhydrous* CH₃CN (10 ml) was heated at reflux, under argon, for 16 h. The mixture was allowed to cool to rt, syringe filtered and the filtrate concentrated under reduced pressure to afford a residual yellow oil. The crude material was purified by column chromatography on neutral alumina (gradient elution; CH₂Cl₂ to 0.5 % CH₃OH : CH₂Cl₂, utilising 0.1 % CH₃OH increments) to yield the *title compound* **39** as an orange crystalline solid (0.379 g, 0.404 mmol, 74 %); R_f = 0.74 (Alumina, CH₂Cl₂ – CH₃OH, 49 : 1 v/v); m.p. 87-89 °C; ¹H NMR (CDCl₃, 500 MHz) δ 1.38 (18H, br s, ^tBu CH₃; ^{Boc} CH₃), 1.46 (6H, d, J = 4.0 Hz, CH₃), 2.61 (8H, br s, cyclen CH₂), 2.82 (4H, br s, cyclen CH₂), 3.07 (4H, br s, cyclen CH₂), 3.33 (2H, br s, CH₂CO), 3.40 (2H, br s, CH₂CO), 3.61 (2H, br s, CH₂ pyridine), 5.12 (2H, br s, CH), 7.19 (1H, d, J

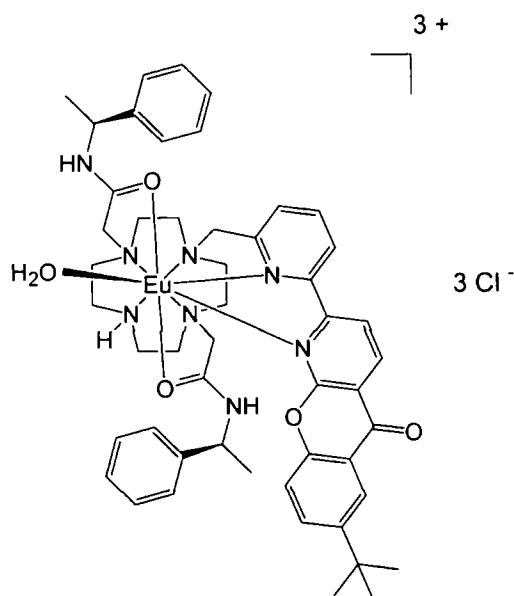
= 8.0 Hz, H^{5'}), 7.26 (10H, br s, Ph), 7.46 (1H, br s, NH), 7.58 (1H, d, *J* = 8.5 Hz, H¹⁰), 7.64 (1H, t, *J* = 8.0 Hz, H^{4'}), 7.74 (1H, br s, NH), 7.82 (1H, dd, *J* = 9.0; 2.5 Hz, H⁹), 8.29 (1H, d, *J* = 2.5 Hz, H⁷), 8.41 (1H, d, *J* = 8.0 Hz, H^{3'}), 8.46 (1H, d, *J* = 8.0 Hz, H²), 8.78 (1H, d, *J* = 8.0 Hz, H³); ¹³C NMR (CDCl₃, 125 MHz, ¹H decoupled 500 MHz) δ 21.3 (1C, CH₃), 22.0 (1C, CH₃), 28.7 (3C, 'Boc CH₃), 31.5 (3C, C¹⁴), 35.1 (1C, C¹³), 48.0 (1C, CH), 48.4 (1C, CH), 52.5 (2C, cyclen CH₂), 53.2 (2C, cyclen CH₂), 53.8 (2C, cyclen CH₂), 54.6 (2C, cyclen CH₂), 59.4 (1C, CH₂ pyridine), 59.8 (1C, CH₂CO), 60.6 (1C, CH₂CO), 80.2 (1C, 'Boc_(q)), 116.6 (1C, C⁴), 118.3 (1C, C¹⁰), 121.1 (1C, C^{3'}), 121.3 (1C, C⁶), 122.7 (1C, C⁷), 124.8 (1C, C^{5'}), 126.5 (1C, P_(o/m)), 126.8 (1C, P_(o/m)), 127.3 (2C, P_(o/m)), 127.8 (2C, P_(o/m)), 128.7 (1C, P_(o/m)), 128.9 (1C, P_(o/m)), 133.8 (1C, C⁹), 137.6 (1C, C^{4'}), 138.5 (1C, C³), 143.0 (1C, Ph_(q)), 143.8 (1C, Ph_(q)), 148.2 (1C, C⁸), 153.8 (1C, C^{1'}), 154.2 (1C, C¹¹), 156.1 (1C, 'Boc C = O), 158.0 (1C, C⁶), 160.1 (1C, C¹), 160.3 (1C, C¹²), 170.1 (2C, amide C = O), 177.8 (1C, C⁵); MS (ES⁺) *m/z* 937.5 (100 %, [M + H]⁺); HRMS (ES⁺) *m/z* found 937.5331 [M + H]⁺ C₅₅H₆₉O₆N₈ requires 937.5334.

2-[4-[6-(6-*tert*-Butyl-10-oxo-10*H*-9-oxa-1-aza-anthracen-2-yl)-pyridin-2-ylmethyl]-7-[[*(S)*-1-phenyl-ethylcarbamoyl]-methyl]-1,4,7,10-tetraaza-cyclododec-1-yl]-*N*-[[*(S)*-1-phenyl-ethyl]-acetamide (40)



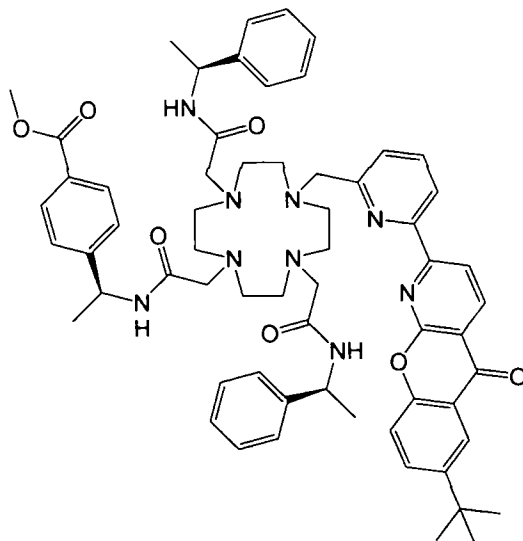
A solution of 7-[6-(6-*tert*-butyl-10-oxo-10*H*-9-oxa-1-aza-anthracen-2-yl)-pyridin-2-ylmethyl]-4,10-bis-[[*(S)*-1-phenyl-ethylcarbamoyl]-methyl]-1,4,7,10-tetraaza-cyclododecane-1-carboxylic acid *tert*-butyl ester **39** (0.320 g, 0.341 mmol) in CH₂Cl₂ – TFA

(2 : 1 v/v, 6 ml) was stirred at rt, in a sealed flask, for 12 h, to afford a yellow solution. The solvent was removed under reduced pressure to yield a glassy solid. The crude material was repeatedly (x 3) dissolved in CH₂Cl₂ (5 ml) and the solvent removed under reduced pressure to facilitate elimination of excess acid and *tert*-butyl alcohol. The residue was finally taken into 0.2 M KOH (aq) (10 ml) and extracted with CH₂Cl₂ (3 x 15 ml). The organic layers were combined, dried over K₂CO₃, filtered and the filtrate concentrated under reduced pressure to yield the *title compound* **40** as an orange coloured crystalline solid (0.254 g, 0.304 mmol, 89 %); m.p. 92-95 °C; ¹H NMR (CDCl₃, 500 MHz) δ 1.38 (9H, s, ^tBu CH₃), 1.47 (6H, d, *J* = 7.0 Hz, CH₃), 2.58 (8H, br s, cyclen CH₂), 2.64 (8H, br s, cyclen CH₂), 3.09 (4H, q, *J* = 17.0 Hz, CH₂CO), 3.60 (1H, d, *J* = 15.0 Hz, CH₂ pyridine), 3.68 (1H, d, *J* = 15.0 Hz, CH₂ pyridine), 5.14 (2H, q, *J* = 7.5 Hz, CH), 7.16 (3H, q, *J* = 8.0 Hz, H⁵: Ph_(p)), 7.24 (4H, t, *J* = 7.5 Hz, Ph_(m)), 7.30 (4H, d, *J* = 7.5 Hz, Ph_(o)), 7.56 (1H, d, *J* = 9.0 Hz, H¹⁰), 7.62 (1H, t, *J* = 7.5 Hz, H⁴), 7.82 (1H, dd, *J* = 8.5; 2.0 Hz, H⁹), 8.06 (2H, d, *J* = 8.5 Hz, NH), 8.28 (1H, d, *J* = 2.5 Hz, H⁷), 8.37 (1H, d, *J* = 7.5 Hz, H³), 8.44 (1H, d, *J* = 8.5 Hz, H²), 8.77 (1H, d, *J* = 8.5 Hz, H³); ¹³C (CDCl₃, 125 MHz, ¹H decoupled 500 MHz) δ 21.7 (2C, CH₃), 31.5 (3C, C¹⁴), 35.0 (1C, C¹³), 47.4 (2C, cyclen CH₂), 48.6 (2C, CH), 52.5 (2C, cyclen CH₂), 53.4 (2C, cyclen CH₂), 53.7 (1C, cyclen CH₂), 54.8 (1C, cyclen CH₂), 58.7 (1C, CH₂ pyridine), 60.2 (2C, CH₂CO), 116.6 (1C, C⁴), 118.3 (2C, C²; C¹⁰), 121.0 (1C, C³), 121.3 (1C, C⁶), 122.7 (1C, C⁷), 125.0 (1C, C⁵), 126.7 (4C, Ph_(o)), 127.5 (2C, Ph_(p)), 128.8 (4C, Ph_(m)), 133.8 (1C, C⁹), 137.6 (1C, C⁴), 138.5 (1C, C³), 143.5 (2C, Ph_(q)), 148.2 (1C, C⁸), 153.6 (1C, C¹), 154.2 (1C, C¹¹), 158.0 (1C, C⁶), 160.2 (1C, C¹), 160.3 (1C, C¹²), 170.8 (2C, amide C=O), 177.8 (1C, C⁵); MS (ES⁺) *m/z* 837.5 (100 %, [M + H]⁺); HRMS (ES⁺) *m/z* found 837.4817 [M + H]⁺ C₅₀H₆₁O₄N₈ requires 837.4810.

[EuL⁸]

A stirring solution of 2-{4-[6-(6-*tert*-butyl-10-oxo-10*H*-9-oxa-1-aza-anthracen-2-yl)-pyridin-2-ylmethyl]-7-[(*S*)-1-phenyl-ethylcarbamoyl)-methyl]-1,4,7,10-tetraaza-cyclododec-1-yl}-*N*-[(*S*)-1-phenyl-ethyl]-acetamide **40** (0.020 g, 0.024 mmol) and Eu(OTf)₃·6H₂O (0.017 g, 0.024 mmol) in *anhydrous* CH₃CN (1 ml) was heated at reflux, under argon, for 14 h. The solution was allowed to cool to rt followed by the removal of solvent under reduced pressure to afford a glassy orange solid. CH₂Cl₂ (10 ml) was added to the solid, and the mixture sonicated for 10 min. The solvent was then decanted and the solid material dissolved in a minimum volume of CH₃CN (0.5 ml). The solution was added dropwise onto diethyl ether (25 ml) to induce precipitation. The solid material was isolated by centrifugation, and the process of induced precipitation repeated twice more to yield the complex as its triflate salt. The pale yellow coloured solid was made water soluble by the exchange of triflate anions for chloride anions using 'DOWEX 1 x 8 200-400 mesh Cl⁻' resin. The solid material was dissolved in a mixture of H₂O – CH₃OH (1:1 v/v, 10 ml) and 0.5 g of prepared resin added to the solution, which was stirred at room temperature, for 3 h. The resin was removed by filtration, and the filtrate concentrated under reduced pressure to yield the *title complex* [EuL⁸] as a colourless solid (0.009 g, 0.008 mmol, 34 %); λ_{max} (H₂O) = 355 nm; τ (H₂O) = 0.36 ms; HPLC (Method A) t_R = 11.0 min.

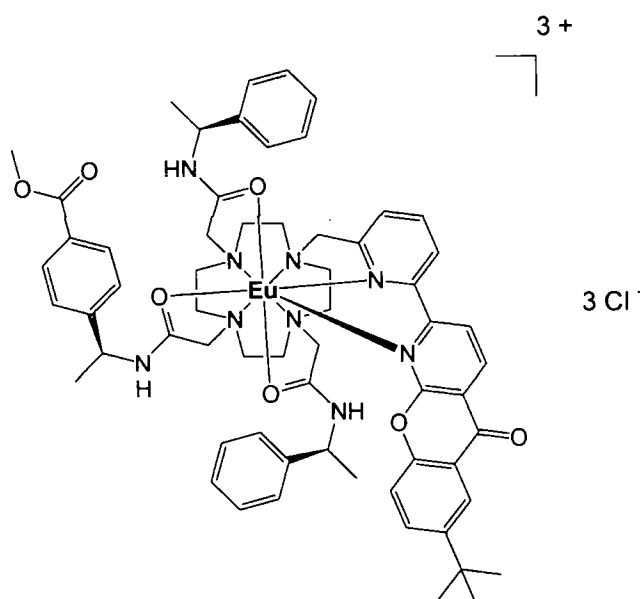
4-[(S)-1-(2-{7-[6-(6-*tert*-Butyl-10-oxo-10*H*-9-oxa-1-aza-anthracen-2-yl)-pyridin-2-ylmethyl]-4,10-bis-[(S)-1-phenyl-ethylcarbamoyl]-methyl]-1,4,7,10-tetraaza-cyclododec-1-yl}-acetylamino)-ethyl]-benzoic acid methyl ester ([L⁹])



A stirring mixture of 2-{4-[6-(6-*tert*-butyl-10-oxo-10*H*-9-oxa-1-aza-anthracen-2-yl)-pyridin-2-ylmethyl]-7-[(S)-1-phenyl-ethylcarbamoyl]-methyl]-1,4,7,10-tetraaza-cyclododec-1-yl}-*N*-((S)-1-phenyl-ethyl)-acetamide **40** (0.131 g, 0.157 mmol), 4-[(S)-1-(2-chloro-acetylamino)-ethyl]-benzoic acid methyl ester **30** (0.050 g, 0.196 mmol) and K₂CO₃ (0.043 g, 0.313 mmol) in *anhydrous* CH₃CN (7 ml) was heated at reflux, under argon, for 18 h. The resultant mixture was allowed to cool to rt, syringe filtered and the filtrate concentrated under reduced pressure to afford a residual orange oil. The crude material was purified by column chromatography on neutral alumina (gradient elution; CH₂Cl₂ to 1.0 % CH₃OH : CH₂Cl₂, utilising 0.1 % CH₃OH increments) to yield the *title compound* as an orange crystalline solid (0.105 g, 0.102 mmol, 64 %); *R*_F = 0.27 (Alumina, CH₂Cl₂ – CH₃OH, 49 : 1 v/v); m.p. 87-89 °C; ¹H NMR (CDCl₃, 500 MHz) δ 1.40 (9H, s, ^tBu CH₃), 1.44 (9H, d, *J* = 7.0 Hz, CH₃), 2.71 (16 H, br s, cyclen CH₂), 3.25 (6H, br s, CH₂CO), 3.75 (2H, s, CH₂ pyridine), 3.84 (3H, s, C(O)OCH₃), 5.05 (3H, q, CH), 7.16 (2H, d, *J* = 8.0 Hz, H⁵; Ph_(p)), 7.28 (10H, m, Ph), 7.33 (2H, d, *J* = 8.0 Hz, Ph_(o/m)), 7.60 (1H, d, *J* = 8.5 Hz, H¹⁰), 7.73 (1H, t, *J* = 8.0 Hz, H⁴), 7.85 (1H, dd, *J* = 8.5; 2.5 Hz, H⁹), 7.89 (2H, d, *J* = 8.0 Hz, Ph_(o/m)), 8.30 (1H, d, *J* = 2.5 Hz, H⁷), 8.43 (2H, d, *J* = 8.0 Hz, H²; H³), 8.77 (1H, d, *J* = 8.0 Hz, H³); ¹³C (CDCl₃, 125 MHz, ¹H decoupled 500

MHz) δ 21.9 (3C, CH₃), 31.5 (3C, C¹⁴), 35.0 (1C, C¹³), 48.9 (3C, CH), 51.5 (2C, cyclen CH₂), 52.3 (1C, C(O)OCH₃), 52.5 (2C, cyclen CH₂), 53.0 (2C, cyclen CH₂), 53.7 (2C, cyclen CH₂), 58.5 (3C, CH₂CO), 60.2 (1C, CH₂ pyridine), 116.6 (1C, C⁴), 118.3 (2C, C²; C¹⁰), 121.3 (1C, C³), 121.4 (1C, C⁶), 122.7 (1C, C⁷), 125.4 (2C, Ph), 126.2 (2C, Ph), 126.5 (4C, Ph), 127.5 (1C, C⁵), 128.8 (4C, Ph), 129.2 (1C, Ph), 130.1 (2C, Ph), 133.8 (1C, C⁹), 137.8 (1C, C⁴), 138.6 (1C, C³), 143.5 (2C, Ph_(q)), 148.2 (1C, C⁸), 153.6 (1C, C¹), 154.2 (1C, C¹¹), 159.9 (1C, C⁶), 160.2 (1C, C¹), 160.3 (1C, C¹²), 166.9 (1C, C(O)OCH₃), 170.8 (3C, amide C = O), 177.8 (1C, C⁵); MS (ES⁺) m/z 1056.6 (100 %, [M + H]⁺); HRMS (ES⁺) m/z found 1056.5733 [M + H]⁺ C₆₂H₇₄O₇N₉ requires 1056.5706.

[EuL⁹]

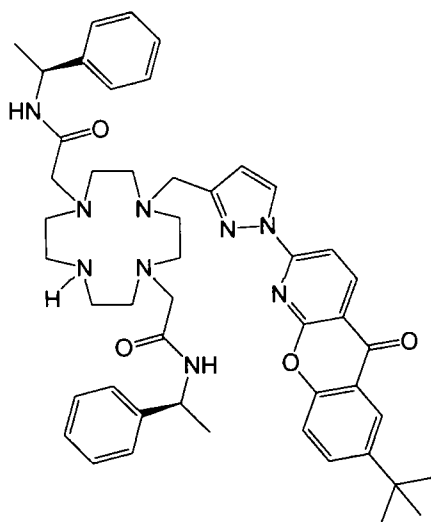


A stirred solution of 4-[(*S*)-1-(2-{7-[6-(6-*tert*-butyl)-10-oxo-10*H*-9-oxa-1-aza-anthracen-2-yl]-pyridin-2-ylmethyl}-4,10-bis-[(*S*)-1-phenyl-ethylcarbamoyl]-methyl]-1,4,7,10-tetraaza-cyclododec-1-yl)-acetyl-amino)-ethyl]-benzoic acid methyl ester [L⁹] (0.061 g, 0.057 mmol) and Eu(OTf)₃·6H₂O (0.045 g, 0.063 mmol) in *anhydrous* CH₃CN (2ml) was heated at reflux, under argon, for 17 h. The resultant solution was allowed to cool to rt followed by the removal of solvent under reduced pressure to afford a glassy orange solid. CH₂Cl₂ (10 ml) was added to the solid, and the mixture sonicated for 10 min. The solvent was then decanted and the solid material dissolved in a minimum volume of CH₃CN (1.0 ml). The solution was added dropwise onto diethyl ether (50 ml) to induce

precipitation. The solid material was isolated by centrifugation, and the process of induced precipitation repeated twice more to yield the complex as its triflate salt. The yellow solid was made water soluble by the exchange of triflate anions for chloride anions using ‘DOWEX 1 x 8 200-400 mesh Cl’ resin. The solid material was dissolved in a mixture of H₂O – CH₃OH (1:1 v/v, 20 ml) and 0.8 g of prepared resin added to the solution, which was stirred at rt, for 6 h. The resin was removed by filtration, and the filtrate concentrated under reduced pressure to yield the *title complex* [EuL⁹] as a pale yellow coloured solid (0.044 g, 0.036 mmol, 64 %); λ_{max} (H₂O) = 348 nm; τ (H₂O) = 1.02 ms; τ (D₂O) = 1.34 ms; HPLC (Method A) t_{R} = 10.9 min.

7.4.4 Pyrazoyl-azaxanthone Amide Conjugate Complex

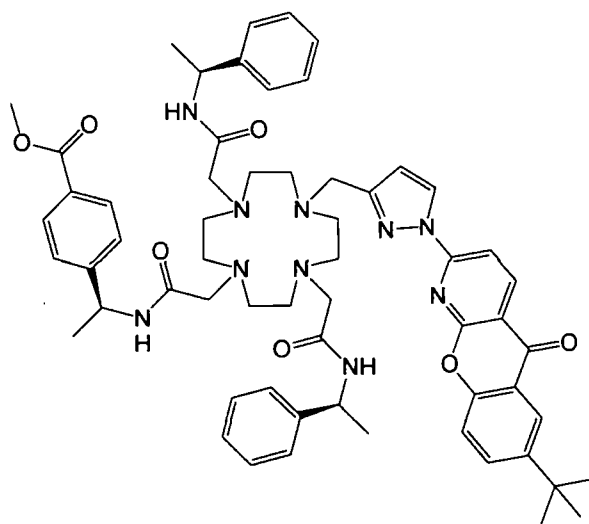
2-{4-[1-(6-*tert*-Butyl-10-oxo-10*H*-9-oxa-1-aza-anthracen-2-yl)-1*H*-pyrazol-3-yl methyl]-7-[(*S*)-1-phenyl-ethylcarbamoyl]-methyl]-1,4,7,10-tetraaza-cyclododec-1-yl}-*N*-[(*S*)-1-phenyl-ethyl]-acetamide (34)



A stirring mixture of *N*-[(*S*)-1-phenyl-ethyl]-2-(7-[(*S*)-1-phenyl-ethylcarbamoyl]-methyl)-1,4,7,10-tetraaza-cyclododec-1-yl)-acetamide **33** (0.104 g, 0.211 mmol), 2-(3-bromomethyl-pyrazol-1-yl)-6-*tert*-butyl-9-oxa-1-aza-anthracen-10-one **12** (0.087 g, 0.211 mmol) and NaHCO₃ (0.020 g, 0.231 mmol) in *anhydrous* CH₃CN (5 ml) was heated at 60 °C, under argon, for 18 h. The resultant mixture was allowed to cool to rt, syringe filtered and the filtrate concentrated under reduced pressure to afford a yellow residue. The crude material was purified by column chromatography on neutral alumina (gradient elution:

CH₂Cl₂ to 0.5 % CH₃OH : CH₂Cl₂, utilising 0.1 % CH₃OH increments) to yield the *title compound 34* as a pale yellow coloured solid (0.124 g, 0.150 mmol, 71 %); m.p. 152-154 °C; ¹H NMR (CDCl₃, 500 MHz) δ 1.40 (9H, s, ^tBu CH₃), 1.47 (6H, d, *J* = 7.0 Hz, CH₃), 2.58 (4H, br s, cyclen CH₂), 2.79 (4H, br s, cyclen CH₂), 2.91 (8H, br s, cyclen CH₂), 3.36 (4H, s, CH₂C(O)), 3.71 (2H, s, CH₂ pyrazole), 5.07 (2H, q, *J* = 14.0; 7.5 Hz, CH), 6.31 (1H, d, *J* = 2.5 Hz, H²), 7.13 (2H, t, *J* = 7.5 Hz, Ph), 7.21 (4H, t, *J* = 7.5 Hz, Ph), 7.35 (4H, d, *J* = 7.5 Hz, Ph), 7.54 (1H, d, *J* = 9.0 Hz, H¹⁰), 7.84 (1H, dd, *J* = 8.5; 2.5 Hz, H⁹), 7.91 (2H, br s, NH), 7.98 (1H, d, *J* = 8.5 Hz, H²), 8.29 (1H, d, *J* = 2.5 Hz, H⁷), 8.55 (1H, d, *J* = 2.5 Hz, H¹), 8.76 (1H, d, *J* = 8.5 Hz, H³); MS (ES⁺) *m/z* 826.0 (100 %, [M + H]⁺); HRMS (ES⁺) *m/z* found 826.4769 [M + H]⁺ C₄₈H₆₀N₉O₄ requires 826.4763.

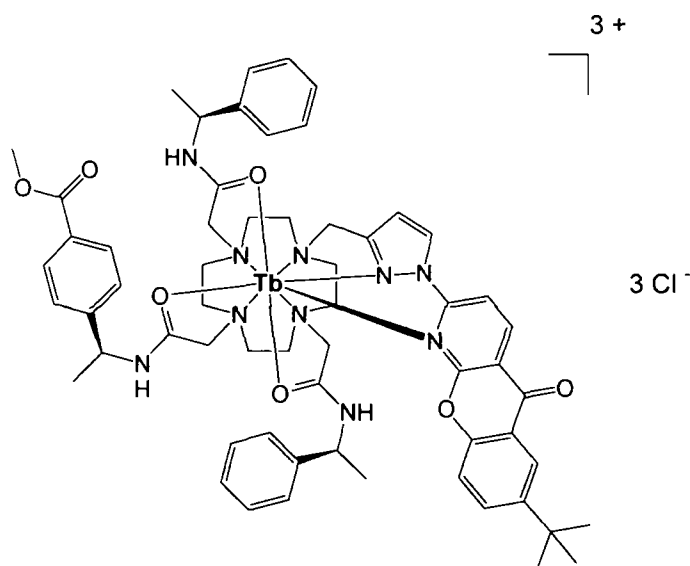
4-[(*S*)-1-(2-{7-[1-(6-*tert*-Butyl-10-oxo-10*H*-9-oxa-1-aza-anthracen-2-yl)-1*H*-pyrazol-3-ylmethyl]-4,10-bis-[(*S*)-1-phenyl-ethylcarbamoyl]-methyl]-1,4,7,10-tetraaza-cyclododec-1-yl}-acetylamino)-ethyl]-benzoic acid methyl ester ([L¹⁰])



A stirring mixture of 2-{4-[1-(6-*tert*-butyl-10-oxo-10*H*-9-oxa-1-aza-anthracen-2-yl)-1*H*-pyrazol-3-ylmethyl]-7-[(*S*)-1-phenyl-ethylcarbamoyl]-methyl]-1,4,7,10-tetraaza-cyclododec-1-yl}-*N*-[(*S*)-1-phenyl-ethyl]-acetamide **34** (0.060 g, 0.073 mmol), 4-[(*S*)-1-(2-chloro-acetylamino)-ethyl]-benzoic acid methyl ester **30** (0.021 g, 0.084 mmol) and Cs₂CO₃ (0.031 g, 0.095 mmol) in *anhydrous* CH₃CN (5 ml) was heated at reflux, under argon, for 16 h. The resultant mixture was allowed to cool to rt, syringe filtered and the

filtrate concentrated under reduced pressure to afford a yellow residue. The crude material was purified by column chromatography on neutral alumina (gradient elution: CH_2Cl_2 to 0.5 % $\text{CH}_3\text{OH} : \text{CH}_2\text{Cl}_2$, utilising 0.1 % CH_3OH increments) to yield the *title compound* [**L¹⁰**] as a pale yellow coloured solid (0.060 g, 0.058 mmol, 79 %); $R_f = 0.68$ (Alumina, $\text{CH}_2\text{Cl}_2 - \text{CH}_3\text{OH}$, 49 : 1 v/v); m.p. 187-189 °C; $^1\text{H NMR}$ (CDCl_3 , 400 MHz) δ 1.41 (12H, br s, $t\text{Bu CH}_3$; CH_3), 1.45 (6H, d, $J = 7.0$ Hz, CH_3), 2.57 (16H, br, cyclen CH_2), 2.86 (2H, br s, CH_2CO), 2.99 (4H, br s, CH_2CO), 3.62-3.84 (5H, br, CH_2 pyrazole; CO_2CH_3), 5.14 (3H, q, $J = 7.0$ Hz, CH), 6.30 (1H, d, $J = 2.5$ Hz, H^2), 6.21-7.32 (12H, br, Ph), 7.47 (2H, d, $J = 8.0$ Hz, Ph), 7.55 (1H, d, $J = 9.0$ Hz, H^{10}), 7.82 (1H, dd, $J = 8.0$; 2.5 Hz, H^9), 7.98 (1H, d, $J = 8.0$ Hz, H^2), 8.31 (1H, d, $J = 2.5$ Hz, H^7), 8.78 (1H, d, $J = 8.0$ Hz, H^3); MS (ES^+) m/z 1067.7 (100 %, $[\text{M} + \text{Na}]^+$); HRMS (ES^+) m/z found 1045.5706 $[\text{M} + \text{H}]^+$ $\text{C}_{60}\text{H}_{73}\text{N}_{10}\text{O}_7$ requires 1045.5698.

[TbL¹⁰]

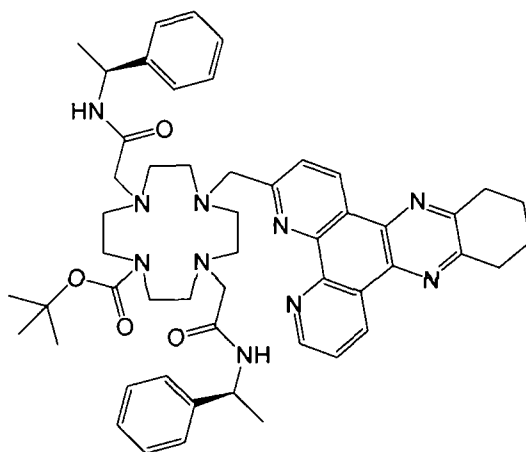


A solution of 4-[(*S*)-1-(2-{7-[1-(6-*tert*-butyl-10-oxo-10*H*-9-oxa-1-aza-anthracen-2-yl)-1*H*-pyrazol-3-ylmethyl]-4,10-bis-[(*S*)-1-phenyl-ethylcarbamoyl]-methyl]-1,4,7,10-tetraaza-cyclododec-1-yl}-acetyl-amino)-ethyl]-benzoic acid methyl ester [**L¹⁰**] (0.054 g, 0.051 mmol) and $\text{Tb}(\text{OTf})_3 \cdot 6\text{H}_2\text{O}$ (0.033 g, 0.054 mmol) in *anhydrous* CH_3CN (1 ml) was heated at reflux, under argon, for 16 h. The resultant solution was allowed to cool to rt followed by the removal of solvent under reduced pressure to afford a glassy orange solid. CH_2Cl_2 (10 ml) was added to the solid, and the mixture sonicated for 10 min. The

solvent was then decanted and the solid material dissolved in a minimum volume of CH₃CN (0.5 ml). The solution was added dropwise onto diethyl ether (25 ml) to induce precipitation. The solid material was isolated by centrifugation, and the process of induced precipitation repeated twice more to yield the complex as its triflate salt. The yellow solid was made water soluble by the exchange of triflate anions for chloride anions using 'DOWEX 1 x 8 200-400 mesh Cl' resin. The solid material was dissolved in a mixture of H₂O – CH₃OH (1:1 v/v, 14 ml) and 0.6 g of prepared resin added to the solution, which was stirred at rt, for 6 h. The resin was removed by filtration, and the filtrate concentrated under reduced pressure to yield the *title complex* [TbL¹⁰] as a pale yellow coloured solid (0.037 g, 0.028 mmol, 55 %); λ_{\max} (H₂O) = 348 nm, τ (H₂O) = 2.27 ms; ϕ_{Tb} (H₂O; pH 6.0; λ_{exc} 355 nm) = 63 %; HPLC (Method A) t_{R} = 10.9 min.

7.4.5 Tetraazatriphenylene Amide Conjugate Complex

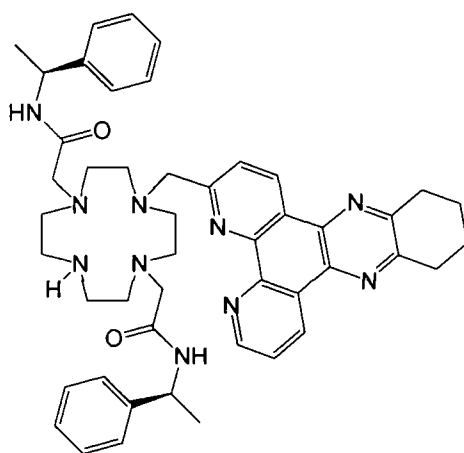
4,10-bis-(((S)-1-Phenyl-ethylcarbamoyl)-methyl)-7-(10,11,12,13-tetrahydro-4,5,9,14-tetraaza-benzo[*b*]triphenylen-6-ylmethyl)-1,4,7,10-tetraaza-cyclododecane-1-carboxylic acid *tert*-butyl ester (41)



A stirring mixture of 4,10-bis-(((S)-1-phenyl-ethylcarbamoyl)-methyl)-1,4,7,10-tetraaza-cyclododecane-1-carboxylic acid *tert*-butyl ester **37** (0.131 g, 0.218 mmol), 3-chloromethyl-10,11,12,13-tetrahydrodipyrido-[3,2a:2',3'-c]-phenazine (0.080 g, 0.240 mmol) and K₂CO₃ (0.045 g, 0.327 mmol) in *anhydrous* CH₃CN (5 ml) was heated at reflux, under argon, for 16 h. The resultant mixture was allowed to cool to rt, syringe filtered and the filtrate concentrated under reduced pressure to afford a residual yellow

oil. The crude material was purified by column chromatography on neutral alumina (gradient elution; CH₂Cl₂ to 2 % CH₃OH : CH₂Cl₂, utilising 0.1 % CH₃OH increments) to yield the *title compound 41* as a yellow coloured crystalline solid (0.171 g, 0.190 mmol, 87 %); *R_F* = 0.61 (Alumina, CH₂Cl₂ – CH₃OH, 19 : 1 v/v); m.p. 149-150 °C; ¹H NMR (CDCl₃, 500 MHz) δ 1.35 (6H, d, *J* = 2.5 Hz CH₃), 1.39 (9H, s, 'Boc CH₃), 2.08 (4H, br s, H¹⁰; H¹³), 2.43 (4H, br s, cyclen CH₂), 2.78 (6H, br s, CH₂CO), 3.05 (4H, br s, cyclen CH₂), 3.24 (8H, br s, cyclen CH₂), 3.54 (2H, s, CH₂ dpqC), 5.00 (2H, q, *J* = 8.0 Hz, CH), 7.07-7.15 (10H, m, Ph), 7.60 (1H, d, *J* = 8.0 Hz, H²), 7.84 (1H, dd, *J* = 8.0; 4.5 Hz, H⁷), 8.07 (2H, br s, NH), 8.97 (1H, dd, *J* = 4.5; 1.5 Hz, H⁶), 9.44 (1H, d, *J* = 8.0 Hz, H¹), 9.56 (1H, d, *J* = 8.0 Hz, H⁸); ¹³C NMR (CDCl₃, 125 MHz, ¹H decoupled 500 MHz) δ 22.3 (2C, C¹⁰, C¹³), 22.9 (2C, CH₃), 28.8 (3C, 'Boc CH₃), 33.1 (2C, C¹¹, C¹²), 47.3 (1C, CH), 48.9 (1C, CH), 50.4 (2C, cyclen CH₂), 51.5 (2C, cyclen CH₂), 52.9 (2C, cyclen CH₂), 53.7 (2C, cyclen CH₂), 55.9 (2C, CH₂CO), 61.1 (1C, CH₂ dpqC), 80.3 (1C, C'Bu), 124.8 (1C, C²), 125.5 (1C, C⁷), 126.4 (2C, Ph_(o/m)), 126.7 (2C, Ph_(o/m)), 126.9 (2C, Ph_(o/m)), 127.1 (2C, Ph_(o/m)), 128.5 (2C, Ph_(p)), 134.7 (1C, C⁸), 135.0 (1C, C¹), 137.1 (1C, Ar_(q)), 137.4 (1C, Ar_(q)), 144.5 (2C, Ph_(q)), 146.1 (1C, Ar_(q)), 146.3 (1C, Ar_(q)), 150.6 (1C, Ar_(q)), 155.1 (1C, Ar_(q)), 155.3 (1C, Ar_(q)), 160.2 (1C, Ar_(q)), 170.3 (2C, amide C = O); MS (ES⁺) *m/z* 915.5 (100 %, [M + Na]⁺); HRMS (ES⁺) *m/z* found 915.5011 [M + Na]⁺ C₅₂H₆₄O₄N₁₀²³Na₁ requires 915.5004.

***N*-((*S*)-1-Phenyl-ethyl)-2-[7-(((*S*)-1-phenyl-ethylcarbamoyl)-methyl)-4-(10,11,12,13-tetrahydro-4,5,9,14-tetraaza-benzo[*b*]triphenylen-6-ylmethyl)-1,4,7,10-tetraaza-cyclododec-1-yl]-acetamide (36)**



Procedure A:

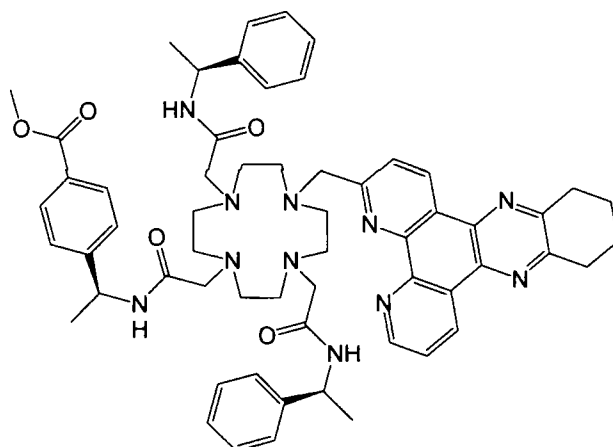
A stirring mixture of *N*-((*S*)-1-phenyl-ethyl)-2-(7-(((*S*)-1-phenyl-ethylcarbamoyl)-methyl)-1,4,7,10-tetraaza-cyclododec-1-yl)-acetamide **33** (0.370 g, 0.748 mmol), 3-chloromethyl-10,11,12,13-tetrahydrodipyrido-[3,2a:2',3'-c]-phenazine (0.250 g, 0.748 mmol) and NaHCO₃ (0.069 g, 0.823 mmol) in *anhydrous* CH₃CN (8 ml) was heated at 55 °C, under argon, for 7 h. The reaction mixture was allowed to cool to rt, syringe filtered and the filtrate concentrated under reduced pressure to afford an orange solid. The crude material was purified by column chromatography on neutral alumina (gradient elution: CH₂Cl₂ to 0.5 % CH₃OH : CH₂Cl₂) to yield the *title compound* **36** as a pale cream coloured solid (0.330 g, 0.416 mmol, 56 %); ¹H NMR (CDCl₃, 500 MHz) δ 1.35 (6H, d, *J* = 2.5 Hz CH₃), 2.08 (4H, br s, H¹⁰; H¹³), 2.43 (4H, br s, cyclen CH₂), 2.78 (6H, br s, CH₂CO), 3.05 (4H, br s, cyclen CH₂), 3.24 (8H, br s, cyclen CH₂), 3.58 (2H, s, CH₂ dpqC), 5.00 (2H, q, *J* = 8.0 Hz, CH), 7.07-7.15 (10H, m, Ph), 7.60 (1H, d, *J* = 8.0 Hz, H²), 7.84 (1H, dd, *J* = 8.0; 4.5 Hz, H⁷), 8.07 (2H, br s, NH), 8.97 (1H, dd, *J* = 4.5; 1.5 Hz, H⁶), 9.44 (1H, d, *J* = 8.0 Hz, H¹), 9.56 (1H, d, *J* = 8.0 Hz, H⁸), 10.61 (1H, br s, cyclen NH); ¹³C NMR (CDCl₃, 125 MHz, ¹H decoupled 500 MHz) δ 22.3 (2C, C¹⁰, C¹³), 22.9 (2C, CH₃), 33.1 (2C, C¹¹, C¹²), 47.3 (1C, CH), 48.9 (1C, CH), 50.4 (2C, cyclen CH₂), 51.5 (2C, cyclen CH₂), 52.9 (2C, cyclen CH₂), 53.7 (2C, cyclen CH₂), 55.9 (2C, CH₂CO), 61.1 (1C, CH₂ dpqC), 124.8 (1C, C²), 125.5 (1C, C⁷), 126.4 (2C, Ph_(o/m)), 126.7 (2C, Ph_(o/m)), 126.9 (2C, Ph_(o/m)), 127.1 (2C, Ph_(o/m)), 128.5 (2C, Ph_(p)), 134.7 (1C, C⁸), 135.0 (1C, C¹), 137.1 (1C, Ar_(q)), 137.4 (1C, Ar_(q)), 144.5 (2C, Ph_(q)), 146.1 (1C, Ar_(q)), 146.3 (1C, Ar_(q)), 150.6 (1C, Ar_(q)), 155.1 (1C, Ar_(q)), 155.3 (1C, Ar_(q)), 160.2 (1C, Ar_(q)), 170.3 (2C, amide C = O); MS (ES⁺) *m/z* 793.6 (100 %, [M + H]⁺); HRMS (ES⁺) *m/z* found 793.4660 [M + H]⁺ C₄₇H₅₇N₁₀O₂ requires 793.4660.

Procedure B:

A solution of 4,10-bis-(((*S*)-1-phenyl-ethylcarbamoyl)-methyl)-7-(10,11,12,13-tetrahydro-4,5,9,14-tetraaza-benzo[*b*]triphenylen-6-ylmethyl)-1,4,7,10-tetraaza-cyclododecane-1-carboxylic acid *tert*-butyl ester **41** (0.159 g, 0.177 mmol) in CH₂Cl₂ – TFA (2 : 1 v/v, 6 ml) was stirred at rt, in a sealed flask, for 5 h, to afford an orange solution. The solvent was removed under reduced pressure to yield a glassy solid. The

crude material was repeatedly (x 3) dissolved in CH₂Cl₂ (10 ml) and the solvent removed under reduced pressure to facilitate elimination of excess acid and *tert*-butyl alcohol. The residue was finally taken into 1 M KOH_(aq) (10 ml) and extracted with CH₂Cl₂ (2 x 20 ml). The organic extracts were combined, dried over K₂CO₃, filtered and the filtrate concentrated under reduced pressure to yield the *title compound 36* as an orange coloured crystalline solid (0.129 g, 0.162 mmol, 92 %). *Characterisation was identical to that reported in procedure A.*

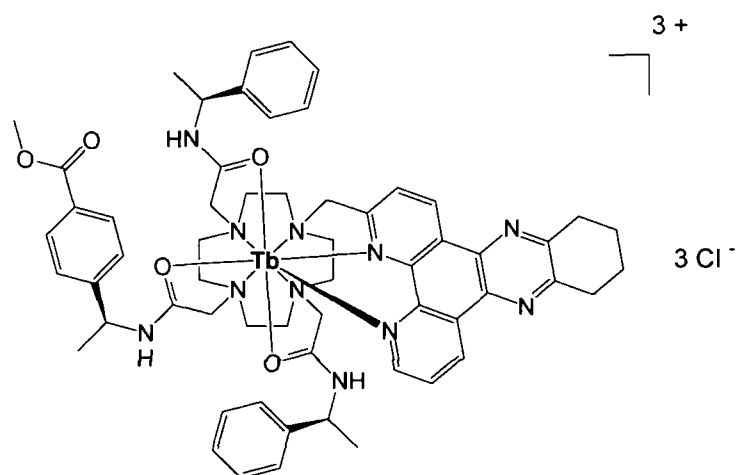
4-((*S*)-1-{2-[4,10-bis-[[(*S*)-1-Phenyl-ethylcarbamoyl]-methyl]-7-(10,11,12,13-tetrahydro-4,5,9,14-tetraaza-benzo[*b*]triphenylen-6-ylmethyl)-1,4,7,10-tetraaza-cyclododec-1-yl]-acetamino}-ethyl)-benzoic acid methyl ester ([L¹¹])



A stirring mixture of *N*-((*S*)-1-phenyl-ethyl)-2-[7-[[(*S*)-1-phenyl-ethylcarbamoyl]-methyl]-4-(10,11,12,13-tetrahydro-4,5,9,14-tetraaza-benzo[*b*]triphenylen-6-ylmethyl)-1,4,7,10-tetraaza-cyclododec-1-yl]-acetamide **36** (0.100 g, 0.126 mmol), 4-[(*S*)-1-(2-chloro-acetylamino)-ethyl]-benzoic acid methyl ester **30** (0.037 g, 0.145 mmol) and Cs₂CO₃ (0.049 g, 0.151 mmol) in *anhydrous* CH₃CN (5 ml) was heated at reflux, under argon, for 18 h. The resultant mixture was allowed to cool to rt, syringe filtered and the filtrate concentrated under reduced pressure to afford an orange solid. The crude material was purified by column chromatography on neutral alumina (gradient elution: CH₂Cl₂ to 0.5 % CH₃OH : CH₂Cl₂) to yield the *title compound [L¹¹]* as a free flowing cream coloured solid (0.117 g, 0.115 mmol, 92 %); ¹H NMR (CDCl₃, 500 MHz) δ 1.43 (3H, d, *J*

= 2.0 Hz, CH₃), 1.45 (6H, d, $J = 2.0$ Hz, CH₃), 2.09 (4H, br s, H¹⁰; H¹³), 2.29-2.63 (16H, br s, cyclen CH₂), 3.23 (4H, br s, H¹¹; H¹²), 3.86 (3H, s, CO₂CH₃), 4.10 (2H, s, CH₂ dpqC), 5.14 (3H, q, $J = 7.5$ Hz, CH), 7.15-7.23 (10H, m, Ph), 7.30 (2H, d, $J = 8.0$ Hz, Ph), 7.38 (2H, d, $J = 8.0$ Hz, H²), 7.72 (2H, dd, $J = 8.5$; 4.5 Hz, Ph), 7.90 (2H, d, $J = 8.0$ Hz, H⁷), 9.19 (1H, dd, $J = 4.5$; 1.5 Hz, H⁶), 9.33 (1H, d, $J = 8.5$ Hz, H¹), 9.48 (1H, dd, $J = 8.5$; 2.0 Hz, H⁸); δ_{C} (CDCl₃, 125 MHz) 21.6 (3C, CHCH₃), 23.0 (C¹⁰, C¹³), 33.1 (C¹¹, C¹²), 48.3 (2C, CH), 48.4 (1C, CH), 52.3 (1C, CO₂CH₃), 53.6 (2C, cyclen CH₂), 53.7 (2C, cyclen CH₂), 53.8 (2C, cyclen CH₂), 53.9 (2C, cyclen CH₂), 59.8 (3C, CH₂CO), 62.6 (1C, CH₂ dpqC), 123.3 (1C, C²), 123.9 (1C, C⁷), 126.3 (2C, Ph_(o/m)), 126.4 (2C, Ph_(o/m)), 126.5 (2C, Ph_(o/m)), 127.7 (2C, Ph_(o/m)), 127.8 (2C, Ph_(o/m)), 128.8 (2C, Ph_(p)), 128.9 (2C, Ph_(o/m)), 133.6 (1C, C⁸), 137.7 (1C, C¹), 137.8, 143.3 (1C, Ar_(q)), 146.8 (1C, Ar_(q)), 147.0 (1C, Ar_(q)), 148.7 (1C, Ar_(q)), 151.8 (1C, Ar_(q)), 154.0 (1C, Ar_(q)), 154.2 (1C, Ar_(q)), 161.3 (1C, Ar_(q)), 166.9 (1C, ester C = O), 170.14 (1C, amide C = O), 170.2 (2C, amide C = O). MS (ES⁺) m/z 1034.7 (100 %, [M + Na]⁺); HRMS (ES⁺) m/z found 1012.55580 [M + H]⁺ C₅₉H₇₀N₁₁O₅ requires 1012.55559.

[TbL¹¹]



A solution of 4-((*S*)-1-{2-[4,10-bis-[(*S*)-1-phenyl-ethylcarbamoyl]-methyl]-7-(10,11,12,13-tetrahydro-4,5,9,14-tetraaza-benzo[*b*]triphenylen-6-ylmethyl)-1,4,7,10-tetraaza-cyclododec-1-yl]-acetylamino}-ethyl)-benzoic acid methyl ester [L¹¹] (0.035 g, 0.035 mmol) and Tb(OTf)₃·6H₂O (0.023 g, 0.038 mmol) in *anhydrous* CH₃CN (1 ml) was heated at reflux, under argon, for 18 h. The solution was allowed to cool to rt,

followed by the removal of solvent under reduced pressure to afford a glassy orange solid. CH_2Cl_2 (10 ml) was added to the solid, and the mixture sonicated for 10 min. The solvent was then decanted and the solid material dissolved in a minimum volume of CH_3CN (1.0 ml). The solution was added dropwise onto diethyl ether (50 ml) to induce precipitation. The solid material was isolated by centrifugation, and the process of induced precipitation repeated twice more to yield the complex as its triflate salt. The yellow solid was made water soluble by the exchange of triflate anions for chloride anions using 'DOWEX 1 x 8 200-400 mesh Cl' resin. The solid material was dissolved in a mixture of $\text{H}_2\text{O} - \text{CH}_3\text{OH}$ (1:1 v/v, 20 ml) and 0.8 g of prepared resin added to the solution, which was stirred at rt, for 4 h. The resin was removed by filtration, and the filtrate concentrated under reduced pressure to yield the *title complex* [**TbL¹¹**] as a colourless solid (0.033 g, 0.026 mmol, 74 %); λ_{max} (H_2O) = 348 nm; τ (H_2O) = 1.57 ms; HPLC (Method A) t_{R} = 10.9 min.

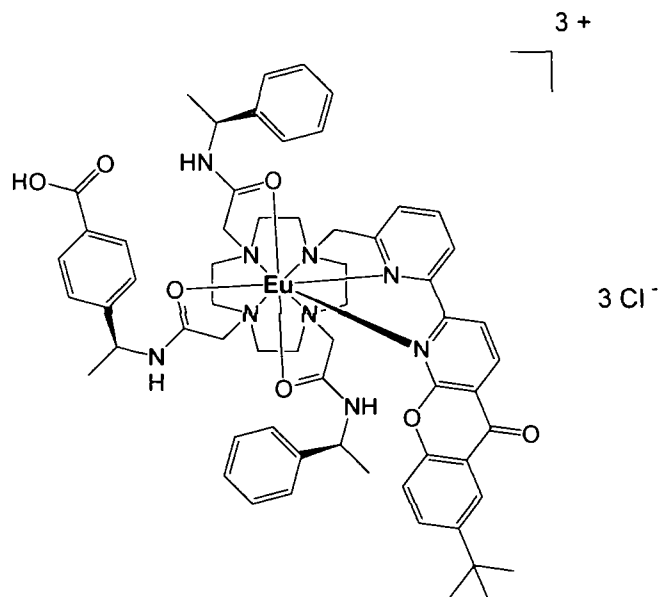
[**EuL¹¹**]

An analogous procedure to that described for [**TbL¹¹**] was followed using 4-((*S*)-1-{2-[4,10-bis-[(*S*)-1-phenyl-ethylcarbamoyl]-methyl]-7-(10,11,12,13-tetrahydro-4,5,9,14-tetraaza-benzo[*b*]triphenylen-6-ylmethyl)-1,4,7,10-tetraaza-cyclododec-1-yl]-acetylamino}-ethyl)-benzoic acid methyl ester [**L¹¹**] (0.031 g, 0.031 mmol) and $\text{Eu}(\text{OTf})_3 \cdot 6\text{H}_2\text{O}$ (0.019 g, 0.034 mmol) in *anhydrous* CH_3CN (1 ml). The procedure yielded the *title complex* [**EuL¹¹**], as a colourless solid (0.025 g, 0.021 mmol, 69 %); λ_{max} (H_2O) = 348 nm; τ (H_2O) = 1.04 ms.

7.5 Activation and Conjugation of Conjugate Complexes

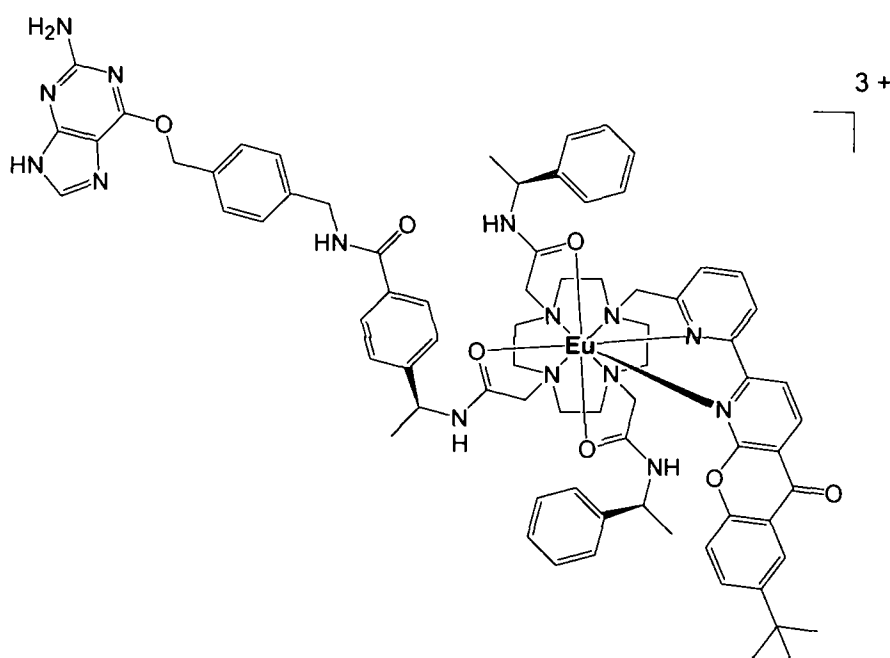
7.5.1 Pyridyl-azaxanthone, [EuL⁹]

[EuL⁹_CO₂H]



A solution of [EuL⁹] (1.5 μmol) in CH₃OH – 0.02 M KOH_(aq) (1:1 v/v, 2 ml) was stirred at rt. The progress of hydrolysis was monitored by reverse phase HPLC using a Chromolith performance RP18e 100 x 4.6 mm column. (*Method D*; t_R (ester) = 6.40 mins, t_R (acid) = 6.24 mins).

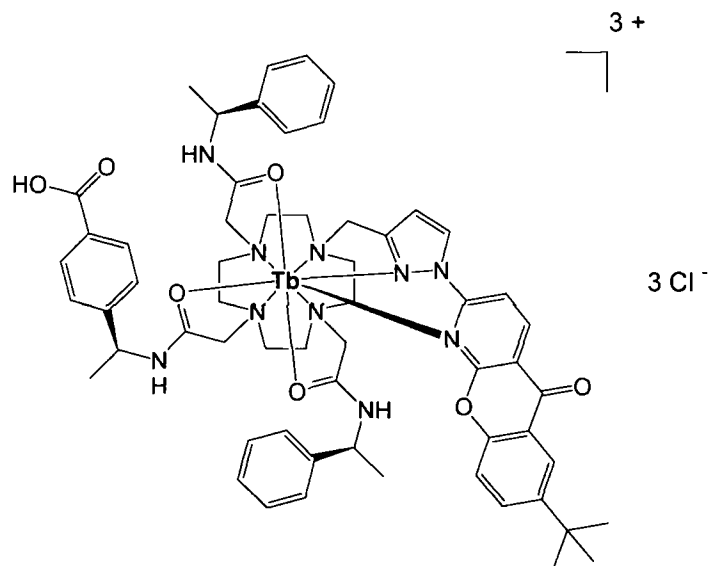
The reaction ran to completion in approximately 2 h and was neutralised using a dilute HCl_(aq) solution. The solvent was removed under reduced pressure and the crude residue used directly in the next step without further purification.

[EuL⁹_CONHBG]

To a stirred solution of **[EuL⁹_CO₂H]** in *anhydrous* DMF (2 ml) was added incremental equivalents of TSTU and DIPEA (50 μ l of a 100 mM solution in DMF in each case, 5 μ mol). The progress of the reaction was monitored by reverse phase HPLC using a Chromolith performance RP18e 100 x 4.6 mm column.

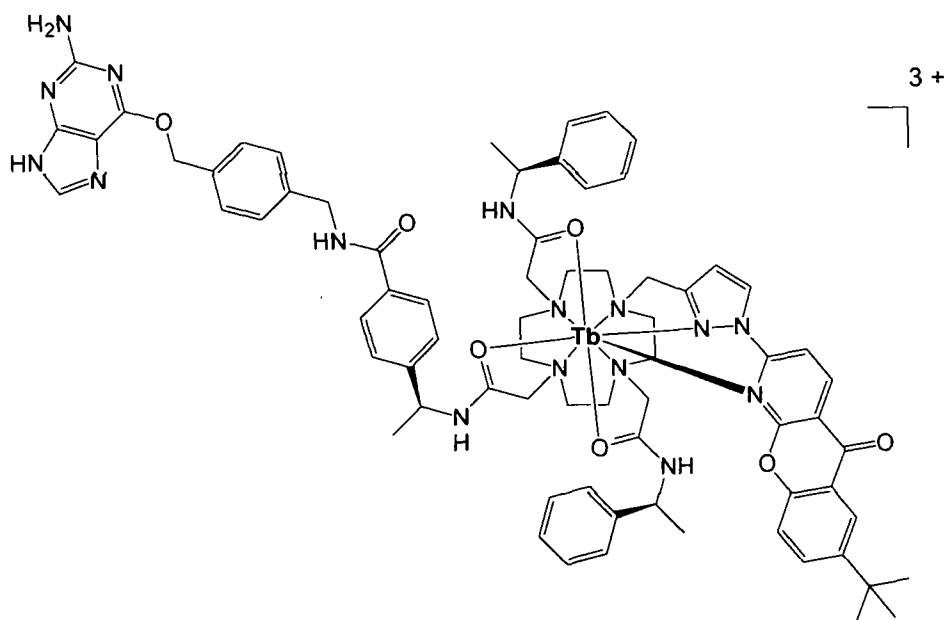
BG-NH₂ was added to the stirred solution of in situ **[TbL¹⁰_NHS]** (1 μ mol) in *anhydrous* DMF (400 μ l). The mixture was stirred at rt and the progress of the reaction was monitored by reverse phase HPLC using a Chromolith performance RP18e 100 x 4.6 mm column. (*Method D*; t_R (NHS) = 6.28 mins, t_R (BG) = 5.97 mins).

The reaction ran to completion in approximately 1 h. The product was purified by reverse phase semi-preparative HPLC using a Chromolith performance RP18e 100 x 10 mm column. (*Method E*; t_R (BG) = 6.67 mins). The product was obtained as a colourless solid (320 nmol, 34 %).

7.5.2 Pyrazoyl-azaxanthone, [TbL¹⁰][TbL¹⁰_CO₂H]

A solution of [TbL¹⁰] (1.3 μmol) in $\text{CH}_3\text{OH} - 0.02 \text{ M KOH}_{(\text{aq})}$ (1:1 v/v, 2 ml) was stirred at rt. The progress of hydrolysis was monitored by reverse phase HPLC using a Chromolith performance RP18e 100 x 4.6 mm column. (*Method C*; t_R (ester) = 6.07 mins, t_R (acid) = 5.78 mins).

The reaction ran to completion in approximately 2 h and was neutralised using a dilute $\text{HCl}_{(\text{aq})}$ solution. The solvent was removed under reduced pressure and the crude residue used directly in the next step without further purification; MS (ES^+) m/z 594 $[\text{M} - \text{H}]^{2+}$; 1187 $[\text{M} - 2\text{H}]^+$.

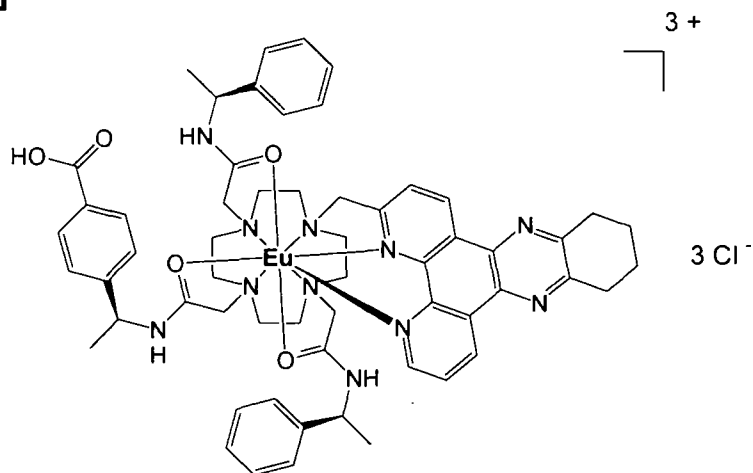
[TbL¹⁰_CONHBG]

To a stirred solution of [TbL¹⁰_CO₂H] in *anhydrous* DMF (2 ml) was added incremental equivalents of TSTU and DIPEA (50 μl of a 100 mM solution in DMF in each case, 5 μmol). The progress of the reaction was monitored by reverse phase HPLC using a Chromolith performance RP18e 100 x 4.6 mm column. (*Method C*; t_R (acid) = 6.07 mins, t_R (NHS) = 6.28 mins).

BG-NH₂ was added to the stirred solution of in situ [TbL¹⁰_NHS] (1 μmol) in *anhydrous* DMF (400 μl). The mixture was stirred at rt and the progress of the reaction was monitored by reverse phase HPLC using a Chromolith performance RP18e 100 x 4.6 mm column. (*Method C*; t_R (NHS) = 6.28 mins, t_R (BG) = 5.97 mins).

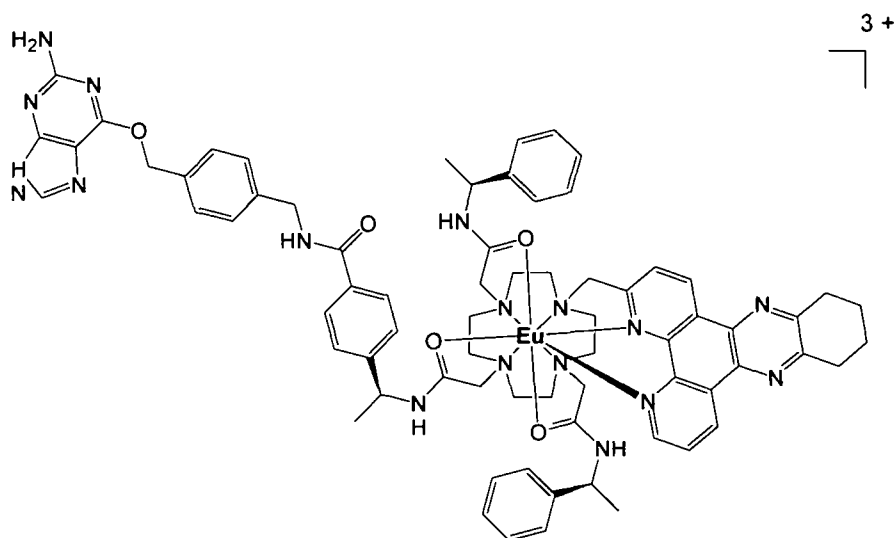
The reaction ran to completion in approximately 15 min. The product was purified by reverse phase semi-preparative HPLC using a Chromolith performance RP18e 100 x 10 mm column. (*Method E*; t_R (BG) = 5.23 mins).

The product was obtained as a colourless solid (380 nmol, 38 %); MS (ES⁺) m/z 721 [M - H]²⁺; 1440 [M - 2H]⁺.

7.5.3 Tetraazatriphenylene, [EuL¹¹][EuL¹¹-CO₂H]

A solution of [EuL¹¹] (5 μmol) in CH₃OH – 0.02 M KOH_(aq) (1:1 v/v, 4 ml) was stirred at rt. The progress of hydrolysis was monitored by reverse phase HPLC using a Chromolith performance RP18e 100 x 4.6 mm column. (*Method B*; t_R (Ester) = 5.17 mins, t_R (acid) = 4.93 mins).

The reaction ran to completion in approximately 2 h and was neutralised using a dilute HCl_(aq) solution. The solvent was removed under reduced pressure and the crude residue used directly in the next step without further purification; MS (ES⁺) m/z 1154 [M – 2H]⁺.

[EuL¹²_CONHBG]

To a stirred solution of **[EuL¹²_CO₂H]** in anhydrous DMF (2 ml) was added incremental equivalents of TSTU and DIPEA (50 μ l of a 100 mM solution in DMF in each case, 5 μ mol). The progress of the reaction was monitored by reverse phase HPLC using a Chromolith performance RP18e 100 x 4.6 mm column. (*Method C*; t_R (acid) = 4.90 mins, t_R (NHS) = 5.18 mins).

After the reaction had ran to completion, the material was used directly in the next step, without further purification.

BG-NH₂ was added to a stirred solution of **[EuL¹²_NHS]** (1 μ mol) in *anhydrous* DMF (400 μ l). The mixture was stirred at rt and the progress of the reaction was monitored by reverse phase HPLC using a Chromolith performance RP18e 100 x 4.6 mm column. (*Method C*; t_R (NHS) = 5.12 mins, t_R (BG) = 4.93 mins).

The reaction ran to completion in less than 30 mins. The product was purified by reverse semi-preparative HPLC using a Chromolith performance RP18e 100 x 10 mm column. (*Method F*; t_R (BG) = 11.49 mins).

The product was obtained as a colourless solid (380 nmol, 38 %); MS (ES⁺) m/z 1406 [M - 2H]⁺.

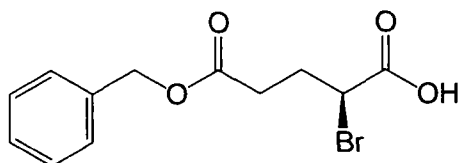
[TbL¹²]

Analogous procedures to that described for **[EuL¹²]** were followed using **[TbL¹²]** to yield **[TbL¹²_BG]**.

7.6 Carboxylate Conjugate Complexes

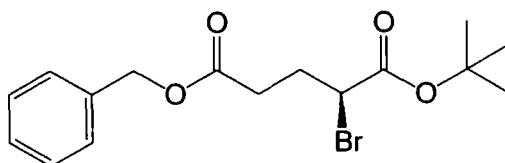
7.6.1 Carboxylate Conjugate Arm

(S)-2-Bromo-pentanedioic acid 5-benzyl ester ¹² (44)



A solution of NaNO₂ (5.50 g, 80.1 mmol) in H₂O (50 ml) was added dropwise over 30 min to a stirred solution of (*S*)-glutamic acid 5-benzyl ester (10.0 g, 42.1 mmol) and NaBr (16.0 g, 116 mmol) in 1 M HBr (250 ml), cooled at -5 °C. After 10 h, conc. H₂SO_{4(aq)} (5 ml) was slowly added to the reaction mixture, which was then extracted with diethyl ether (3 x 300 ml). The combined organic extracts were washed with brine (200 ml), dried over Na₂SO₄, filtered and the filtrate concentrated under reduced pressure. The crude material was purified by column chromatography on silica (gradient elution: Hexane – 20 % EtOAc : Hexane, utilising 1 % EtOAc increments) to yield the *title compound* **44** as a yellow oil (7.40 g, 24.6 mmol, 58 %); R_F = 0.25 (Silica, Hexane – EtOAc 17 : 3 v/v); ¹H NMR (CDCl₃, 700 MHz) δ 2.30 (1H, m, CH₂CHBr), 2.42 (1H, m, CH₂CHBr), 2.60 (2H, m, CH₂CH₂CHBr), 4.41 (1H, dd, *J* = 9.0; 6.0 Hz, CH), 5.14 (2H, s, CH₂Ph), 7.33-7.39 (5H, m, Ph); ¹³C NMR (CDCl₃, 176 MHz, ¹H decoupled 700 MHz) δ 29.7 (1C, CH₂CH₂CHBr), 31.6 (1C, CH₂CHBr), 44.2 (1C, CH), 66.9 (1C, CH₂Ph), 128.4 (1C, Ph_(o/m)), 128.5 (1C, Ph_(o/m)), 128.6 (1C, Ph_(o/m)), 128.7 (1C, Ph_(o/m)), 128.8 (1C, Ph_(p)), 135.8 (1C, Ph_(q)), 172.1 (1C, Cbz C = O), 173.4 (1C, Acid C = O); MS (ES⁺) *m/z* 323.2 (100 %, [M + H]⁺).

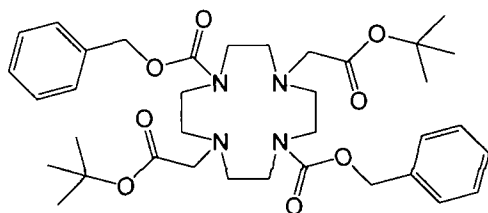
(S)-2-Bromo-pentanedioic acid 5-benzyl ester 1-tert-butyl ester (45)



A solution of (*S*)-2-bromo-pentanedioic acid 5-benzyl ester **44** (2.00 g, 6.85 mmol) in *tert*-butyl acetate (25 ml) and HClO₄ in H₂O (70 %, 0.34 mmol) was stirred, at rt, for 16 h. H₂O (35 ml) was added to the reaction mixture, and the organic phase separated. The organic phase was washed with H₂O (25 ml), followed by 5 % Na₂CO₃ (aq) (25 ml). The solvent was removed under reduced pressure to yield the *title compound* **45** as a yellow coloured oil (2.15 g, 6.03 mmol, 88 %); ¹H NMR (CDCl₃, 700 MHz) δ 1.46 (9H, s, 'Boc CH₃), 2.25 (1H, m, CH₂CHBr), 2.35 (1H, m, CH₂CHBr), 2.55 (2H, m, CH₂,CH₂,CHBr), 4.23 (1H, q, *J* = 5.5; 2.0 Hz, CH), 5.12 (2H, s, CH₂Ph), 7.31-7.36 (5H, m, Ph); ¹³C NMR (CDCl₃, 176 MHz, ¹H decoupled 700 MHz) δ 27.9 (3C, 'Boc CH₃), 29.9 (1C, CH₂CH), 31.8 (1C, CH₂CH₂), 46.9 (1C, CH), 66.7 (1C, CH₂Ph), 82.8 (1C, 'Boc_(q)), 128.4 (1C, Ph_(o/m)), 128.5 (1C, Ph_(o/m)), 128.6 (1C, Ph_(o/m)), 128.7 (1C, Ph_(o/m)), 128.8 (1C, Ph_(p)), 136.0 (1C, Ph_(q)), 168.5 (1C, 'Boc C = O), 172.2 (1C, Cbz C = O); MS (ES⁺) *m/z* 379.0 (100 %, [M + Na]⁺).

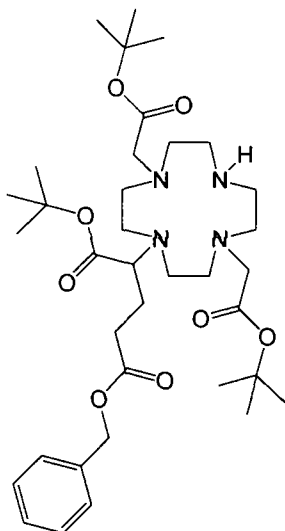
7.6.2 Cyclen Intermediates

4,10-bis-*tert*-Butoxycarbonylmethyl-1,4,7,10-tetraaza-cyclododecane-1,7-dicarboxylic acid dibenzyl ester ¹³ (**46**)



A stirred mixture of 1,4,7,10-tetraaza-cyclododecane-1,7-dicarboxylic acid dibenzyl ester **31** (2.65 g, 6.02 mmol), *tert*-butyl bromoacetate (2.64 g, 2.00 ml, 13.5 mmol) and Cs₂CO₃ (5.88 g, 18.1 mmol) was heated at reflux in *anhydrous* CH₃CN (25 ml), under argon, for 18 h. The reaction mixture was allowed to cool to rt, syringe filtered and the filtrate concentrated under reduced pressure to yield a residual yellow oil. The crude material was purified by column chromatography on silica (gradient elution: CH₂Cl₂ to 1.5 % CH₃OH : CH₂Cl₂, utilising 0.1 % CH₃OH increments) to yield the *title compound* **46** as a yellow coloured oil (2.46 g, 3.68 mmol, 61 %); R_F = 0.53 (Silica, CH₂Cl₂ – CH₃OH, 39 :

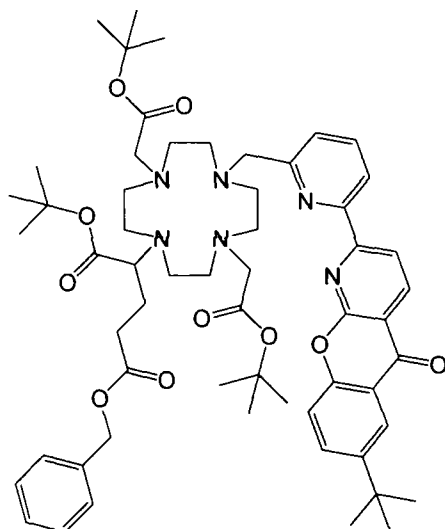
2-(4,10-bis-*tert*-Butoxycarbonylmethyl-1,4,7,10-tetraaza-cyclododec-1-yl)-pentanedioic acid 5-benzyl ester 1-*tert*-butyl ester (49)



A stirred mixture of (7-*tert*-butoxycarbonylmethyl-1,4,7,10-tetraaza-cyclododec-1-yl)-acetic acid *tert*-butyl ester **47** (0.369 g, 0.925 mmol), (*S*)-2-bromo-pentanedioic acid 5-benzyl ester 1-*tert*-butyl ester **45** (0.325 g, 0.923 mmol) and NaHCO₃ (0.074 g, 0.925 mmol) was heated at 55 °C in *anhydrous* CH₃CN (15 ml), under argon, for 18 h. The reaction mixture was allowed to cool to rt, syringe filtered and the filtrate concentrated under reduced pressure to afford an orange residual oil. The crude material was purified by column chromatography on neutral alumina (gradient elution: CH₂Cl₂ – 1.0 % CH₃OH : CH₂Cl₂, utilising 0.1 % CH₃OH increments) to yield the *title compound* **49** as a yellow coloured solid (0.373 g, 0.552 mmol, 60 %); *R*_F = 0.28 (Alumina, CH₂Cl₂ – CH₃OH, 49 : 1 v/v); ¹H NMR (CDCl₃, 700 MHz) δ 1.34 (27H, s, ^tBoc CH₃), 1.80 (2H, m, arm CH₂), 2.41 (4H, m, cyclen CH₂; arm CH₂), 2.70 (6H, m, cyclen CH₂), 3.05 (8H, m, cyclen CH₂), 3.24 (4H, q, CH₂CO), 3.31 (1H, t, *J* = 7.5 Hz, CH), 5.03 (2H, q, *J* = 12.5; 5.5 Hz, Cbz CH₂), 7.19-7.27 (5H, m, Ph); ¹³C NMR (CDCl₃, 176 MHz, ¹H decoupled 700 MHz) δ 25.0 (1C, CH₂), 28.3 (9C, ^tBoc CH₃), 30.9 (1C, CH₂), 46.6 (2C, cyclen CH₂), 49.8 (2C, cyclen CH₂), 50.8 (2C, cyclen CH₂), 51.4 (2C, cyclen CH₂), 56.5 (2C, CH₂CO), 60.8 (1C, CH), 66.6 (1C, Cbz CH₂), 81.7 (2C, ^tBoc_(q)), 82.2 (1C, ^tBoc_(q)), 128.4 (2C, Ph_(o/m)), 128.5 (1C, Ph_(p)), 128.7 (2C, Ph_(o/m)), 136.0 (1C, Ph_(q)), 170.4 (2C, ^tBoc C = O), 171.4 (1C, ^tBoc C = O), 172.9 (1C, Cbz C = O); MS (ES⁺) *m/z* 677.4 (100 %, [M + H]⁺); HRMS (ES⁺) *m/z* found 677.4484 [M + H]⁺ C₃₆H₆₁O₈N₄ requires 677.4484.

7.6.3 Pyridyl-azaxanthone Carboxylate Conjugate Complex

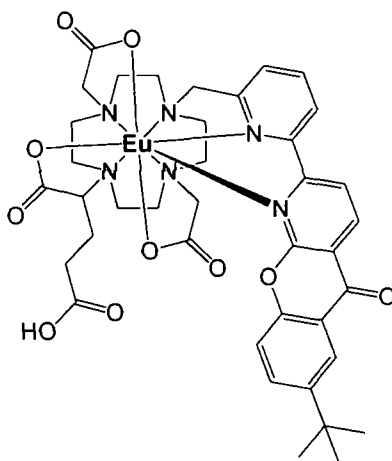
2-{4,10-bis-*tert*-Butoxycarbonylmethyl-7-[6-(6-*tert*-butyl-10-oxo-10*H*-9-oxa-1-aza-anthracen-2-yl)-pyridin-2-ylmethyl]-1,4,7,10-tetraaza-cyclododec-1-yl}-pentanedioic acid 5-benzyl ester 1-*tert*-butyl ester ([L¹²])



A stirred mixture of 2-(6-bromomethyl-pyridin-2-yl)-6-*tert*-butyl-9-oxa-1-aza-anthracen-10-one **9** (0.110 g, 0.318 mmol), 2-(4,10-bis-*tert*-butoxycarbonylmethyl-1,4,7,10-tetraaza-cyclododec-1-yl)-pentanedioic acid 5-benzyl ester 1-*tert*-butyl ester **49** (0.195 g, 0.289 mmol) and K₂CO₃ (0.086 g, 0.636 mmol) in *anhydrous* CH₃CN (10 ml) was heated at reflux, under argon, for 40 h. The reaction mixture was allowed to cool to rt, filtered and the filtrate concentrated under reduced pressure to afford an orange residual oil. The crude material was purified by column chromatography on neutral alumina (gradient elution: CH₂Cl₂ – 1.0 % CH₃OH : CH₂Cl₂, utilising 0.1 % CH₃OH increments) to yield the *title compound* [**L¹²**] as a yellow oil (0.188 g, 0.116 mmol, 40 %); *R_F* = 0.37 (Alumina, CH₂Cl₂ – CH₃OH, 19 : 1 v/v); ¹H NMR (CDCl₃, 700 MHz) δ 1.34 (27H, s, ^tBoc CH₃), 1.38 (9H, s ^tBu CH₃), 2.37 (4H, m, cyclen CH₂; arm CH₂), 2.73 (6H, m, cyclen CH₂), 3.07 (8H, m, cyclen CH₂), 3.26 (4H, q, CH₂CO), 3.31 (1H, t, *J* = 7.5 Hz, CH), 5.04 (2H, q, *J* = 12.5; 5.5 Hz, Cbz CH₂), 7.19-7.27 (6H, m, Ph; H⁵), 7.54 (1H, d, *J* = 8.5 Hz, H¹⁰), 7.72-7.78 (2H, br s, H⁴; H⁹), 8.24 (1H, d, *J* = 3.0 Hz, H⁷), 8.32 (1H, d, *J* = 8.0 Hz, H³), 8.40 (1H, br s, cyclen NH), 8.48 (1H, d, *J* = 7.0 Hz, H²), 8.75 (1H, d, *J* = 8.0 Hz, H³); ¹³C NMR (CDCl₃, 176 MHz, ¹H decoupled 700 MHz) δ 25.0 (1C, CH₂),

28.3 (9C, ^tBoc CH₃), 30.9 (1C, CH₂), 31.5 (3C, C¹⁴), 34.9 (1C, C¹³), 46.6 (2C, cyclen CH₂), 49.8 (2C, cyclen CH₂), 50.8 (2C, cyclen CH₂), 51.4 (2C, cyclen CH₂), 56.5 (2C, CH₂CO), 63.3 (1C, CH), 66.6 (1C, Cbz CH₂), 81.7 (2C, ^tBoc_(q)), 82.2 (1C, ^tBoc_(q)), 116.4 (1C, C⁴), 118.3 (1C, C¹⁰), 118.5 (1C, C²), 119.7 (1C, C⁵), 121.3 (1C, C⁶), 122.7 (1C, C⁷), 123.8 (1C, C²), 128.4 (2C, Ph_(o/m)), 128.5 (1C, Ph_(p)), 128.7(2C, Ph_(o/m)), 133.6 (1C, C⁹), 136.1 (1C, Ph_(q)), 137.9 (1C, C⁴), 138.4 (1C, C³), 148.1 (1C, C⁸), 153.6 (1C, C¹), 154.2 (1C, C¹¹), 158.6 (1C, C⁶), 160.2 (1C, C¹), 160.6 (1C, C¹²), 170.4 (2C, ^tBoc C = O), 171.4 (1C, ^tBoc C = O), 172.9 (1C, Cbz C = O), 177.8 (1C, C⁵); MS (ES⁺) *m/z* 1019.6 (100 %, [M + H]⁺); HRMS (ES⁺) *m/z* found 1019.5866 [M + H]⁺ C₅₈H₇₉O₁₀N₆ requires 1019.5852; HPLC (Method A) *t_R* = 12.0 min.

[EuL¹²]



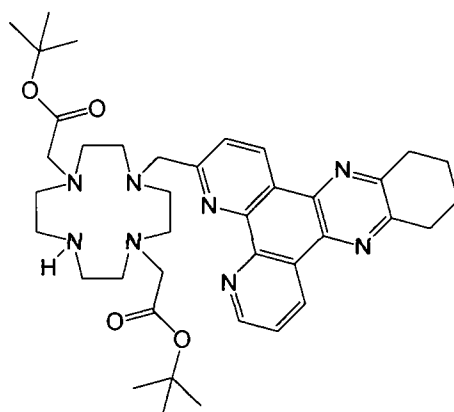
A stirred mixture of 2-{4,10-bis-*tert*-butoxycarbonylmethyl-7-[6-(6-*tert*-butyl-10-oxo-10H-9-oxa-1-aza-anthracen-2-yl)-pyridin-2-ylmethyl]-1,4,7,10-tetraaza-cyclododec-1-yl}-pentanedioic acid 5-benzyl ester 1-*tert*-butyl ester [**L¹²**] (0.021 g, 0.021 mmol) in hydrobromic acid (5 ml) was heated at 40 °C, for 4 h. The solvent was removed under reduced pressure to yield a glassy solid. The crude material was analysed by ¹H NMR to ensure complete deprotection, with the material used immediately for complexation. HPLC (Method A) *t_R* = 10.83 min.

The deprotected ligand was dissolved in CH₃OH – H₂O (2 : 2 v/v, 4 ml) and Eu(OAc)₃·6H₂O (0.008 g, 0.023 mmol) added to the solution. The pH of the solution was raised to 5.4 by the addition of 1 M KOH (aq), then stirred and heated at 90 °C, for 14 h. The reaction mixture was allowed to cool to rt before raising the pH of the solution to

10.0 using dilute KOH (aq). The reaction mixture was stirred for 1 h to allow precipitation of excess Eu metal as its hydroxide salt, Eu(OH)₃. The solid precipitate was removed by syringe filtration and the pH of the colourless aqueous filtrate reduced to pH 5.5 using a solution of 1 M HCl (aq). The solvent was removed under reduced pressure using a freeze-drier to yield the *title complex* [EuL¹²] as a colourless solid (0.008 g, 0.009 mmol, 45 %); $\lambda_{\text{max}}(\text{H}_2\text{O}) = 355 \text{ nm}$.

7.6.4 Tetraazatriphenylene Carboxylate Conjugate Complex

[7-*tert*-Butoxycarbonylmethyl-4-(10,11,12,13-tetrahydro-4,5,9,14-tetraaza-benzo[*b*]triphenylen-6-ylmethyl)-1,4,7,10-tetraaza-cyclododec-1-yl]-acetic acid *tert*-butyl ester (48)



A stirred mixture of (7-*tert*-butoxycarbonylmethyl-1,4,7,10-tetraaza-cyclododec-1-yl)-acetic acid *tert*-butyl ester (0.195 g, 0.488 mmol), 3-chloromethyl-10,11,12,13-tetrahydrodipyrido-[3,2a:2',3'-c]-phenazine (0.125 g, 0.374 mmol) and NaHCO₃ (0.063 g, 0.750 mmol) was heated at 60 °C in *anhydrous* CH₃CN (15 ml), under argon, for 18 h. The reaction mixture was allowed to cool to rt, syringe filtered and the filtrate concentrated under reduced pressure to afford a yellow solid. The crude material was purified by column chromatography on neutral alumina (gradient elution: CH₂Cl₂ – 0.8 % CH₃OH : CH₂Cl₂, utilising 0.1 % CH₃OH increments) to yield the *title compound* **48** as a pale yellow coloured solid (0.220 g, 0.315 mmol, 84 %); R_F = 0.21 (Alumina, CH₂Cl₂ – CH₃OH 19 : 1 v/v); m.p. 175-177 °C; ¹H NMR (CDCl₃, 500 MHz) δ 1.29 (18H, s, ^tBoc CH₃), 2.06 (4H, s, cyclen CH₂) 2.67 (4H, s, cyclen CH₂), 2.80 (4H, s, cyclen CH₂), 2.99

(4H, s, cyclen CH₂), 3.21 (4H, cyclen CH₂), 3.57 (4H, s, CH₂CO), 4.02 (2H, s, CH₂ dpqC), 7.65 (1H, m, H⁷), 7.75 (1H, m, H²), 8.76 (1H, dd, $J = 5.0; 1.5$ Hz, H⁶), 9.42 (1H, m, H¹), 9.48 (1H, m, H⁸); ¹³C NMR (CDCl₃, 126 MHz, ¹H decoupled 500 MHz) δ 28.2 (6C, 'Boc CH₃), 44.5 (2C, cyclen CH₂), 49.6 (2C, cyclen CH₂), 49.8 (2C, cyclen CH₂), 53.7 (2C, CH₂CO), 55.7 (2C, cyclen CH₂), 81.6 (2C, 'Boc_(q)), 123.6 (1C, C²), 123.9 (1C, Ar), 126.2 (1C, C Ar), 127.7 (1C, Ar), 133.5 (1C, Ar), 133.9 (1C, Ar), 137.2 (1C, C⁸), 137.5 (1C, C¹), 145.8 (1C, C Ar), 146.4 (1C, Ar), 152.2 (1C, C⁶), 154.5 (1C, Ar), 154.6 (1C, Ar), 159.6 (1C, Ar), 170.4 (2C, C = O); MS (ES⁺) m/z 699.4 (100 %, [M + H]⁺); HRMS (ES⁺) m/z found 699.4335 [M + H]⁺ C₃₉H₅₅N₈O₄ requires 699.4340.

References

- 1.) F. J. Villani, T. A. Mann, E. A. Wefer, J. Hannon, L. L. Larca, M. J. Landon, W. Spivak and D. Vashi, *J. Med. Chem.*, 1975, **18**, 1.
- 2.) U. S. Schubert, C. Eschbaumer and M. Heller, *Org. Lett.*, 2000, **2**, 3373
- 3.) O. Reany, T. Gunnlaugsson and D. Parker, *J. Chem. Soc. Perkin. Trans 2.*, 2000, 1819.
- 4.) R. A. Poole, G. Bobba, M. J. Cann, J-C. Frias, D. Parker and R. D. Peacock, *Org. Biomol. Chem.*, 2005, **3**, 1013.
- 5.) S. Brandes, C. Gros, F. Denat, P. Pullumbi and R. Guilard, *B. Soc. Chim. Fr.*, 1996, **133**, 65.
- 6.) R. S. Dickins, J. A. K. Howard, C. L. Maupin, J. M. Moloney, D. Parker, J. P. Riehl, G. Siligardi and J. A. G. Williams, *Chem. Eur. J.*, 1999, **5**, 1095.
- 7.) E. Fischer and R. Shultze, *Chem. Ber.*, 1907, **40**, 908.
- 8.) B. B. Shankar, B. J. Lavey, G. Zhou, J. A. Spitler, L. Tong, R. Rizvi, D-Y. Yang, R. Wolin, J. A. Kozlowski, N-Y. Shih, J. Wu, R. W. Hipkin, W. Gonsiorek and C. A. Lunn, *Bioorg. Med. Chem. Lett.*, 2005, **15**, 4417.
- 9.) M. Woods and A. D. Sherry, *Inorg. Chim. Acta*, 2003, **351**, 395.
- 10.) Z. Kovacs and A. D. Sherry, *J. Chem. Soc., Chem. Commun.*, 1995, **2**, 185.
- 11.) L-O. Pålsson, R. Pal, B. S. Murray, D. Parker and A. Beeby, *Dalton Trans.*, 2007, 5726.
- 12.) K-P. Eisenwiener, P. Powell and H. R. Mäcke, *Bioorg. Med. Chem. Lett.*, 2000, **10**, 2133.
- 13.) Z. Kovacs and A. D. Sherry, *Synthesis.*, 1997, **7**, 759.

Appendices

Appendix 1 – Substituted Pyrazoyl-azaxanthone Characterisation

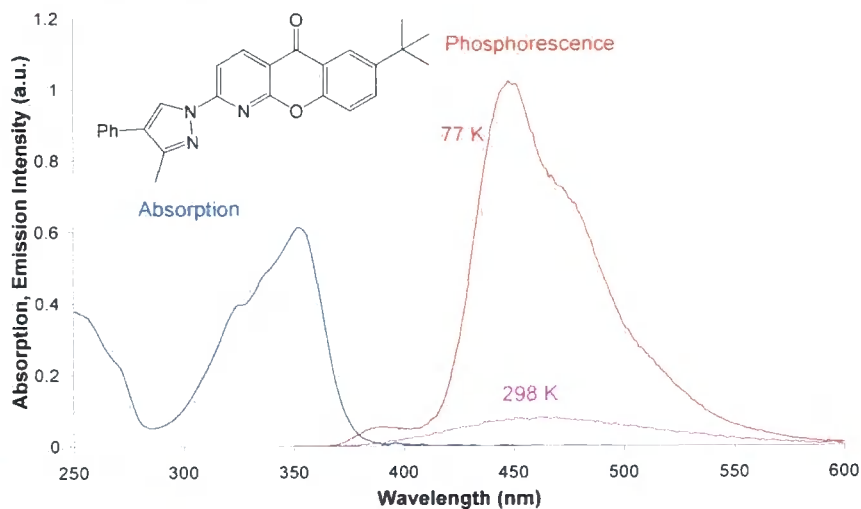


Figure 7.1: Absorption (left) and Phosphorescence (right) spectrum of Ph-pyrazoyl-azaxanthone (Absorption 298 K, MeOH; Phosphorescence 77 K, EPA)

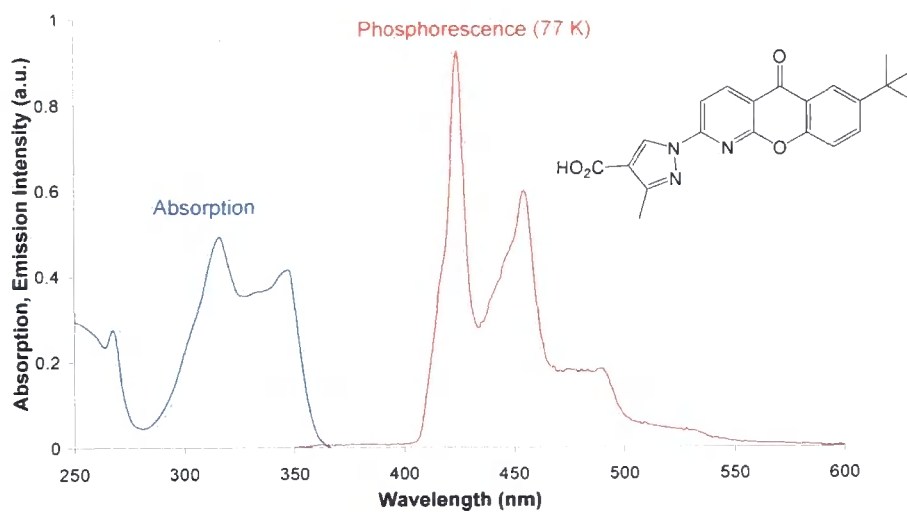


Figure 7.2: Absorption (left) and Phosphorescence (right) spectrum of CO₂H-pyrazoyl-azaxanthone (Absorption 298 K, MeOH; Phosphorescence 77 K, EPA)

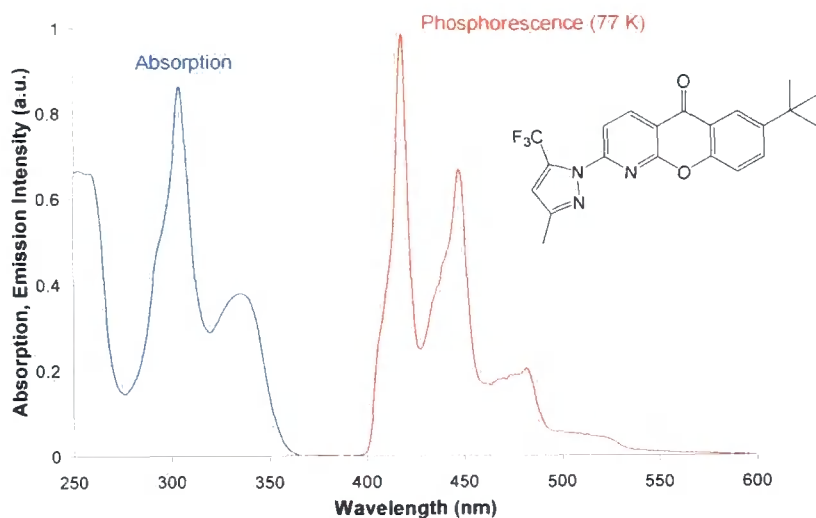


Figure 7.3: Absorption (left) and Phosphorescence (right) spectrum of CF_3 -pyrazol-azaxanthone (Absorption 298 K, MeOH; Phosphorescence 77 K, EPA)

Appendix 2 – Analytical Reverse Phase HPLC Analysis / Characterisation

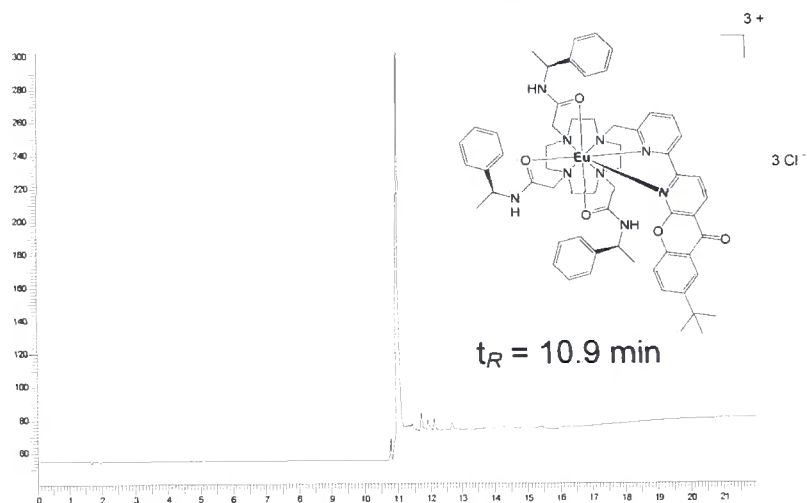


Figure 7.4: HPLC analysis of $[EuL^4]$ (Chromolith RP18e Column, Method A)

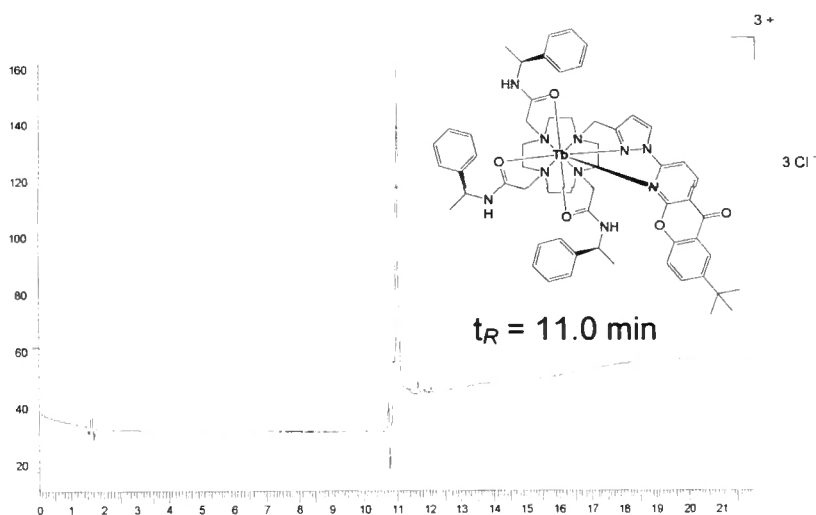


Figure 7.5: HPLC analysis of [TbL⁵] (Chromolith RP18e Column, Method A)

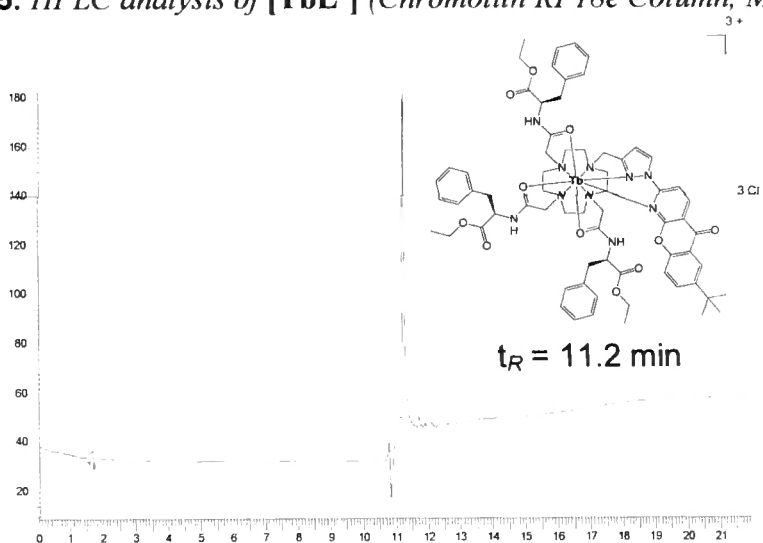


Figure 7.6: HPLC analysis of [TbL⁶] (Chromolith RP18e Column, Method A)

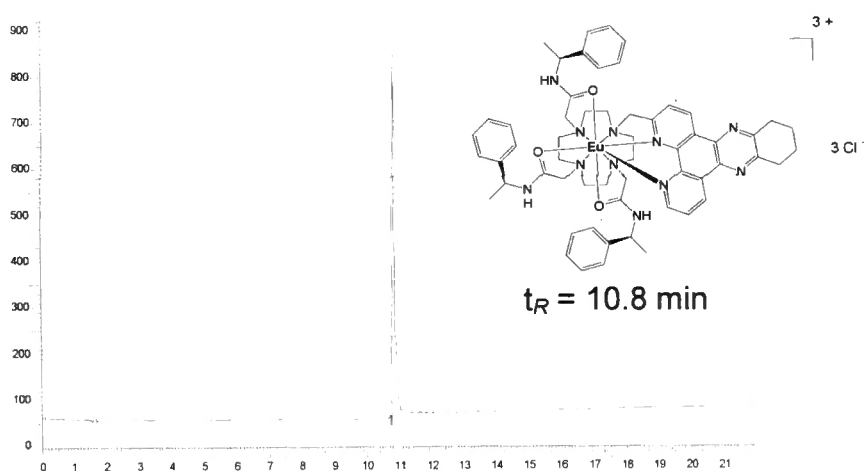


Figure 7.7: HPLC analysis of [EuL⁷] (Chromolith RP18e Column, Method A)

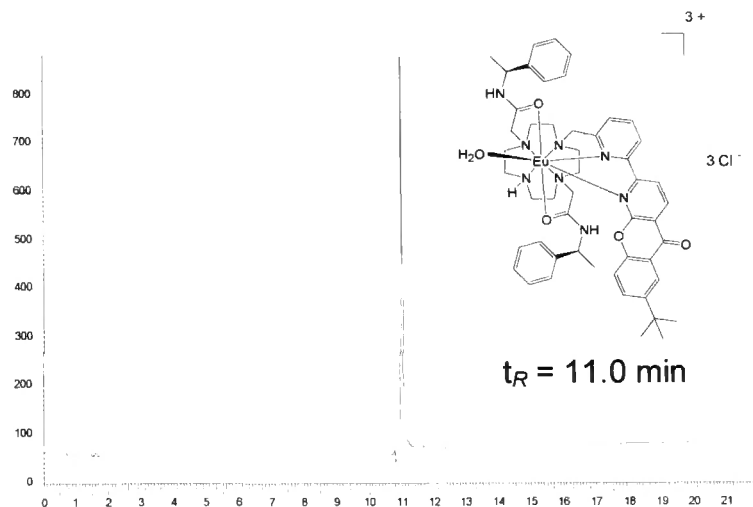


Figure 7.8: HPLC analysis of $[\text{EuL}^8]$ (Chromolith RP18e Column, Method A)

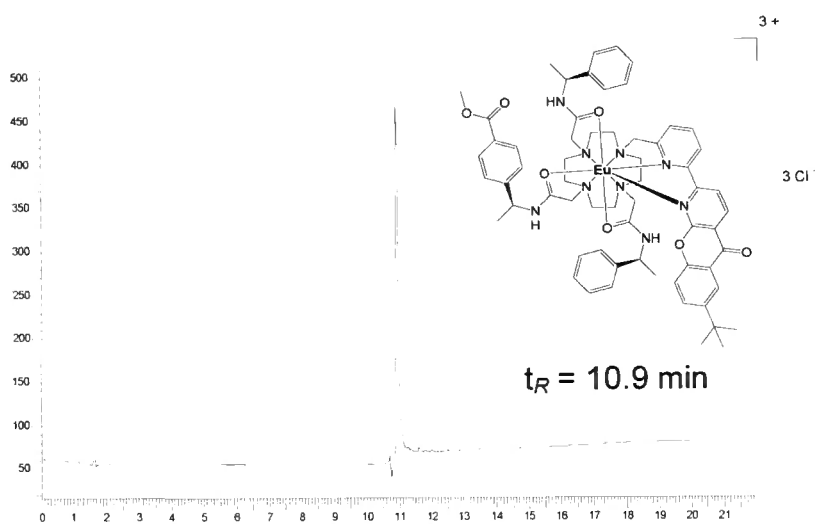


Figure 7.9: HPLC analysis of $[\text{EuL}^9]$ (Chromolith RP18e Column, Method A)

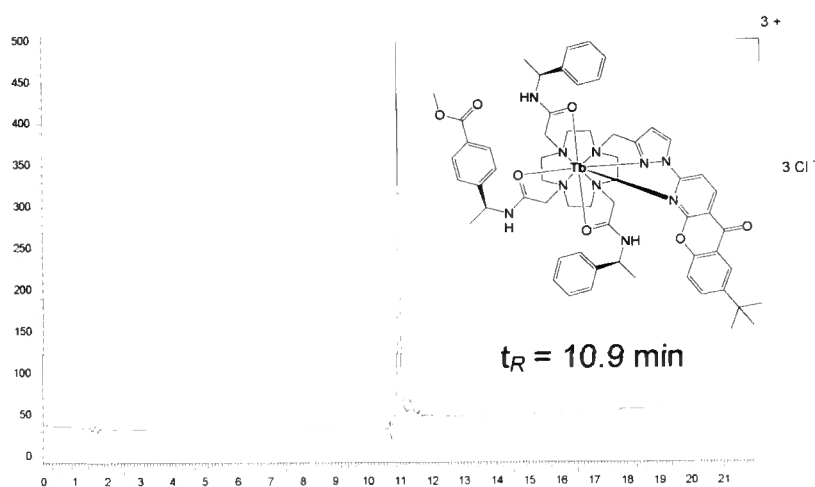


Figure 7.10: HPLC analysis of $[\text{TbL}^{10}]$ (Chromolith RP18e Column, Method A)

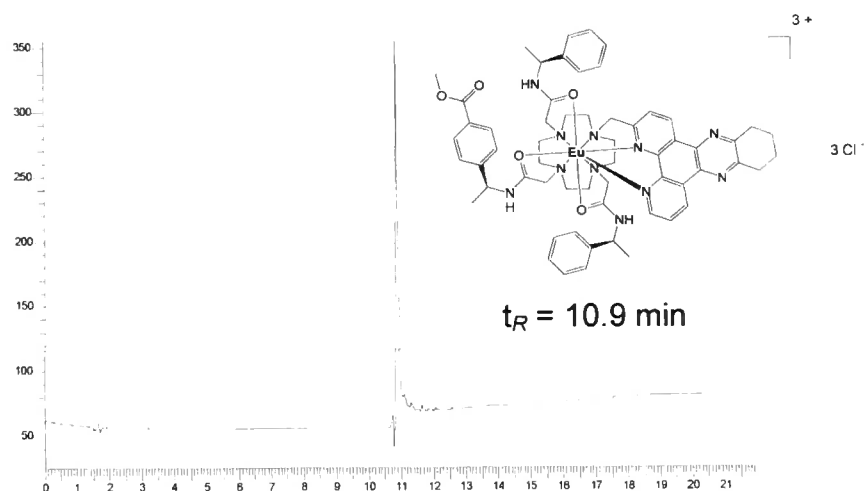


Figure 7.11: HPLC analysis of [EuL¹¹] (Chromolith RP18e Column, Method A)

Appendix 3 – Crystal Data and Structure Refinement Parameters

	Methylpyridyl-azaxanthone 8	Bromopyrazoyl-azaxanthone 12
Empirical Formula	C ₂₂ H ₂₀ N ₂ O ₂	C ₂₀ H ₁₈ BrN ₃ O ₂
Molecular Weight	344.40	412.28
Crystal System	Monoclinic	Monoclinic
Space Group	<i>P</i> 2 ₁ / <i>c</i>	<i>P</i> 2 ₁ / <i>c</i>
Crystal Size / nm	0.54 x 0.36 x 0.13	0.50 x 0.05 x 0.05
Temperature / K	120	120
<i>a</i> / Å	13.4718 (3)	17.044 (3)
<i>b</i> / Å	6.7227 (7)	13.303 (2)
<i>c</i> / Å	19.4491 (19)	8.0788 (12)
Volume / Å ³	1760.7 (3)	1817.6 (3)
<i>Z</i>	4	4
Density / g cm ⁻³	1.299	1.507
μ / mm ⁻¹	0.08	2.28
<i>R</i> _{int}	0.028	0.104
Data [<i>I</i> > 2σ(<i>I</i>)]	4671	3201
<i>R</i> ₁ / w <i>R</i> ₂ [<i>I</i> > 2σ(<i>I</i>)]	0.042 / 0.118	0.073 / 0.125
Goodness of fit (<i>S</i>)	1.03	1.14
N ^o of variables	315	228

